ASTRONOMICAL INSTITUTE
of the
ROMANIAN ACADEMY

Str. Cutitul de Argint 5, Bucharest
RO-040558, Romania

OBSERVATOIRE DE PARIS
SYSTÈMES DE RÉFÉRENCE TEMPS-ESPACE
UMR8630 / CNRS

61, avenue de l'Observatoire, Paris
F-75014, France

Astrometry from ground and from space

Astrométrie au sol et dans l'espace

Edited by

(Actes publiés par)

N. CAPITAINE and M. STAVINSCHI

JOURNÉES 2002 ⋆

SYSTÈMES DE RÉFÉRENCE SPATIO-TEMPORELS

⋆ BUCHAREST, 25-28 SEPTEMBER

ISBN 2-901057-48-9

ISBN 973-558-108-6

TABLE OF CONTENTS

PRÉFACE

Les Journées 2002 "Systèmes de référence spatio-temporels", avec le sous-titre "Astrométrie au sol et dans l'espace", ont été organisées à Bucarest du 25 au 28 Septembre 2002. Leur organisation conjointe par l'Institut Astronomique de l'Académie Roumaine et l'Observatoire de Paris reflète la longue tradition de coopération entre astronomes Roumains et Français et, plus géneralement, d'échanges culturels entre nos deux pays. Leur réussite doit beaucoup au Ministère de l'Education et de la Recherche Roumain et au Service Culturel de l'Ambassade de France en Roumanie que nous remercions très vivement pour leur soutien. L'Institut Français à Bucarest a chaleureusement accueilli ces Journées en leur permettant le meilleur déroulement possible. Nous remercions particulièrement son Directeur, M. Colombani, Mme Ravanel et tout son personnel. Nous sommes également redevables à l'Observatoire de Paris qui a pris en charge la publication de ces Actes.

Le but général de ces "Journées" est de discuter les problèmes relatifs aux systèmes de référence d'espace et de temps, depuis le concept et la réalisation, jusqu'à l'interprétation scientifique des observations les plus précises. Ces Journées ont été organisées annuellement depuis 1988, tout d'abord à Paris jusqu'en 1992 et, depuis 1994, alternativement à Paris et dans d'autres villes européennes : Varsovie en 1995, Prague en 1997, Dresde en 1999 et Bruxelles en 2001.

Les Journées 2002 ont inclus, comme c'est l'usage, des sessions relatives aux systèmes de référence d'espace et de temps, la rotation de la Terre et l'astrométrie. Les sessions générales ont été intitulées "Repères de référence cinématiques et dynamiques", "Repères de référence célestes et terrestres", "Théorie de la rotation de la Terre", "Temps, transfert de temps et rotation de la Terre", chaque session incluant des exposés invités et des contributions orales. La session poster a été précédée de courtes présentations orales. De plus, une session spéciale du Groupe de travail de la Division I de l'UAI intitulé "Future Development of Ground-Based Astrometry" a été organisée sous forme d'une table ronde pour discuter des programmes scientifiques qui peuvent être encore entrepris avec succès à partir d'instruments astrométriques au sol.

Environ 70 participants de 14 pays ont participé à ces Journées. En plus des 15 conférences invitées, des 26 communications orales et des 26 posters, les participants ont pu assister à deux conférences publiques: "Références astronomiques - Références spirituelles" et "Références spatio-temporelles dans le cadre de l'activité spatiale Roumaine". La réunion s'est terminée par la visite de l'Observatoire de Bucarest de l'Institut Astronomique de l'Académie Roumaine. Il a été décidé de publier les Actes comme c'est l'usage et d'y inclure les contributions aux discussions du Groupe de travail de l'UAI, de poursuivre les discussions de ce groupe, en particulier sur sa page web et également d'en élargir sa composition.

Les Actes sont divisés en 5 chapitres qui correspondent aux différentes sessions et contiennent l'ensemble des contributions invitées, orales et posters. La liste des participants est donnée en pages viii et ix, le Programme scientifique en pages x à xii, la Table des matières en pages iii à v et la Postface en page 261. Celle-ci annonce les "Journées" 2003 à St.Petersbourg.

Nous remercions le Comité Scientifique d'Organisation pour sa contribution essentielle à la préparation du programme scientifique ainsi que tous les auteurs qui ont transmis leur texte pour la publication, sous la forme demandée et dans les délais requis.

Nous remercions le personnel de l'Observatoire de Bucarest, et en particulier Vasile Mioc et Petre Popescu, pour leur travail très efficace au sein du Comité Local d'Organisation avant et pendant la réunion, ainsi qu'Olivier Becker pour son aide technique pour la publication des Actes.

Les organisatrices des "Journées 2002",

Nicole CAPITAINE et Magda STAVINSCHI

28 août 2003

PREFACE

The Journées 2002 "Systèmes de référence spatio-temporels", with the sub-title "Astrometry from Ground and from Space", have been held from 25 to 28 September 2002 in Bucharest. They have been organized jointly by the Astronomical Institute of the Romanian Academy and Paris Observatory, with the help of the Ministry of Education and Research and of the Cultural Service of the French Embassy in Romania. The Journées 2002, reflecting the long term tradition of cooperation between Romanian and French astronomers, were the fourteenth conference in this series. The purpose is to discuss the problems, from the concepts and realizations of space and time reference systems, up to the scientific interpretations of precise observations referred to these systems. The previous Journées have been organized in Paris each year from 1988 to 1992 and alternately, since 1994, in Paris and other European cities as follows: Warsaw (1995), Paris (1996), Prague (1997), Paris (1998), Dresden (1999), Paris (2000) and Brussels (2001).

These Journées 2002 included, as usual, sessions related to space and time reference systems, Earth rotation and astrometry. The general sessions were "Kinematical and Dynamical celestial reference systems", "Celestial and Terrestrial Reference Systems", "Theory of Earth Rotation", "Time, Time Transfer and Earth Rotation". Each session included invited papers and oral contributions and the poster session was introduced by short oral presentations. In addition, a special round table of the IAU Division 1 Working Group "Future Development of Ground-Based Astrometry" was organized to discuss the scientific programs that can still be successfully performed with ground-based instruments.

About 70 participants from 14 countries attended this meeting. Beside 15 invited papers, 26 oral communications and 26 posters, the participants could attempt two public conferences: "Astronomical references - Spiritual references" and "Space-time references in the Romanian Space Activity". The meeting ended by visiting the Bucharest Observatory of the Astronomical Institute of the Romanian Academy. It was decided that the Proceedings of Journées 2002 be published including the contribution from the Working Group "Future Development of Ground-Based Astrometry" and that the discussions held during the round table of this WG will continue, especially on its own site and with a group enlarged with new members.

We are grateful to Service culturel de l'Ambassade de France en Roumanie, Ministry of Education and Research and Astronomical Institute of the Romanian Academy for helping this meeting and especially to the Institut Français in Bucharest which has hosted the sessions and the reception. We especially thank his Director, M. Colombani, Mrs Ravanel and all its staff. The Proceedings are published thanks to the financial support of Paris Observatory.

These Proceedings are divided into five sections corresponding to the sessions of the meeting including, for each session, the invited talks, as well as the oral and poster contributions which have been presented during the meeting. The list of participants is given on pages viii and ix, the scientific programme on pages x to xii. A Table of Contents and a Postface are given on pages iii to v and 261 respectively. The Postface gives the announcement for "Journées" 2003 in St. Petersburg (Russian Federation).

We thank the Scientific Organizing Committee for its valuable contribution to the elaboration of the scientific programme and all the authors of the papers who have sent their contribution in the required form and within the required deadline. We would like to thank especially Vasile Mioc and Petre Popescu for their very efficient work before and during the meeting within the Local Organizing Committee and the staff of the Bucharest Observatory as well. We are grateful to Olivier Becker for his efficient technical help for the publication.

The organizers of the "Journées 2002",

Nicole CAPITAINE and Magda STAVINSCHI

28 August 2003

Liste des participants / List of Participants

ANDREI *Alexandre Humberto*, Brazil, oat1@on.br
BARKIN *Yuri*, Russia, barkin@sai.msu.ru
BAZYEV *Nataliya*, Russia, Ii1966@mail.ru
BIZOUARD *Christian*, France, Christian.bizouard@obspm.fr
BOCSA *Gheorghe*, Romania, gbocsa@aira.astro.ro
BOUGEARD *Mireille*, France, bougeard@hpopa.obspm.fr
BOURDA *Geraldine*, France, Geraldine.Bourda@obspm.fr
BRZEZINSKI *Aleksander*, Poland, alek@cbk.waw.pl
CAPITAINE *Nicole*, France, nicole.capitaine@obspm.fr
CHAPRONT *Jean*, France, jean.chapront@obspm.fr
CHARLOT *Patrick*, France, charlot@observ.u-bordeaux.fr
COLL *Bartolomé*, France, bartolome.coll@obspm.fr
COSTACHE *Doru*, Romania, Dcostache@home.ro
DAIGNE *Gerard*, France, daigne@observ.u-bordeaux.fr
DAMLJANOVIC *Goran*, Yugoslavia, gdamljanovic@aob.bg.ac.yu
DE VIRON *Olivier*, Belgium, o.deviron@oma.be
DEBARBAT *Suzanne*, France, Suzanne.Debarbat@obspm.fr
DROBITKO *Eugene*, Russia, siggy@paloma.spbu.ru
DUCOURANT *Christine*, France, ducourant@observ.u-bordeaux.fr
ESCAPA *Alberto*, Spain, Alberto.Escapa@ua.es
FUJISHITA *Mitsumi*, Japan, mfuji@ktmail.ktokai-u.ac.jp
GAMBIS *Daniel*, France, daniel.gambis@obspm.fr
KAZAKEVICH *Elena*, Russia, elen@ek3286.spb.edu
KORSUN' *Alla*, Ukraine, akorsun@mao.kiev.ua
KOSEK *Wieslaw*, Poland, kosek@cbk.waw.pl
KOVALEVSKY *Jean*, France, Jean.Kovalevsky@obs-azur.fr
KUDLAY *Oleksandr*, Ukraine, kudlay@mao.kiev.ua
LAMBERT *Sébastien*, France, Sebastien.Lambert@obspm.fr
LANGHANS *Ralf*, Germany, langhans@astro.geo.tu-dresden.de
MANDACHE *Cipriana*, Romania, cipriana@opdaf1.obspm.fr
MIOC *Vasile*, Romania, vmioc@aira.astro.ro
MUINOS HARO *Jose L*, Spain, ppmu@roa.es
NICULESCU *Anca*, Romania, Ancan@inm.ro
PARASCHIV *Petre*, Romania, Paras@aira.astro.ro
PINIGIN *Gennady*, Ukraine, pinigin@mao.nikolaev.ua
POPESCU *Petre*, Romania, petre@aira.astro.ro
POPESCU *Radu*, Romania, pradu@aira.astro.ro
PRUNARIU *Dumitru Dorin*, Romania, prunariu@rosa.ro
RON *Cyril*, Czech R., ron@ig.cas.cz
RUSU *Mircea*, Romania, Mrusu@dnt.ro

SCHUH *Harald*, Austria, hschuh@luna.tuwien.ac.at
SHULGA *Alexander*, Ukraine, japetus@mao.nikolaev.ua
SOFFEL *Michael*, Germany, soffel@rcs.urz.tu-dresden.de
SOMA *Mitsuru*, Japan, somamt@cc.nao.ac.jp
STAVINSCHI *Magda*, Romania, magda@aira.astro.ro
SOUCHAY *Jean*, France, Jean.Souchay@obspm.fr
TANG *Zhenghong*, China, zhtang@center.shao.ac.cn
TEIXEIRA *Ramachrisna*, Brazil, Rama@sider.net
TEYSSANDIER *Pierre*, France, Pierre.Teyssandier@obspm.fr
VERTYPOLOKH *Oleksandr*, Ukraine, Verto@observ.univ.kiev.ua
VONDRAK *Jan*, Czech Republic, Vondrak@ig.cas.cz
XIA *Yifei*, China, Yfxia@nju.edu.cn
YATSKIV *Yaroslav*, Ukraine, Yatskiv@mao.kiev.ua
ZHANG *Chengzhi*, China, czzhang@nju.edu.cn
ZHAROV *Vladimir*, Russia, zharov@sai.msu.ru
ZHU *Zi*, China, zhuzi@ms.sxso.ac.cn

JOURNÉES 2002 SYSTÈMES DE RÉFÉRENCE SPATIO-TEMPORELS

"Astrometry from ground and from space"
"Astrométrie au sol et dans l'espace"

***Scientific Organising Committee*:** Brzezinski A., Poland; Capitaine N. (Chair), France; Defraigne P., Belgium; Kovalevsky J., France; Soffel M., Germany; Vondrák J., Czech R.; Yatskiv Y., Ukraine.
***Local Organising Committee*:** Mioc V., Popescu P., Stavinschi M. (Chair)
Astronomical Institute of the Romanian Academy, Bucharest, RO-040558, Romania
***Venue* :** Institut Français (Bucharest)

SCIENTIFIC PROGRAMME

Wednesday, 25 September: 14 h 30 – 18 h 00

OPENING OF THE JOURNÉES 2002 : Introduction and presentation
N. Capitaine and M. Stavinschi

SESSION 1a. – KINEMATICAL AND DYNAMICAL CELESTIAL REFERENCE SYSTEMS
Invited papers
M. SOFFEL, S. KLIONER : *Relativity for astrometry at the microarcsecond level*
J. CHAPRONT, G. FRANCOU: *The lunar ephemeris ELP2000 revisited*

Oral communications
G. DAMLJANOVIC, J. SOUCHAY: *Cross-identification of* HIPPARCOS-2MASS *second incremental data release*
Z. ZHU: *Hipparcos proper-motion system with respect to FK5 and SPM 2.0 systems*
G. PINIGIN et al.: *Refinement of linking optical-radio reference frames on the basis of collaborative observatories in international joint project*
R. TEIXEIRA et al.: *Optical position and proper motion of X-Ray sources south-eastern of the Ophiuchus molecular clouds*
B. COLL: *A principal positioning system for the Earth*

Oral presentation of posters (Sessions 1 and 2)

Thursday, 26 September: 9 h 00 – 13 h 00

SESSSION 1b – CELESTIAL AND TERRESTRIAL REFERENCE SYSTEMS

Invited papers
P. CHARLOT: *Extending and improving the ICRF*
J. VONDRÁK, C. RON: *An improved optical reference frame for long-term Earth rotation studies*
H. SCHUH, W. SCHLUETER, N. VANDENBERG: *Prospective improvements of IVS products and evolvement of observing programs*
Ya. YATSKIV et al.: *Recent compiled catalogue of radio source postions RSC(GAO UA) 01 C01*
N. CAPITAINE: *Accurate formulation for the transformation between the Terrestrial and Celestial Reference Systems*

Oral communications
R. POPESCU, P. POPESCU and O. BĂDESCU: *Deflection of the vertical in Bucharest derived from geodetic astronomical observations*
S. LAMBERT, Ch. BIZOUARD: *Positioning the Terrestrial Ephemeris Origin in the International Terrestrial Reference Frame*
V. MIOC: *Earth's rotation and stability of satellite orbits*

Oral presentation of posters (Sessions 3 and 4)

Thursday, 26 September: 14 h 30 – 18 h 00

SESSION 2 – THEORY OF EARTH ROTATION

Invited papers

A. BRZEZINSKI, S. MATHEWS: *Recent advances in modeling the lunisolar perturbation in polar motion corresponding to high frequency nutation: report on the discussion of the IAU Comm.19 WG on Nutation*
O. de VIRON et al.: *Nutation residuals and physics of the Earth's interior*
A. ESCAPA, J. GETINO, J. M. FERRANDIZ: *Variational approach to the rotational dynamics of a three-layer Earth model; fluid outer core dynamics*
Ch. BIZOUARD, S. LAMBERT: *Variable processes in polar motion and length of day*

Oral communications

W. KOSEK: *Polar motion prediction by different methods in polar coordinates system*
O. KUDLAY: *Precise Analysis of EOP Series; an attempt to distinguish chaotic and non-stationary processes*
J. SOUCHAY, M. FOLGUEIRA: *Free motion of rigid and elastic bodies with respect to inertial frame*
V. E. ZHAROV, S. L. PASYNOK: *Theory of nutation of the non-rigid Earth with the atmosphere*
V. MIOC, M. STAVINSCHI: *Martian rotation influence on eccentric trajectories of orbiters*

POSTER SESSION

CONFERENCE : 19 h 00

Friday, 27 September: 9 h 00 – 12 h 00

SESSION 3 – SPACE AND GROUND-BASED ASTROMETRY

Oral communications

G. DAIGNE: *Al-sky surveys and optical interferometers: complementary tools in building frames?*
F. MIGNARD , J. KOVALEVSKY: *Space astrometry missions: common principles and objectives*
M. STAVINSCHI: *The IAU Working Group "Future developments in ground-based astrometry"*
J. L. MUINOS et al.: *Observations with our CCD transit circle in Argentina*
A.H. ANDREI et al.: *Solar diameter observations on the maximum of Cycle 23*
G. BOCSA: *Precise positions and magnitude for Pluto* in 1932 and *1967-1975 at Bucharest Observatory*
C. RON, J. VONDRÁK: *An improved star catalogue for Ondrejov PZT*
C. DUCOURANT et al.: *Proper motion survey in the Bordeaux M2000 zone*

Discussion of the IAU Working Group including short communications

G. PINIGIN: *Limit capabilities of ground-based optical astrometry instrumentation*
R. POPESCU, P. POPESCU, P. PARASCHIV: *Preliminary tests for CCD observations of mutual phenomena in Bucharest*

CONFERENCE : 12 h 00 -13 h 00

Concluding paper of Session 3 and discussion

J. KOVALEVSKY: *Synthesis of possible programs using small ground-based astrometric instruments*

Friday, 27 September: 14 h 00 – 18 h 00

SESSION 4 – TIME, TIME TRANSFER AND EARTH ROTATION

Invited papers

S. DEBARBAT, M. LERNER: *La rotation de la Terre de l'Antiquité à l'aube du XXe siècle*
D. GAMBIS, D. ABARCA del RIO and D. SALSTEIN: *Solar activity and Earth rotation variability from interannual to decadal times scales*

Oral communications

M. SOMA, K. TANAKAWA, K.A. KAWABATA: *Earth's rotation in the 7^{th} century derived from eclipse records in Japan and China*
P. TEYSSANDIER, B. LINET: *Time transfer and frequency shift to the order $1/c^4$ in the field of an axisymmetric rotating body*
C. MANDACHE et al.: *The atomic frequency standards and the time measurement*
P. PARASCHIV, P. POPESCU: *Long-term stability of Rhode&Schwarz quartz clocks*

CLOSING SESSION OF THE JOURNEES 2002

LIST OF POSTERS

SESSIONS 1a and 1b – REFERENCE SYSTEMS

Yu. BABENKO et al.: *Reduction of compiled catalogue in the selected extragalactic radio sources fields*
E. DROBITKO, V. VITYAZEV: *HIPPARCOS Kinematics of nearby and distant stars*
M. FUJISHITA: *Problems to construct the radio celestial reference frame using VERA*
E. KAZAKEVICH, V. ORLOV, V. VITYAZEV: *HIPPARCOS, search for stellar groups*
E. KAZAKEVICH, V. VITYAZEV: *TYCHO2, the wavelet search for stellar groups*

SESSION 2 – THEORY OF EARTH ROTATION

G. BOURDA: *Earth rotation and gravitational potential*
A. ESCAPA, J. M. FERRÁNDIZ, J. GETINO: *Quasi-semmidiurnal nutations induced by the indirect effect of the triaxiality of the Earth : Rigid and non-rigid models*
A. KORSUN, G. KURBASOVA: *Dynamical study of Siberian anticyclone and Earth rotation*
Y. XIA, C. ZHANG: *Martian precession and nutation*
V. E. ZHAROV, S.L. PASYNOK, J. GETINO: *Comparative analysis of the new nutation series*

SESSION 3 – SPACE AND GROUND-BASED ASTROMETRY

A. H. ANDREI et al.: *Radio structure effects on the optical and radio representations of the ICRF*
Yu. BABENKO et al.: *Kyiv meridian axial telescope observation programs: First results*
M. BOUGEARD: *Statistical methods in application to astrometry*
R. LANGHANS: *A universal computer program for high precision position determination of minor planets on CCD-frames*
R. LANGHANS, V. MALYUTO, H. POTTHOFF: *Calculated differential color refraction confronted with observed stellar positions*
M. POGORELTSEV, O.VERTYPOLOKH, Yu.BABENKO: *Application of the "Scanner+MIDAS" complex for processing astrometric photographic plates*
Z. TANG et al.: *Rigorous vectorial formulae for block-adjustment and application extending FOV of CCD*
O. VERTRYPOLOKH, YU. BABENKO, P. LAZORENKO: Devices for reduction of CCD distortion under scan mode

Session Ia

KINEMATICAL AND DYNAMICAL CELESTIAL REFERENCE SYSTEMS

SYSTÈMES DE RÉFÉRENCE CINÉMATIQUES ET DYNAMIQUES

RELATIVITY FOR ASTROMETRY AT THE MICROARCSECOND LEVEL

S.A. KLIONER, M. SOFFEL
Lohrmann Observatory, Dresden Technical University
01062 Dresden, Germany

ABSTRACT. The current state of relativistic modeling of positional observations with microarcsecond accuracy is reviewed. The requirements which should satisfy a reasonable relativistic model as well as the structure of a standard relativistic model are both discussed. Some subtle relativistic effects playing a role in the model are elucidated. Additional relativistic effects due to gravitational fields produced outside of the solar system which potentially could be larger than 1 μas are also briefly mentioned.

1. INTRODUCTION

Fifteen years after the idea of positional measurements with an accuracy of a microarcsecond was seriously discussed for the first time microarcsecond astrometry is gradually becoming reality. Two space missions GAIA and SIM approved by ESA and NASA should be launched and produce first results within the next decade. Being rather different in goals and technical means these two missions have one thing in common – the accuracy of ~ 1 μas. One microarcsecond is the apparent thickness of a sheet of paper as seen from the other side of the Earth. This amazing technical accuracy requires very careful theoretical modeling. It is clear that very complicated instrumental calibrations and models are necessary here. It is also clear that in many cases the sources themselves (quasars, stars, solar system bodies, etc.) have angular extensions exceeding 1 μas and, thus, adequate astrophysical models of the sources are needed to interpret the photocenters of the corresponding images with required accuracies. This paper deals with what lies between these two parts of the overall modeling: here we briefly describe a standard relativistic model of positional observations of point-like sources with microarcsecond accuracy.

2. SOME REQUIREMENTS TO A RELATIVISTIC MODEL OF POSITIONAL OBSERVATIONS

Let us first formulate some simple requirements which any reasonable relativistic model of positional observations should satisfy.

A. The model should be compatible with state-of-the-art relativistic models of other kind of observations (i.e. geodetic VLBI observations which are used to construct the ICRS). This indispensably means that the model must be compatible with the IAU 2000 Resolutions on relativity (Soffel *et al.* 2003).

B. The model should be complete. The suggested relativistic framework should not only give

the possibility to model the positional observations, but also should provide the community with relativistic models for translational and rotational motion of the satellite, etc.

C. The model should be valid for any trajectory of the satellite (although the types of the orbits for GAIA and SIM are fixed, actual orbits will be affected by various non-gravitational effects and other factors and cannot be calculated in advance).

D. The model should take into account a realistic model of the solar system (i.e. all gravitating bodies producing a light deflection of 1 μas and more should be taken into account).

E. The model should be formulated in such a way that any model of the motion of solar system bodies can be used (i.e. any ephemeris can be plugged into the model).

F. The model should be valid for any light source: from a near-earth asteroid to a quasar.

G. The model should contain all effects in light propagation which may amount to 1 μas in real observations.

H. The model should be as simple as possible (i.e. any formulas and calculations affecting the results at levels below 1 μas should be avoided).

I. The model should be configurable. Since the accuracy of the observations will crucially depend on the brightness of the source it is important to efficiently calculate the observed quantities with a given accuracy (1 μas or worse) and not just with a fixed accuracy of 1 μas. Furthermore, for detailed investigations of the observational data it is necessary to switch off and on particular physical effects.

J. The model should be formulated in such a way that we could test general relativity against at least some class of alternative theories of gravity.

3. THE STRUCTURE OF THE MODEL

A model satisfying all the requirements formulated above was elaborated and refined by several authors during more than a decade. After the pioneering works of Brumberg, Klioner and Kopeikin (1990) and Klioner and Kopeikin (1992) the model was substantially refined and simplified by Klioner (2000, 2002, 2003a). Full details of the model are given in Klioner (2003a). Here we just give an overview of its structure. The model uses the Barycentric Celestial Reference System (BCRS) of the IAU to describe the translational motion of the satellite and the solar system bodies as well as the light propagation from the source to the satellite. The Geocentric Celestial Reference System (GCRS) of the IAU is used only for the purpose of satellite orbit determination (this implies the use of Earth-based observations of the satellite itself). The model also uses a local reference system of the satellite (or a tetrad attached to the satellite) kinematically nonrotating relative to the BCRS to describe the observable direction of the light propagation and any local physical processes in the satellite (e.g. its rotational motion). Let us introduce five vectors:

1. $\mathbf{s}$ is the unit observed direction (the word "unit" means here and below that the formally Euclidean scalar product $\mathbf{s}\cdot\mathbf{s}=s^i\,s^i$ is equal to unity). This vector is defined with respect to the tetrad attached to the satellite's center of mass and kinematically non-rotating with respect to the spatial axes of the BCRS.

2. $\mathbf{n}$ is the unit tangent vector to the light ray at the moment of observation.

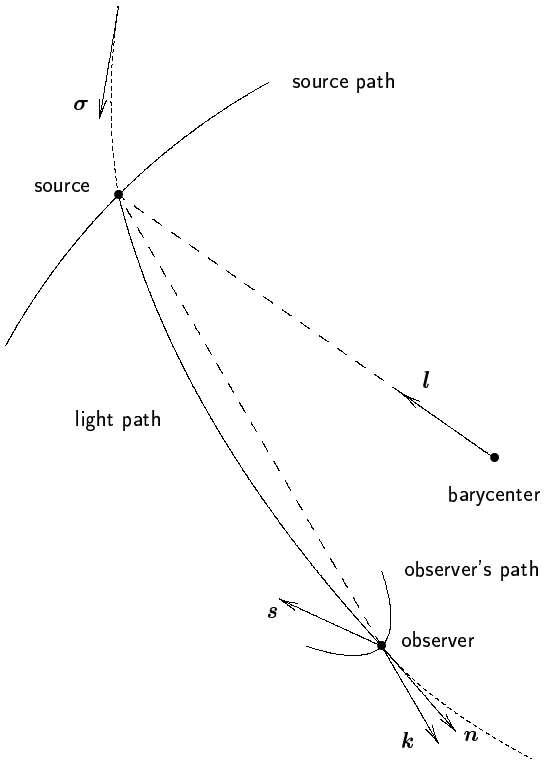

Figure 1: Five principal vectors used in the model: $\mathbf{s}$, $\mathbf{n}$, $\boldsymbol{\sigma}$, $\mathbf{k}$, $\mathbf{l}$.

3. $\boldsymbol{\sigma}$ is the unit tangent vector to the light ray at $t = -\infty$.

4. $\mathbf{k}$ is the unit coordinate vector from the source to the observer.

5. $\mathbf{l}$ is the unit vector from the barycenter of the Solar system to the source.

Note that the last four vectors are defined formally in the coordinate space of the BCRS. The five vectors used in the model are illustrated on Fig. 1. The calculations constituting the model lead to subsequent transformations of the five vectors mentioned above into each other. The physical content of these transformations can be formulated as follows:

$\mathbf{s} \leftrightarrow \mathbf{n}$ Aberration and gravitational effects affecting the observable light direction as compared to the coordinate direction of light propagation at the point of observation.

$\mathbf{n} \leftrightarrow \boldsymbol{\sigma}$ Gravitational light deflection for infinitely distant sources.

$\mathbf{n} \leftrightarrow \mathbf{k}$ Gravitational light deflection for sources situated at finite distances.

$\mathbf{k} \leftrightarrow \mathbf{l}$ Parallax.

The transformation sequence for a solar system source is $\mathbf{s} \rightarrow \mathbf{n} \rightarrow \mathbf{k}$. A number of vectors $\mathbf{k}$ derived for several epochs of observations allows one to determine (or refine) the BCRS orbit of the observed body. The transformation sequence for a source outside of the solar system is $\mathbf{s} \rightarrow \mathbf{n} \rightarrow \boldsymbol{\sigma} = \mathbf{k} \rightarrow \mathbf{l}$. In general the vector $\mathbf{l}$ depends on time. A reasonable parametrization of that time dependence allows one to obtain the proper motion of the source (and, additionally, orbital elements for binary stars, etc.).

The most complicated part of the transformations is the calculation of the gravitational light deflection. At the level of 1 μas this must include

1. post-Newtonian effects of motionless mass monopoles (in principle, not only the major planets should be taken into account here, but also a number of satellites and even Ceres),
2. post-Newtonian effects of motionless mass quadrupoles (important only for the four giant planets of the solar system), and
3. effects of translational motion of the gravitating bodies.

The effects of rotational motion of Jupiter are also marginally important. Moreover, although the post-post-Newtonian effects in the framework of general relativity are expected to play no role at the level of 1 μas (accounting for the minimal Sun avoidance angle of at least 35 degrees), one has to include a reasonable parametrization of post-post-Newtonian effects in the light propagation in the framework of a class of alternative theories of gravity. The reason is that the expected accuracy of the determination of the PPN parameter γ (of order $\sim 10^{-7}$) is close to the validity limit of the post-Newtonian approximation.

4. A SUBTLE POINT OF THE MODEL: LIGHT PROPAGATION IN THE FIELD OF MOVING BODIES

One of the most complicated points in the whole relativistic model of positional observations is the effect of translation motion of gravitating bodies on the light propagation. Hellings (1986) was probably the first who treated the problem from a rather intuitive point of view: he recommended to use the standard post-Newtonian formulas for the light propagation in the gravitational field of a motionless body and to substitute in those formulas the position of each gravitating body at the moment of closest approach of that body and the photon. The next step has been done by Klioner (1989) where the problem has been solved rigorously for the bodies moving with a constant velocity in the first post-Newtonian approximation. The effects of accelerations of the bodies have been further treated by Klioner and Kopeikin (1992) where it was shown that if the coordinates and velocities of the bodies are computed at the moments of closest approach of the corresponding body and the photon, the residual terms of the solution are in some sense minimized. The complete solution of the problem for arbitrarily moving bodies in the first post-Minkowskian approximation was found by Kopeikin and Schäfer (1999) who succeeded to integrate analytically the post-Minkowskian equations of light propagation in the field of arbitrarily moving mass monopoles. The Kopeikin-Schäfer solution has been rewritten explicitly by Klioner (2003b) who also showed how to get the Kopeikin-Schäfer solution in a very clear and straightforward way for a uniformly moving body as well as how to generalize the Kopeikin-Schäfer solution for bodies with full multipole structure. Recently, Klioner and Peip (2003) performed a series of numerical simulations to investigate the practical accuracy of various analytical formulas for the case of a GAIA-like observing satellite. The authors concluded that if an accuracy of 0.2 μas is sufficient, the initial suggestion of Hellings (1986) can be used. If higher accuracy is needed both the Klioner-Kopeikin and Kopeikin-Schäfer solutions can be used (the difference between them being less than 0.002 μas).

5. BEYOND THE STANDARD MODEL

The model sketched above can be called a "standard model". That model guarantees the accuracy of 1 μas provided that all gravitational effects in the light propagation come from the Solar system itself. In reality this cannot be always assumed and the standard model should be

extended to include some additional gravitational effects in the light propagation in some specific cases. Just to give some examples, let us mention that a more complicated model is necessary to describe the motion of light sources which are members of nearly edge-on binary systems. Gravitational light deflection caused by stars near the line of sight (microlensing) or by whole galaxies (macrolensing) is an important issue (Belokurov, Evans, 2002) as is the gravitational light deflection caused by gravity waves (Kopeikin *et al.* 1999). Finally, the expansion of the universe has to be considered for light-sources at cosmic distances (larger than say a few 100 Mpc). To this end the BCRS metric has to be 'matched' to the cosmic metric that contains the scale factor $a(t)$ of the universe (Soffel, Klioner, 2003).

6. REFERENCES

Belokurov, V.A., & Evans, N.W. 2002, *Mon. Not. R. Astr.Soc.*, 331, 649

Brumberg, V.A., Klioner, S.A., & Kopejkin, S.M. 1990, in Inertial Coordinate System on the Sky, ed. J.H. Lieske & V.K. Abalakin (Dordrecht: Kluwer), 229

Hellings, R. W. 1986, *Astron. J.*, 91, 650

Klioner, S. A. 1989, Propagation of the Light in the Barycentric Reference System considering the Motion of the Gravitating Masses, Soobschch. Inst. Prik. Astron. No 6, p.21 (Communications of the Institute of Applied Astronomy, No 6, St. Petersburg, in Russian)

Klioner, S.A. 2000, in: Towards Models and Constants for Sub-Microarcsecond Astrometry, ed. by K.J. Johnston, D.D. McCarthy, B.J. Luzum, G.H. Kaplan, Proceedings of the IAU Colloquium 180, Washington D.C., 308

Klioner, S.A. 2002, in: GAIA: a European Space Project, ed. by O. Bienaymé, C. Turon, EAS Publications Series, Vol. 2 (Proceeding of Les Houches Summer School "GAIA: a European Space Project", 14-17 May 2001) (Les Ulis: EDP Sciences), 93

Klioner, S.A. 2003a, *Astron. J.*, 125, 1580–1597

Klioner, S.A. 2003b, *Astron. Astrophys.*, 404, 783

Klioner, S. A., Kopeikin, S. M. 1992, *Astron. J.*, 104, 897

Klioner, S. A., Peip, M. 2003, *Astron. Astrophys.*, submitted (preprint available as `http://arxiv.org/abs/astro-ph/0305204`)

Kopeikin, S. M., Mashhoon, B. 2002, *Physical Review* **D**, 65, ID 64025

Kopeikin, S. M., Schäfer, G. 1999, *Physical Review* **D**, 60, ID 124002

Kopeikin, S.M., Schäfer, G., Gwinn, C.R., & Eubanks, T.M. 1999, *Physical Review* **D**, 59, ID 084023

Soffel, M., Klioner, S.A., 2003, in preparation

Soffel, M., Klioner S.A., Petit, G. et al. 2003, *Astron. J.*, in press (preprint available as `http://arxiv.org/abs/astro-ph/0303376`)

THE LUNAR THEORY ELP2000 REVISITED

J. CHAPRONT and G. FRANCOU
SYRTE - Observatoire de Paris - UMR 8630/CNRS
61, avenue de l'Observatoire, 75014 Paris, France
e-mail: jean.chapront@obspm.fr

ABSTRACT. The construction of the complete lunar theory ELP goes back to the 1980s. Among all the components which form the solution, planetary perturbations contribute mainly to its deficiency. A new solution has been build that makes use of the planetary perturbations (MPP01) constructed recently by (Bidart 2000). After several transformations and tests, this new solution is called ELP/MPP02.
Fitting the constants and the reference frame, ELP/MPP02 has been extensively compared to various JPL ephemerides and mainly DE405/DE406 (Standish 1998) to test its accuracy on a short time interval of one century and on a long time interval covering several millennia. Compared to ELP, over a few centuries, a significant improvement of the precision - in particular on the radius vector - is put in evidence. On the long range, the planetary contributions with long periods are noticeably improved.
Taking advantage of the partials included in ELP, this new solution is fit directly to LLR observations. Our future ephemerides shall be based on this contribution using our LLR fits.

1. THE SOLUTION ELP

ELP is a semi-analytical solution for the orbital motion of the Moon. Its construction, under a complete form, containing all sensible perturbations, goes back to the 1980s. It is named ELP2000-82 (Chapront-Touzé, Chapront 1983). The main components of the solution includes:
• *The Main Problem.* It represents the motion of Earth, Moon and Sun where the Earth-Moon barycenter EMB is moving along a keplerian orbit; it includes partials with respect to various lunar and planetary parameters which are used when fitting to observations.
• *The Earth's figure perturbations* including the nutational motion of the Earth.
• *The direct and indirect planetary perturbations.* The direct perturbations are due to the action of the planets on the Earth; indirect perturbations are induced by the deviation of EMB from a keplerian orbit. Planetary perturbations contain in particular the secular motions of EMB (eccentricity and perihelion) and of the ecliptic. The motions of the planets come from VSOP82 (Bretagnon 1982).
• *The relativistic effects.*
• *The tidal perturbations.*
• *The Moon's figure perturbations and coupling with libration.*
The first version of ELP has not been fit directly to observations but via the JPL lunar ephemeris DE200-LE200. VSOP82 used the same source of comparisons and fits. A brief description of the various versions of ELP and derived ephemerides is given in Table 1.

Table 1. The different versions of ELP

Version	*Date*	*Fit*	*Characteristics*
ELP2000-82	1983	DE200	Planetary motions: VSOP82 (Bretagnon 1982)
ELP2000-85	1988	DE200	Secular motions of high degree n in time: t^n
ELP2000-82B	1996	DE245	Improved masses, gravitational parameters, tides etc...
ELP2000-96	1997	LLR	Numerical complements ρ_{245}
Lunar librations			Moon's lunar libration theory completed
ELP/MPP02	2002	LLR	Planetary motions VSOP2000 (Moisson 2000)

Before the present solution, our last version was ELP2000-96 obtained by adding numerical complements to ELP on the basis of the JPL ephemeris DE245; a complete analysis of Lunar Laser Ranging observations from 1972 till 1998 has been performed using this solution and the analytically completed Moon's theory of the lunar libration (Chapront et al. 1999).
ELP provides the polar coordinates σ (longitude V, latitude U and distance r) under the general formulation:

$$\sigma = \sum_{n\geq 0} t^n \sum_{i_1,i_2,...,i_p} A^{(n)}_{i_1,i_2,...,i_p} \times \sin\left(i_1\lambda_1 + i_2\lambda_2 + ... + i_p\lambda_p + \phi^{(n)}_{i_1,i_2,...,i_p}\right) \quad (1)$$

In the case of V one has to add to the previous formula the secular mean longitude $w_1 = w_1^{(0)} + w_1^{(1)}t + w_1^{(2)}t^2 + ...$ $A^{(n)}_{i_1,i_2,...,i_p}$ are numerical coefficients, $\phi^{(n)}_{i_1,i_2,...,i_p}$ are numerical phases and λ_j are literal arguments standing for polynomial functions of the time: $\lambda_j = \sum_{k\geq 0} \lambda_j^{(k)} t^k$. In the case of the Main Problem, we have also at our disposal the derivatives of the coefficients $A^{(n)}_{i_1,i_2,...,i_p}$ and the mean motions $\lambda_j^{(1)}$ with respect to several constants (sidereal mean motions of Moon and Sun, lunar and solar eccentricities, inclination, ratios of masses,...). The Main Problem depends on 4 arguments, D, F, l and l' (Delaunay's arguments). For Earth's figure perturbations, we add the argument $\zeta = w_1 + pt$, where p is the precession constant for J2000. For planetary perturbations the components λ_j are Delaunay's arguments, and planetary secular mean longitudes known from a planetary theory. The reference plane of the theory is the mean dynamical ecliptic at J2000.

2. A NEW SOLUTION ELP/MPP02

We knew that in ELP the main limitation in precision resulted from the computation of the series for direct and indirect planetary perturbations. A new solution for planetary perturbations in the orbital motion of the Moon has been elaborated by P. Bidart. It is named MPP01 and described in (Bidart 2000, 2001). It has been constructed within the framework of ELP solution and the perturbation method is inspired by Brown's lunar theory whose basic concepts are discussed in (Chapront-Touzé and Chapront 1980). The aim of MPP01 was to improve the accuracy taking advantage of two recent progresses: the availability of numerical tools able to handle very large Poisson series (Software GREGOIRE) and the appearance of a new semi-analytical planetary theory, VSOP2000 (Moisson 2000).

VSOP2000 is more precise than VSOP82 which has been used in ELP and introduces a recent set of planetary masses (IERS92). It contains formal developments similar to ELP: the planetary coordinates (osculating elements) are developed under the form of Poisson series as in (1). The numerical values of the coefficients depend on the masses but also on the values of the

osculating elements for a given epoch (J2000). These elements have not been obtained directly from a fit to observations but via a comparison of the analytical solution to the JPL ephemeris DE403. The angles are linear combinations of the planetary mean longitudes which have been derived with a better accuracy than in VSOP82. MPP01 takes advantage of this improvement, in particular in the integration process of arguments with long periods.

Fig 1. Longitude.

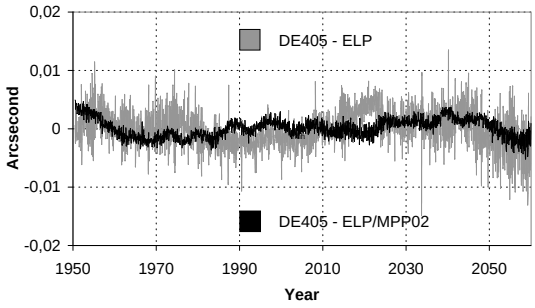

Fig 2. Latitude.

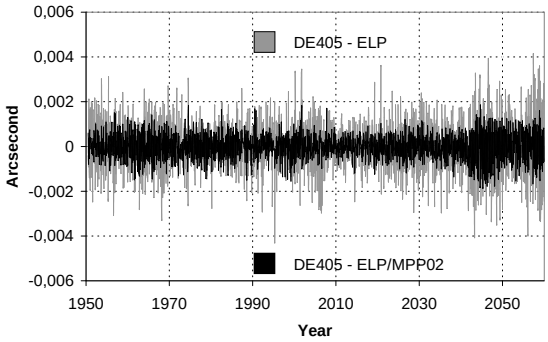

Fig 3. Distance.

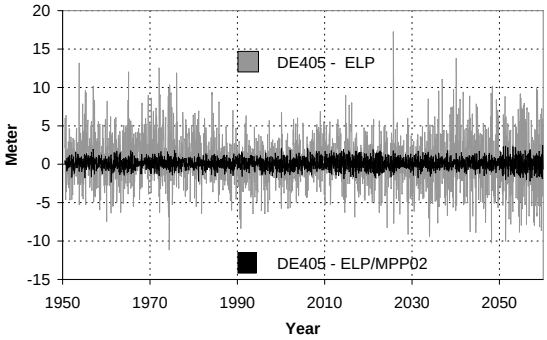

On the basis of MPP01 we have derived a new solution ELP/MPP02. Its planetary component MPP02 has the following characteristics:
• *Number of terms*: after various numerical tests, compared to MPP01, the number of terms has been diminished to reduce the round-off errors of large sums (for example, in longitude we kept 16000 arguments instead of 128000)
• *Moving perigee and plane of orbit*: we have used the original series used in ELP2000-82B, more precise than in MPP01.
• *Secular motions in lunar perigee, node and mean longitude*: we have used the original polynomials of ELP2000-82B in t, t^2, t^3, t^4 since Bidart's solution has been achieved only in t^2.
After fitting the constant to DE405 over one century $[+1950; +2060]$, we have made a comparison of the differences between ELP/MPP02 and DE406 on this time interval. Figs 1 to 3 illustrate this comparison. We observe in particular the sensible improvement of ELP/MPP02 (in dark) compared to the original solution ELP (in light).

3. A FIT TO LLR OBSERVATIONS

Fig 4. Longitude.

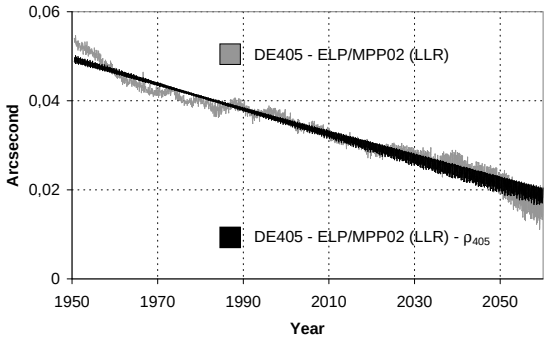

Fig 5. Latitude.

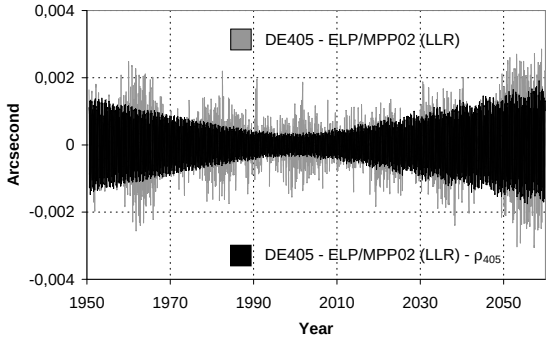

Fig 6. Distance.

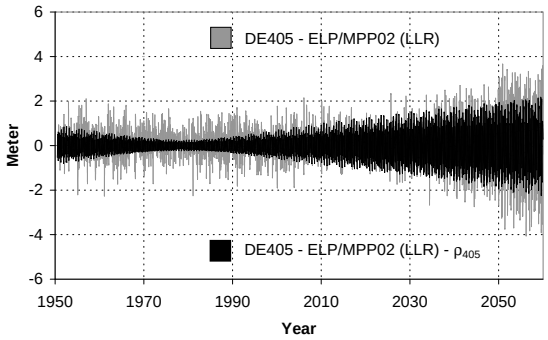

Following the same method as we have applied earlier with DE245 (Chapront et al. 1999) we build numerical complements with DE405 that we call ρ_{405} in such a manner that: DE405 = ELP/MPP02(405) + ρ_{405}, over the time span $[+1950; +2060]$. The notation ELP/MPP02(405) means than the constants are derived from the fit to DE405. This solution which is nothing else than DE405 is now compared to LLR observations. A new set of constants is provided with this comparison. We finally substitute in our analytical solution this new set, and we obtain the solution ELP/MPP02(LLR) which results from our fit to LLR observations. Adding the numerical complements ρ_{405} which are insensible to the change of constants at the millimeter level, the so-completed solution ELP/MPP02(LLR) + ρ_{405} keeps the precision of a numerical integration. Figs. 4, 5 and 6 show the comparison of these 2 solutions to DE405.
We see on Fig.4 an offset in the longitudes of about $0.''036$ which is due to a difference between the two reference frames (ELP/MPP02 and DE405). The slope which amounts to $0.025''$/century is within the estimated error on the mean motion in longitude. (Shelus et al. 2001) give an estimate of $0.015''$/century for this error. The discrepancies as large as 30 cm in distance in the mid period of laser observation show that, in spite of post-fit residuals of about 2 to 3 cm, part of the difference arises from the models and the determinations of various parameters (lunar and solar parameters, libration, positions of reflectors and stations, tidal coefficients,...).

4. A COMPARISON WITH DE406 OVER 6 MILLENNIA

In order to estimate the precision of the solution on a very long range we have made a comparison between ELP/MPP02(405) and DE406 over the long interval $[-3000; +2500]$. Figs 7 to 9 illustrate the crude differences (in light). If one wants to keep closer to DE406, we can compute a new solution ELP/MPP02* which is the same as ELP/MPP02 but with secular variations of the lunar arguments w_i (mean longitude, perigee and node) fitted on DE406, i.e.: $w_i^{(2)}t^2 + w_i^{(3)}t^3 + w_i^{(4)}t^4 + w_i^{(5)}t^5$. The determination of the polynomial coefficients $w_i^{(k)}$ is realized by a mean square fit.

Fig 7. Longitude.

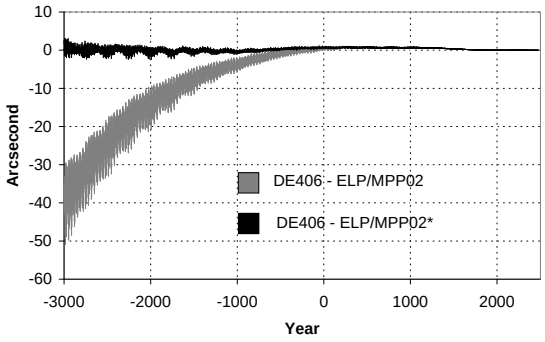

Fig 8. Latitude.

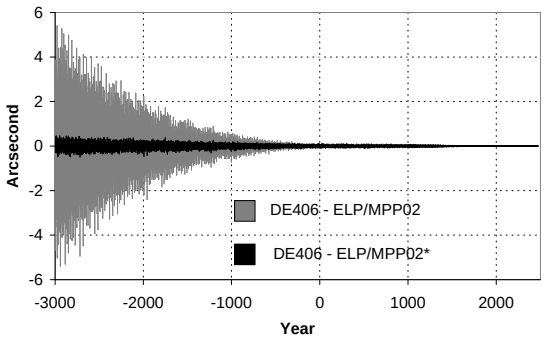

Fig 9. Distance.

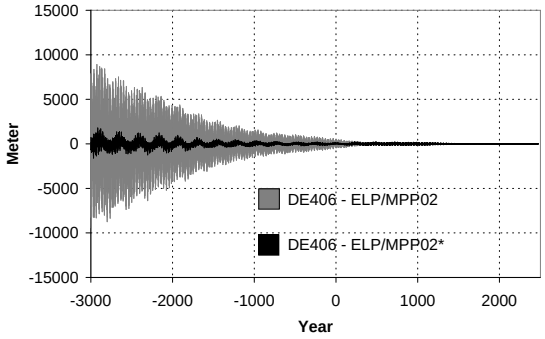

We obtain a noticeable reduction of the differences with DE406 (in dark). Indeed, these 'empirical corrections' are a fit rather than an improvement of the secular variations of the angles in the theory. Although DE406 and ELP/MPP02 are very close one should be aware of the uncertainty on secular acceleration in longitude which is very much larger than these empirical corrections. Besides such a fit absorbs the numerical drift of the numerical integration.

5. CONCLUSION

ELP/MPP02(LLR) whose constants are fit to LLR data is our new analytical version of ELP that replaces ELP2000-82B. Practically ELP/MPP02 is presented in form of Fourier series for the Main Problem and its partials plus Poisson series for perturbations to the Main Problem. Two sets of constants are provided as well as literal expressions for the arguments (Moon, Sun and Planets):

• Constants fit to LLR data for ELP/MPP02 (LLR);

• Constants fit to DE405 (one century around J2000) for ELP/MPP02(405).

When it is coupled to a solution for the lunar libration and other physical models, the new ephemeris ELP/MPP02(LLR) + ρ_{405} is used for the comparisons to LLR and the determination of various parameters: lunar and solar parameters, but also tidal acceleration, position of the dynamical reference frame, correction to the precession constant, libration parameters, position of the stations ...

A solution with secular correction to the lunar angles (ELP/MPP02*) 'reproduces' DE406 on the long range (6 millenia) within a few arcsecond.

6. REFERENCES

Bidart, P.: 2000, Les perturbations planétaires dans le mouvement orbital de la Lune, Thèse de Doctorat, Observatoire de Paris

Bidart, P.: 2001, MPP01, A new solution for planetary perturbations in the orbital motion of the Moon, *Astron. Astrophys.*, **366**, 351

Bretagnon, P.: 1982, Théorie du mouvement de l'ensemble des planètes, la solution VSOP82, *Astron. Astrophys.*, **114**, 278

Chapront, J., Chapront-Touzé, M. and Francou, G.: 1999, Determination of the lunar orbital and rotational parameters and of the ecliptic reference system orientation from LLR measurements and IERS data, *Astron. Astrophys.*, **343**, 624

Chapront-Touzé, M. and Chapront, J.: 1980, Les perturbation planétaires de la Lune, *Astron. Astrophys.*, **91**, 233

Chapront-Touzé, M. and Chapront, J.: 1983, The lunar ephemeris ELP2000,*Astron. Astrophys.*, **124**, 50

Moisson, X.: 2000, Intégration du mouvement des planètes dans le cadre de la relativité générale, Thèse de Doctorat, Observatoire de Paris

Shelus P., J., Ries, J., G., Williams J., G. and Dickey J. O.: 2001, A Summary of LLR Activity and Science Results, 12th International Workshop in Laser Ranging, Matera

Standish, E.M.: 1998, JPL Planetary and Lunar Ephemerides, DE405/LE405, IOM, 312.F-98-048, Pasadena

CROSS - IDENTIFICATION OF HIPPARCOS - 2MASS SECOND INCREMENTAL DATA RELEASE

G. DAMLJANOVIC [1], J. SOUCHAY [2]
[1] Astronomical Observatory
Volgina 7 , 11160 Belgrade, Yugoslavia
e-mail: gdamljanovic@aob.bg.ac.yu
[2] SYRTE/UMR8630 – CNRS, Observatoire de Paris
61 avenue de l'Observatoire, 75014 Paris, France
e-mail: Jean.Souchay@obspm.fr

ABSTRACT. This paper is in line with the current efforts to link large stellar catalogues, both in the visible and infrared, to the ICRF (International Celestial Reference Frame). We did the cross – identification between HIPPARCOS (HIgh Precision PARallax COllecting Satellite) and 2MASS (Two Micron All Sky Survey) and presented here the main results. It was found 37940 common stars, after selecting a rejection criterion, that we set to a 3σ value. Our cross-identification is more than 68.5% successful. There were 117955 HIPPARCOS stars, and 162195232 2MASS Second Incremental Data Release ($\sim$ 47% of the sky) ones in our basic selection. It means, the programme of 3σ criterion is adequate for cross – identification of new catalogues of millions of stars. After that, we calculated the standard error of unit weight of differences $\Delta\alpha$ and $\Delta\delta$, and it was close to $0.''10$, in good agreement with other results (Cutri *et al.* 2001).

1. INTRODUCTION

From 1997, the HIPPARCOS Catalogue (ESA 1997) is considered as the primary optical counterpart of the ICRF. After a decision of the IAU (International Astronomical Union) General Assembly in Kyoto 1997, the ICRF was adopted to materialize the ICRS (International Celestial Reference System) from the beginning of 1998. It is based on a catalogue of 608 compact radio sources (Ma *et al.* 1998) which are determined with an internal precision of 0.3 to 0.5 mas (milliarcsecond). It has been updated recently by the ICRF – Ext.1, which includes 59 new sources (IERS Annual report 1999).

The HIPPARCOS contains roughly 110 000 stars, brighter than magnitude 12, mostly range between $V = 7$ and $V = 9$, which is far too restricting nowadays when searching reference stars for astrometric calibration. The mean density is less than 3 stars/square degree, which is not enough to insure a suitable astrometric reduction in the case of observations carried out in small fields with CCD detectors (more precisely, for the reductions of observations of fainter stars). Therefore it is necessary to produce large stellar catalogues with fainter sources (in the visible and in the infrared) and linked to the ICRF. The HIPPARCOS stars positions and proper motions are bases of the optical frame HCRF (Hipparcos Celestial Reference Frame).

The HIPPARCOS Catalogue, as an optical frame, gives for each object, among a very large number of parameters, the position with an accuracy of the order of 1 mas at 1991.25 (the epoch of the catalogue), and the proper motions in $\mu_\alpha \cos\delta$ and μ_δ with a standard error of about 1 mas/yr.

Let us mention some features of the Tycho-2 Catalogue (Hog *et al.* 2000): it is an astrometric reference catalogue with positions at the precision of 60 mas for all the stars, proper motions with a 2.5 mas/yr accuracy, and two-colour photometric data for roughly 2.5 million brightest stars in the sky. About 4% stars are without proper motion data. The corresponding star density, which depends on the galactic latitude b is about 150 stars/sq.deg. for $b = 0^o$, 50 for $b = \pm 30^o$, and 25 for $b = \pm 90^o$. The limiting magnitude V is near 11.5 mag and the completeness reaches about 90 % .

The attention should be maintained of various recent catalogues which should help to the densification of the ICRF, not only at optical wavelengths, but also at other ones (infrared, radio, X, etc.). Some of them are available in that aim, such as the Tycho-2 Catalogue, the USNO CCD Astrograph Catalogue (UCAC), the 2MASS (infrared), DENIS (Deep Near Infrared Survey of the Southern Sky), etc. One of the most interesting projects is the 2MASS of the near infrared sky which is based on two highly automated 1.3 m telescopes for both hemispheres, equipped with a three channel camera to observe the sky simultaneously at J (1.25 microns), H (1.65 microns) and K_S (2.17 microns).

In this paper we perform the cross – identification of HIPPARCOS – 2MASS PSC stars. Our cross – identification results, based on the programme of 3σ criterion, are hopeful for similar jobs of the cross – identification of new big stellar catalogues. It is in accordance with lot of nowadays efforts to link large stellar catalogues to the ICRF.

2. THE 2MASS CATALOGUE

The 2MASS Second Incremental Data Release includes a Point Source Catalogue (PSC), with positions and photometry for 162213354 sources, an Extended Source Catalogue (XSC) with positions and photometry in the three survey band passes for 585056 objects and an Atlas Images (1897017 FITS images in the three survey bands). The 2MASS catalogue is a joint project between the University of Massachusetts and the Infrared Processing and Analysis Center California Institute of Technology (Cutri *et al.* 2001), with observing facilities at Mt. Hopkins – AZ (N $31^o40'50.''8$, W $110^o52'41.''3$, 2306 m elevation) for the northern and Cerro Tololo – Chile (S $30^o10'3.''7$, W $70^o48'18.''3$, 2171 m elevation) for the southern hemisphere. The 2MASS telescopes map the sky with overlapping strips (tiles), about 6^o in length (in δ direction) and $8.'5$ in width (in α direction) by using a freeze-frame scanning technique. They are operated by the Smithsonian Astrophysical Observatory (SAO) and the National Optical Astronomy Observatories (NOAO); the 2MASS is formed by the National Aeronautics and Space Administration (NASA) and the National Science Foundation (NSF).

The PSC of the 2MASS Second Incremental Data Release has been divided onto 49 right ascension segments, $0^h \leq \alpha < 24^h$, ordered by increasing declination within each segment. The data are covering 19681 square degrees, which means about 47 % of the sky. The relevant observations were carried out between 1997 June 7^{th} and 1999 February 20^{th} (329 northern and 239 southern nights with at least one photometric period). The northern 2MASS telescope began to observe in June 1997, and the southern one in March 1998. The PSC consists of brightness data in three survey bands and positions, without proper motions. The magnitude limits are: 15.8 mag for J band, 15.1 mag for H one, and 14.3 mag for K_S one. Each telescope is equipped with the three-channel camera, and each channel has got 256x256 array of HgCdTe detectors. The final 2MASS catalogues will contain about 470 million stars and 1.6 million galaxies. The positions are accurate to $< 0.''2$, and α and δ done for J2000 (each star has got

the epoch of observation). The PSC occupies a total of 49 GB (uncompressed data). Because of the very big amount of 2MASS data, it is necessary to use DVD – ROM, big hard disk, fast computer and other modern equipment. The positions of the 2MASS sources are correlated with the ACT or USNO-A optical catalogues. Note that positional associations do not mean necessarily identifications. The positions of 2MASS objects are tied to the ICRS via the ACT Reference Catalogue. Some positional solution may have a random walk as much as $1.''0$ from the ICRS frame. About 77% of the PSC objects have $|b| < 20^o$ (the majority of point sources are concentrated towards the Galactic plane).

3. THE POSITIONAL ERRORS OF STARS OF 2MASS PSC CATALOGUE

Some data from the ACT (Urban *et al.* 1998) or USNO-A catalogues are included in the 2MASS PSC records, but these are not identifications between the infrared and optical sources. These are only associations, and the optical associations for the 2MASS sources are found using a simple closest positional algorithm. The astrometric accuracy of 2MASS PSC is $< 0.''2$. It was reached via the comparison of the positions of stars in the PSC with those in the Tycho-2 and UCAC catalogues (which are not used in 2MASS position reconstruction). The accuracy of 2MASS positions is on line with the number and distribution of ACT astrometric reference stars in each tile. The ACT catalogue has got 988 758 stars to about $V = 11$ mag and with positional error $< 0.''03$. The tiles with few or poorly distributed reference stars have got bad astrometric solution and bigger discrepancy from the reference frame. Concerning the possible sources of 2MASS positions errors, let mention a relative sparsity of ACT reference stars near the Galactic poles, problems of observations/reductions near the Galactic center and near tile ends, etc.

In the Analysis part of the 2MASS Second Incremental Data Release Explanatory Supplement, three astrometric tests were done. They consist on a comparison of 2MASS positions with those given by the ACT catalogue (used in the reconstruction), with the Tycho-2 catalogue and with the UCAC catalogue, these two last ones having been released respectively just before and after the 2MASS Second Incremental Data Release. After the comparison to ACT Reference Catalogue positions and the analysis of $\Delta\alpha$ and $\Delta\delta$ of 2MASS the standard deviation was roughly $\sigma \approx 0.''11$, (slightly higher in δ and lower in α) and the mean differences could be rounded to $\approx 0.''0$. For some tiles, the number and distribution of ACT stars were insufficient (as reference stars during 2MASS data processing). In these specific cases, for which the reconstruction errors are typically larger, the USNOA catalogue was used. Note that because of the procedure, the 2MASS positional errors are small in the vicinity of ACT reference stars, but errors would grow in the intervals between them.

The Tycho-2 catalogue includes the same set of stars as those contained in the ACT. For the comparison only the set of new Tycho-2 stars which are supposed to be single, and whose proper motions data are available, have been retained (~ 1.5 million stars). From the 2MASS catalogues only stars detected in all three bands, with $J < 15.8$ mag, $H < 15.1$ mag and $K_S < 14.3$ mag were used. The position r.m.s. was $\sigma \approx 0.''18$.

The 2MASS positions comparison to the UCAC positions show residuals for a huge set of ~ 10 million stars in common with a brightness up to $V = 12.5$ mag. The agreement between 2MASS and UCAC is noticeably better than the equivalent one between 2MASS and Tycho-2, with a value of $\sigma \approx 0.''12$. The UCAC is the first release of the U.S. Naval Observatory CCD Astrograph Catalogue which contains most of the southern hemisphere stars with brightness up to $V = 16$ mag and a δ range between -90^o and -5^o. Therefore UCAC positions seem to be more accurate and with higher density than the Tycho-2 ones. The above results might point

out an inconsistency of UCAC with Tycho-2.

4. THE CROSS - IDENTIFICATION OF HIPPARCOS - 2MASS

The first step consists of carrying out HIPPARCOS - 2MASS cross - identification, after selecting a rejection criterion, that we set to a 3σ value. In the present paper we make the 2MASS PSC positions comparison with respect to the positions given by the HIPPARCOS Catalogue. The mean density of Hipparcos Catalogue is about 3 stars per sq.deg., while 2MASS density is about 8 242 stars per square degree (2 stars per square arc minute). Thanks to easy comparison, we did separately the cross - identification in each of 49 segments adopted for 2MASS, and our cross - identification programme made it only into 3^m long α respective segments (not across the all celestial Hipparcos sphere for each 2MASS star). Of course, we made a matrix with the information about the 3^m segments locations for the Hipparcos Catalogue. In that way, for a suitable limited Hipparcos zone of the sky, each 2MASS star was compared with some numbers of Hipparcos ones. The identification was considered as effective when the Hipparcos star could be coupled to only one 2MASS star within a 3σ vicinity in both coordinates (α and δ).

At the beginning of our cross - identification procedure, we tested our method inside a very small part of the sky including a few Hipparcos stars, just to check the quality of our results, and we ran our detection algorithm within the 49 above mentioned 2MASS segments. Some stars were without enough data and we removed these stars before beginning the cross-identification procedure. Therefore 18 122 stars, which represent about 0.01% of the 2MASS PSC were removed from this catalogue. In a similar way, 263 stars were removed from the Hipparcos Catalogue (about 0.22%), because of the absence of proper motion data. Finally, we had 117 955 Hipparcos stars.

For each star, we calculated the standard deviation σ both in the α direction and in the δ one, respectively σ_α and σ_δ, by using Hipparcos and 2MASS data. There were enough data to do it. The calculated value of σ_α (and σ_δ) depends of few parts, $\sigma_\alpha^2 = \sigma_{\alpha 1}^2 + \sigma_{\alpha 2}^2 + \sigma_{\alpha 3}^2 + ...$ (and $\sigma_\delta^2 = \sigma_{\delta 1}^2 + \sigma_{\delta 2}^2 + \sigma_{\delta 3}^2 + ...$). The values $\sigma_{\alpha 1}$ and $\sigma_{\delta 1}$ are on line with the standard errors of the Hipparcos positions, and calculated by using the Hipparcos data. The values $\sigma_{\alpha 2}$ and $\sigma_{\delta 2}$ are on line with the observational epochs difference between Hipparcos and 2MASS (both catalogues data) and the errors of proper motions $\mu_\alpha \cos\delta$ and μ_δ (from Hipparcos data). The values $\sigma_{\alpha 3}$ and $\sigma_{\delta 3}$ are on line with the position error ellipse, and calculated by using the 2MASS data. The position error ellipse 2MASS data have: major axis ($2a$), minor axis ($2b$), and position angle (β). The position angle is in degrees, with the zero point in the northern direction N and via the eastern E one (of the error ellipse major axis). It was necessary that $\sigma_{\alpha 1}$ and $\sigma_{\alpha 3}$ ($\sigma_{\delta 1}$ and $\sigma_{\delta 3}$) are consistent between each other, and because of it we calculated the values of the standard error ellipse in the α direction

$$\sigma_{\alpha 3} = \left[x'^2 + y'^2\right]^{1/2} = \frac{ab}{\left[(a\cos\beta)^2 + (b\sin\beta)^2\right]^{1/2}} \qquad (1)$$

and in the δ one

$$\sigma_{\delta 3} = \left[x^2 + y^2\right]^{1/2} = \frac{ab}{\left[(a\sin\beta)^2 + (b\cos\beta)^2\right]^{1/2}} \qquad (2).$$

We did it by using the next formulas (determined from the ellipse formula which is done in rectangular plane coordinates):

$$x' = \frac{ab\sin\beta}{\left[(a\cos\beta)^2 + (b\sin\beta)^2\right]^{1/2}} \quad (3)$$

$$y' = \frac{-ab\cos\beta}{\left[(a\cos\beta)^2 + (b\sin\beta)^2\right]^{1/2}} \quad (4)$$

$$x = \frac{ab\cos\beta}{\left[(a\sin\beta)^2 + (b\cos\beta)^2\right]^{1/2}} \quad (5)$$

$$y = \frac{ab\sin\beta}{\left[(a\sin\beta)^2 + (b\cos\beta)^2\right]^{1/2}} \quad (6),$$

where $(x/a)^2 + (y/b)^2 = 1$ with $x = r\cos\beta$, $y = r\sin\beta$, $x' = r'\sin\beta$ and $y' = -r'\cos\beta$. The star is the coordinate origin of mentioned rectangular plane which is the tangent plane of the sphere. The value r is the distance between the star and the cross - point of the star's error ellipse with major axis; the cross - point has got the coordinates x and y. The value r' is the same, but with minor axis; the coordinates of that cross - point are x' and y'. The directions r and r' have got 90^o between each other. We get the Eq. (1), Eq. (2), Eq. (3), Eq. (4), Eq. (5) and Eq. (6) after a few trigonometric transformations.

The epoch of Hipparcos observations is 1991.25, and each star of 2MASS PSC has its own epoch of observation. Because of it, it is necessary to take into account the standard error rate for the proper motions influence by using the values of $\mu_\alpha\cos\delta = \mu_{\alpha*}$, μ_δ and the epoch differences t (in years). Therefore, the positions in both catalogues are on line with J2000.0 epoch. It means, before carrying out the cross - identification procedure by using $3\sigma_\alpha$ rejection threshold in the α direction and $3\sigma_\delta$ one in the δ one, we took into account the changes of the Hipparcos coordinates α_H and δ_H due to the epoch differences t (in years) by using the Hipparcos proper motions $\mu_{\alpha*}$ and μ_δ, $\alpha_{Hipp} = \alpha_H + \mu_{\alpha*}t/\cos\delta$ and $\delta_{Hipp} = \delta_H + \mu_\delta t$, where α_{Hipp} and δ_{Hipp} are at the epoch of 2MASS observations. Finally, we did the cross - identification of Hipparcos - 2MASS, and our cross - identification procedure identifies the common star if its position satisfies
$\alpha_{Hipp} - \alpha_{2MASS} = \Delta\alpha < 3\sigma_\alpha$ and
$\delta_{Hipp} - \delta_{2MASS} = \Delta\delta < 3\sigma_\delta$.

Following this principle we found 37 940 common stars, which represents about 32.2% of the 117 955 Hipparcos stars in our basic selection. Because of the fact that the 2MASS Second Incremental Data Release covers about 47% of the sky, this means that our cross - identification procedure is more than 68.5% successful. At present, one of the reasons for $100\% - 68.5\% = 31.5\%$ cases is the systematic part of σ_α (and σ_δ) which we did not know at the beginning of our cross - identification procedure. If we suppose that the the systematic error between HIPPARCOS and 2MASS coordinates is less than $0.''1$ (in line with our preliminary investigations about the systematic discrepancies of HIPPARCOS-2MASS coordinates), and put it into our 3σ programme, we can reach near 80 % of common stars. Another reason is that the 2MASS PSC Second Incremental Data Release covers 47% of the sky. Some of the stars are not presented in both catalogues, but only in one of them. We removed 18122 stars from the 2MASS PSC and 263 stars from the HIPPARCOS because these stars were without enough data for our programme, etc.

Our set is divided into 19 572 common stars with $\delta \geq 0^o$ (northern hemisphere) and 18 368 ones with $\delta < 0^o$ (southern one). As a total, only two unsuccessful cross – identifications (of

37 940 common stars) have been found. Each of the Hipparcos stars H16658 and H85045 can be associated with two 2MASS objects. In the Hipparcos Catalogue, the star H16658 is noted as a single star, but the star H85045 is noted as a double star (WDS17229+1628, J1248 AB). From our results, both H16658 and H85045 are close double stars, or maybe the star H16658 is not double, but there is another one with close coordinates. During the next step of our investigations we need to include more data (the magnitude, for example) to solve these cases even there are only two cases for now.

5. CONCLUSIONS

In this paper, only two unsuccessful cross - identifications of 37940 detected common stars have been found. We conclude that these two cases are close double stars or just near each other on the sphere: H85045 is already marked as a double star (WDS17229+1628), H16658 is marked as the single star in the Hipparcos Catalogue. In the future, for these kinds of cases we are going to include the cross – identification part with photometric data into 3σ criterion. If we compare any two catalogues with hundreds millions stars each of them and if there are many unsuccessful (astrometrical) cross - identification cases, it is good to create the cross - identification part with photometric data to solve them.

The cross – identification of HIPPARCOS – 2MASS stars are presented by using our programme based on the 3σ criterion and the information of the positions of stars, the proper motions, etc. It is on line with the similar actions about the cross – identifications of new catalogues of millions stars. It is the part of nowadays efforts to link big stellar catalogues (the visible and infrared ones) to the ICRF.

Acknowledgements

This publication makes use of data products from the Two Micron All Sky Survey, which is a joint project of the University of Massachusetts and the Infrared Processing and Analysis Center/California Institute of Technology, funded by the National Aeronautics and Space Administration and the National Science Foundation.

6. REFERENCES

Cutri, R. M., Skrutskie, M. F., Van Dyk, S., Chester, T., Evans, T., Fowler, J., Gizis, J., Howard, E., Huchra, J., Jarrett, T., Kopan, E. L., Kirkpatrick, J. D., Light, R. M., Marsh, K. A., McCallon, H., Schneider, S., Stiening, R., Sykes, M., Weinberg, M., Wheaton, W. A., Wheelock, S., 2001, Explanatory Supplement to the 2MASS Second Incremental Data Release, University of Massachusetts and the Infrared Processing and Analysis Center/California Institute of Technology, NASA and NSF.

ESA, 1997, The Hipparcos and Tycho Catalogues, ESA SP - 1200.

Hog, E., Fabricius, C., Makarov, V. V., Urban, S., Corbin, T., Wycoff, G., Bastian, U., Schwekendiek, P., Wicenec, A., 2000, The Tycho - 2 Catalogue, Copenhagen.

International Earth Rotation Service (IERS), 1999, Annual Report 1999, Observatoire de Paris.

Ma, C. *et al.*, 1998, *Astron. J.*, 116, p. 516.

Urban, S. E., Corbin, T. E., Wycoff, G. L., 1998, *AJ* 115, p. 2161.

HIPPARCOS PROPER-MOTION SYSTEM WITH RESPECT TO FK5 AND SPM 2.0 SYSTEMS

Z. ZHU
Astronomical Department, Nanjing University
Nanjing 210093, China
e-mail: zhuzi@nju.edu.cn

ABSTRACT. Carrying out a kinematical analysis of the Galaxy for proper-motion systems of the FK5 and Hipparcos, a large difference in proper motions between two systems is found, even if the precessional correction to the FK5 system has been considered. Comparing the PPM and ACRS proper motions, which are constructed on the FK5 system, with those of the Hipparcos, an interiorly nonrigid rotation existing in the FK5 proper-motion system is detected. Proper-motion differences between the FK5 and Hipparcos systems cannot be explained by the constant of the FK5 precessional correction, which is given by the VLBI and LLR observations. Analyzing proper motions of the Hipparcos and SPM 2.0 systems, the component ω_y of the rotational vector of the SPM 2.0 proper-motion system related to the Hipparcos is obtained, that is almost as large as twice 0.25 mas yr^{-1} for the uncertainty of the Hipparcos inertiality.

1. INTRODUCTION

More than 100,000 stars were measured by the Hipparcos astrometric satellite. The capability of accurate wide-angle measurements over the whole sky of the Hipparcos mission has ensured that the system of stellar positions, proper motions, and parallaxes is characterized by a high degree of internal consistency. The positions and proper motions in the Hipparcos Catalogue define a reference frame which is likely to be accurate, on a global scale, to about 0.1 mas at the epoch J1991.25 and 0.1 mas yr^{-1}. It is not doubtful that the system can be considered to be free of regional errors, when we compare it with any existing global catalogue. Considering its observations were made in space and its high internal precision of about 1 mas for positions and 1 mas yr^{-1} for proper motions, there is no evidence to suspect the color- and magnitude-dependent systematics in the Hipparcos system to a significant level. Because of the favorable internal systematics, the Hipparcos Catalogue provides us the best optical materialization to analyze internal systematic errors of other catalogues.

The Hipparcos data were preliminarily adjusted to the FK5 system, which was formally based on the mean equator and dynamical equinox of J2000.0. The final catalogue was subsequently linked to the International Celestial Reference System (ICRS), which was defined and realized by a set of radio sources observed by the VLBI technique. The estimated uncertainty of the Hipparcos link corresponds to a standard error of 0.6 mas in the alignment of the axes at the catalogue epoch J1991.25 and 0.25 mas yr^{-1} in the rate of rotation of the system with respect to distant extragalactic objects (Kovalevsky et al. 1997).

On the other hand, the FK5 has been constructed by applying dynamical as well as kinematical concepts. In order to tie the FK5 system to an inertial coordinate system, a constant of the lunisolar precessional correction and a correction of the fictitious motion of the equinox should be applied to the FK5 proper-motion system. Several years observations by the VLBI and LLR have given a coincident value of the precessional correction $\Delta p = -3.0 \pm 0.2$ mas yr^{-1}(Charlot et al. 1995, Chapront et al. 1999, Fukushima 2000). If one considers the FK5 system, in the global sense, as a rigid frame ignoring its regional errors, the proper-motion system should differ from the ICRS only by the lunisolar precessional correction to Newcomb's value and by the fictitious motion of the equinox.

Properties of the proper-motion system play a critical role in the evaluation of the galactic kinematics via the proper-motion data of stars, as well as in the characterization of the inertiality of the coordinate system itself. In order to understand the overall properties of proper motions of the Hipparcos system and examine the systematic errors in proper motions of other catalogues, we concentrate our present work on proper-motion analysis.

2. KINEMATICAL ANALYSIS FOR PROPER-MOTION SYSTEMS

The kinematical parameters of the Galaxy can be statistically derived from the stellar proper motions in an inertial coordinate system. Analyzing proper-motion data from the ACRS Part1 catalogue that is in the FK5 system, Miyamoto & Sôma (1993) have studied the local kinematics from the galactic K-M giants. They have derived the kinematic parameters of the conventional Oort constants A and B, yielded the precessional correction $\Delta p = -2.67 \pm 0.28$ mas yr^{-1} and the correction of the fictitious motion of the equinox $\Delta e + \Delta\lambda = -1.16 \pm 0.26$ mas yr^{-1} to the FK5 system. Using the proper motions from the ACRS catalogue, Miyamoto, Sôma, and Yoshizawa (1993) have investigated further the kinematics for the young O-B stars.

Based on the Hipparcos proper motions of stars, we have analyzed the galactic kinematics for the late type K-M giants and the young O-B5 stars (Miyamoto & Zhu 1998, Zhu & Yang 1999, Zhu 2000a). The Oort constants A and B, derived from the ACRS and Hipparcos proper motions, are listed in Table 1, where the rotational velocities of the Galaxy V_0 are given at the galactic distance of the Sun $R_0 = 8.5$ kpc. It is obviously shown that the rotational velocities derived from the Hipparcos proper motions are more large than those derived from the conventional FK5 proper motions. For the K-M giants, the difference of the rotational speeds ΔV_0 is as large as 70 km s^{-1}, while the velocity difference for the O-B stars reaches to 50 km s^{-1}.

To inspect the systematic difference between the two proper-motion systems, we have further analyzed the proper-motion differences between the ACRS Part 1 and the Hipparcos Catalogue for about 24,000 K-M giants. Prior to making the proper- motion differences $\Delta\mu_\ell^* = (\mu_\ell^*)_{ACRS} - (\mu_\ell^*)_{HIP}$, the precessional correction and the equinoctial motion correction are applied to the ACRS proper motions. According to the classical Oort-Lindblad model for the galactic differential rotation, we have the following equation

$$\kappa\Delta\mu_\ell^* = r^{-1}(\Delta S_1 \sin\ell - \Delta S_2 \cos\ell) + (\Delta A \cos 2\ell + \Delta B)\cos b, \qquad (1)$$

where $\kappa = 4.74047$ is the conversion factor of units and r is the heliocentric distance of the star; S_1 and S_2 are the components of the local solar motion toward the galactic center and in the direction of the galactic rotation.

Applying the least squares to the equation, we found

$$\Delta S_1 = -0.12 \pm 0.20 \ \text{km s}^{-1} \ , \quad \Delta S_2 = -0.13 \pm 0.21 \ \text{km s}^{-1},$$
$$\Delta A = -0.61 \pm 0.15 \ \text{mas yr}^{-1}, \quad \Delta B = 1.03 \pm 0.10 \ \text{mas yr}^{-1}.$$

Table 1: Parameters of the galactic kinematics derived from the ACRS and Hipparcos proper motions. The rotational velocities V_0 are given at the galactic distance of the Sun $R_0 = 8.5$ kpc.

Proper motions	A (mas yr^{-1})	B (mas yr^{-1})	V_0 (km s^{-1})
ACRS gK-gM	2.63±0.12	−1.76±0.10	177.1±6.2
ACRS O-B	2.85±0.19	−2.60±0.15	219.9±9.8
Hipparcos gK-gM	3.27±0.14	−2.93±0.10	249.6±7.0
Hipparcos O-B	3.39±0.24	−3.28±0.18	268.7±11.9

The difference in the galactic rotation is thus obtained as $\Delta V_0 = -\ 66.1 \pm 7.2$ km s^{-1}. The present solution coincides well with the large difference in the galactic rotation individually derived from the ACRS proper motions and from the Hipparcos proper motions.

3. REGIONAL ERRORS IN THE PPM AND ACRS PROPER MOTIONS

As the star density in the FK5 is so low, we selected stars from the PPM Star Catalogue and the Astrographic Catalog Reference Stars (ACRS) Part 1 in the present analysis, and compared their proper motions with the Hipparcos system. The PPM and ACRS are all sky catalogues constructed on the FK5 system. The PPM catalogue contains 93,772 Hipparcos stars, while the ACRS Part1 includes 83,188 stars common to the Hipparcos Catalogue. For a general description of the PPM and ACRS catalogues, see Röser (1994).

The regional errors of proper motions were derived in such a way: first, we divided the whole celestial sphere into 36°×18° cells which run from 0° to 360° in galactic longitude and from −90° to +90° in galactic latitude. Each cell is 10°×10° in size, containing from several tens to hundreds of stars depending on the galactic latitude zonal.Then, in the galactic coordinate system, the mean differences of proper motions of stars in each cell were calculated for the two coordinates ($\Delta\mu_\ell^*$, $\Delta\mu_b$), in sense of considered catalogue minus Hipparcos. Note that stars with large residuals of proper motions were removed from the calculation (>2.6 σ). The vector diagram in Figure 1 shows distributions of the proper-motion differences in the galactic coordinate system, where the top panel gives relative errors in proper motions between the PPM and Hipparcos catalogues, and the bottom panel demonstrates those between the ACRS and Hipparcos.

Regional differences of the PPM and ACRS related to Hipparcos exhibit a similar distribution over the whole sky and appear to have alike systematics. But quantitatively, they are obviously inconsistent for the same individual region, even if both catalogues were aligned to the same FK5 system. This is probably due both to their own localized errors of proper motions existing in the PPM and ACRS catalogues and to different accuracies of the alignments to the FK5 system. Therefore, these regional errors of the PPM and ACRS cannot be fully recognized as the representation of local errors of the FK5 itself. Figure 1 shows remarkably large residual velocities from both the PPM and ACRS catalogues, which are mainly around the axis from the south celestial pole (SCP) to the north celestial pole (NCP).This rotation of residual velocities in the southern hemisphere is more pronounced than the northern part. From the kinematic point of view, such a structure of the velocity distribution will lead to decreasing the determined absolute values of Oort constants A and B of the galactic kinematics. That is one of the reason why we have found a remarkably larger galactic rotation from the Hipparcos proper motions than that from the ACRS proper motions.

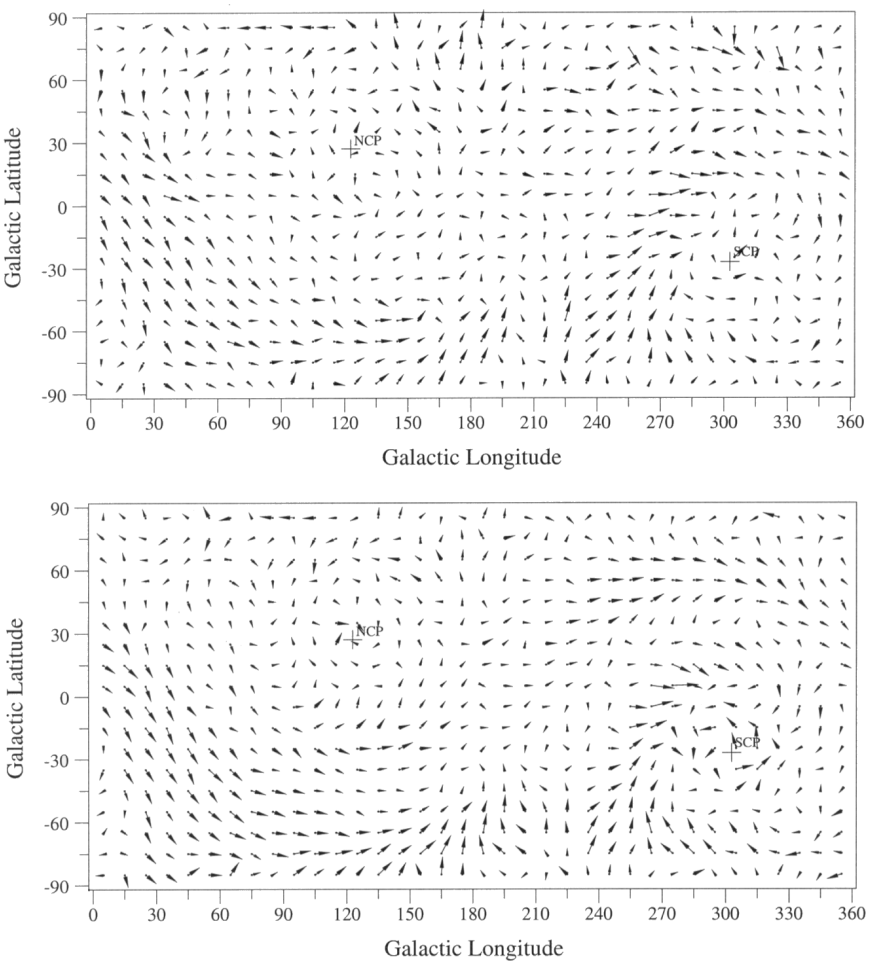

Figure 1: Regional differences of proper motions between the PPM and Hipparcos in sense PPM−Hipparcos (*top panel*), and between the ACRS and Hipparcos in sense ACRS−Hipparcos (*bottom panel*), in the galactic coordinate system .

4. MAGNITUDE AND COLOR EQUATIONS IN PROPER MOTIONS

In our previous work, we have analyzed the magnitude- and color-dependent differences in proper motions between the PPM and Hipparcos, and between the ACRS and Hipparcos (Zhu 2000b). A strong magnitude-dependent systematics were found both in the PPM and ACRS proper-motion system. Especially for the component in $\Delta\mu_\alpha^*$, it increases rapidly at the fainter magnitude and behaves more strongly for the ACRS proper motions (see Figure 6 in Zhu 2000b). The color-dependent systematics shows a similar variation in proper-motion differences for both PPM−Hipparcos and ACRS−Hipparcos (see Figure 7 in Zhu 2000b). Stars with the lowest color index exhibit more large systematics in their proper-motion differences.

From the proper-motion comparison between the PPM and Hipparcos, and between the ACRS and Hipparcos, we found clear systematic differences of proper motions depended both on magnitudes and colors. The PPM and ACRS catalogues suffer a quite similar fashion in their color and magnitude equations with respect to the Hipparcos proper-motion system.

The Southern Proper Motion (SPM) Program is the southern-sky complement to the Northern Proper Motion (NPM) Program (Platais et al. 1998a). The SPM 2.0 Catalog contains 321,608 stars (9,386 single stars common to Hipparcos) between declinations of $-22°$ and $-43°$ observed in 156 fields. The absolute proper motions were measured on an inertial reference system defined by faint galaxies. Analyzing the proper-motion differences related to the Hipparcos,

Table 2: Global rotation derived from FK5, PPM, ACRS, and SPM 2.0, relative to the Hipparcos proper-motion system. The units are in mas yr^{-1}.

Component	FK5−HIP	PPM−HIP	ACRS−HIP	SPM−HIP
ω_x	-0.30 ± 0.10	-0.67 ± 0.03	-0.42 ± 0.10	-0.05 ± 0.18
ω_y	$+0.60\pm0.10$	$+0.84\pm0.03$	$+0.56\pm0.10$	-0.49 ± 0.15
ω_z	$+0.70\pm0.10$	$+0.18\pm0.03$	-0.08 ± 0.10	$+0.15\pm0.16$

we found that there are neither strong systematics nor large regional errors existing in the SPM 2.0 Catalog (Zhu 2001), except a common shift $< \Delta\mu_\delta > = 0.46$ mas yr^{-1} between the two systems.

5. GLOBAL ROTATION

The basic relation of the global rotation between two proper-motion systems can be described by a pure rigid-body rotation:

$$\begin{aligned} \Delta\mu^*_\alpha &= -\omega_x \sin\delta\cos\alpha - \omega_y \sin\delta\sin\alpha + \omega_z\cos\delta, \\ \Delta\mu_\delta &= +\omega_x \sin\alpha - \omega_y\cos\alpha. \end{aligned} \tag{2}$$

Where the vector $\boldsymbol{\omega} = (\omega_x, \omega_y, \omega_z)$ represents the rotational difference between the two frames, taken in sense of considered catalogue minus Hipparcos. By means of an overall pattern comparison of the FK5 proper-motion system with Hipparcos via PPM and ACRS proper-motion data, we have determined the vectors of the global rotation between the PPM and Hipparcos, and between the ACRS and Hipparcos, proper-motion systems (Zhu & Yang 1999). A later work by Mignard & Frœschlè (2000) gave the global rotation between the FK5 and Hipparcos, and between the PPM and Hipparcos. Comparing the SPM 2.0 system with the Hipparcos, the rotational difference between the two proper-motion systems was derived (Zhu 2001). We collect all the results listed in Table 2.

The precessional correction Δp represents an additional systematic error of the FK5 proper-motion system to an inertial coordinate system, thus the FK5 proper-motion system should differ from the Hipparcos only by a precessional correction and by a correction of the fictitious motion of the equinox. Taking the precessional correction $\Delta p = -3.0 \pm 0.2$ mas yr^{-1} into account, which is independently determined by the VLBI and LLR, and accepting $\Delta e + \Delta\lambda = -1.16 \pm 0.26$ mas yr^{-1} for the correction of the fictitious motion of the equinox proposed by Miyamoto & Sôma (1993), we cannot find a consistent explanation directly from solutions in Table 2 (FK5−HIP, PPM−HIP, ACRS−HIP).

Both the SPM 2.0 and Hipparcos proper-motion systems are constructed on the ICRS. Ignoring the internal systematic errors affecting the SPM 2.0 proper-motion system and neglecting the remaining rotations of the SPM and Hipparcos systems with respect to the ICRS, then the proper-motion system of the SPM 2.0 should coincide with the Hipparcos proper-motion system. The rotational vector for the SPM 2.0 proper motions with respect to the Hipparcos shows that the two components ω_x and ω_z are apparently less than the value of 0.25 mas yr^{-1} for the uncertainty of the Hipparcos inertiality, while the component ω_y is almost as large as twice that value. It is noticed that our result is in a good agreement for all three components with the mean values of the residual spin components derived from the mean-per-field SPM-data solution

using a recalibrated magnitude equation by Platais et al. (1998b).

6. CONCLUSION

On the basis of the Hipparcos data, whose system is believed to be quasi-inertial to within ± 0.25 mas yr^{-1} and to represent an internally consistent reference frame, we have performed analysis on the FK5 proper-motion system via two large astrometric catalogues, the PPM and ACRS catalogues, both constructed on the FK5 system. The regional differences of proper motions between the PPM and Hipparcos, and between the ACRS and Hipparcos, show a remarkably large residual velocity around the axis from the south celestial pole to the north celestial pole. The regional differences on the southern hemisphere are larger than those on the northern part. Considering the magnitude- and color-dependent pattern of the proper-motion difference, we have found that the PPM and ACRS catalogues suffer a quite similar fashion in their color and magnitude equations with respect to the Hipparcos proper-motion system. These reflect, at least qualitatively, the internal inconsistency of the FK5 proper-motion system. It implies that the FK5 proper-motion system is practically interiorly nonrigid, which rotates differentially from region to region, from magnitude to magnitude, and from spectral type to spectral type.

The global rotation of proper motions between the PPM and Hipparcos, and between the ACRS and Hipparcos, shows a large offset compared with the correction of the precessional constant determined by the VLBI and LLR, especially for the components of ω_x and ω_z. It could be largely due to the internal nonrigid feature of the FK5 proper-motion system and to the lower accuracy of alignment of the PPM or ACRS system to the system of the FK5.

From the proper-motion comparison between the SPM 2.0 and Hipparcos catalogues, we found that the regional differences of the SPM 2.0 proper motions exhibit neither strong systematics nor large regional errors. The global rotation related to the Hipparcos frame is slower than 0.25 mas yr^{-1} except the component along the y-axis.

Acknowledgments This work was supported by the National Natural Science Foundation of China (NSFC).

7. REFERENCES

Chapront, J., Chapront-Touzé, M., & Francou, G. 1999, *Astron. Astrophys.*, 343, 624
Charlot, P., et al. 1995, *Astron. J.*, 109, 418
Fukushima, T. 2000, in IAU Coll. 180, ed. J. Kenneth et al. (Washington DC: USNO), 417
Kovalevsky, J., et al. 1997, *Astron. Astrophys.*, 304, 189
Mignard, F., Frœschlè, M. 2000, *Astron. Astrophys.*, 354, 732
Miyamoto, M., Sôma, M. 1993, *Astron. J.*, 105, 691
Miyamoto, M., Sôma, M., & Yoshizawa, M. 1993, *Astron. J.*, 105, 2138
Miyamoto, M., Zhu, Z. 1998, *Astron. J.*, 115, 1483
Platais, I., et al. 1998a, *Astron. J.*, 116, 2556
Platais, I., et al. 1998b, *Astron. Astrophys.*, 331, 1119
Röser, S. 1994, in Astronomy from Wide-Field Imaging, ed. H. T. MacGillivray et al. (Dordrecht: Kluwer), 261
Zhu, Z., Yang, T. G. 1999, *Astron. J.*, 117, 1103
Zhu, Z. 2000a, *Publ. Astron. Soc. Japan*, 52, 1133
Zhu, Z. 2000b, *Publ. Astron. Soc. Pacific*, 112, 1103
Zhu, Z. 2001, *Publ. Astron. Soc. Japan*, 53, L33

REFINEMENT OF LINKING OPTICAL-RADIO REFERENCE FRAMES ON THE BASIS OF THE INTERNATIONAL JOINT PROJECT BETWEEN COLLABORATIVE OBSERVATORIES

Z. ASLAN[3], R. GUMEROV[4], E. HAMITOV[3] W. JIN[2], N. MAIGUROVA[1], G. PINIGIN[1], Yu. PROTSYUK[1], A. SHULGA[1], Z. TANG[2], S. WANG[2]

1) Nikolaev Astronomical Observatory,
Observatorna 1, Nikolaev, 54030 UKRAINE;
e-mail: dir@mao.nikolaev.ua; pinigin@mao.nikolaev.ua;
2) Shanghai Astronomical Observatory,
Nandan Road 80, Shanghai, 200030 CHINA;
e-mail: zhtang@center.shao.ac.cn; jwj@center.shao.ac.cn;
3) Turkish National Observatory TUG,
Antalya, 07058 TURKEY;
e-mail: aslan@tug.tug.tubitak.gov.tr;
4) Kazan State University,
Kremlevskaya 18, Kazan, 420008 RUSSIA;
e-mail: Rustem.Gumerov@ksu.ru

ABSTRACT. Results of the Joint Project between observatories from China, Turkey, Russia and Ukraine on improvement of linking optical and radio reference systems are discussed. The 300 extragalactic radio sources (ERS) observation program is extended at the expense owing to the increase of observation in a southern hemisphere up to -40^0 declinations. The stars from catalogues USNO-A2.0 and UCAC1 were used as reference one. The analysis of ERS position (optical – radio) differences in observations with different telescopes showed about ±40mas accuracy. The observations of more than 100 ERS made with 1.5m RTT150 in Turkey and two telescopes in China were used. The intermediate internal estimation of angles between optical and radio systems on the base of ERS coordinates selected in the -40^0 +75^0 declinations zone was made: ω_x =7±24, ω_y =-3±24, ω_{zy} = -12 ± 21 (s.e.) mas.

1. INTRODUCTION

- Due to the epoch difference between optical and radio reference frames it is very important for modern astrometry to refine frame's link by different methods and instruments [1].
- The task of collaborated programme (Joint Project) between astronomical observatories from China, Turkey, Russia and Ukraine is the refinement of optical / radio linking [2,3].
- It will be appropriate for enhancing of optical-radio link accuracy. It can be shown that rotation parameter's precision of about 5 mas will be reached by using of 300 extragalactic radio sources (ERS) with positional precision not worse than 20 mas [3].

2. PROGRAM AND INSTRUMENTATION

The final collaborated program list includes about 300 ERS for declination zone from -40^o to $+90^o$. There are about 200 ERS optical counterparts in the northern sky and 100 ERS in the southern sky. At present several CCD telescopes are used by collaborated observatories for the Joint Project:

- Nikolaev astronomical observatory (Ukraine): AMC - Axial meridian circle (180,2480) and Zone astrograph (160,2044) of the Nikolaev astronomical observatory equipped with the similar CCDs ISD017A (1040x1160, 16 x 16 mkm, $1.''6$/pix);
- Kazan state university (Russia) and Turkish national observatory (Turkey): RTT150 – Russian-Turkish Telescope (1500,11600) of the Kazan state university installed in Turkey (TUG) for joint using. Right now it is equipped with the CCD ST-8 (1530 x 1020, 9 x 9 mkm, $0.''16$/pix);
- Shanghai astronomical observatory (China): Yunnan observatory 1m telescope (FOV $6'.5$x$6'.5$, focal length 13m, scale 0.024mm/pixel and $0.''3737$/pixel); Beijing astronomical observatory 2.16m telescope (FOV $10'$x$10'$, focal length 13m, scale 0.015mm/pixel and $0.''3$/pixel).

3. OBSERVATION AND REDUCTION

3.1. *Reduction Methods*

Reduction of the CCD images with software including flat field correction, digital image filtration, identification of star-like objects, display of the images and calculation of star-like objects' CCD coordinates was made. It is possible to operate with CCD fields made in stare and drift-scan modes [4].

Positions of the ERS optical counterparts were obtained by CCD direct imaging on the collaborated telescopes, using the secondary reference star positions from the catalogues USNO-A2.0 and UCAC1.

For an accurate reduction by small CCD fields with enough number of secondary reference stars it was decided to use the compiled catalogue as a reference one that was made of some new CCD catalogues [5]. Creation of compiled catalogue with stars of $12\text{-}15^m$ for about 300 ERS fields in declination zone -20^0 $+90^0$ is in progress from 2001. Seven separate catalogues made by observatories in Kiev (PIRS and MAC1), Bucharest, La Palma (CAMC1-11), USNO and Hamburg observatories (ERL), Pulkovo, Nikolaev (AMCIB) with CCD and photographic telescopes are used.

3.2*Observation in Chinese observatories*

The observations of 22 ERS in the southern hemisphere and optical positions determination relative to the UCAC1 were carried out [6]. The internal accuracy of comparison between optical and radio ERS positions is on the level of 60mas and 45 mas in right ascension and declination, respectively. UCAC1 is good connected with the ICRF. Additionally, there were obtained 65 ERS observed in Yunnan and Beijing observatories on the level of a good quality of about 30mas in both coordinates. Preliminary calculation has shown a possibility to use them for angles data processing.

Observation with the RTT150 in Antalya: The observations of 26 ERS in the southern hemisphere and optical positions determination relative to the USNOA2.0 were carried out in Antalia in accordance with the Joint Project. The internal accuracy of comparison between optical and radio ERS positions is on the level of 43mas and 34 mas in right ascension and declination, respectively. USNOA2.0 is not so accurate catalogue as UCAC1 and its connection with the ICRF is of the same order. The observations of 44 ERS in northern hemisphere and optical positions relative to USNOA2 were carried out in Antalia. The internal accuracy of

comparison between optical and radio positions is 31 mas and 38 mas in right ascension and declination, respectively.

4. DETERMINATION OF PRELIMINARY ANGLES BETWEEN OPTICAL AND RADIO REFERENCES FRAMES

The values of angles between optical and radio reference frames in accordance with the data of observation with RTT150 in Turkey and 1-m telescope in China were also calculated by common formulas:

$\Delta\alpha_{\ O-R}$ Cosδ = ω_x Sinδ Cosα + ω_y Sinδ Sinα - ω_z Cosδ , (1)

$\Delta\delta_{\ O-R}$ = - ω_x Sinα + ω_y Cosα ,

where: $\Delta\alpha_{O-R} = \alpha_O$ - α_R and $\Delta\delta_{\ O-R} = \delta_O$ - δ_R are ERS coordinate differences in optical and radio reference frames; ω_x,ω_y,ω_z - rotation angles about the x,y,z axes, respectively.

It is to be noted that some differences in position between USNO-A2.0 and ICRF are available due to systematic errors: position errors depending from star brighness and declination, unknown proper motion of secondary reference stars, regional differences in positions between ICRF and USNO-A2.0; also, distorsion of drift scanning CCD fields, some reduction errors of the CCD images made by stare and drift-scan modes, by operation with pointlike and extended objects from the ERS counterparts.

As a first analysis free terms $\Delta\alpha_0$Cosδ and $\Delta\delta_0$ were determined in two equations (1) for consideration of differences between USNO-A2.0 and ICRF. Resulting values of these terms made $\Delta\alpha_0$Cosδ = +0.″11 ±0.″04 and $\Delta\delta_0$= +0.″14 ±0.″02 and are similar to those discussed in [7-8]. After taking it into accout the unknown angles values from available observations in the ICRF were determined.

The second estimation of obtained angles are given in the Tabl.1 in comparison with the angles determined by different authors [9-19].

Table 1. Optical-radio rotational parameters

Source	ω_x (mas)	ω_y (mas)	ω_z (mas)	N	σ_1 (mas)	$\sigma_{(O-R)}$ mas
Hamburg(1990), [13]	30±20	53±20	23±20	28	±86	
CAMC+Bord (1990), [14]	32±18	10±19	13±18	20	66	±66
Kiev(1992), [16]	0±30	70±30	20±20	251	365	
Jonston et al (1994), [17]	43±19	31±19	-29±18	43		
FASTT(1994), [10]	-20±17	28±16	11±13	99	122	42
Kumkova et al (1995), [18]	38±18	22±16	-17±16	78		146
Andrei et al(1995), [15]	-30±20	30±30	20±20	29	170	
FASTT(1997), [11,12]	-2.2±3.3	-2.2±3.4	3.4±2.9	689		
Zacharias et al (1999), [19]	-0.2±3.9	-5.4±3.9	-2.5±3.9	318	58	50
Joint Project (2002), [9]	**7± 24**	**-3± 24**	**-12± 21**	**92**	**175**	**40**

The column N gives the number of ERS sources in the solution, $\omega_{x,y,z}$ - rotation angles with

their standard errors; σ_1 – error of unit weight; $\sigma_{(O-R)}$ – accuracy of the ERS optical position with respect to the radio reference frame.

Comparing the data from different observatories it should be noted the internal accuracy of obtained angles in Tabl.1 is dependent mainly from the position accuracy of USNOA2.0 stars. It is possible to obtain good accuracy results with help of the best secondary reference stars position by using the future compiled catalog , new UCAC in the northern hemisphere, also by increasing the ERS number.

At present, there are additional available observations (about 100 ERS) made by collaborated telescopes. Also, we intend to obtain enough number of ERS observations in the next year accordingly the final program list (about 300 ERS).

5. CONCLUSION

Current processing of the optical/radio differences of 92 ERS with the average position accuracy of 40 mas by using the secondary reference stars from the USNO-A2.0 permits to determine rotation parameters with accuracy of 21-24 mas.

The expected accuracy of the optical/radio linking could be of about 5 mas by using the collaborated telescopes that will provide sufficient number of ERS (about 300) with their position accuracy of 20 mas and accuracy of secondary reference stars on the level of 40-50 mas.

This work is partly supported by Russian Foundation of Basic Research (Grants No.02-02-17076a).

6. REFERENCES

1. Stavinschi M., 2001, In: Extention and Connection of reference Frames using CCD ground-based Technique, G.Pinigin (ed.), Atoll, Nikolaev, pp.29-34.
2. Tang Z.H., Jin W.J., Wang S.H. et al., 2000, In: IAU Colloquium N180, USNO, 57.
3. Pinigin G., Shulga A., Maigurova N.V. et al., 2000, In: Kinematics and Physics of Celestial Bodies, Suppl. Ser., N3, Astronomy in Ukraine-2000 and Beyond (impact of international cooperation), Y. Yatskiv (ed.), Kiev, p. 59-63.
4. Protsyuk Y., 2000, In: Baltic Astronomy, 9, 554.
5. Vertipolokh A., BabenkoYu., Danil'tsev O. et al., In: Journees 2002 Reduction of Compiled Catalogue in the Selected ERS Fields, This Volume.
6. Tang Z. H., Wang S. H. Jin W. J., 2002, AJ, V.123, 125.
7. Assafin M., Andrei A., Vieira Martins R. et al. 2001, Astroph.J., 552, 380.
8. Dario N., Da Silva Neto, A.N., Andrei A. et al, 2000, AJ, 119, pp.1470-1479.
9. Maigurova N., Pinigin G., Protsyuk Yu. et al., 2001, In Extention and Connection of reference Frames using CCD ground-based Technique, G.Pinigin (ed), Atoll, Nikolaev, pp.52-57.
10. Stone R.C.,1994, A.J. V.108,N1, pp.313-325.
11. Stone R.C., 1997, A.J., V.114, N2, pp.850-858.
12. Stone R.C.,1998, Astrophys.J.Letters V.506,N2, P.2 pp.L93-L96.
13. Ma C. et al., 1990, AJ, 1224.
14. Morrison A.N. et al, 1990, A&A, 236, 256.
15. Andrei A.N. et al, 1995, AJ, 109, 428.
16. Tel'nyuk-Adamchuk V.V. et al, 1992, Kinematics and Physics of Celestial Bodies,V. 8, 17 (in Russian).
17. Johnston K.J. et al, 1994, Bull. Am. Astron. Soc., V.26, No.2, 901.
18. Kumkova I.I. et al, 1995, IAU Simp. No 166 Astronomical and Astrophysical Objectives of Sub-Millarcsecond Optical Astronomy, eds E.Hog, P.K.Seidelmann,383.
19. Zacharias N., Zacharias M.I., Hall D.M. et al., A.J. 118, pp.2511-2525.

OPTICAL POSITION AND PROPER MOTION FOR X-RAY SOURCES SOUTHEASTERN OF THE OPHIUCHUS MOLECULAR CLOUDS

R. TEIXEIRA[1,2], C. DUCOURANT[2,1], M.J. SARTORI[3], P. BENEVIDES-SOARES[1]
J.L. MUIÑOS[4], J.P. PÉRIÉ[2], J. GUIBERT[5] and C. MALLAMACI[6]

1- Instituto de Astronomia, Geofísica e Ciências Atmosféricas, Brazil
2- Observatoire de Bordeaux, France
3- Laboratório Nacional de Astrofísica, Brazil
4- Real Instituto y Observatorio de la Armada, Spain
5- Observatoire de Paris, France
6- Universidad Nacional de San Juan, Argentina
e-mail: teixeira@astro.iag.usp.br

ABSTRACT. Here we are interested in defining the optical counterpart and to determine acurate positions and proper motion of approximately three hundred X-ray sources observed by ROSAT. These sources are distributed in a region at the southeastern of the Ophiuchus molecular cloud complex. This region is specially interesting mainly due to the fact that it contains PMS stars that are "isolated" from molecular clouds. The identification of new PMS stars and the proper motion measurements in this region is important to understand why these stars are far from the molecular clouds and their formation mechanism. The X-ray sources considered here form a list of new possible PMS stars candidates that were selected by using X-ray hardness ratios.

1. WORK MOTIVATION AND DEVELOPMENT

The knowledge of proper motion of young stars can contribute significantly with the study of their formation mechanism (Lépine and Duvert 1994) and their membership properties. They can contribute too for the detection of young star candidates.

The work presented here, is part of a more general project that aim the measurements of positions and proper motions of a big number of pre-main sequence (PMS) stars already identified in the literature, detection of new PMS stars and study of their kinematics.

Here, we present the preliminary results of the measurements of positions and proper motions of the optical conterpart of about 300 ROSAT All-Sky Survey sources. These sources are in a region southeastern of the Ophiuchus star-forming clouds where are found some "isolated" T Tauri stars. As the PMS stars have been over the years, found and associated to molecular clouds the presence of these "isolated" T Tauri stars here, is interesting and claim for an explication. Naturaly, the detection of other young stars in this region and the kinematic parameters for these stars, are essential to understand as these stars can be "isolated" from the star-forming region.

We work with ROSAT data because the T Tauri stars are X-ray sources. Of course, the possible young nature of some of these objects can only be deduced by spectral observations.

We obtain the positions and proper motions by combining recent and ancient optical positions by weighted least square (Teixeira et al. 2000). The recent positions come from CCD meridian observations at Bordeaux (Viateau et al. 1999), El Leoncito (Muiños et al. 2003) and Valinhos (Dominici et al. 2000) and also, observations with the Danish 1.5m ESO telescope. The old positions come from the literature: AC2000(Urban et al. 1998), USNO(Monet et al. 1998), UCAC1 (Zacharias et al. 2000), Tycho2 (Hog et al. 2000), and from the digitalization of plates at MAMA (Guibert et al. 1984).

In Figure 1 we show the VPD for about 180 sources X where we highlight some PMS and ZAMS stars indentified in the literature. We can note a reasonable coincidence between the proper motions of some of these PMS stars but this fact doesn't point out a particular distribution for these stars.

We make an external check of our results by comparing the proper motions obtained here with the Tycho 2 one. The Figures 2 and 3 show the comparison in right ascension and declination proper motion. As we can see we have a very good coincidence with Tycho 2 proper motions in both coordinates. Our data don't show systematic tendency. The mean difference is 0.1mas/yr and the standard deviation 2.2 and 2.5 mas/yr to right ascension and declination, respectively. However, we have to keep in mind that this comparison was made only with the brightest stars and an analysis for the fainter stars is necessary.

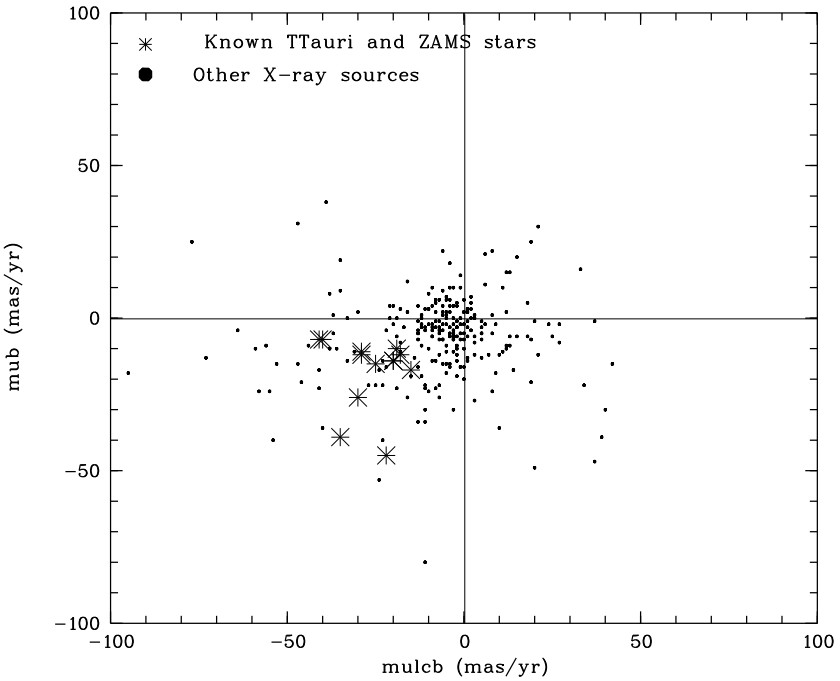

Figure 1: Proper motion diagram

Our results are very preliminary and many recent observations have still to be added to our data. We expect then to solve some identification problems and to improve the quality of the position and proper motion measurements

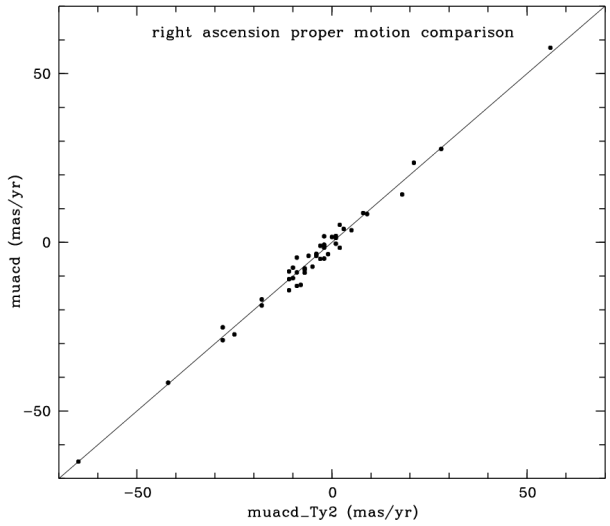

Figure 2: Right ascension proper motion comparison with Tycho 2 data

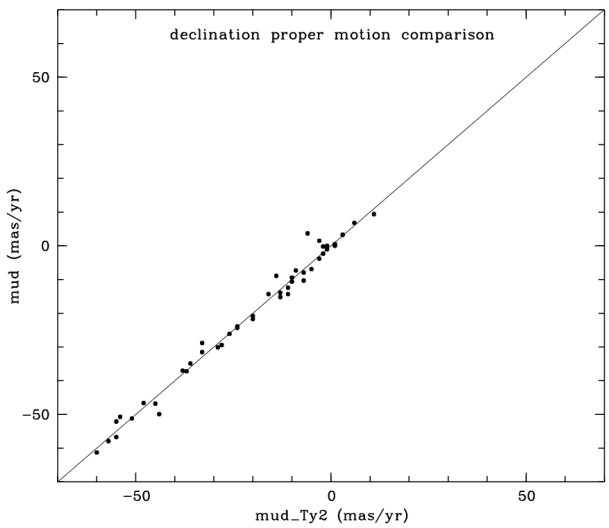

Figure 3: Declination proper motion comparison with Tycho 2 data

2. REFERENCES

Dominici T.P., Teixeira R., Horwath J.E., Medina-Tanco G.A and Benevides-Soares P., 1999, A&ASS 136, 261-167

Guibert J., Charvin P., Stoclet P., 1984, Coll. 78 UAI

Hog E., Fabricius C., Makarov V.V. et al., 2000, A&A, 357, 367

Lépine J.R.D. and Duvert G., 1994, A&A, 286, 60-71

Monet D., Bird A., Canzian B. et al.,1998, USNO - A2.0. A cataloog of Astrometric Standards

Muiños J.L. et al. 2003 in this proceeedings

Teixeira R., Ducourant C., Sartori M.J. et al., 2000, A&A, 361,1143-1151

Urban S.E., Corbin T.E., Wycoff G.L. et al., 1998, AJ 115, 1212

Viateau B., Réquième Y., Le Campion J.F. et al. 1999, A&ASS, 134, 173-186

A PRINCIPAL POSITIONING SYSTEM FOR THE EARTH

B. COLL
SYRTE/UMR8630-CNRS
Observatoire de Paris, 61 avenue de l'Observatoire, 75014 Paris, France
e-mail: bartolome.coll@obspm.fr, http://coll.cc

ABSTRACT. The project SYPOR wishes to use the global navigation satellite system GALILEO as an autonomous relativistic positioning system for the Earth. Motivations and a sketch of the basic concepts underlying the project are presented. For non geodetic (perturbed) satellites, a two-dimensional example describes how the dynamics of the constellation of satellites and that of the users may be deduced from the knowledge of the dynamics of only one of the satellites during a partial interval.

1. INTRODUCTION

The current conception of the global navigation satellite systems (GNSS), like GPS, is based on a Newtonian model corrected numerically of some "relativistic effects". The *direct* relativistic theory suggests not only amelioration in accuracy, but also new functions for such GNSS systems.

The project *SYPOR* (*Sy*stème de *Po*sitionnement *R*elativiste) proposes the ideas and instruments needed to carry out these new possibilities. Particularly it aims to endow the constellation of satellites of GALILEO of the necessary elements to constitute, by itself, a *primary, autonomous positioning system* for the Earth and its neighbors. The word "autonomous" refers here to the capability of the constellation to provide complete relativistic metric information, i.e. to describe the *kinematics* and the *dynamics* both, of the constellation itself and of the users (possibility of gravimetry).

For this goal, the project *SYPOR* envisages, for the first time in physics and astronomy, to construct in the neighbors of the Earth a relativity-compatible physical coordinate system (relativistic positioning system).

In this paper we sketch the general lines of the project (Section 2), as well as the underlying physical concepts, namely that of *relativistic positioning systems* (Section 3) and the way to make such systems *autonomous*, which is illustrated in the two-dimensional case (Section 4).

Some of the ideas and results on this subject are the fruit of a long and friendly collaboration with Lluís Bel (Univ. Pais Vasco, Bilbao, Spain), Joan Josep Ferrando and Juan Antonio Morales (Univ. Valencia, Burjassot, Spain), and Albert Tarantola (Inst. Physique du Globe, Paris, France).

2. SKETCH OF THE PROJECT

For most of the needs of geodesy and positioning, the Earth may be considered as a *Newtonian system*, for which classical mechanics is enough to explain its essential properties. But a constellation of satellites around the Earth, endowed with clocks exchanging their proper times, is a *relativistic system* in its own right (mainly due to Doppler and gravitational potential "relativistic effects"). Consequently, the natural conceptual frame to study GNSS is relativity theory.

At present, the GNSS involve the Earth and the constellation of satellites as a sole, coupled system. They start from a terrestrial, non relativistic coordinate system (Coll, 2001) and use the satellites of the constellation as moving beacons to indicate to the users their position with respect to this system.

The project SYPOR offers this result in two steps, that have different levels of conceptual precision and practical accuracy:

1. At the first level, SYPOR proposes the concepts and means to use the sole constellation of satellite-borne clocks as the most accurate, primary, autonomous, relativistically valid, positioning system for the neighbors of the Earth. At this level, any user may know its coordinates with respect to the satellites, its dynamical state (acceleration, rotation), the exact internal configuration of the constellation, and their situation with respect to the ICRS (i.e. all what an user may hope to obtain from a primary system), and any two users may know their relative position, distance and relative orientation.

Such a positioning system is a non usual one, with light-like (rapidly variable) coordinate surfaces, but any conventional system may be defined with respect to it. It is to be noted that, at this level, no synchronization of clocks is at all necessary.

2. At the second level, the usual data of the control segment on the trajectories of the satellites, are "read" as the data defining the coordinate change to (secondary, non relativistic) terrestrial coordinates (WGS 84 or ITRF classical eference systems).

At this level, any user may know its position (with terrestrial precision) with respect to the Earth, as with the current GPS conception.

The possibility appears for a space agency to concentrate its interest in the first level, the autonomous positioning system, and delegate to global and local Earth agencies the control of the terrestrial coordinates.

To realize these performances, every satellite must be endowed with the following kinematic devices:

- a device, on every satellite, allowing to exchange proper times with its neighbors (internal control of the parts of the system) (Hammesfahr, 1999),
- a device, on four at least of the satellites, pointing to the ICRS (International Celestial Reference System) in order to define virtual local charts "at rest" with respect to the ICRS (external control of the system as a whole),
- a device, on every satellite, broadcasting over the Earth, beside its proper time, those of their neighbors (strong integrity: control by the users segment).

3. POSITIONING SYSTEMS

Relativity theory may be used:

* as a wise algorithm to sprinkle Newtonian expressions with terms corresponding to the "relativistic effects" necessary for the obtention of the correct numerical values, or

* as the adequate starting frame to rise and to approach the physical situations with the most recent concepts and developments on the space-time.

The first use is undoubtedly correct in some particular scenarios, as may be in approximate numerical computations or for the abstract comparison of the equations of the two theories. The analysis shows that in fact this first use may be correct in the situations in which the physical determination of the coordinates either does not matter, or may be numerically identified to their Newtonian geometric determinations. But it is obviously useless to take advantage of the progress and specific developments of relativity theory in its proper domain, as it is the case in advanced GNSS.

The basic arena of relativity theory is its space-time. Relativistic space-time differs from Newtonian space-time in the following essential point: "the space" and "the present" are not now "physical objects", but inessential local arbitrary conventions. The three-dimensional Newtonian space has as much physical reality as have the Ptolemaic cristal spheres, and "past", "present" and "futur" are not exhaustive complementary parts of the space-time. Consequently, "objects" in their usual sense, like galaxies, stars, planets, mountains do not exist in the relativistic space-time. What one can find in it are rather the "absolute invariants" that they generate, that is to say, their "histories". It is with the histories of the satellites that a relativistic theory of GNSS must be constructed.

A *locationing system* is a detailed description for the physical construction of a coordinate system. To construct a coordinate system is either to construct its coordinate lines, or to construct its coordinate (hyper-)surfaces. But the choice of one or the other, and the protocol of their physical construction, give rise to very different physical properties (Coll, 2001).

Thus, when the protocol of their physical construction allows a particular observer (generally situated at the origin) to attach to every point of his neighbor a set of coordinates, one has what is currently called a *reference system*. But if this protocol allows every point of a neighbor to know its proper coordinates, then one has a *positionning system*.

In Newtonian physics, these functions are exchangeable, and perhaps this is why they are frequently mistaken. But in relativistic physics these two functions have very different physical properties:

* they are always *incompatible* for a sole coordinate system. So that the "reference" or "positioning" character of a locationing system must be previously chosen,

* it is always *impossible* to construct a positioning system starting from a reference system,

* it is always *possible* (and very easily) to construct a reference system starting from a positioning one.

As a consequence, the *first* element to be conceived in a relativistic GNSS must imperatively be its positioning system, and not its terrestrial reference system (WG 84 or IERS) as it is currently the case.

Remember (Coll, 2001) that relativistic positioning systems are *generic, free,* and *immediate*, three very important physical properties that no other locationing system may simultaneously offer. Thus, for example, Cartesian coordinates are not generic, the standard synchronization (two-way signals) usual in the construction of reference systems does not give rise to immediate systems; harmonic conditions are generic, but not free, etc.

A general analysis of rigorous mathematical results, physical possibilities and present tech-

nical developments leads to the important epistemic result that, among all the relativistic locationing systems, the set of relativistic positioning systems exists but constitute a very little class. And the simplest representative of this class is the one formed by electromagnetic signals broadcasting the proper time τ_i of four independent clocks S_i $(i = 1, ..., 4)$.

From now on, we suppose these clocks carried by (non necessarily geodetic) satellites.

In the space-time, the above wave fronts signals, parameterized by the proper time of the clocks, draw four families of physical hypersurfaces moving at the velocity of light, realizing a *covariantly null coordinate system* $\{\tau_i\}$.

Coordinate systems of this class are very unusual. Very different from the current relativistic ones, and still more from the Newtonian ones, they have been studied by a very restricted number of specialists in relativity. For an almost exhaustive bibliography, see (Blagojević et al., 2001).

In such covariantly null coordinate systems, the Minkowski metric of the space-time, $\eta_{\alpha\beta} = diag\{1, -1, -1, -1\}$ adopts the form:

$$\eta_{\alpha\beta} = \begin{pmatrix} 0 & f & g & h \\ f & 0 & \ell & m \\ g & \ell & 0 & n \\ h & m & n & 0 \end{pmatrix} \tag{1}$$

where $f, g, h, \ell, m, n,$ are strictly positive functions of the coordinates τ_i.

We see that in such coordinates there is no time-like asymmetry, the four coordinate surfaces playing exactly the same role. The nullity of all the diagonal terms in the above real expression seems to have erroneously suggested in the past that such coordinate systems would be "somewhere degenerate"; this uncorrect intuitive feeling is perhaps the cause of the absence of studies on them and of their slow re-discovery by some authors.

The four proper times $\{\tau_i\}$ read at a space-time event by a receptor constitute its (covariantly null) coordinates with respect to the four satellites. But such a system can not be considered as *primary* (with respect to the space-time structure) if we have not sufficiently information to relate to it any other coordinate system (Cartesian, harmonic, etc). And for this task, we need to know the (dynamical) space-time trajectories of the satellites. In principle, there are many ways to do that, one simple one being to force satellites to follow prescribed trajectories, for example geodesics. But the most complete one is that in which these information is generated and broadcasted at every instant by the system of satellites itself, *whatever* be their trajectories. When this happens, we call the primary system *autonomous*.

4. AUTONOMOUS POSITIONING SYSTEMS

How to make autonomous such a system of embarked clocks , arbitrarily synchronized, broadcasting their proper times? The answer is very simple: broadcasting, not only their proper time, but also the proper time of their neighboring satellite's clocks.

In other words: let τ_{ij}, $i \neq j$, be the proper time of the satellite's clock j received by the satellite i at its proper time instant τ_i. Then, the broadcasting of the data $\{\tau_i, \tau_{ij}\}$ allow to make autonomous the covariantly null space-time positioning system $\{\tau_i\}$.

Observe that the sixteen data $\{\tau_i, \tau_{ij}\}$ received by an observer contains, of course, the coordinates $\{\tau_i\}$ $(i = 1, ..., 4)$, of this observer but also the coordinates $\{\tau_i, \tau_{ij}\}$ of *every* satellite i in the totally covariant null coordinate system that the four satellites are generating.

In a four-dimensional Cartesian grid of axis τ_i $(i = 1, ..., 4)$, the data $\{\tau_i, \tau_{ij}\}$ received by

an user represent at every instant the proper position of the user as well as the positions of the satellites. During an arbitrary interval, these data allow the user to draw in this grid its proper space-time trajectory as well as the trajectory of the four satellites. Of course, two different users will found, in their corresponding grids, that their personal trajectories are different, but in the covering domain of proper times, the trajectories of the four satellites will be necessarily the same.

Such grids are diffeomorphic to the corresponding domain of the space-time, but they are not *isometric*. The precise deformation that relates them is nothing but the *metric tensor* $g_{ij}(\tau_\ell)$ of this domain, which gives the dynamical properties of the trajectories (their inertial and/or gravitational characteristics).

When the grid trajectories of the satellites are particularly simple, their space-time dynamical ones are easy to obtain. For example, in the two-dimensional Minkowski case, if the grid trajectories of the two satellites are non parallel straight lines, one can show that necessarily the satellites follow convergent geodesics, meanwhile if the grid trajectories are parallel straight lines, the two satellites are necessarily uniformly accelerated.

When the grid trajectories are arbitrary, an important general result may be prove: the knowledge of the dynamics of *one of the satellites* during a *relative acausal interval*, allows to know the dynamics of both of the satellites as well as that of the user at any later instant.

In other words: if 1 and 2 denote the two clocks, the relative acausal interval of the satellite 1 with respect to the satellite 2 at the "instant" τ_2 is the interval of the trajectory of the satellite 1 between its proper times $\tau_1' = \tau_{21}$ and τ_1'' such that $\tau_{12} = \tau_2$. Then our result states that the dynamical knowledge of the satellite 1 during its proper time interval (τ_1', τ_1'') suffices to know its dynamical trajectory for any $\tau_1 \geq \tau_1''$ and of 2 and the user for any $\tau_2 \geq \tau_{12}$.

The relative acausal interval of, say, the satellite 1 with respect to the satellite 2, at the "instant" τ_2 is the interval of the trajectory of the satellite 1 between its proper times $\tau_1' = \tau_{21}$ and τ_1'' such that $\tau_{12} = \tau_2$. Then, in other words, our result states that the dynamical knowledge of the satellite 1 during its proper time interval (τ_1', τ_1'') suffices to know its dynamical trajectory for any $\tau_1 \geq \tau_1''$ and of 2 and the user for any $\tau_2 \geq \tau_{12}$.

Of course, around the Earth more than four satellites will be convenient. Every four neighboring ones will constitute a *local chart* of the *atlas* of covariantly null coordinate systems enveloping the Earth. From this atlas, appropriate virtual global conventional coordinate system may be defined.

5. REFERENCES

Blagojević, M., Garecki, J., Hehl, F., Obukhov, Yu., 2001. Real Null Coframes in General Relativity and GPS type coordinates, *Phys. Rev.* D65 (2002) 044018, e-print: gr-qc/0110078. Almost exhaustive bibliography.

Coll, B., 2001. Physical Relativistic Frames, in *Journées 2001 Systèmes de Référence Spatio-Temporels*, Brussels, Belgium, 24-26 September 2001, also http://coll.cc. Some properties of classical and relativistic coordinate systems are pointed out.

Hammesfahr, J. et al., 1999. Intersatellite Ranging and Autonomous Ephemeris Determination for future Navigation Systems, Deutsches Zentrum für Luft- und Raumfahrt (DLR), document number ISR-DLR-REP-002. Excellent report on the possibility of intersatellite links (ISL).

Session Ib

CELESTIAL AND TERRESTRIAL REFERENCE SYSTEMS

SYSTÈMES DE RÉFÉRENCE CÉLESTES ET TERRESTRES

EXTENDING AND IMPROVING THE INTERNATIONAL CELESTIAL REFERENCE FRAME

P. CHARLOT
Observatoire de Bordeaux–CNRS/UMR 5804
BP 89, 33270 Floirac, France
e-mail: charlot@obs.u-bordeaux1.fr

ABSTRACT. The International Celestial Reference Frame (ICRF) currently includes a total of 667 extragalactic radio sources distributed over the entire sky, whose positions were measured based on data acquired with the Very Long Baseline Interferometry (VLBI) technique during the past two decades. This paper reviews the ongoing VLBI observational efforts to densify the frame with new sources and to extend the ICRF to higher radio frequencies. Analysis and modeling refinement to further improve the quality of the ICRF are also discussed with particular emphasis on astrophysical modeling of the emission structure of the sources.

1. THE INTERNATIONAL CELESTIAL REFERENCE FRAME (ICRF)

The International Celestial Reference Frame (ICRF) (Ma *et al.* 1998) became effective as the fundamental celestial reference frame on 1 January 1998, following a resolution adopted by the XXIIIrd General Assembly of the International Astronomical Union (IAU) on 1997 August 20 in Kyoto, Japan. The ICRF differs from the previous realization of the celestial frame, the FK5 stellar catalog, in two important ways: (i) it relies on extragalactic objects, and (ii) its axes are no longer related to the equator and ecliptic planes. Instead, the ICRF axes are specified through quasi-inertial coordinates of extragalactic objects, as measured with the Very Long Baseline Interferometry (VLBI) technique.

The VLBI data set used for the ICRF includes all applicable dual-frequency 2.3 GHz and 8.4 GHz Mark III VLBI measurements obtained from August 1979 to July 1995 (1.6 million pairs of group delay and phase delay rate observations). From a total of ∼600 extragalactic sources observed during this period, a subset of 212 sources distributed over the entire sky was selected to define the initial direction of the ICRF axes (Ma *et al.* 1998). These *defining* sources were chosen based on their observing histories with the VLBI networks and the stability and accuracy of their position estimates. The accuracy of the individual source positions is as small as 250 microarcseconds (μas) for the best objects while the orientation of the ICRF coordinate axes is good at the 20 μas level. Positions for 294 less-observed *candidate* sources and 102 *other* sources with less-stable coordinates were also reported, primarily to densify the frame (Ma *et al.* 1998). The first extension of the ICRF, ICRF–Ext.1, provides coordinates for an additional 59 *new* sources and refines the positions of candidate sources, based on further VLBI data acquired through April 1999 (IERS 1999).

Continued VLBI observation of the ICRF sources is essential to maintain the viability and

integrity of the frame on the long term because extragalactic objects evolve in impredictable ways. Both their strength (total flux density) and radio structure (as imaged with high resolution VLBI) may change on time scales of a few months to a few years. The bulk of the observations for the ICRF maintenance is acquired through the so-called "RDV" (Research and Development with the VLBA) experiments. These are carried out every two months with a network comprising the 10 stations of the Very Long Baseline Array (VLBA)[1] plus other stations in North America, Europe, Asia and the Pacific. A total of ∼70 sources is observed in every RDV experiment and both the astrometric positions of these sources and images of their emission structures are derived from the data. Additionally, a small portion of certain geodetic VLBI sessions is used to observe ICRF sources so that each ICRF source, except in the far south, is observed recurrently.

Identification of new sources and modeling refinement are equally important to further improve the quality of the ICRF. Section 2 reviews the current VLBI observing programs for extending the ICRF. These include programs aimed at increasing the number of sources and programs to extend the frame to higher radio frequencies. The actual limitations to the VLBI astrometric accuracy are discussed in Sect. 3 with particular emphasis on the astrophysical modeling of the emission structure of the sources.

2. DENSIFICATION AND EXTENSION OF THE ICRF

The current observational efforts for extending the ICRF are directed towards either the densification of the frame at the standard geodetic observing frequencies (2.3 GHz and 8.4 GHz) or its extension to higher radio frequencies (24 GHz and 43 GHz). ICRF densification programs include single-epoch VLBI surveys to identify new candidate sources plus subsequent VLBI experiments dedicated to improve their astrometric positions, whereas ICRF extension experiments focus on observation of current ICRF sources. Each of these VLBI observing programs is discussed in turn below.

2.1 The VLBA Calibrator Survey

The VLBA Calibrator Survey (VCS1) (Beasley *et al.* 2002) consists of ten VLBA survey sessions conducted between August 1994 and August 1997, each of which observed a particular declination belt of 10–20° between −30° and +90° declination. The goals of this survey were: (*a*) to increase the surface density of known geodetic-grade calibrators with milliarcsecond-accurate positions, providing candidate sources for future extensions of the ICRF; (*b*) to facilitate routine VLBI phase-referencing to most regions of the northern and equatorial sky, allowing high-resolution radio imaging of weak scientific targets (Beasley & Conway 1995); and (*c*) to provide a uniform VLBI image data-base at 2.3 GHz and 8.4 GHz for use in scientific research, including active galactic nuclei and gravitational lensing studies, and cosmology.

Overall, a total of 1811 candidate calibrators were observed, most of which selected from the Jodrell Bank–VLA astrometric survey (Patnaik *et al.* 1992, Browne *et al.* 1998, Wilkinson *et al.* 1998). The analysis of this massive data set, recently published as the VCS1 catalog, reports unpreviously-measured VLBI astrometric positions for 1332 sources along with survey VLBI images[2] at 2.3 GHz and 8.4 GHz for most of these sources (Beasley *et al.* 2002). Two additional survey sessions have been carried out in January 2002 and May 2002 to fill existing holes in the VCS1 sky coverage of calibrators: in the declination range −20° to −45°; near the galactic plane; and for ICRF sources with somewhat limited structural information. These observed a further 500 potential calibrators which will form the basis for the VCS2 extension (Fomalont *et al.* 2002).

[1]The VLBA is a facility of the National Radio Astronomy Observatory (NRAO) which is operated by Associated Universities, Inc., under cooperative agreement with the National Science Foundation.

[2]Available through the NRAO www site at http://magnolia.nrao.edu/vlba_calib/index.html.

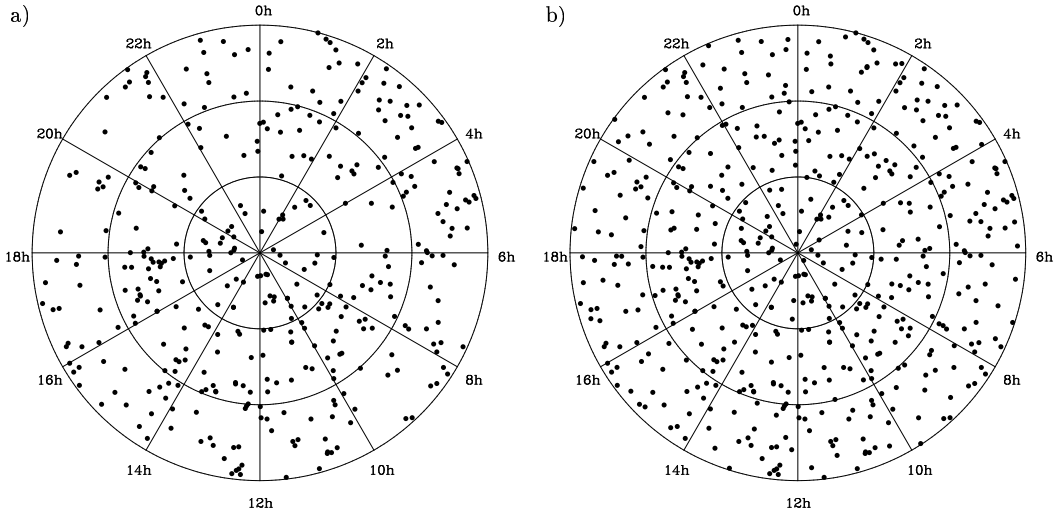

Figure 1: Northern-sky source distribution in polar coordinates: *a*) for the ICRF–Ext.1 frame; *b*) after completing the densification proposed by Charlot *et al.* (2000). The successive circles correspond to declinations of 0° (outer circle), 30°, 60°, and 90° (inner central point).

While the magnitude of the position errors is comparable for the ICRF–Ext.1 and VCS1 catalogs, it should be emphasized that the observing geometry of the VLBA Calibrator Survey was quite different from that of usual geodetic or astrometric sessions. Geodetic sessions attempt to observe uniformly the entire mutually visible sky as well as the local sky at each station to limit geometric and tropospheric systematic errors. As explained above, these conditions were not met in the VLBA Calibrator Survey, and it is possible that the VCS1 systematic errors are rather different. Additional observations of a large-enough sample of VCS1 sources in standard astrometric mode would thus be desirable to further assess the accuracy of this frame.

2.2 Densifying the northern sky

One of the deficiencies of the ICRF is the inhomogeneous sky distribution of the sources. While the frame contains an average of one source per $8° \times 8°$ on the sky, the angular separation to the nearest ICRF source for any randomly-selected sky location is up to 13° in the northern sky and 15° in the southern sky (Charlot *et al.* 2000). This non-uniform coverage makes it difficult to assess and control any local deformations of the frame which for example might be caused by tropospheric propagation effects or the apparent motions of the sources due to their variable emission structures. It also precludes the use of the ICRF as a catalog of calibrators for phase-referencing observations because the angular separation between the calibrator and target source should be a few degrees at most in such observations (Beasley & Conway 1995).

As shown by Charlot *et al.* (2000), this deficiency could be largely reduced if adding a limited number of sources at specific sky locations. For example, an additional 150 sources in the northern sky would reduce the angular separation to the nearest ICRF source from a maximum of 13° to a maximum of 6°. This improvement is illustrated in Fig. 1 where the current northern-sky coverage in ICRF–Ext.1 is compared to that which would be obtained with such a densification. Based on the VLBA Calibrator Survey, Charlot *et al.* (2000) have further identified 150 such sources to fill the appropriate empty holes in the frame. Their source selection strategy was also designed to select only sources with no or limited extended structure, so that these constitute a priori high-quality candidates for the densifying the ICRF.

Observation of these sources was initiated in May 2000 with a large VLBI network of 12 tele-

scopes comprising the European VLBI Network (EVN)[3] plus additional geodetic stations in USA and Canada. During this experiment, an initial 50 sources was observed, 49 of which were successfully detected, thus confirming that the source selection scheme was adequate. Preliminary astrometric analysis of these data indicates agreement at the milliarcsecond level with the VCS1 results for the majority of the sources. A further 50 sources have been observed in June 2002 with a similar VLBI network, the data of which should be correlated soon, while the rest of the sources is scheduled for observation in 2003.

2.3 Strengthening the southern sky

Another deficiency of the ICRF is the limited number of defining sources in the south (see the distribution of defining sources in Ma *et al.* 1998) and their somewhat less-accurate astrometric positions, as a result of the lack of well-established VLBI networks in the southern hemisphere. It is therefore of primary importance to devote special observational efforts to the southern sky to attempt to improve this situation in future ICRF realizations.

Along this line, a dedicated five-year observing program, including both astrometric and imaging experiments, has recently been initiated as a collaborative project between the US Naval Observatory (USNO) and the Australia Telescope National Facility (ATNF) (Fey *et al.* 2000). The objectives of this project are twofold: (*a*) improve the position accuracy of the existing southern ICRF sources and increase the density of candidate sources in the south; and (*b*) image at 8.4 GHz a complete sample of compact flat-spectrum sources south of -20° declination.

As reported by Ojha (2002), four full 24-hour astrometric sessions on existing ICRF sources along with short observations of 81 candidate sources have already been carried out. These used ATNF-accessible telescopes plus other geodetic stations in the southern hemisphere. Additionally, first-epoch VLBI imaging observations of 184 southern ICRF sources have been completed. Ultimately, the astrometric sessions should provide a strong tie between the northern and southern sky through the overlapping common sources at moderate southern declinations whose positions have already been measured with the northern VLBI networks.

2.4 Extension to higher radio frequencies

As mentioned above, the foundational work of the ICRF was done based on observations acquired at the standard geodetic frequencies of 2.3 GHz and 8.4 GHz. A number of developments have now converged to make future years an opportune time to pursue the extension of the ICRF to radio frequencies in the 24–43 GHz range. First, the 2.3 GHz environment is becoming increasingly cluttered by radio frequency interference making continued dual-frequency observations at 2.3 GHz and 8.4 GHz ever more difficult. Second, high-frequency amplifiers are now (24 GHz and 43 GHz) or will shortly be (32 GHz) available for use by the VLBI technique. Third, radio tracking systems for planetary probes are moving to the 32 GHz band and will soon require a sub-milliarcsecond-accurate high-frequency reference frame for deep space navigation. Additionally, extension to higher frequencies should enable improved VLBI astrometry, because the extragalactic sources are expected to be more compact at higher frequencies.

Based on this appreciation, a team of collaborators from several institutions (NASA, NRAO, USNO and Bordeaux Observatory) has been assembled in the fall of 2001 to initiate the extension of the ICRF in the 24–43 GHz range. As described by Jacobs *et al.* (2002), the major motivations for undertaking this large observational effort are: (*a*) to improve state-of-the-art VLBI astrometry; (*b*) to extend the list of VLBI calibrators in the 24–43 GHz range to enhance phase-referencing at high frequencies; (*c*) to study the high-frequency VLBI source morphology and its temporal evolution; and (*d*) to prepare for future deep space navigation. Along these lines, an initial proposal requesting VLBA observing time for three test experiments at 24 GHz and 43 GHz, with both astrometric and imaging goals, was approved in January 2002.

[3]See http://www.evlbi.org/ for an overview of the European VLBI Network.

Table 1: VLBI systematic error budget (adapted from Jacobs *et al.* [1998])

Component of error	Error (μas)
Troposphere[†]	150–250
Instrumentation	50–100
Source structure	0–1000
A priori nutation model	20
Tides	20
Plasma effects	15
Relativity	10–40
Numerical stability	2

[†]Assuming that azimuthal asymmetries (tropospheric gradients) are modeled.

The first experiment, carried out in May 2002, observed 65 sources at 24 GHz and 43 GHz, all of which have been successfully detected and imaged at both frequencies. A comparison of these images with existing maps at lower frequencies (8.4 GHz and 2.3 GHz) confirms that the emission structures are generally more compact at high frequency. On the astrometric side, a preliminary analysis indicates consistency at the milliarcsecond level with the current ICRF source positions. The second experiment, carried out in August 2002, has just been correlated and is about to be analyzed, while the third experiment is planned for the end of year. Not awaiting the results of these, a new proposal has been submitted to the VLBA for further observing in 2003 based on this initial success.

3. IMPROVING THE ACCURACY OF THE ICRF

3.1 Limits on astrometric accuracy

Increasing the accuracy of VLBI astrometry requires improving the overall VLBI observing, calibration, and analysis system. This includes instrumentation as well as physical modeling of the observed VLBI quantities. Current estimates of the systematic "error budget" for VLBI astrometry, as that from Jacobs *et al.* (1998) in Table 1, provide directions for such improvements.

The troposphere causes the largest errors, at the level of 150–250 μas, mostly because of water vapor turbulence, temperature profile mismodeling, and mapping function approximations. The next largest errors are due to the instrumentation (atomic clock instabilities, receiver sensitivity, instrumental phase calibration errors) which may contribute a total of 50–100 μas. Source structure errors vary widely; for most of the sources, it is not the dominant error, but for a small fraction of them – perhaps 10% – it is the dominant error (see below for further details). Smaller errors are caused by nutation and tidal mismodeling, plasma effects (miscalibration due to the Earth's magnetic field, scintillation at low Sun angle), and relativistic mismodeling (both General Relativity and Special Relativity), which may each contribute from 10 to 40 μas, while numerical errors are thought to be negligible.

In the future, specific efforts should be directed at improving the troposphere calibration and modeling if significant reduction of the 250 μas systematic errors of the ICRF is to be sought. When this error is routinely reduced, e.g. by water-vapor-radiometer calibration (Naudet *et al.* 2002), the focus should be on instrumental calibration and source structure modeling. Recent progress for the latter is reviewed in the next section.

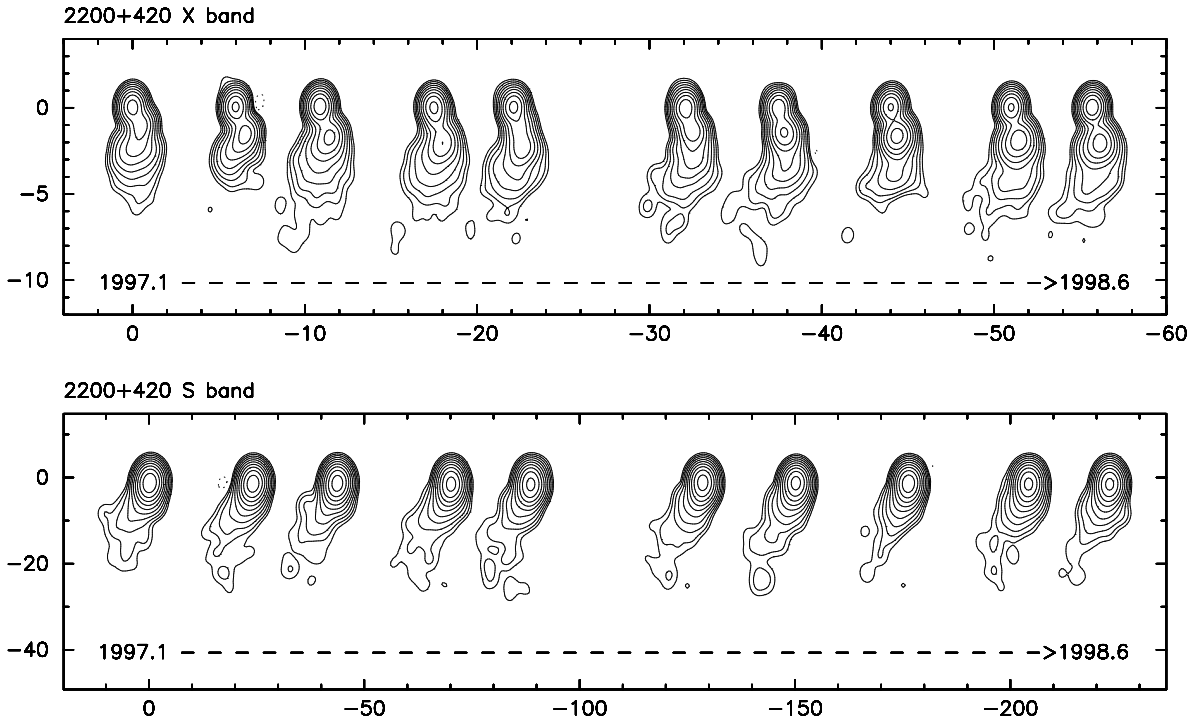

Figure 2: VLBI images of 2200+420 at 8.4 GHz (top panel) and 2.3 GHz (bottom panel) for 10 successive epochs spanning the period 1997.1–1998.6 (available from the USNO Radio Reference Frame Image Data Base). The maps are aligned horizontally according to the northern structural component (scale in milliarcseconds) and are spaced linearly according to their observing epochs. See Charlot (2002) for a discussion of source structure.

3.2 Astrophysical modeling of source structure

At the milliarcsecond scale, most of the extragalactic radio sources exhibit spatially-extended and variable emission structures which limit the VLBI astrometric accuracy if not modeled (Fey & Charlot 1997, 2000). The algorithm to model source structure (Charlot 1990) requires identification of a truly kinematically-stable morphological feature for each source and calculation of corrections derived from structure maps for the astrometric VLBI quantities. Exploratory work in this area showed that such modeling significantly improves the positional stability for the extended core-jet source 3C273 (1223+026) intensively observed during the 1980's, and reduces the rms delay residuals (Charlot 1994). A similar analysis based on VLBI data up to 1997 revealed that the long-term proper motion detected for the source 4C39.25 (0923+392) largely cancels out when incorporating source structure modeling, thus confirming that the peculiar systematic motion for this source is not real, but instead caused by its structural evolution (Charlot 2000).

Just recently, such exploratory studies have been extended to a much larger scale with a data set including 160 sources observed over up to 10 epochs and a total of 800 maps to correct for source structure (Sovers *et al.* 2002). Overall, the weighted rms delay residuals were found to decrease by 8 ps in quadrature upon introducing source maps to model the structure delays. The angular equivalent of this improvement is approximately 100 μas for typical VLBI baselines and amounts to a significant fraction of the 250 μas systematic error of the ICRF, thus confirming that source structure does affect VLBI analysis even though it is not currently the dominant error. For some sources with extended or fast-varying structures like the BL Lac object 2200+420 (see maps in Fig. 2), improvements were as large as 40 ps. In such cases, the scatter of the "arc" source positions over time was also found to decrease substantially (Fig. 3).

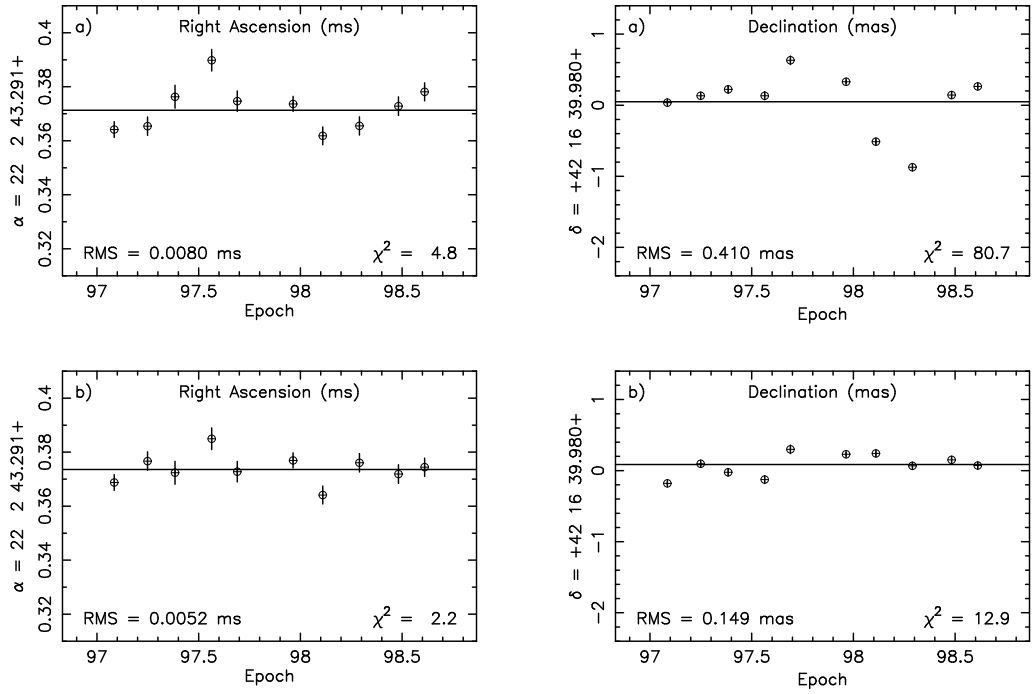

Figure 3: Estimated right ascension and declination coordinates of 2200+420 for 10 successive epochs spanning the period 1997.1–1998.6: *a*) no source structure modeling; *b*) with source structure modeled. Note the improved coordinate stability (reduced RMS scatter) for the latter. See Charlot (2002) for further details.

Future work in this area should be targeted at lengthening the time base, which was limited to 1.5 yr in the analysis of Sovers et al. (2002), in order to investigate source structure errors on longer time scales. Detailed studies of time sequence of maps are also necessary to permit identification of the invariant fiducial points within individual sources and further improve modeling (see Charlot [2002] for a discussion of this aspect).

4. CONCLUSION

The ICRF, as realized by VLBI astrometry, has been a great step forward. Compared with previous stellar realizations of the celestial frame, it is intrinsically simpler, much more accurate, more stable, and less susceptible to systematic errors, even though it requires continued VLBI observations to maintain these qualities on the long term. Further observations are underway to strengthen the southern sky, to densify the frame, and to extend it to other radio frequencies for wider applications of the ICRF. On the modeling side, the major areas to focus on for further improvements are the troposphere calibration and modeling, the instrumental calibration, and source structure modeling.

Immediate attention within the next year will be focused on the preparation of the 2003 IAU General Assembly. Current plans include: (*a*) assembling a second ICRF extension – with similar modeling as for ICRF and ICRF–Ext.1 and no revision of source categories – in order to publish the positions of the new sources observed since 1999; (*b*) detailed investigations of how a new ICRF realization could be improved upon ICRF (modeling refinement, revised analysis strategies, handling of source structure and source position variations); and – if time permits – (*c*) generation of a prototype ICRF–2 with revised *defining*, *candidate*, and *other* source categories.

5. REFERENCES

Beasley, A. J., Conway, J. E.: 1995, Very Long Baseline Interferometry and the VLBA, J. A. Zensus, P. J. Diamond and P. J. Napier (Eds.), *ASP Conf. Ser.*, **82**, p. 327.

Beasley, A. J., Gordon, D., Peck, A. B., Petrov, L., MacMillan, D. S., Fomalont, E. B., Ma, C.: 2002, *Astrophys. J. Suppl. Ser.*, **141**, 13.

Browne, I. W. A., Patnaik, A. R., Wilkinson, P. N., Wrobel, J. M.: 1998, *Mon. Not. R. Astr.Soc.*, **293**, 257.

Charlot, P.: 1990, *Astron. J.*, **99**, 1309.

Charlot, P.: 1994, VLBI Technology: Progress and Future Observational Possibilities, T. Sasao, S. Manabe, O. Kameya, and M. Inoue (Eds.), Terra Scientific Publishing Company, Tokyo, Japan, p. 287.

Charlot, P.: 2000, Proceedings of IAU Colloquium 180, Towards Models and Constants for Sub-Microarcsecond Astrometry, K. J. Johnston, D. D. McCarthy, B. J. Luzum, and G. H. Kaplan (Eds.), U. S. Naval Observatory, Washington, D. C., USA, p. 29.

Charlot, P.: 2002, International VLBI Service for Geodesy and Astrometry 2002 General Meeting Proceedings, N. R. Vandenberg and K. D. Baver (Eds.), NASA/CP-2002-210002, p. 233.

Charlot, P., Viateau, B., Baudry, A., Ma, C., Fey, A., Eubanks, M., Jacobs, C., Sovers, O.: 2000, International VLBI Service for Geodesy and Astrometry 2000 General Meeting Proceedings, N. R. Vandenberg and K. D. Baver (Eds.), NASA/CP-2000-209893, p. 168.

Fey, A. L., Charlot, P.: 1997, *Astrophys. J. Suppl. Ser.*, **111**, 95.

Fey, A. L., Charlot, P.: 2000, *Astrophys. J. Suppl. Ser.*, **128**, 17.

Fey, A. L., Johnston, K. J., Jauncey, D. L., Reynolds, J. E., Tzioumis, A., Lovell, J. E. J., McCulloch, P. M., Costa, M. E., Ellingsen, S. J., Nicolson, G. D.: 2000, International VLBI Service for Geodesy and Astrometry 2000 General Meeting Proceedings, N. R. Vandenberg and K. D. Baver (Eds.), NASA/CP-2000-209893, p. 164.

Fomalont, E., Beasley, T., Peck, A., Gino, C.: 2002, International VLBI Service for Geodesy and Astrometry 2002 General Meeting Proceedings, N. R. Vandenberg and K. D. Baver (Eds.), NASA/CP-2002-210002, p. 360.

IERS: 1999, 1998 IERS Annual Report, Observatoire de Paris, D. Gambis (Ed.), p 87.

Jacobs, C. S., Sovers, O. J., Naudet, C. J., Coker, R. F., Branson, R. P.: 1998, *TMO Progress Report 42-133*, 1.

Jacobs, C. S., Jones, D. L., Lanyi, G. E., Lowe, S. T., Naudet, C. J., Resch, G. M., Steppe, J. A., Zhang, L. D., Ulvestad, J. S., Taylor, G. B., Sovers, O. J., Ma, C., Gordon, D., Fey, A. L., Boboltz, D. A., Charlot, P.: 2002, International VLBI Service for Geodesy and Astrometry 2002 General Meeting Proceedings, N. R. Vandenberg and K. D. Baver (Eds.), NASA/CP-2002-210002, p. 350.

Ma, C., Arias, E. F., Eubanks, T. M., Fey, A. L., Gontier, A.-M., Jacobs, C. S., Sovers, O. J., Archinal, B. A., Charlot, P.: 1998, *Astron. J.*, **116**, 516.

Naudet, C. J., Keihm, S., Lanyi, G., Linfield, R., Resch, G., Riley, L., Rosenberger, H., Tanner, A.: 2002, International VLBI Service for Geodesy and Astrometry 2002 General Meeting Proceedings, N. R. Vandenberg and K. D. Baver (Eds.), NASA/CP-2002-210002, p. 194.

Ojha, R.: 2002, *ATNF News*, **47**, 10.

Patnaik, A. R., Browne, I. W. A., Wilkinson, P. N., Wrobel, J. M., 1992, *Mon. Not. R. Astr.Soc.*, **254**, 655.

Sovers, O. J., Charlot, P., Fey, A. L., Gordon, D.: 2002, International VLBI Service for Geodesy and Astrometry 2002 General Meeting Proceedings, N. R. Vandenberg and K. D. Baver (Eds.), NASA/CP-2002-210002, p. 243.

Wilkinson, P. N., Browne, I. W. A., Patnaik, A. R., Wrobel, J. M., Sorathia, B.: 1998, *Mon. Not. R. Astr.Soc.*, **300**, 790.

AN IMPROVED OPTICAL REFERENCE FRAME FOR LONG-TERM EARTH ROTATION STUDIES

J. VONDRÁK, C. RON
Astronomical Institute, Academy of Sciences of the Czech Republic
Boční II, 141 31 Prague 4, Czech Republic
e-mail: vondrak@ig.cas.cz, ron@ig.cas.cz

ABSTRACT. The Earth orientation parameters, based on optical astrometry observations of latitude/universal time variations and the Hipparcos Catalogue, covering the interval 1899.7-1992.0, were determined in past years at the Astronomical Institute in Prague, in close cooperation with the Czech Technical University in Prague. During the solution we discovered that not all Hipparcos stars are suitable for such a long-term study; many of them proved to have large errors in proper motions, mostly due to their multiplicity and shortness of the Hipparcos mission. Eventually, we had to improve about 20% of the proper motions from the same observations that we used to estimate the Earth orientation parameters.

New catalogues have appeared recently that are based on the combination of the Hipparcos Catalogue with past ground-based observations: FK6, TYCHO 2, and most recently ARIHIP, being a selection of the Combination Catalogues FK6, GC+HIP, TYC2+HIP and HIP. We made the inventory of all stars observed in Earth orientation programs at 33 observatories during the 20th century, and found 4480 different stars. Out of these we construct the Earth Orientation Catalogue (EOC) that is basically given in the International Celestial Reference System (ICRS). Whenever possible, we take over the positions, proper motions, parallaxes and radial velocities from the following catalogues, in the order of their importance: ARIHIP (3023 stars), TYCHO 2 (1271 stars), and Hipparcos (140 stars); 46 stars were identified in none of them. However, not all of these stars are astrometrically excellent in the sense of the classification introduced by Wielen et al.; only 1982 belong to categories 1-3. The positions and proper motions of the remaining 2498 stars will therefore be thoroughly checked and, if necessary, improved on the basis of the latitude/universal time observations.

1. INTRODUCTION

During the past years, three different solutions of Earth orientation in the Hipparcos reference frame were derived, in close cooperation of the Astronomical Institute and Czech Technical University in Prague, all of them covering the interval 1899.7–1992.0:

1. Solution OA97 (Vondrák et al. 1998), based on observations made with 45 different instruments (48 series) located at 31 observatories. 4.32 million individual observations of latitude/universal time variations were used, and 11% of Hipparcos star proper motions and/or positions were corrected from the series of Earth orientation observations.

2. Solution OA99 (Vondrák et al. 2000), based on observations with 47 instruments (merged into 39 series, with the steps caused by different coordinates of the instruments located at the same observatory removed) at 33 observatories. 4.45 million observations were used, and 20% of Hipparcos star proper motions/positions were corrected. We increased the percentage of the corrections, by changing the statistical criteria, because we found that more stars are probably double than we originally expected.

3. Solution OA00, based on 47 different instruments (merged into 41 series, with slightly different steps in data removed) at 33 observatories. 4.44 million observations were used, 20% of the Hipparcos stars corrected.

The above mentioned corrections of Hipparcos proper motions/positions were applied because we had problems with double and multiple stars, whose motions are not linear.

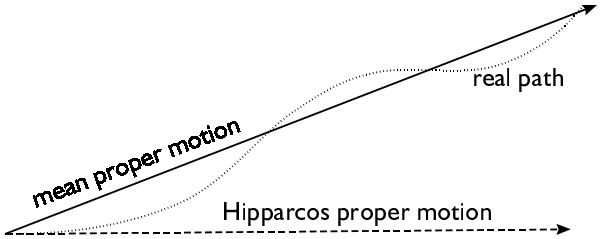

Figure 1: Real path of one of the components of a double star, mean and Hipparcos proper motion

The Hipparcos mission was shorter than 4 years, and therefore the Hipparcos proper motion reflect the instantaneous motion of one of the components of the star that is not suitable for extrapolation of the position to the epochs distant from the mean epoch of Hipparcos Catalogue (see Fig. 1). It was also sometimes not quite clear which of the components was observed in Earth orientation programmes – it might be different from the one for which the position and/or proper motion in the Hipparcos entry is given. These corrections were therefore computed and applied when found statistically significant, either to proper motions, or to positions or to both, for each instrument separately. The corrections were derived from the deviations of individual observations of the same star from 5-day average latitude/universal time values. Statistical criteria such as sufficient number of observations, length of the interval covered by the observations and the ratio of biases and/or drifts to the uncertainty in their estimations have been used.

These problems led us to the idea of creating a unique star catalogue consisting of all stars observed during the twentieth century in Earth orientation programmes. The catalogue is meant to be eventually used for future reanalysis of Earth Orientation Parameters from old optical observations. In order to do that we decided to utilize the catalogues that came out of the combination of observations both from space and ground. Quite naturally, the intensive astrometric observations of latitude/universal time made during the most of the last century at many observatories that we collected must not be abandoned in this work.

2. RECENT STAR CATALOGUES

New star catalogues, given in the Hipparcos reference frame, appeared recently. They are based on combination of space mission Hipparcos (Hipparcos and Tycho Catalogues) with older

ground-based catalogues. Therefore, mainly the proper motions are improved since much longer time span covered by observations is used. They are as follows:

- **FK6** (Wielen et al. 1999, 2000) containing 878 basic and 3272 additional fundamental stars, these parts are denoted here as **F61** and **F63**, respectively. The catalogue was created from the combination of Hipparcos and FK5 catalogues;
- **TYCHO-2** (Høg et al. 2000) containing 2.5 million stars, here denoted as **TYC2**. Combination of Tycho with 144 ground-based catalogues was used to derive this catalogue;
- **GC+HIP** (Wielen et al. 2001a) containing 20 thousand stars, here denoted as **GCH**. It comes from the combination of Hipparcos with Boss' General Catalogue;
- **TYC2+HIP** (Wielen et al. 2001b) containing 90 thousand stars, here denoted as **T2H**. This is the combination of Hipparcos with proper motions from TYCHO-2;
- **ARIHIP** (Wielen et al, 2001c) containing 91 thousand stars. It is the selection of 'best' stars from above mentioned **FK6, GCH, T2H, HIP** catalogues.

Wielen et al. (1999) introduced the classification of the stars according to their 'astrometrical excellence' into three categories by assigning the number of asterisks to each star, and utilized it in their above mentioned catalogues. It goes from *** (highest rank) to * (lowest rank); no asterisk means that the star is probably a component of double or multiple system, and therefore not astrometrically excellent. In the following we use these catalogues, in combination with astrometric observations of latitude/universal time, to derive the new Earth Orientation Catalogue.

3. EARTH ORIENTATION CATALOGUE

First of all, we made an inspection of all optical data of Earth orientation programs available, and found 4480 different stars observed during 1899.7–1992.0 at 33 observatories. The distribution of these stars on the sky and the histogram of their magnitude distribution are displayed in Fig. 2. Its asymmetric character (due to the concentration of the observatories on northern hemisphere) is evident. These stars were then identified in the catalogues described in Section 2, and their catalogue entries (i.e., magnitudes, positions, proper motions, parallaxes and radial velocities) were taken over to the new Earth Orientation Catalogue (EOC), in the following order of importance:

1. **ARIHIP**, from which we took over the majority, i.e. 3023 stars;
2. **TYC2**, from which we took over 1271 stars;
3. **HIP**, from which we took over only 140 stars;
4. **XXX**, or 'local' catalogues (i.e., those used by the observatories and often improved from their own observations), from which we took over the remaining 46 stars that could be identified in none of the preceding catalogues.

This procedure, during which we searched for only the stars that had not been identified in the preceding step, assures that the most accurate positions/proper motions available in the most recent catalogues are used in the new catalogue.

The numbers of the stars in EOC are constructed in the following way:

- Hipparcos number is used if the star is contained in HIP and is either single or its component A was observed.

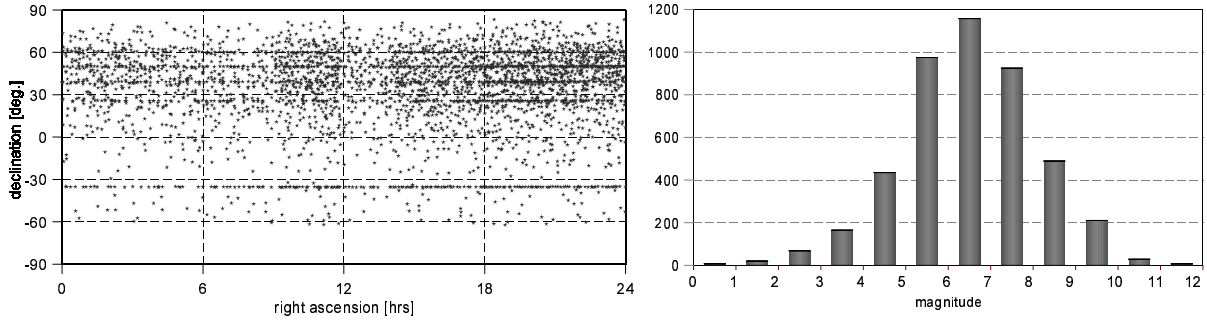

Figure 2: Distribution of EOC stars on the sky (left), and their magnitude distribution (right).

- Numbers 200001, 200002, ... for the stars that are not contained in Hipparcos Catalogue; there are only 107 such stars (61 being taken over from TYC2 and 46 from local catalogues).
- HIP number + 300000 for the stars that are contained in HIP but either photocenter or other component than A is observed. Number of these stars is not exactly known at the moment, it will gradually increase as the positions of 'astrometrically not excellent' stars are checked against the observations (see below).

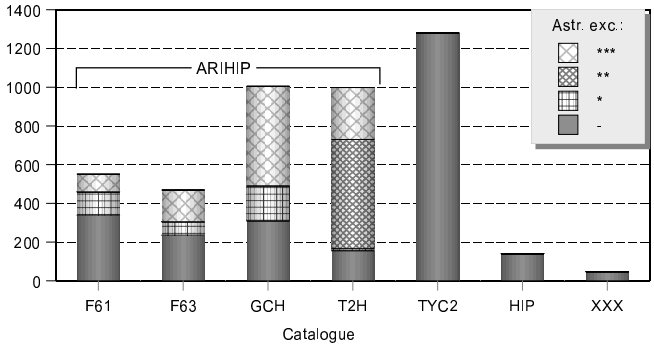

Figure 3: Catalogue of origin and 'astrometrical excellency'.

The origin of EOC entries is shown in Fig. 3, where a more detailed statistics is given – the entries taken over from ARIHIP are further subdivided into the four original subcatalogues of ARIHIP (F61, F63, GCH, and T2H). The statistics of the astrometric excellence classification is also depicted, in different textures (see legend). Out of the total number of 4480 stars, only 1982 are classified as 'astrometrically excellent', with one of the categories *, **, ***. Obviously, the majority of EOC stars that are not 'astrometrically excellent' require a thorough check of their positions and proper motions, and probably an improvement of many of them. To achieve this, two possible methods are presently under consideration:

- Simpler method, similar to the one that we used in our previous work: each observation of the star in question is used to determine its position with respect to 'astrometrically excellent' stars at each night, for each instrument separately. Then the observations of the same star at different epochs from all observatories are put together, Hipparcos position with a proper weight is added (only if the component observed is identical with the entry in Hipparcos Catalogue), and if the difference is statistically significant the position/proper motion is determined by linear regression.
- More complicated method, consisting in the application of a modified chain method (Vondrák 1980) that is used to determine positions and proper motions of all stars observed

by each instrument, alternatively in combination with properly weighted Hipparcos positions (Ron & Vondrák, this volume). These 'local' catalogues are then tied to the ICRS via 'astrometrically excellent' stars, and the catalogue entry for the same star combined from all individual instruments.

The following three examples demonstrate some typical cases that we can meet when checking the 'non-excellent' stars. All of them are based on the observations with PZT's at Richmond, Florida. The first above mentioned method was used, and the corrections of positions and proper motions with respect to original catalogues, referred to J2000.0, are shown.

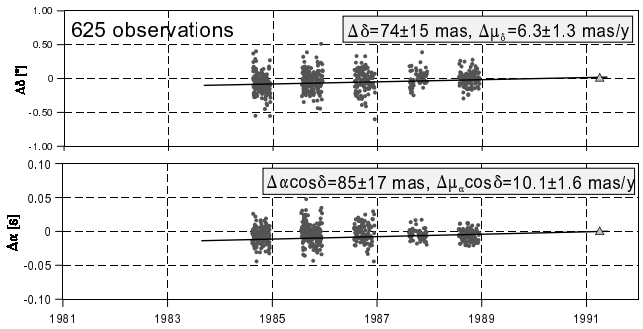

Figure 4: Richmond PZT observations of the star EOC716.

The first example (Fig. 4) shows the case of the star EOC716, whose entry comes from T2H catalogue (mag=6.2, $\alpha = 0^h08^m52.13633^s$, $\delta = 25°27'46.7454''$), that can be constrained to Hipparcos position. It is most probably a single star, whose proper motion nevertheless require a correction. PZT observations (small circles) are combined with the position in the Hipparcos Catalogue at the epoch J1991.25 (triangles). In linear regression (full line), all individual PZT observations are given weights equal to 1, while the Hipparcos position is assigned the weight of 1000, reflecting its superior accuracy. This practically assures the constraint to the position in the Hipparcos Catalogue at its mean epoch. The corrections of proper motion evidently exceed their formal uncertainties.

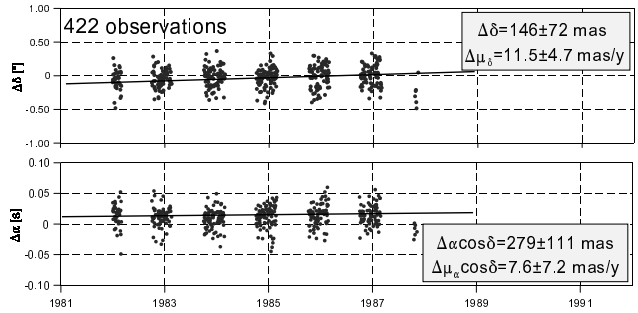

Figure 5: Richmond PZT observations of the star EOC326947.

The second example, depicted in Fig. 5, shows the case when not only proper motion but also position of the star requires a correction. Double star HIP26947 (angular distance of the components is $2.67''$, according to Hipparcos), whose entry comes from TYC2 catalogue and refers to component A (mag=8.6, $\alpha = 5^h43^m03.18405^s$, $\delta = 25°21'47.6756''$), was probably seen as a single star on PZT photographic plate, and its photocenter was measured. The full black regression line fitted to individual observations obviously does not intersect the baseline at the

epoch 1991.25. The star number becomes EOC326947 if these corrections, witnessing that the observed object is different from component A, are confirmed by observations made at other observatories.

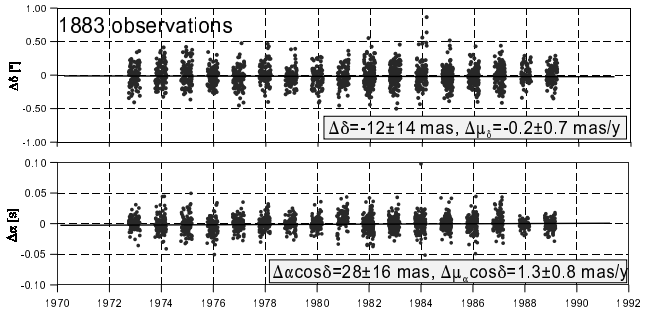

Figure 6: Richmond PZT observations of the star EOC200028.

The third example is shown in Fig. 6. It demonstrates the case of the star whose entry, that was taken over from the TYC2 catalogue, does not require a correction. The star is not contained in the Hipparcos Catalogue, and therefore it was given a new number EOC200028. Neither the position nor the proper motion of the star (mag=8.0, $\alpha = 6^h05^m05.59794^s$, $\delta = 25°48'03.3309''$), as given in TYC2 catalogue, evidently require a correction, as can be seen from the full black regression line fitted to individual observations; the corrections found are quite comparable with their formal uncertainties and are therefore statistically insignificant.

4. CONCLUSIONS

The new Earth Orientation Catalogue is being constructed that will hopefully be more accurate than the Hipparcos catalogue, in a long-term sense. To this end, the combination of ground-based optical observations in Earth orientation programmes with space observations (Hipparcos, Tycho) will be used to improve proper motions of some of the stars that are not 'astrometrically excellent' in Wielen's sense. The EOC, when finished, is planned to be used in a newly prepared solution of Earth Orientation Parameters from optical astrometry in the interval 1899.7–1992.0.

Acknowledgements. This project is supported by the grant No. 3205 awarded by the Grant Agency of the Academy of Sciences of the Czech Republic.

5. REFERENCES

Høg E., Fabricius C., Makarov V.V. et al. (2000) The Tycho-2 Catalogue of the 2.5 million brightest stars. *Astron. Astrophys.* **355**, L27–L30.

Ron C., Vondrák J. (2003) An improved star catalogue for Ondřejov PZT. In: N. Capitaine (ed.) *Journées 2002 Systèmes de référence Spatio-temporels*, Observatoire de Paris, this volume

Vondrák J. (1980) The determination of mean positions and proper motions of 304 stars from PZT observations at Ondřejov. *Bull. Astron. Inst. Czechosl.* **31**, 89-101.

Vondrák J., Pešek I., Ron C., Čepek A. (1998) Earth orientation parameters 1899.7–1992.0 in the ICRS based on the HIPPARCOS reference frame. *Publ. Astron. Inst. Acad. Sci. Czech R.* **87**, 1–56

Vondrák J., Ron C., Pešek I. (2000) Survey of observational techniques and Hipparcos reanalysis. In: S. Dick, D.D. McCarthy, B. Luzum (eds.) *Polar motion: Historical and Scientific Problems, Proc. IAU Coll. 178*, ASP Conf. Series **208**, 206–213.

Wielen R., Schwan H., Dettbarn C. et al. (1999) Sixth Catalogue of fundamental stars (FK6), Part I Basic fundamental stars with direct solutions. *Veröff. Astron. Rechen-Inst. Heidelberg* No. 35, Kommissions-Verlag G. Braun, Karlsruhe.

Wielen R., Schwan H., Dettbarn C. et al. (2000) Sixth Catalogue of fundamental stars (FK6), Part III Additional fundamental stars with direct solutions. *Veröff. Astron. Rechen-Inst. Heidelberg* No. 37, Kommissions-Verlag G. Braun, Karlsruhe.

Wielen R., Schwan H., Dettbarn C. et al. (2001a) Astrometric Catalogue GC+HIP derived from a combination of Boss' General Catalogue with the HIPPARCOS Catalogue. *Veröff. Astron. Rechen-Inst. Heidelberg* No. 38, Kommissions-Verlag G. Braun, Karlsruhe.

Wielen R., Schwan H., Dettbarn C. et al. (2001b) Astrometric Catalogue TYC2+HIP derived from a combination of the HIPPARCOS Catalogue with the proper motions given in the TYCHO-2 Catalogue. *Veröff. Astron. Rechen-Inst. Heidelberg* No. 39, Kommissions-Verlag G. Braun, Karlsruhe.

Wielen R., Schwan H., Dettbarn C. et al. (2001c) Astrometric Catalogue ARIHIP containing stellar data selected from the combination catalogues FK6, GC+HIP, TYC2+HIP and from the HIPPARCOS Catalogue. *Veröff. Astron. Rechen-Inst. Heidelberg* No. 40, Kommissions-Verlag G. Braun, Karlsruhe.

PROSPECTIVE IMPROVEMENTS OF IVS PRODUCTS AND EVOLVEMENT OF OBSERVING PROGRAMS

H. SCHUH (1), W. SCHLUETER (2), AND N. VANDENBERG (3)

(1) Institute of Geodesy and Geophysics, Vienna University of Technology, Wien, Austria
(2) Bundesamt für Kartographie und Geodäsie, Kötzting, Germany
(3) NVI, Inc./GSFC, Greenbelt, U.S.A.
e-mail: hschuh@luna.tuwien.ac.at

ABSTRACT. Geodetic and astrometric VLBI is fundamental for the establishment and maintenance of the ICRF and contributes extensively to the generation of the ITRF. It plays an essential role in geodesy and astrometry due to its uniqueness in observing the complete set of Earth orientation parameters (EOPs) which describes the transformation between the ICRF and ITRF stable over a time span longer than a few days. VLBI provides the reference frames and EOPs consistent over decades on the highest accuracy level. Within the International VLBI Service for Geodesy and Astrometry (IVS) a Working Group (WG2) reviewed the usefulness and appropriateness of the current generation of IVS products and the quality and appropriateness of existing observing programs with respect to accuracy, timeliness and redundancy. A report of the WG2 was presented in November 2001. The report is the basis for continuous improvements and for related research within IVS over the next few years. The results of the report will help IVS to meet the objectives and future requirements set up by the IAG and IAU for research in the geosciences and astronomy.

1. INTRODUCTION

The International VLBI Service for Geodesy and Astrometry (IVS) is a Service of the International Association of Geodesy (IAG), International Astronomical Union (IAU) and of the Federation of Astronomical and Geophysical Data Analysis Services (FAGS). The charter and the basis for international collaboration is given by the Terms of Reference (ToR) accepted by IAG and IAU and by the proposals provided by individual agencies in response to the call for participation.
IVS is an international collaboration of organizations that operate or support Very Long Baseline Interferometry (VLBI) components. The goals are

- to provide a service to support geodetic, geophysical and astrometric research and operational activities,
- to promote research and development activities in all aspects of the geodetic and astrometric VLBI technique,

- to interact with the community of users of VLBI products and to integrate VLBI into a global Earth observing system.

As IVS has no funds of its own, but is tasked by IAG and IAU for the provision of timely, highly accurate products (Earth Orientation Parameters (EOPs), Terrestrial Reference Frame (TRF), Celestial Reference Frame (CRF), etc.), IVS is dependent on the support of individual agencies.

In order to maintain the strong requirement for consistency, which is the basis for realizing and maintaining global reference frames such as the CRF and TRF, IVS initially employed and accepted existing infrastructure, observing programs such as the National Earth Orientation Service (NEOS), coordinated by the US Naval Observatory, or the Continuous Observations of the Rotation of the Earth (CORE), initiated by NASA. During its first two years of existence, the efforts of IVS were concentrated on the installation of new components and adoption of new IVS tasks. Coordination of activities within the service took effort, resources and time to mature.
All the activities of the first years are documented in the Annual Reports of the IVS for the years 1999, 2000 and 2001 [1], [2], [3]. The first General Meeting was held in Kötzting/Germany in February 2000, the second General Meeting was held in Tsukuba/Japan in February 2002 and several technical meetings concerning analysis and technology aspects were conducted. Proceedings of the General Meetings are available [4],[5].

Emphasis was placed on data analysis, coordinated by the Analysis Coordinator. Today six analysis centers provide a timely, reliable, continuous solution for the entire set of five Earth Orientation Parameters (EOPs) - two polar motion coordinates, Universal Time 1 determined by the rotation of the Earth minus Coordinated Universal Time (UT1-UTC), two celestial pole coordinates. The IVS Analysis Coordinator makes a combined solution - the official IVS product - as timely input for the IERS and its combination with the GPS-, SLR/LLR- and DORIS solutions. It turns out that the IVS combined solution gains 20% in accuracy over the single VLBI solutions.

2. REVIEW OF PRODUCTS AND OBSERVING PROGRAMS

At the 4th IVS Directing Board meeting held in September 2000 in Paris, the requirement for reviewing the products and the related observing programs was discussed with the view that IVS must meet its service requirements and improve its products. Because such a review requires overall expertise, a broad discussion and acceptance within the entire community, a Working Group (WG2) for Product Specification and Observing Programs was established at the 5th Directing Board Meeting in February 2001. (The Minutes of all meetings are published and made available on the IVS web site.) The assignment of WG2 was to

- review the usefulness and appropriateness of the current definition of IVS products and suggest modifications,
- recommend guidelines for accuracy, timeliness, and redundancy of products,
- review the quality and appropriateness of existing observing programs with respect to the desired products,
- suggest a realistic set of observing programs which should result in achieving the desired products, taking into account existing agency programs,
- set goals for improvements in IVS products and suggest how these may possibly be achieved in the future,

- present a written report to the IVS Directing Board at its next meeting.

The Working Group suggested a realistic set of observing programs, in order to achieve the desired products by taking into account existing agency programs. Moreover goals were set for improvements and suggestions were made as to how the improvements may possibly be realized in the future. A report of the WG2 was presented in November 2001. The IVS Directing Board reviewed the final version and accepted it for publication, which is available under http://ivscc.gsfc.nasa.gov/WG/wg2 or in the Annual Report 2001 [6].

Based on the WG report the IVS observing program for 2002 - 2005 was established, with the overall observing time increasing by 30% in 2002 to more than 100% in 2005. The IVS observing program includes components equipped with Mk4, S2 and K4 technology. Significant improvements in accuracy and in timeliness, i.e. shorter time delay from observation to the availability of products, can be expected. Involving all internationally available IVS components the observing program will enable IVS to provide continuous temporal coverage.

3. CONCLUSIONS

IVS has the capacity to meet the requirements set up by IAG and IAU in the realization of the reference frames and related products. In general, precise time series of the products, with sufficient accuracy (bias free), density, and timeliness must be generated. IVS as a Technique Center of IERS must guarantee the realization of precise celestial and terrestrial reference frames that are consistent over decades.

To meet this guarantee, improvements are required in the availability and reliability of the network stations. Automation for unattended observing will help to overcome the weekend gaps. More capacity is required in data transmission media, which will be solved by the development of a modern disk based recording system (Mk5) and by the ability to transfer data via the Internet (e-VLBI). These new systems will reduce the time delay and dramatically reduce expenses currently needed for tapes and tape drives. The global network configuration has to be improved, especially in the southern hemisphere, and more observing time is required. Encouraging additional related institutions and including the S2 and K4 technologies will also improve the situation. High priority has to be placed on rapid turnaround sessions at the correlator. To avoid backlogs the throughput at the correlators has to be improved. More analysis centers with different software are required to improve the analysis and to increase the robustness of the products.

IVS's primary duty is to provide the best possible results through optimized and efficient coordination of all the resources available. The new product specifications and the new related observing programs should give the basis for cooperation and for contributions by collaborating institutions. Nevertheless, the current IVS situation is highly dependent on only a few institutions and requires the strong, continued support and contributions of those key players.

4. REFERENCES

[1] Vandenberg, N.R. (editor): Annual Report 1999, NASA/TP-1999-209243, Greenbelt, MD, August 1999

[2] Vandenberg, N. R., Baver K.D.(editors): Annual Report 2000, NASA/TP-2001-209979, Greenbelt, MD; February 2001

[3] Vandenberg, N. R., Baver K.D.(editors): Annual Report 2001, NASA/TP-2002-210001, Greenbelt, MD; February 2002
[4] Vandenberg, N. R., Baver K.D.(editors): 2000 General Meeting Proceedings, NASA/CP-2000-209893, Greenbelt, MD; June 2000
[5] Vandenberg, N. R., Baver K.D.(editors): 2002 General Meeting Proceedings, NASA/CP-2002-210002, Greenbelt, MD; June 2002
[6] Schuh, H. et al.; IVS Working Group 2 for Product Specification and Observing programs, Final Report, Annual Report 2001, page 13 - 45, NASA/TP-2002-210001, Greenbelt, MD; February 2002
All references can be downloaded from the IVS homepage (http://ivscc.gsfc.nasa.gov)

RECENT COMPILED CATALOGUE OF RADIO SOURCE POSITIONS RSC (GAOUA) 01 C 01

YA. YATSKIV[1], O. MOLOTAJ[2], A. KUR'YANOVA[1] and
V. TEL'NYUK–ADAMCHUK[2]

[1] Main Astronomical Observatory, NAS of Ukraine
27 Akademika Zabolotnoho St, 03680 Kyiv, Ukraine
e-mail: yatskiv@mao.kiev.ua
[2] Astronomical Observatory, Taras Shevchenko National University
3 Observatorna St., 04053 Kyiv-53, Ukraine
e-mail: vtel@observ.univ.kiev.ua

ABSTRACT. The GAOUA series of compiled catalogue of radio source positions is briefly described. New catalogue RSC(GAOUA) 01 C 01 is compiled and compared with ICRF.

1. INTRODUCTION

The preparation of the GAOUA series of compiled catalogues of radio source positions has been started in 1989. The Kyiv arc length method proposed by Ya. Yatskiv and A. Kur'yanova, 1990, has been used for this purpose. It consists of several steps:

* selection of "basic"catalogues of radio source (RS) positions as subset of the collected individual catalogues;

* search for defining RSs common to each selected "basic" catalogues;

* calculation of arc lengths (in the following simply "arcs") between common defining RSs in each "basic" catalogue:

* intercomparison of calculated arcs for all "basic" catalogues, which resulted in evaluation of catalogue weights; determination of mean values of the arcs and "arc minus mean arc" residuals;

* construction of the so-called individual "rigid"frames which are based on the arcs and system of which are defined by positions of two selected RSs (in the following "basic" RS) ;

* construction of combined "rigid" frame using the data of previous steps;

* alignment of this combined "rigid" frame to a standard celestial reference frame in particular to the ICRF, and construction of a compiled reference frame under the following conditions: absence of a net rotation ; minimum displacements among common defining RSs of the standard and compiled frames;

* extension of the combined reference frame realized by common defining RSs to additional RSs, involved in process of constructing the frame.

2. THE GAOUA SERIES OF COMPILED CATALOGUE OF RADIO SOURCE POSITIONS OVER 1991 - 2000

By using the approach described above the seven combined solutions based on individual catalogues of RS positions provided by IERS CB and/or IERS AC were obtained (O.Molotaj et al, 2000; A.Kur'yanova and O.Molotaj, 2001). Table 1 gives overview of individual VLBI frames used to construct corresponding compiled catalogues of the GAOUA type.

Table 1. Statistics of individual celestial reference frames and the GAOUA series of compiled catalogues. N is the number of RSs in a frame; N_d is the number of the defining RSs, which are common for "basic" frames; σ_α and σ_δ are the averaged formal uncertainties (in $0.001''$) for right ascension and declination, respectively; W is the weight of "basic" frame used for constructing the combined "rigid" frame; $\overline{\Delta\alpha}^*$ and $\overline{\Delta\delta}$ are the mean differences in terms of "Frame - ICRF" calculated for defining RSs; $<\Delta\alpha^*>$ and $<\Delta\delta>$ are the m.r.s. of those differences

Frame	N	N_d	σ_α	σ_δ	W	$\overline{\Delta\alpha}^*$	$\overline{\Delta\delta}$	$<\Delta\alpha^*>$	$<\Delta\delta>$
				1991					
RSC(GSFC)90 R 01	72	6	0.11	0.20	0.60				
RSC(JPL)90 R 02	197	6	0.39	0.55	0.17				
RSC(NGS)90 R 01	70	6	0.16	0.30	0.23				
RSC(USNO)90 R 02	77	4	0.18	0.25	–				
RSC(GAOUA)91 C 02	228	59	0.75	1.15	–	-.05	.17	1.82	1.36
RSC(GAOUA)91 C 02	228	6	0.15	0.17	–	-.02	.15	.24	.25
				1993					
RSC(GSFC)92 R 01	357	10	0.10	0.15	0.35				
RSC(NOAA)92 R 01	84	10	0.18	0.29	0.29				
RSC(JPL)92 R 01	282	10	0.19	0.27	0.36				
RSC(NAOMZ)92 R 01	125	9	0.22	0.23	–				
RSC(USNO)92 R 02	113	6	0.07	0.10	–				
RSC(GAOUA)93 C 02	426	158	0.48	0.52	–	-.01	.24	.88	1.04
RSC(GAOUA)93 C 02	426	15	0.08	0.10	–	.02	.12	.16	.14
				1994					
RSC(GSFC)93 R 05	449	25	0.14	0.21	0.55				
RSC(JPL)92 R 02	333	25	0.13	0.16	0.17				
RSC(NOAA)93 R 02	107	25	0.36	0.69	0.28				
RSC(USNO)93 R 09	125	5	0.12	0.15	–				
RSC(GIUB)93 R 01	44	11	0.26	0.31	–				
RSC(GAOUA)94 C 02	505	195	0.52	0.55	–	.03	.27	.92	1.54
RSC(GAOUA)94 C 02	505	58	0.21	0.19	–	.02	.33	.25	.32

Frame	N	N_d	σ_α	σ_δ	W	$\overline{\Delta\alpha^*}$	$\overline{\Delta\delta}$	$<\Delta\alpha^*>$	$<\Delta\delta>$
				1997					
RSC(USNO)95 R 04	556	27	0.07	0.08	0.57				
RSC(GSFC)95 R 01	550	27	0.12	0.09	0.33				
RSC(JPL)95 R 01	287	27	0.14	0.21	0.03				
RSC(NOAA)95 R 01	249	27	0.18	0.25	0.07				
RSC(GIUB)95 R 01	89	5	0.17	0.24	–				
RSC(SHA)95 R 01	45	3	0.06	0.08	–				
RSC(GAOUA)97 C 01	598	212	0.15	0.18	–	.00	.20	.27	.31
				1998					
RSC(USNO)97 R 08	615	82	0.15	0.18	0.36				
RSC(GSFC)97 R 01	600	82	0.14	0.18	0.49				
RSC(JPL)97 R 01	287	82	0.20	0.28	0.15				
RSC(GIUB)97 R 01	266	26	0.78	0.59	–				
RSC(GAOUA)97 R 01	129	17	0.21	0.38	–				
RSC(GAOUA)98 C 01	631	212	0.11	0.13	–	.00	.00	.24	.26
				1999					
RSC(SHA)99 R 01	720	205	0.15	0.18	0.09				
RSC(USNO)99 R 01	652	205	0.12	0.14	0.46				
RSC(GSFC)99 R^{**}	644	205	0.11	0.14	0.25				
RSC(GIUB)99 R 01	602	205	0.15	0.17	0.20				
RSC(IAA)99 R 01	506	82	0.46	0.56	–				
RSC(FFI)99 R 01	431	58	0.16	0.12	–				
RSC(GAOUA)99 C 03	726	212	0.06	0.07	–	.00	.00	.23	.27
				2000					
RSC(SHA)00 R 01	636	204	0.15	0.18	0.30				
RSC(GSFC)00 R 01	624	204	0.11	0.13	0.42				
RSC(BKGI)00 R 01	621	204	0.15	0.17	0.28				
RSC(IAA)00 R 03	312	81	0.13	0.20	–				
RSC(GAOUA)00 R 01	191	47	0.22	0.39	–				
RSC(FFI)00 R 01	104	41	0.13	0.11	–				
RSC(GAOUA)00 C 01	669	212	0.07	0.08	–	.00	.01	.24	.26

3. NEW REALISATION OF CELESTIAL REFERENCE FRAME RSC(GAOUA)01 C 01

Table 2 gives some characteristics of the four individual reference frames which have been used for construction of RSC(GAOUA)01 C 01 by the Kyiv arc method. Three frames, namely RSC(BKGI)01 R 01, RSC(GSFC)01 R 01 and RSC(SHA)01 R 01 had sufficient number of defining sources to be used as individual "basic" frames in process of constructing the compiled catalogue of the GAOUA type. RS 1606+106 and RS 2145+067 were selected as "basic" sources in our approach.

Compiled and individual frames have been compared to the ICRF-Ext.1 and RSC(GAOUA)01 C 01 respectively by using the IERS model represented in equations (1):

$$\begin{aligned} A_1 \tan\delta\cos\alpha + A_2 \tan\delta\sin\alpha - A_3 + D_\alpha(\delta-\delta_\circ) &= \alpha_1 - \alpha_2 \\ -A_1\sin\alpha + A_2\cos\alpha + D_\delta(\delta-\delta_\circ) + B_\delta &= \delta_1 - \delta_2 \end{aligned} \qquad (1)$$

where A_1, A_2, A_3 are rotation angles between two frames under consideration; D_α, D_δ, B_δ represent the systematic effects by three deformation parameters, namely D_α – drift in right ascension as a function of the declination; D_δ – drift in declination as a function of the declination; B_δ – bias in declination.

Table 2. List of VLBI frames under consideration. N is the number of radio sources in the frame; N_b is the number of defining RSs common for the first three catalogues: σ is internal r.m.s. uncertainty ($0.001''$); W is frame weight used for constructing the combined "rigid" frame

Frame	N	N_b	σ_α	σ_δ	W
RSC(BKGI)01 R 01	578	202	0.13	0.16	0.30
RSC(GSFC)01 R 01	552	202	0.08	0.11	0.31
RSC(SHA)01 R 01	660	202	0.14	0.17	0.39
RSC(IAA)01 R 02	331	86	0.25	0.27	–
RSC(GAOUA)01 C 01	670	202	0.08	0.09	–

Only defining sources common to each frame and RSC(GAOUA)01 C 01 were used in the comparisons. The transformation parameters were evaluated by a least squares fit without weights. The relative global orientation and the deformation parameters are given in Tables 3 and 4 respectively.

Table 3. Relative orientation between individual frames and RSC(GAOUA) 01 C 01 (below GAOUAc). A_1, A_2, A_3 are the rotation angles which transform coordinates from the individual VLBI frames to GAOUAc. N_d is the number of common defining sources. Unit: $0.001''$

Frames	N_d	A_1	A_2	A_3
BKGI–GAOUAc	209	$+0.040 \pm 0.011$	$+0.033 \pm 0.011$	-0.031 ± 0.012
GSFC–GAOUAc	202	$+0.007 \pm 0.009$	$+0.000 \pm 0.009$	$+0.012 \pm 0.011$
SHA–GAOUAc	209	$+0.045 \pm 0.015$	$+0.019 \pm 0.015$	-0.021 ± 0.017
IAA–GAOUAc	86	$+0.050 \pm 0.048$	$+0.072 \pm 0.050$	-0.140 ± 0.060
GAOUAc–ICRF	211	-0.011 ± 0.025	-0.023 ± 0.025	-0.004 ± 0.029

Table 4. Drift and biases evaluated in the comparison between individual frames and RSC(GAOUA)01 C 01. D_α, D_δ are the drifts in right ascension and declination respectively, B_δ is the bias in declination. They are evaluated in a global solution together with the rotation angles. Units: $0.001''/deg$ for the drifts, $0.001''$ for the biases

Frames	D_α	D_δ	B_δ
BKGI–GAOUAc	$+0.000 \pm 0.000$	$+0.000 \pm 0.000$	-0.014 ± 0.009
GSFC–GAOUAc	$+0.000 \pm 0.000$	$+0.000 \pm 0.000$	$+0.018 \pm 0.008$
SHA–GAOUAc	$+0.000 \pm 0.001$	$+0.000 \pm 0.000$	-0.027 ± 0.013
IAA–GAOUAc	-0.003 ± 0.002	$+0.001 \pm 0.001$	-0.048 ± 0.051
GAOUAc–ICRF	-0.001 ± 0.001	$+0.000 \pm 0.000$	$+0.010 \pm 0.022$

The four individual celestial frames used for construction of RSC(GAOUA) 01 C 01 have been compared to ICRF-Ext.1 at Celestial System Section (CSS) of the IERS Central Bureau (IERS Annual Report, 2000). No significant slopes in RA and Dec were detected in any individual frames. Moreover constrains applied to align the respective frames as well as GAOUAc to ICRF have resulted in agreements of frames at a few tens of microarcsecond (see values in Table 3).

Figures 1 and 2 show, for the defining sources common to GAOUAc and ICRF, the postfit residuals in RA and in Dec as a function of the declination, and the normalized residuals in Dec as a function of RA respectively.

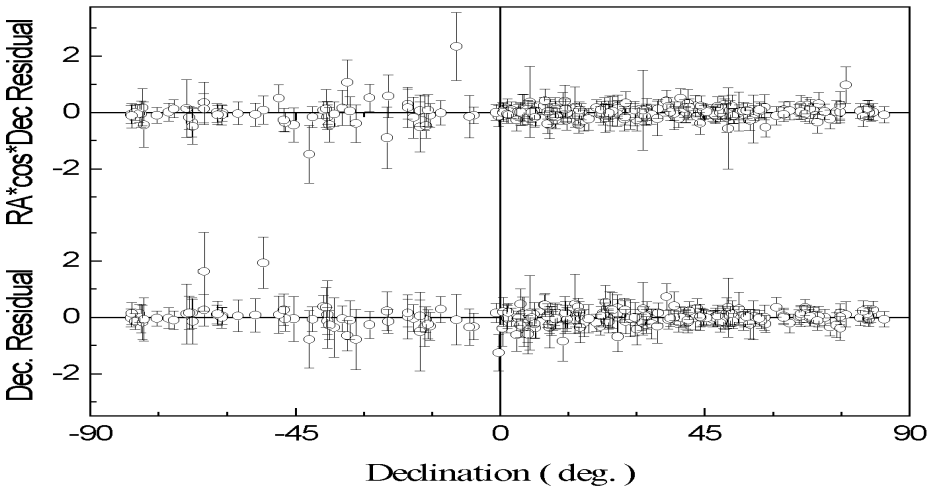

Figure 1: Postfit residuals "GAOUAc–ICRF" against declination for common defining RSs

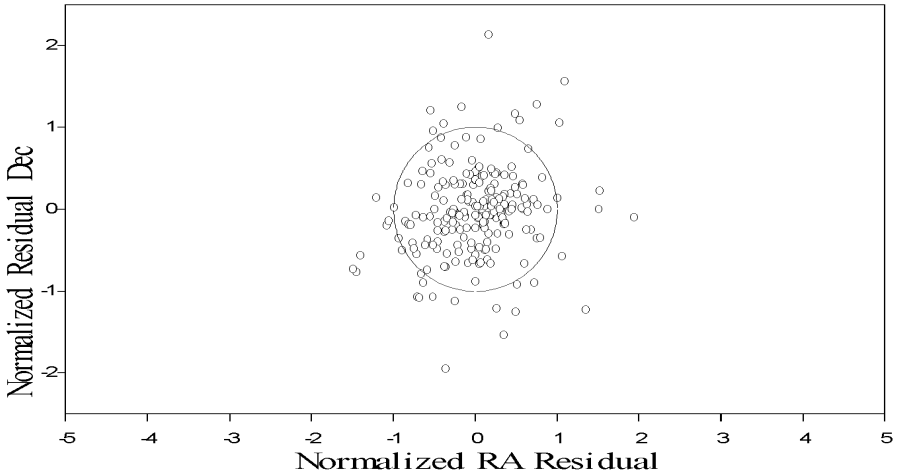

Figure 2: Distribution of normalized residuals "GAOUAc–ICRF" for common defining RRs

4. ON THE INCONSISTENCY OF INDIVIDUAL AND COMPILED CATALOGUES OF RADIO SOURCES WITH THE ICRF

It is pointed out in the report of CSS(see, IERS Annual Report 2000, p.46) that the four individual catalogues under consideration were not inconsistent with the ICRF, at its expected level of accuracy ($\sim 0.25mas$). We try to verify this statment based on the following calculations:

a) formal average values of positions of radio sources were derived for different set of individual and combined/compiled catalogues (SO - system);

b) differences d_{io} between positions of i-th frame and SO-system were calculated and used for determination of the coefficient of correlation r_{ij} between i-th frame and j-th frame.

Table 5. Statistics of individual and compiled catalogues derived from their mutual comparison ($\bar{a}$ is mean differences in RA and in Dec for catalogues under consideration, σ is root squares differences in RA and Dec respectively, and r is the correlation coefficient between the frames under consideration)

Frames		ICRF-Ext.1			RSC(GAOUA)01C 01		
		$\bar{a}$	σ	r	$\bar{a}$	σ	r
RSC(GAOUA)01 C 01	RA	0.011	0.162	-0.01			
	Dec	-0.005	0.194	0.06			
RSC(BKGI)01 R 01	RA	0.008	0.157	0.19	-0.003	0.096	0.35
	Dec	0.005	0.253	-0.51	0.010	0.135	0.05
RSC(GSFC)01 R 01	RA	0.012	0.181	0.00	0.002	0.056	0.88
	Dec	-0.042	0.206	0.17	-0.036	0.077	0.86
RSC(SHA)01 R 01	RA	0.010	0.159	0.10	0.000	0.069	0.58
	Dec	0.002	0.247	-0.31	0.007	0.141	0.12
RSC(IAA)00 R 02	RA	0.014	0.408	-0.56	0.003	0.366	-0.78
	Dec	0.021	0.409	-0.38	0.026	0.375	-0.76

Table 5 gives overview of statistics of the catalogues derived for the common defining radio sources . All catalogues exept RSC(IAA)00 R 02 are consistent with the ICRF at the level of accuracy ~ 0.25 mas.

5. REFERENCES

IERS Annual Report. 2000, Central Bureau of IERS – Bundesamt fur Kartographie und Geodesie, Frankfurt am Main.

Kur'yanova A., Molotaj O., 2001. Compiled catalogues of positions of the extragalactic radio sources RSC(GAOUA)91 C 02, RSCIGAOUA)93 C 02, and RSC(GAOUA)94 C 02, Kinematics and Physics of Celestial Bodies, **4**, No 1, pp. 383-385.

Molotaj O., Tel'nyuk - Adamchuk V., and Yatskiv Ya., 2000. The GAOUA series of compiled celestial reference frames, Kinematics and Physics of Celestial Bodies, Supplement, No 3, pp. 55-58.

ACCURATE FORMULATION FOR THE TRANSFORMATION BETWEEN THE TERRESTRIAL AND CELESTIAL SYSTEMS

N. CAPITAINE
SYRTE - Observatoire de Paris - UMR 8630/CNRS
61, avenue de l'Observatoire
75014 Paris - France
e-mail: capitain@syrte.obspm.fr

ABSTRACT. The use of the International Celestial Reference System (ICRS) since 1998 together with the adoption of IAU 2000 Resolutions and the achieved accuracy in VLBI observations of the celestial pole have brought fundamental changes regarding reference systems and Earth rotation. This allows for an highly accurate formulation of the transformation between the International Terrestrial Reference System (ITRS) and the Geocentric Celestial Reference System (GCRS). This formulation is based on the IAU 2000A precession-nutation and on the IAU refined definition of the Celestial Intermediate Pole (CIP). The IAU recommended paradigm for the terrestrial-to-celestial transformation involves ITRS and GCRS coordinates of the CIP and the use of the Terrestrial and Celestial Ephemeris Origins, TEO and CEO (i.e. "non rotating origin" in the ITRS and GCRS, respectively) to define the Earth Rotation Angle. IAU Resolutions have moreover recommended that the IERS continue to provide users with data and algorithms for the conventional transformation. The implementation of the IAU 2000 resolutions thus requires microarcsecond expressions for both classical and new quantities that must be compliant with the IAU 2000 precession-nutation model. This paper reports on this implementation.

1. INTRODUCTION

There have been fundamental changes regarding reference systems and Earth rotation, namely the use of the International Celestial Reference System (ICRS) since 1998, the adoption of IAU 2000 Resolutions and the unprecedented precision, that modify the expressions to be used in the transformation between the terrestrial and celestial systems.

This paper first emphasizes the consequences of these recent changes and then reports on the implementation of the new formulation and the IAU 2000 expressions for Earth Rotation.

2. RECENT FUNDAMENTAL CHANGES

2.1 Consequences of the adoption of the ICRS

The ICRS, adopted by the IAU as the International Celestial Reference System since the 1st January 1998, is based on barycentric directions of distant extragalactic objects (Ma *et al* 1998) and its definition is independent of the models used for precession and nutation and of the Earth's orbital motion as well. IAU 2000 Resolution B1.3 has clarified the definition of the

system of space-time coordinates within the framework of General Relativity for the Earth or Solar System, respectively. It has also specified the metric tensor to be used in both systems and the 4-dimensional space-time transformation between BCRS and GCRS.

Consequently, the celestial reference system for the Earth Orientation Parameters (EOP) has been changed from the FK5 to the GCRS.

2.2 Consequences of the submilliarcsecond determination of the nutation offsets

VLBI observations being sensitive to the actual orientation of the equator with respect to the GCRS, currently provide, with a submillarcsecond accuracy, the "nutation offsets" that include both the inaccuracies in the precession-nutation model and the frame bias of the mean equator at the reference epoch of the model in the GCRS.

Series of these VLBI observables during a 20-year period, have been used for determining the Basic Earth Parameters (BEP) of the geophysically-based MHB theory (Mathews *et al.* 2002) that has been adopted as the IAU 2000A precession-nutation.

2.3 Consequences of the adoption of the IAU 2000 Resolutions

IAU 2000 Resolutions B1.6 to B1.8 have recommended refined definitions, models and formulations for the celestial to terrestrial transformation.

The new definition of the pole (Resolution B1.7) to which the Earth's rotation refers (i.e. the Celestial Intermediate Pole, CIP) explicitly considers the high frequency variations (for more detail, see Capitaine 2000a and 2000b). According to this definition of an intermediate pole between the ITRS and the GCRS, the new precession-nutation model has to provide nutations with periods greater than two days; in contrast, nutations with periods lower than two days in the GCRS are considered as being variations of polar motion.

The IAU 2000 precession-nutation model adopted by Resolution B1.6 is based on the rigid Earth nutation model (Souchay *et al.* 1999) and on the transfer function of Mathews *et al.* (2002). This model includes two versions with associated precession and obliquity rates and celestial pole offsets at epoch. The most accurate version, denoted IAU 2000A, provides the direction of the celestial pole in the GCRS with a 0.2 mas accuracy (Mathews *et al.* 2002), whereas it shorter version, denoted IAU 2000 B, provides a 1 mas accuracy (McCarthy & Luzum 2003). The IAU 2000A model includes more than 1300 nutations with in-phase and out-of-phase periodic components in longitude and obliquity.

The new paradigm for the transformation between the ITRS and GCRS, which is recommended by Resolution B1.8, is based on the use of the non-rotating origin (Guinot 1979) both in the GCRS (i.e. the Celestial Ephemeris Origin (CEO)) and in the ITRS (i.e. the Terrestrial Ephemeris Origin, TEO). The CEO replaces the equinox as the origin for the Earth Rotation Angle (ERA) and the TEO provides an exact definition of the "instantaneous origin" of longitudes in the ITRS. Moreover, the classical precession and nutation quantities are replaced by the coordinates X and Y of the CIP in the GCRS that include combined precession, nutation and frame biases, together with their coupling effects. In addition to providing an explicit separation between precession-nutation of the equator from Earth rotation, this new paradigm is more simple, compact and direct than the classical one, which is a non-negligible advantage for achieving accuracies at the level of a few microarcseconds.

3. IMPLEMENTATION OF THE NEW FORMULATION

3.1 Implementing the IAU Resolutions

Two equivalent ways of implementing the IAU Resolutions in the transformation from ITRS to GCRS can be used, namely (a) the new paradigm based on the direct use of the CEO and

the ERA and (b) the classical paradigm based on the equinox and GST, but using the CEO and the ERA indirectly (for more detail, see Capitaine *et al.* 2000). They are called respectively "CEO-based" and "equinox-based" transformations in the following.

Common to both paradigms is the polar-motion matrix, which requires, in addition to the coordinates x_p, y_p of the CIP in the ITRS, the use of the quantity s' for providing the position of the TEO in the ITRS, which was neglected in the classical form prior to 1 January 2003. Implementation of the IAU 2000A precession-nutation model using the new paradigm requires expressions for the positions of the CIP and the CEO in the GCRS computed to an accuracy of a few microarcseconds over a time span of a few hundred years, in order to meet the requirements of high-accuracy applications. Implementation using the classical paradigm requires expressions for the various precession and nutation angles and Greenwich Sidereal Time (GST) as well.

3.2 Position of the CIP in the ITRS

In order to realize the CIP as recommended by Resolution B1.7, nutations with periods less than two days are to be considered using a model for the corresponding motion of the pole in the ITRS. The prograde diurnal nutations correspond to prograde and retrograde long periodic variations in polar motion, and the prograde semidiurnal nutations correspond to prograde diurnal variations in polar motion.

Models have been developed to provide such variations in polar motion that are due to tidal gravitation (see Brzeziński & Mathews 2003, this Volume) and are to be considered together with the variations of polar motion due to oceanic tides that appear at the same periods.

3.3 Position of the CIP in the GCRS

The x and y coordinates of the CIP unit vector in the GCRS, denoted X and Y, include (see Capitaine 1990) (i) precession and nutation referred to a fixed conventional ecliptic, (ii) coupling between precession and nutation giving rise to Poisson terms, (iii) celestial offsets ξ_0, η_0 of the CIP at J2000.0 w.r.t. the GCRS (associated with the precession-nutation model) and (iv) the coupling between offset in right ascension, $\mathrm{d}\alpha_0$ and precession-nutation.

Whereas the offsets ξ_0, η_0 are derived from VLBI observations, the determination of the equinox offset requires the use of observations which are dependent on the position of the ecliptic. The numerical value that has been used for the implementation of the IAU 2000 precession-nutation model is the GCRS right ascension of the mean dynamical equinox at J2000 (-14.6 ± 0.5 mas) as provided by Chapront *et al.* (2002) from a fit to LLR observations based jointly on the use of a dynamical theory for the Moon and of VLBI Earth Orientation parameters.

3.4 Implementation of the new definition of UT1

The implementation of the new definition of UT1 with the CEO-based transformation (Resolution B1.8) uses the conventional relationship between ERA and UT1 together with the quantity s that positions the CEO on the equator of the CIP.

The expression for GST to be used in the equinox-based transformation is derived from the relationship between ERA and UT1 and the expression for the accumulated precession and nutation (*i.e.* the equinox-based right ascension of the CEO; see Capitaine & Gontier 1993 for more detail) based on the IAU 2000A model.

4. IAU 2000 EXPRESSIONS FOR EARTH ROTATION

Expressions, numerical Tables and software for implementing the IAU 2000 system with either the classical or the new transformation have been made available during the year 2002.

Provisional expressions have been discussed during the IERS Workshop 2002 in Paris and the final versions have been provided in Chapter 5 of the IERS Conventions 2000.

4.1 Expressions for the variations in polar motion

Model for the variations $(\Delta x, \Delta y)_{nutation}$ in polar motion corresponding to diurnal and subdiurnal celestial nutations has been adopted by an *ad hoc* Working Group (Brzeziński, 2002, Brzeziński & Mathews 2003, this Volume)). The model including all components with amplitudes greater than 0.5 μas, is based on nonrigid Earth models and developments of the tidal potential (Brzeziński, 2001, Brzeziński and Capitaine, 2003, Mathews and Bretagnon, 2003). The amplitudes of the diurnal terms are in very good agreement with those estimated by Escapa *et al.* (2003). A Table for operational use is provided in the IERS Conventions 2000.

The diurnal components of these variations should be considered similarly to the diurnal and semidiurnal variations due to ocean tides. They are not part of the polar motion values reported to the IERS and distributed by the IERS and should therefore be added after interpolation. The long-periodic terms, as well as the secular variation, are already contained in the observed polar motion and need not be added to the reported values.

4.2 Expression for the position of the TEO in the ITRS

The quantity s' is only sensitive to the largest variations in polar motion. The expression to be used has been derived from the current mean amplitudes for the Chandlerian and annual wobbles (Lambert & Bizouard 2002):

$$s' = -47\ \mu\text{as}\ t. \tag{12}$$

4.3 Expression to implement the IAU 2000 definition of UT1

The Earth Rotation Angle, θ, is obtained by the use of its conventional relationship with UT1 as given by Capitaine *et al.* (2000),

$$\theta(T_u) = 2\pi(0.7790572732640 + 1.0027378119113544 8T_u), \tag{13}$$

where T_u = (Julian UT1 date − 2451545.0), and UT1 = UTC + (UT1−UTC),

This definition of UT1 based on the CEO is insensitive at the microarcsecond level to the precession-nutation model and to the observed celestial pole offsets.

4.4 IAU 2000 expression for the position of the CIP in the GCRS

IAU 2000 expressions have been developed for the coordinates X and Y of the CIP in the GCRS, valid at the microarcsecond level (Capitaine *et al.*, 2003a); they are based on the IAU 2000A or IAU 2000B model for precession-nutation and on their corresponding pole offset at J2000.0 with respect to the pole of GCRS. The complete series are provided in the IERS Conventions 2000.

4.5 IAU 2000 expression for the position of the CEO in the GCRS

The position of the CEO in the GCRS is provided by the expression for the quantity s using the developments of X and Y as functions of time (Capitaine *et al.*, 2003a). The numerical development is in fact provided for the quantity $s + XY/2$, which requires less terms to reach the same accuracy than a direct development for s.

The constant term for s, which was previously chosen so that $s(J2000) = 0$, has now been fit (Capitaine *et al.*, 2003b) in order to ensure continuity of UT1 at the date of change (1 January 2003) consistent with the Earth Rotation Angle (ERA) relationship and the current VLBI procedure for estimating UT1.

The complete series for $s+XY/2$ with all terms larger than 0.1 μas is available electronically on the IERS Convention Center website.

4.6 IAU 2000 precession-nutation expressions for the classical paradigm

The IAU 2000 expressions for the precession quantities ψ_A, ω_A, ϵ_A, compatible with the IAU 2000 precession-nutation model can be provided by using the developments of Lieske *et al.* (1977) to which the MHB estimated values for the precession rates, $\delta\psi_A$ and $\delta\omega_A$ have to be added. These expressions together with the Lieske *et al.*'s one (1977) for the planetary precession parameter χ_A have been considered as being the "canonical" 4-rotation series.

Then, expressions have been developed (Capitaine *et al.*, 2003c) for the more usual equatorial precession quantities ζ_A, θ_A, z_A in order to match the canonical 4-rotation series to sub-microarcsecond accuracy over 4 centuries.

Numerical comparisons have shown that the equivalence between the two paradigms requires that the classical one take account rigorously of the corrections to precession using the "canonical" four rotations (Wallace 2002), and frame bias, through appropriate rotation matrices.

4.7 IAU 2000 expression for Greenwich Sidereal Time

The IAU 2000 numerical expressions (Capitaine *et al.* 20003b) linking GST and ERA and locating the CEO have been developed such that they produce no discontinuity in UT1 on 1 January 2003 when changing from the current VLBI procedure to the new IAU 2000 system in which ERA(UT1) is a conventional relationship. This takes into account (i) the change from the former IAU relationship between GMST and UT1, (ii) the change from the IAU 1994 equation of the equinoxes to a more accurate expression and (iii) the systematic error of the order of 100 μas due to the incorrect use of UT (instead of TT) for computing precession in RA in the old expression for GST.

The polynomial part of GST is conventionally defined as GMST, whereas the non-polynomial part is the "complete equation of the equinoxes". This is the sum of the *classical* part and the *complementary terms*. The latter (*i.e.* the right ascension of the CEO in the mean frame at J2000) is very similar to the non-polynomial part of the expression for $s+XY/2$.

The expected discontinuity in UT1 rate, shown to be unavoidable due to the improved models and the fixed relationship between ERA and UT1, will have an effect on the determination of UT1 that is less than a few hundreds of microarcseconds over the next century.

5. CONCLUDING REMARKS

The expressions to be used to implement the IAU 2000 formulation based on the IAU 2000 precession-nutation model, either in the new (CEO-based) or classical (equinox-based) transformations between the ITRS and GCRS have been developed and are provided in the IERS Conventions 2000.

Tables and Fortran subroutines implementing the IAU 2000 terrestrial-to-celestial transformations are provided through the IERS Conventions website, and additional software have been released through the SOFA website (Wallace 2000).

Various comparisons and numerical checks have been performed between the IAU 2000 formulations of the classical and the new transformations. These comparisons revealed the need for improvements to the classical form of the transformation in order to achieve the required level of accuracy. Once these improvements are applied, the consistency between (i) the positions of the CIP in the GCRS and (ii) the rotation about the CIP axis, in the CEO-based and equinox-based transformations, when using the IAU 2000 expressions, are at a level of a few microarcseconds after one century (See Figures 1 and 2).

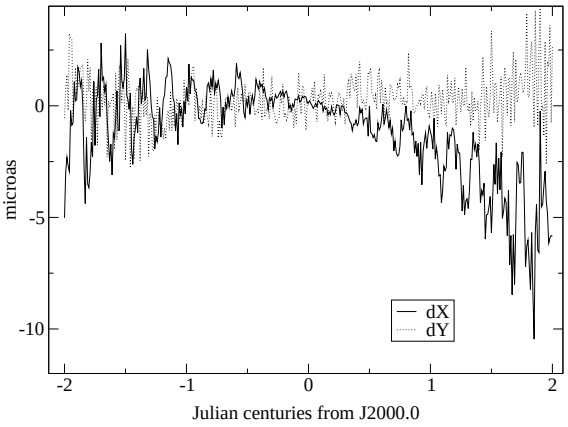

Figure 1: Differences in the GCRS CIP coordinates between the new and classical paradigms using the IAU 2000 expressions (Capitaine et al. 2003a)

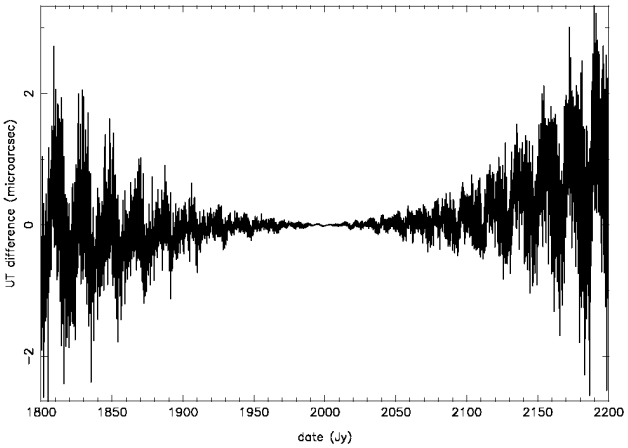

Figure 2: Differences in UT1 between the new and classical paradigms using the IAU 2000 expressions (Capitaine et al. 2003b)

6. REFERENCES

Aoki, S., Guinot, B., Kaplan, G. H., Kinoshita, H., McCarthy, D. D., Seidelmann, P. K., 1982, "The new definition of Universal Time", *Astron. Astrophys.***105**, 359–361.

Brzeziński, A., 2001, "Diurnal and subdiurnal terms of nutation: a simple theoretical model for a nonrigid Earth," in the Proceedings of the *Journées Systèmes de Référence Spatio-temporels* 2000, N. Capitaine (ed), Observatoire de Paris, pp. 243–251.

Brzeziński, A., July 2002, Circular 2, IAU Commission 19 WG "Precession-nutation".

Brzeziński, A., and Capitaine N., 2003, "Lunisolar perturbations in Earth rotation due to the triaxial figure of the Earth: geophysical aspects," in the Proceedings of the *Journées Systèmes de Référence Spatio-temporels* 2001, N. Capitaine (ed), Observatoire de Paris, pp. 51–58.

Brzeziński, A., Mathews, P.M., 2003, "Recent Advances in Modeling the Lunisolar Perturbation in Polar Motion Corresponding to High Frequency Nutation : Report on the Discussion of the IAU Commission 19 WG on Nutation", this Volume.

Capitaine, N., 1990, "The Celestial Pole coordinates", *Celest. Mech. Dyn. Astr.***48**, 127–143.

Capitaine, N., 2000a, in "Polar motion : Historical and scientific problems", ASP Conference series, Vol 208, S. Dick, D.D. McCarthy and B. Luzum eds, pp 573–584.

Capitaine, N., 2000b, "Definition of the Celestial Ephemeris Pole and the Celestial Ephemeris Origin" in "Towards Models and Constants for Sub-microarcsecond Astrometry", K. Johnston, B. Luzum, D.D. McCarthy and G. Kaplan eds, pp 153–163.

Capitaine, N. and Gontier A.-M., 1993, "Accurate procedure for deriving UT1 at a submilliarcsecond accuracy from Greenwich Sidereal Time or from stellar angle," *Astron. Astrophys.***275**, 645–650.

Capitaine, N., Guinot, B., McCarthy, D.D., 2000, "Definition of the Celestial Ephemeris origin and of UT1 in the international Reference Frame," *Astron. Astrophys.***335**, 398–405.

Capitaine, N., Chapront J., Lambert, S., Wallace, P.T, 2003a, "Expressions for the Celestial Intermediate Pole and Celestial Ephemeris Origin consistent with the IAU 2000A precession-nutation model", *Astron. Astrophys.***400**, 1145–1154.

Capitaine, N., Wallace, P.T, McCarthy, D.D., 2003b, "Expressions to implement the IAU 2000 defintion of UT1", *Astron. Astrophys.***406**, 1135–1149.

Capitaine, N., Chapront J., Wallace, P.T, 2003c, "Expressions for IAU 2000 precession quantities", *Astron. Astrophys.*, in press.

Chapront, J., Chapront-Touzé M., and Francou, G., 2002, 'A new determination of lunar orbital parameters, precession constant and tidal acceleration from LLR measurements," *Astron. Astrophys.***387**, 700–709.

Escapa, A., Getino, J., and Ferrándiz, J. M., 2003, "Influence of the triaxiality of the non-rigid Earth on the J2 forced nutations," in the Proceedings of the *Journées Systèmes de Référence Spatio-temporels* 2001, N. Capitaine (ed), Observatoire de Paris, pp. 275–281.

Guinot, B., 1979, "Basic Problems in the Kinematics of the Rotation of the Earth," in *Time and the Earth's Rotation*, McCarthy, D. D. and Pilkington, J. D. (eds), D. Reidel Publishing Company, pp. 7–18.

IERS Conventions 2000, http://www.usno.mil/ Conventions 2000, draft.

IERS Technical Note 29, 2002, N. Capitaine *et al.* eds, Verlag des Bundesamts für Kartographie und Geodäsie, Frankfurt am main.

Lambert, S., Bizouard, C., 2002, "Positioning the Terrestrial Ephemeris Origin in the International Terrestrial Frame," *Astron. Astrophys.***394**, 317–321.

Ma, C.,Arias, E.F., Eubanks, M. Fey, A.L., Gontier, A.-M., Jacobs, C.S., Archninal, B.A., Charlot, P., 1998, "The International Celestial Reference Frame as Realized by Very Long Baseline Intermferometry", *Astron. J.***116**, 516–546.

Mathews, P.M. and Bretagnon P., 2003, "High frequency nutation," in the Proceedings of the *Journées Systèmes de Référence Spatio-temporels* 2001, N. Capitaine (ed), Observatoire de Paris, pp. 28–33.

Mathews, P.M., Herring, T.A., Buffett B.A., 2002, "Modeling of nutation-precession: New nutation series for nonrigid Earth, and insightS into the Earth's Interior," *J. Geophys. Res.*107, B4, 10.1029/2001JB000165.

McCarthy, D. D. and Luzum, B. J., 2003, "An Abridged Model of the Precession-Nutation of the Celestial Pole," *Celest. Mech.***85**, 35-49.

Souchay, J., Loysel, B., Kinoshita, H., and Folgeira, M., 1999, "Corrections and new developments in rigid Earth nutation theory: III. Final tables REN-2000 including crossed-nutation and spin-orbit coupling effects," *Astron. Astrophys.***135**, 111–131.

Wallace, P. T., 2000, in *Towards Models and Constants for Sub-Microarcsecond Astrometry*, K. Johnston, D. D., McCarthy, B. Luzum and G. Kaplan (eds), US Naval Observatory, Washington, D.C., pp. 353–362.

Wallace, P., T. 2002, IERS Technical Note 29, N. Capitaine *et al.* eds, Verlag des Bundesamts für Kartographie und Geodäsie, Frankfurt am main, 65 –67.

DEFLECTION OF THE VERTCAL IN BUCHAREST DERIVED FROM GEODETIC ASTRONOMICAL OBSERVATIONS

R. POPESCU*, P. POPESCU*, O. BADESCU**

*Astronomical Institute of the Romanian Academy
6Str. Cuţitul de Argint 5, RO-752121, Bucharest, Romania
pradu@aira.astro.ro, petre@aira.astro.ro

**Faculty of Geodesy, University of Civil Engineering
Bdul. Lacul Tei 124, Bucharest, Romania
tavone@xnet.ro

ABSTRACT.

In order to develop a zeroth order network of deflection of the vertical, the Astronomical Institute joined with the Faculty of Geodesy has started in Bucharest a scientific project. There were used two very precise instruments: the CCD astrolabe and Leica TC 2002 theodolite. The used software package based on FK5 star catalogue has been designed to work both with classical mechanical theodolite and CCD astrolabe.
This paper emphasizes the methods of observation, reduction techniques, and results. The value of the determined vertical deflection in Bucharest, reported at WGS84 ellipsoid, is about 11".5, while the variance for each component lies under 0".4.

1. DEDUCTION OF VERTICAL DEFLECTION

1.1 Introduction

The connection between space-related observations using GPS technology, and ground based measurements such as VLBI or SLR, demands a better knowledge of the parameters related to the equipotential surface at sea level. These parameters lead to the problem of local vertical deflection reported to the reference ellipsoid. In astronomical geodesy, the local plumb line is related to the astronomical coordinates (Φ, Λ), derived from star observations. In exchange, geodetic coordinates (B, L), obtained by means of GPS technology, give the direction of the normal to the ellipsoid. In the same Earth surface point, the disagreement between the two series of data, i.e. the differences: Φ - B and Λ-L, particularly reflect the unparallelism between the local vertical, and the normal reported to the surface. Transitions regarding these differences in several different local points on Earth's surface could be explained as anomalies in tectonic mass distribution.

1.2 Astrogeodetic method

The main drawback of the gravimetric method is not being straight. The vertical deflection is not immediate, but results after a great amount of calculus performed upon the detected values

of gravitational acceleration. Besides, the method implies expensive hardware(high precision gravimeters).

In comparison with the gravimetric method, the astrogeodetic method is direct, allowing the immediate deduction of the orthogonal components of vertical deflection. That can be easily performed by comparing the astronomical values of coordinates with those obtained by GPS technology.

The first component denoted by ξ is in the plane of local meridian, while the second component η is in the plane of prime vertical

The following relationship gives the angle of vertical deflection (u)

$$u = \sqrt{\xi^2 + \eta^2} \tag{1}$$

The ξ component can be written as the difference between astronomical Φ and geodetic B latitudes, in the same point of observation. Identically, η represents the difference between the two kinds of longitude (Λ and L) corrected of meridian convergence:

$$\xi = \Phi - B, \eta = (\Lambda - L)\cos\Phi \tag{2}$$

2. INTERNATIONAL PROJECTS AND JOINT VENTURES

The beginning of the 9th decade of the last century brought a revolutionary concept in satellitary technique: the GPS. For almost ten years, the scientifically community pointed out toward this new domain, according less interest to the other geodetic technologies

Nevertheless, in the last years one have assisted to sudden technological changes in the domain of terrestrial geodesy (electronic theodolits, gravimeters, EDM instruments), so we can now talk about a link between GPS technology and ground based techniques.

At the beginning of 2000, one have been developed new observational technologies, as a result of a close cooperation between several European research institutes and private entreprises (Swiss Geodetic Commision; Swiss Federal Office of Topography; Swiss Federal Institute of Technology; Leica Heerbrugg; Department of Mathemathical Sciences, University of Trieste, Italy; Istituto Geografico Militare Italiano; Institut für Geodäsie, Universität der Bundeswehr, Neubiberg, Deutschland; Department of Mathematics, Science Faculty, University of Lisbon, Portugal; etc.).

New extensive software packages such as *ICARUS* or *DIADEM* , based on the FK5 star catalogue have been released in order to determine the local vertical deflection, as keystone of geoide fine structure determination.(Bürki, 2002).

These new projects have been tested in several European countries, such as: Swiss, Italy, France, Spain, Greece, Germany, Portugal.

3. ROMANIAN CAMPAIGN OF OBSERVATIONS

3.1 The start of a joint project in Bucharest

The Astronomical Institute joined the Faculty of Geodesy, in the attempt to develop a network of deflections of the vertical. Hence, a new scientific project has been started at Bucharest.

3.2 Observations: sites, instruments and reduction methods

For the very beginning of this project, there have been chosen to points of observation: the first point is located at AIRA, on the astrolabe pilaster and have the GPS coordinates (B=44^o 24'

43". 059, L=26^{o}05' 38". 024). The second site, whose GPS coordinates are (B = 44^o 27' 50". 247, L = 26^o 07' 32". 993), is located at TUCE, on the roof of the Faculty of Geodesy.

The distance between the observational sites is 6 km. There were used two very precise instruments: the CCD astrolabe and Leica TC 2002 theodolite. Astrolabe observations were performed only at AIRA, while visual observations with the mechanical theodolite were performed in both sites.

The used software package, based on FK5 star catalogue, has been designed to work both with classical mechanical theodolite and CCD astrolabe. Usually, the reduction of astronomical data achieved at ground asks for resolution, the classic method *of equal altitude*. All the astronomical data obtained with CCD astrolabe have been reduced by this method. In exchange, the set of observational data obtained with the mechanical theodolite has been reduced by means o a new method called: *measurements checked by unknowns*.

Here, the depart relationship remains as in the classical procedure, the well known expression:

$$F = \sin\varphi \sin\delta + \cos\varphi \cos\delta \cos H - \cos z = 0 \tag{3}$$

Beside $d\lambda$, $d\varphi$, and dr, the unknown vector also contains two additional unknowns(ν_t, ν_z), related to the directly measured parameters, i.e. timing and zenithal distance of stars passage.

The condition equation can be written:

$$\left(\frac{\partial F}{\partial t}\right)\nu_t + \left(\frac{\partial F}{\partial z}\right)\nu_z + \left(\frac{\partial F}{\partial \lambda}\right)d\lambda + \left(\frac{\partial F}{\partial \varphi}\right)d\varphi + \left(\frac{\partial F}{\partial r}\right)dr \tag{4}$$

In order to solve the system, one have to introduce a special matrix, called the pound matrix. The pound for ν_t associated to each observed star is given by formula:

$$p_t = (\cos\delta \sin\omega)^2 \tag{5}$$

while for ν_z, the pound is set to the unity.

Atudorei (1993), and Badescu (2002) present a rigorous demonstration of this method.

3.3 Statistical analysis concerning the results obtained at AIRA (astrolabe pilaster), with both instruments

The observational situation is syntactically described in table1. Unless both of them are based on astronomical observations, there are a lot of differences between the two methods (different instruments, number of nights and observed stars, different dates, and even different mode of synchronizing the time)

As remark, one have to mention that ξ and η , obtained by both methods, are obtained as results of astronomical observations, corrected of polar movement.

Preliminary tests with the CCD astrolabe have begun in 1997(Popescu et al. 1997), but reliable observational data concerning the vertical deflection in Bucharest, have been obtained only since 1998 (Popescu 1999).

The averaged values of obtained data, and their dispersions are shown in table 2. It worth to remark the similarity between both sets of data.

Concerning the observational correctness denominated by σ_ξ, and σ_η, we can say it is 3-4 times better in the case of CCD observations. That can be explained first, by the great quantity of observed stars during the night; as soon as the number of observed stars rises toward 100 by night, σ falls down under 0.2". On the other hand, the computer aided observations with accurate timing (time GPS), increases the accuracy.

Figures 1 and 2 show the variation of ξ and η, obtained with both instruments at the same location, during the period of observation(1998-2002):

Characteristics	**Method#1**	**Method#2**	**Observations**
Location	Astrolabe pilaster A.I.R.A	Astrolabe pilaster A.I.R.A	In the same point have been used both methods of reduction
Period of observation	1998 -2002	2002	Different perriods of observation
Observers	AIRA	TUCE	Different observators.
Instruments	CCD astrolabe (set)	Leica TC 2002 (portable)	Completely different observing instruments with different accuracy
Number of nights of observation	34	9	no observations
Star catalogue	FK5	FK5 GSC	no observations
Observations	Zenithal: almucantharat of 45^o	Both azimuthal and zenital any value	no observations
Time	UTC$\Longrightarrow$GPS + time card	UTC$\Longrightarrow$Internet, portable chronometer	no observations
Average number of observed stars by night	$\approx$30	$\approx$18	Method #1:great variation of observed stars at different nights.; Method #2: no variation of observed stars at different nights
Reduction method	Equal altitudes	Measurements cheked by unknowns	no observations
One observed star $\Rightarrow$	one ecuation	two ecuations	#1 : n stars$\Rightarrow$n ecuations #2 : n stars$\Rightarrow$ 2n ecuations
Number of unknowns	3	3	no observations
Geodetic coordinates	WGS 84	WGS 84	no observations

Table 1:

CCD	$\xi_{\mathbf{avr}}$	$\mathbf{d}_\xi$	$\eta_{\mathbf{avr}}$	$\mathbf{d}_\eta$	**Leica2002**	$\xi_{\mathbf{avr}}$	$\mathbf{d}_\xi$	$\eta_{\mathbf{avr}}$	$\mathbf{d}_\eta$
(”)	11.679	0.349	4.776	0.323	(”)	11.415	0.378	4.578	0.457

Table 2:

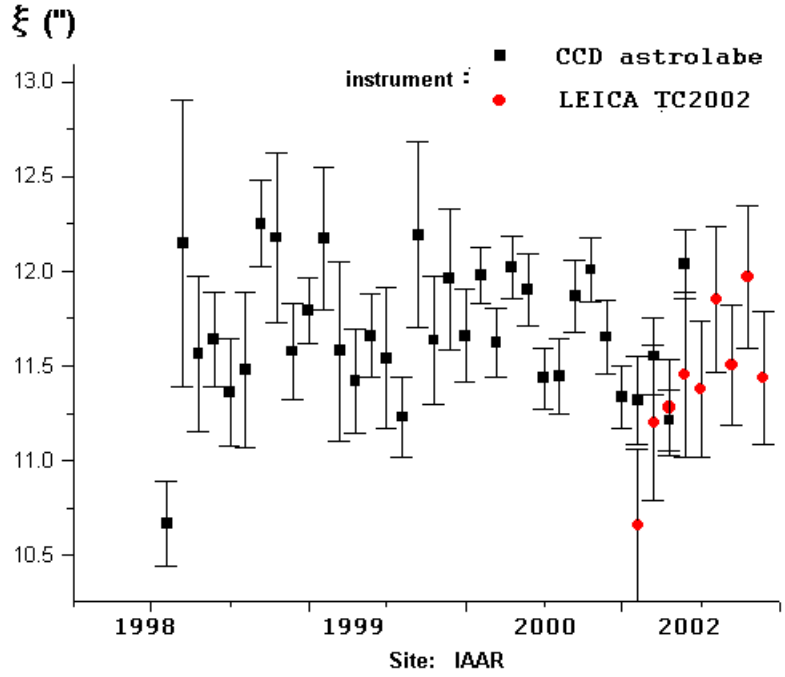

Figure 1: Time variation of ξ since 1998-2002

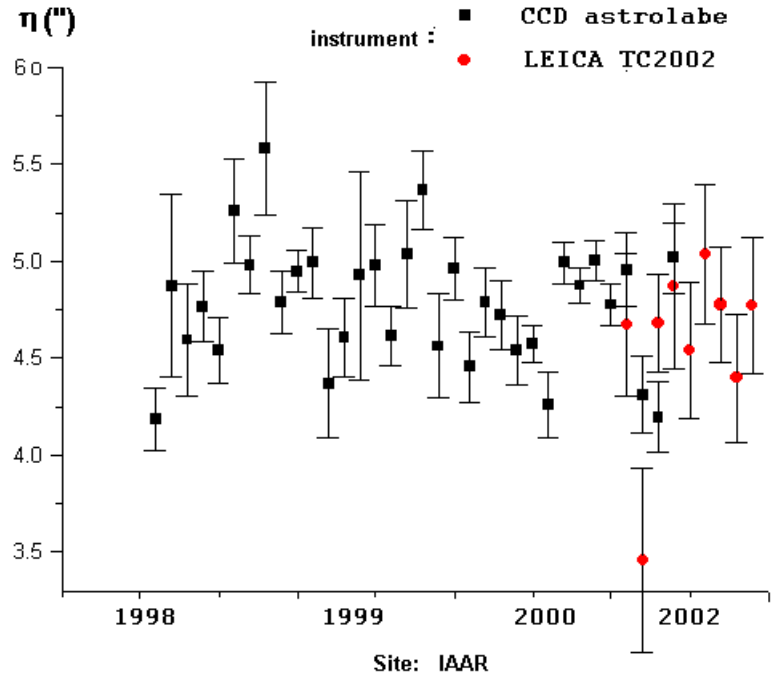

Figure 2: Time variation of η since 1998-2002

4. CONCLUDING REMARKS

- A statistical study concerning the obtained values shows the homogenousness of standard deviations in both cases of of ξ and η, no matter what method was used. That means no significative differences in obtained precisions at different nights of observations. The Barlett test applied on data set shows $\chi^2 = 0.3576$ ¡ χ^2 (P=95% ,f=3-1 = 2) = 5.95 for meridian component (ξ) and c2 = 1.9566 ¡ c2 (P=95%, f=3-1 = 2) = 5.95 for prime vertical component (η).

- The comparation between the two method can be done only at level of data associated dispersions. It consist in verifiing the differences (if there exist) between both statistic populations. After appliing the F test (small number of determinations) it results a significative difference. First method is more precise, as we already attempted. On the other hand, a small number of determinations can't be characteristic and we hope to continue the series of observations.

- None of applied statistic tests confirmed the presence of factors acting sistematicly upon the results

- The mean external accuracies (1σ) for the components of the deflection in latitude and longitude are estimated to be ¡ 0".2, and about 0".4 in case of theodolite observations. The results seems to be reasonable, comparable with those obtained in Netherland (% ¡ 0".3), Italy, and Swiss.

5. REFERENCES

Atudorei, M.:1993,Revista de Geodezie, Cartografie si Cadastru, **2**, 2.
Badescu, O.: 2002, PhD thesis, Bucharest
Bürki, B.: 2002,www.ggl.baug.ethz.ch/research/.
Popescu, P., Popescu, R., Paraschiv, P.:1997a, Romanian Astronomical Journal, **7(2)**, 189.
Popescu, R.: 1999 private communication, Poznan.

POSITIONING THE TERRESTRIAL EPHEMERIS ORIGIN IN THE INTERNATIONAL TERRESTRIAL REFERENCE FRAME

S. LAMBERT, C. BIZOUARD
SYRTE - UMR8630/CNRS, Observatoire de Paris
61 avenue de l'Observatoire 75014 Paris, FRANCE
e-mail: Sebastien.Lambert@obspm.fr

ABSTRACT. Resolution B1.8 adopted by the XXIV General Assembly of the International Astronomical Union (Manchester, august 2000) recommends the use of the Non-Rotating Origin (Guinot 1979) on the moving equator both in the International Celestial Reference System (ICRS) and in the International Terrestrial Reference System (ITRS). The Non-Rotating Origin (NRO) in the ITRS is designated the Terrestrial Ephemeris Origin (TEO). Resolution B1.8 is to be implemented on 1 January 2003 by the International Earth Rotation Service (IERS) which is required to provide the position of the TEO in the ITRS. This paper is devoted to the calculation of this position. Because the TEO depends on the polar motion, which is poorly modeled, its position has been derived from observational data. This has been compared to an analytical model based on a simplified representation of polar motion. We propose then a numerical expression for the displacement of the TEO to be used in the new coordinate transformation from the Celestial Reference System to the Terrestrial Reference System according to the resolution.

1. INTRODUCTION

The study has been realized in the framework of the resolutions adopted by the XXIV General Assembly of the International Astronomical Union (Manchester, August 2000) concerning the transformation between the Celestial Reference System (CRS) and the Terrestrial Reference System (TRS), which are to be implemented in the International Earth Rotation Service (IERS) procedures on 1 January 2003.

Resolution B1.8 recommends the use of the Non-Rotating Origin (NRO) on the moving equator to reckon the angle of rotation of the Earth. The NRO (also called departure point) in the Celestial Reference System (CRS) is defined by the kinematical condition of non-rotation of this point around the rotation axis when the rotation pole moves in the CRS (Guinot 1979). Similarly, the NRO in the Terrestrial Reference System (TRS) is defined by the kinematical condition of non-rotation around the rotation axis when the rotation pole moves in the TRS. The properties of these two points have already been studied in Capitaine *et al.* (1986 and 2000).

In practice, the determination of the Earth orientation refers to the Celestial Intermediate Pole (CIP), defined by IAU 2000 resolution B1.7, which is the pole correponding to an axis closed to the rotation axis (difference smaller than 20 mas). Therefore :

• The NRO as realized by taking into account the motion of the CIP in the Celestial Reference

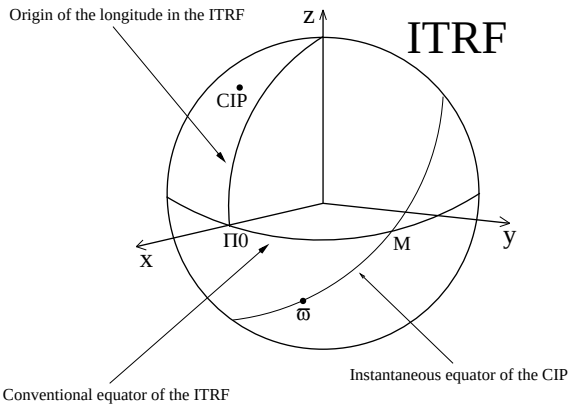

Figure 1: The Non-Rotating Origin with respect to the ITRF.

System (CRS) gives a point on the moving equator of date noted σ and designated by the Celestial Ephemeris Origin (CEO).

• The NRO as realized by taking into account the motion of the CIP in the Terrestrial Reference System (TRS) gives a point on the moving equator of date noted ϖ and designated as the Terrestrial Ephemeris Origin (TEO).

Astrometric and geodetic data analysis software involve the computation of the transformation between the CRS and the TRS. In the framework of the IAU 2000 recommendations, they need an expression for the displacement of the Terrestrial Ephemeris Origin both for the classical transformation and for transformation based on the Non-Rotating Origin representation.

The study is focused on the computation of the position of the TEO in the ITRS.

2. FORMULATION

Consider a displacement of the CIP between dates t_0 and t, the point ϖ along the moving equator defines the broken arc s' (see Figure 1) :

$$s' = \varpi M - \Pi_0 M - (\varpi_0 M_0 - \Pi_0 M_0). \tag{1}$$

In this definition, ϖ and ϖ_0 represent the position of the departure point at dates t and t_0, Π_0 is the origin of the longitude in the ITRF, and M and M_0 are the nodes between the conventional equator of the ITRF and the equators of dates t and t_0. Because of the fact that the kinematical condition does not constrain the position of ϖ_0 along the moving equator, it is convenient to take, by convention (Capitaine *et al.* 1986) :

$$\varpi_0 M_0 - \Pi_0 M_0 = 0. \tag{2}$$

The displacement of the TEO in the ITRS, s', is related, for a date t, to the CIP coordinates u and v in the TRS by the formula :

$$\begin{aligned} s' &= \varpi M - \Pi_0 M \\ &= -\int_{t_0}^{t} \frac{u\dot{v} - \dot{u}v}{2} \mathrm{d}t, \end{aligned} \tag{3}$$

where u corresponds to the coordinate x_p of the CIP in the ITRS, v refers to $-y_p$, and the dot is for the time derivative. The integration is made between dates t_0 and t.

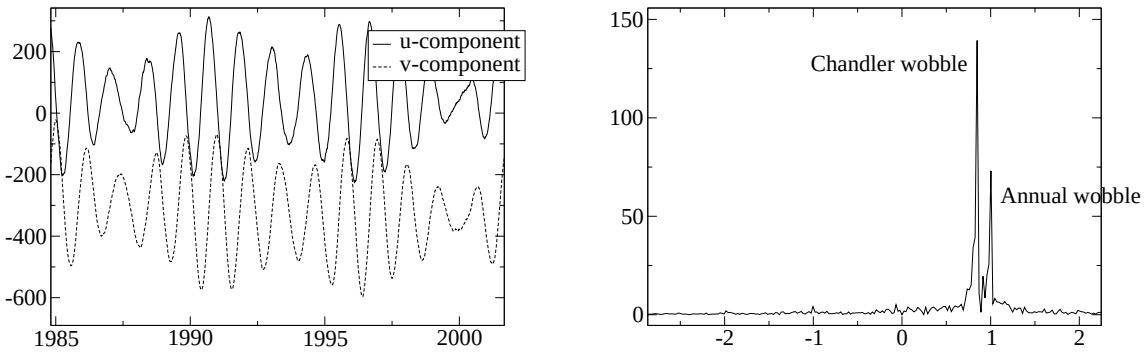

Figure 2: Left side : bserved polar motion during the last two decades from the IERS C04 series, amplitudes are in mas, u-component (x_p) is in full line, v-component ($-y_p$) is in dotted line, the time is given in years. Right side : complex spectrum of polar motion (Fast Fourier Transform) over the total duration of the IERS C04 series (1962-2002), amplitudes are in mas, frequencies are in cycles per year (cpy).

3. POSITIONING FROM GEODETIC DATA

The computation of s' is based upon combined time series C04 for polar motion which is provided by the Earth Orientation Parameters Product Center of the International Earth Rotation Service (IERS EOP-PC) based at the Paris Observatory, France. Such a series is obtained by the combination of individual polar motion series from various spatial and geodetic techniques such as Very Long Baseline radio Interferometry (VLBI), Global Positioning System (GPS, GLONASS), Satellite Laser Ranging (SLR) or Lunar Laser Ranging (LLR). This series give daily averaged values for the CIP coordinates x_p, y_p, the values for $UT1-UTC$ and length-of-day LOD, and the Celestial pole offsets $d\psi$ and $d\epsilon$ which are the corrections to the nutation model IAU 1980. For a sampling of one day (at 0h UTC) the data covers the period from 1962 january 1st until 2002 (see Figure 2).

Let $u = x_p$ and $v = -y_p$ be the CIP coordinates in the ITRS. From time series of u and v, we can compute numerically the quantity s' given by equation (3). The result of the computation is plotted in Figure 3.

We notice that the curve of s' shows a periodic variation with period 2334.4 days with an amplitude that reaches 1 μas and which is also present in the polar motion (see Figure 2). Smaller oscillations with Chandlerian and annual periods are also visible. The trend of the curve is varies during the 40 years depending on the variations of the amplitudes of the chandlerian and annual wobbles. It is a well known fact that the Chandler wobble has undergone some drastic variations in amplitude and phase during the twentieth century. For details see (Guinot 1972) and (Vondrák 1985).

4. POSITIONING BASED ON MODEL FOR POLAR MOTION

It is well known that the polar motion, at low frequencies (periods longer than a few days), is

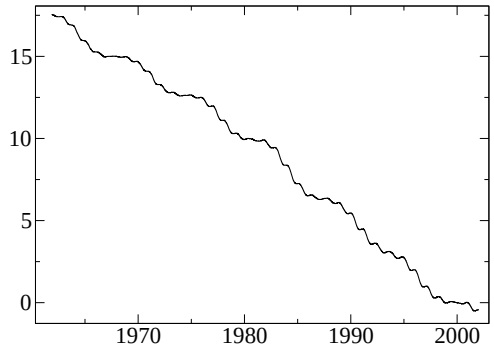

Figure 3: Displacement s' of the Terrestrial Ephemeris Origin over the total duration of the IERS C04 series (1962-2002), the time is given in years, amplitudes are in μas.

mostly a combination of the Chandler wobble, with a period of about 433 days (Lambeck 1988), and the annual oscillation. The combination of these two oscillations causes a modulation of 2334.4 days (about 6.4 years) which is clearly visible in Figure 2. In addition, we observe a linear trend in both coordinates.

In this section, we assume that the observed polar motion is well represented by two prograde circular waves at the above periods and by a linear trend :

$$\begin{aligned} u &= A_c \cos(\sigma_c t + \phi_c) + A_a \cos(\sigma_a t + \phi_a) + u_0 + u_1 t, \\ v &= A_c \sin(\sigma_c t + \phi_c) + A_a \sin(\sigma_a t + \phi_a) + v_0 + v_1 t, \end{aligned} \tag{4}$$

where A_c and A_a are the real amplitudes of the Chandler and annual wobbles respectively and are considered as constant over the span of the series, σ_c and σ_a are the Chandler and annual frequencies, with the respective phases ϕ_c and ϕ_a refered to epoch J2000.0. The non-periodic terms are represented by u_0, v_0, u_1 and v_1. After an analytical integration, we obtain a model for s' in the form :

$$s'(t) = L(t) + B(t) + P(t), \tag{5}$$

where the first term is the linear trend

$$L(t) = -\frac{1}{2}\left[\sigma_c A_c^2 + \sigma_a A_a^2 + v_1 u_0 - u_1 v_0\right] t. \tag{6}$$

The second term contains periodic terms of period 2334.4 days :

$$B(t) = -\frac{1}{2}\frac{\sigma_c + \sigma_a}{\sigma_c - \sigma_a} A_c A_a \sin((\sigma_c - \sigma_a)t + (\phi_c - \phi_a)). \tag{7}$$

The last term is less significant and more complex. It contains Chandler and annual periods and combined terms $t \times \sin$ or $t \times \cos$ (see Lambert and Bizouard 2002).

As we mentionned above, Chandlerian and annual wobbles amplitudes have known variations. To illustrate these variations, least-squares fits of Chandler, annual and linear terms over three windows spanning twenty years were performed. Then we have computed the amplitudes of the main terms expressed in above equations, L and B, for three periods of 20 years. Results are displayed in Table 1. The periodic term $B(t)$ is, with these values, below the desirable accuracy,

Table 1: Values of the main terms of s' as presented in equations (1), (6) and (20) for three different periods and different amplitudes of the Chandler wobble A_c and the annual wobble A_a.

	1962-1982	1972-1992	1982-2002
A_c mas	140	160	178
A_a mas	92	87	80
L μas pjc	-38	-44	-51
B μas	0.4	0.4	0.4

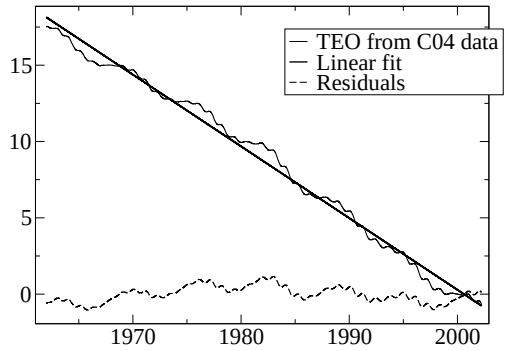

Figure 4: Displacement of the Terrestrial Ephemeris Origin s' over the total duration of the IERS C04 series (1962-2000) and the model given by expression 9. The time is given in years, displacements are in μas.

and should be neglected. At 1 μas accuracy over the last 40 years, the expression for s' is reduced to a linear form :

$$s'(t) - s'(t_0) = -\frac{1}{2}\left[\sigma_c A_c^2 + \sigma_a A_a^2\right] t. \tag{8}$$

The diurnal and subdiurnal tidal variations for polar motion provided by Ray (McCarthy 1996 and Ray 1994) should be added for a more rigourous study due to possible effects from their very short periods in the time integration. These high-frequency contributions are very small compared to the amplitude of the long periodic polar motion : they can reach a maximum of 0.5 mas. The effect is only about 0.06 μas per century and is therefore negligible (Lambert and Bizouard 2002).

5. EXPRESSION FOR POSITIONING THE TEO IN THE ITRF

As a conclusion of this study, we propose a numerical expression for the quantity s'. Although such a model is limited in time because of unpredictable changes in the wobbles amplitudes, it is possible to provide a numerical expression for s' which represents the motion of the TEO in the ITRS with an accuracy of 1 μas over the last 40 years. On this span, variations in the amplitudes of the wobbles will not produce an error larger than 1 μas. The following expression

is fitted on the curve obtained from C04 data :

$$s' = -47.0 \times t, \tag{9}$$

where s' is in μas. The parameter t is the Terrestrial Time (TT) expressed in julian centuries from epoch J2000.0 :

$$t = (\mathrm{TT} - 2000 \text{ january } 1\mathrm{d}\ 12\mathrm{h}\ \mathrm{TT})/36525, \tag{10}$$

with TT in days.

If the Chandler amplitude in the next years does not present variations larger than during the span 1962-2002, then according to Table 1, the uncertainty on the linear trend is 13 μas per julian century. We can ensure that the 1 μas accuracy linear model can be extended for the 10 next years.

Figure 4 shows the linear model of s' corresponding to expression (9) together with the numerical computation from observations. If unexpected variations in the amplitudes of the wobbles occur in the coming years, such a model will have to be updated.

REFERENCES

Capitaine N., Guinot B., Souchay J., 1986, Celest. Mech. 39, 283

Capitaine N., Guinot B., McCarthy D. D., 2000, A&A 355, 398

Guinot B., 1972, A&A 19, 207

Guinot B., 1979, In: McCarthy D. D. and Pilkington J. D. (eds.) Time and the Earth's Rotation. D. Reidel Pub. Co., p. 7

Lambert S., Bizouard C., 2002, A&A 394, 317

Lambeck K., 1988, Geophysical Geodesy - The Slow Deformation of the Earth, Oxford Science Publications

McCarthy D. D., 1996, IERS Conventions. IERS Technical Note 21, Observatoire de Paris

Ray R., Steinberg D. J., Chao B. F., Cartwright D. E., 1994, Science 264, 830

Vondrák J., 1985, Annales Geophysicae 3, 351

PLANETARY ROTATION AND STABILITY OF SATELLITE ORBITS

V. MIOC
Astronomical Institute of the Romanian Academy
Str. Cuţitul de Argint 5, RO-752121 Bucharest, Romania
e-mail: vmioc@aira.astro.ro

ABSTRACT. The planetary rotation acts on the satellite dynamics mainly via the zonal harmonics of the gravitational potential. We study the equatorial satellite orbits in a planetary fieldcharacterized by zonal harmonics up to the fifth order.

To depict the phase-space structure, we resort to McGehee-type coordinates, as well as to foliations by the energy constant and angular momentum constant. Various stability regions are found for each case.

The problem presents interesting features, as for instance: cases when all traiectories (except a separatrix) are stable; existence of stable motion for nonnegative energy levels; positive Lebesgue measure for initial data leading to quasiperiodic and noncircular periodic orbits; important role of the angular momentum.

1. INTRODUCTION

The planetary rotation influences the dynamics of a satellite primarily via the zonal harmonics of the gravitational potential (but through other effects, too). In this paper we study such an influence by tackling the equatorial motion of a satellite in the field of a planet featured by the potential

$$U = \sum_{n=1}^{6} a_n / r^n,$$

where r is the reciprocal distance, whereas a_n are real parameters. We consider $a_1 > 0$, $a_2 = 0$, $a_3 < 0$, as in the general planetary case in the solar system. Also, to obtain the most general situations, we considered the whole sign interplay among a_4, a_5, and a_6.

We work in collision-blow-up coordinates introduced by McGehee (1974). To identify the stability zones, we use the reduced 2D phase space, depicting all possible phase curves for negative, positive, and zero energy, for the collisional ($a_6 > 0$) and noncollisional ($a_6 < 0$) cases, and resorting to a foliation by the angular momentum. We find surprising stability regions for negative-energy levels (Figures 1a, 1d below), and even for nonnegative-energy levels. The stable orbits are either circular (relative equilibria) or noncircular (periodic and quasiperiodic). The initial data that lead to the latter ones have positive Lebesgue measure.

2. BASIC EQUATIONS

The two-body problem associated to our field can be reduced to a central-force problem.

The planar motion of the satellite with respect to the planet is described by the Hamiltonian $H(\mathbf{q},\mathbf{p}) = |\mathbf{p}|^2/2 - \sum_{n=1}^{6} a_n/|\mathbf{q}|^n$, where $\mathbf{q} = (q_1, q_2) \in \mathbf{R}^2 \setminus \{(0,0)\}$, $\mathbf{p} = (p_1, p_2) \in \mathbf{R}^2$ are the configuration vector and the momentum vector of the satellite, respectively. It is clear that the problem admits the first integrals of angular momentum ($q_1p_2 - q_2p_1 = L = \text{constant}$) and of energy ($H(\mathbf{q},\mathbf{p}) = h/2 = \text{constant}$).

To remove the isolated singularity at the origin $\mathbf{q} = (0,0)$, which corresponds to a collision (Mioc and Stavinschi 2001, 2002), we apply the following sequence of McGehee-type transformations (McGehee 1974):

$$\begin{aligned} r &= |\mathbf{q}|, \qquad \theta = \arctan(q_2/q_1), \\ \xi &= \dot{r} = (q_1p_1 + q_2p_2)/|\mathbf{q}|, \qquad \eta = r\dot{\theta} = (q_1p_2 - q_2p_1)/|\mathbf{q}|, \end{aligned} \tag{1}$$

which introduce standard polar coordinates,

$$x = r^3\xi, \qquad y = r^3\eta, \tag{2}$$

which scale down the velocity components, and a Sundman-type rescaling of time $d\tau = r^{-\alpha}dt$, $\alpha \in \mathbf{N}$. (This last transformation does not interest us in what follows.) In this way we obtain regular equations of motion. Under the transformations (1)−(2), the angular momentum integral and the energy integral become respectively

$$y = Lr^2, \tag{3}$$

$$x^2 + y^2 = hr^6 + 2\sum_{n=1}^{6} a_n r^{6-n}, \tag{4}$$

whereas the singularity at $r = 0$ was replaced by the collision manifold $M_0 = \{(r,\theta,x,y) \mid r = 0, \theta \in S^1, x^2 + y^2 = 2a_6\}$ pasted on the phase space.

The regularized equations of motion do not contain θ explicitly, so we can factorize the flow by S^1. Next, we eliminate y between (3) and (4). In this way the phase-space dimension was reduced from 4 to 2. The energy integral in the (r,x)-plane will read

$$x^2 = f(r) = hr^6 + 2a_1r^5 - L^2r^4 + 2a_3r^3 + 2a_4r^2 + 2a_5r + 2a_6,$$

where we took into account the fact that $a_2 = 0$. Remark that, in this plane, M_0 reduces to the points $\mathrm{M}(0, \sqrt{2a_6})$ and $\mathrm{N}(0, -\sqrt{2a_6})$.

We shall describe the phase-space structure for negative, zero, and positive energy levels, analyzing the behaviour of the function $x = \pm\sqrt{f(r)}$. Since $x^2 \geq 0$, we shall consider only the positive roots of the polynomial in the right-hand side of above energy integral. We also shall consider, for the same purpose, the positive roots of the polynomial $\tilde{f}(r) = df(r)/dr = 6hr^5 + 10a_1r^4 - 4L^2r^3 + 6a_3r^2 + 4a_4r + 2a_5$. To deal with the most general case, we suppose that $\tilde{f}(r)$ has four changes of sign (the maximum possible) for $h < 0$. This entails a maximum of five positive roots (according to Descartes' rule) for collisional phase-space ($a_6 > 0$) and four positive roots for noncollisional phase-space ($a_6 < 0$). For $h \geq 0$, we suppose that $\tilde{f}(r)$ has three changes of sign (the maximum possible, which entails a maximum of four/three positive roots for collisional/noncollisional phase-space.

3. PHASE-SPACE STRUCTURE

The phase-space structure for $h < 0$ is plotted in Figure 1. In the collisional case ($a_6 > 0$), there exists a critical energy level $h_c^- < 0$ that creates, along with the interplay of the field parameters, three different portraits: Figures 1a, 1b, 1c for $h < h_c^-$, $h = h_c^-$, and $0 > h > h_c^-$,

respectively. The foliation performed by making $|L|$ increase points out a great variety of phase orbits, as well as bifurcations (corresponding to critical values of L) concretized by relative equilibria: two centres S (stable circular orbits) and two saddles U (unstable circular orbits).

The case illustrated in Figure 1a is the most interesting. There are two kinds of quasiperiodic and periodic orbits. The ones bounded by the loop generated by U_1 and the double loop generated by U_2 (1) have significant osculating eccentricities. Those situated inside the double loop are centered on either S_1 (2) or S_2 (3) and have smaller osculating eccentricities. Such trajectories are recovered in Figures 1b (1', 2') and 1c (1", 2"). All these orbits are stable.

In the noncollisional case ($a_6 < 0$), there also exists a critical energy level, but all situations lead to the phase portrait plotted in Figure 1d. Except the separatrix formed by the double loop associated to the saddle $\bar{U}$ (which creates zones wholly similar to those in Figure 1a), all other orbits are stable.

The phase-space structure for $h > 0$ is plotted in Figure 2. There also exist critical values of the energy level, which create three different phase portraits for $a_6 > 0$, or only one portrait for $a_6 < 0$. The stability zones lie inside the homoclinic loop associated to the saddles U_2 (Figure 2a), U_2" (Figure 2c), $\bar{U}$ (Figure 2d), or inside the heteroclinic loop created by the saddles U_1' and U_2' (Figure 2b). These stable orbits are quasiperiodic or periodic, and are centered on the equilibria S, S', S", $\bar{S}$ (all stable circular orbits).

The case $h = 0$ leads to exactly the same phase portraits as in Figure 2, but now the different pictures are generated only by the interplay of the field parameters.

4. CONCLUDING REMARKS

To search for stability regions in our problem, we depicted the phase portraits for the whole interplay among field parameters, energy level, and angular momentum. The most important features of the model (some of them surprising) are:

4.1. For $h < 0$, there exist cases (Figures 1a, 1d) in which a double loop associated to a saddle creates three zones of stable quasiperiodic and periodic orbits. Moreover, in Figure 1d all trajectories (but the separatrix) are stable.

4.2. There exist quasiperiodic and periodic orbits even for nonnegative energy levels.

4.3. The sets of quasiperiodic and noncircular periodic orbits have positive Lebesgue measure. Indeed, choosing initial data on such an orbit, and considering the foliations performed, in a neighbourhood of this point there exists an open set of initial data that lead to the same kind of orbit.

4.4. The role of the angular momentum is of the same importance as that of the energy. It creates bifurcations without regard to the energy level.

4.5. Our results were obtained for the maximum number of changes of sign of $\tilde{f}(r)$. Simpler mathematical situations entail simpler phase portraits. For instance, in the Earth's case, the phase-space structure is similar to that of Fock's problem (Mioc and Pérez-Chavela 2003): only one type of stable orbits for $h < 0$, and no stable orbit for $h \geq 0$.

4.6. Our results can add something to the explanation of the observed structure of the planetary rings, especially as concerns the existence of gaps.

5. REFERENCES

McGehee, R.: 1974, *Invent. Math.* **27**, 191.
Mioc, V., Stavinschi, M.: 2001, *Phys. Lett. A* **279**, 223.
Mioc, V., Stavinschi, M.: 2002, *Phys. Scripta* **65**, 193.
Mioc, V., Pérez-Chavela, E.: 2003, *J. Math. Phys.* **44** (to appear).

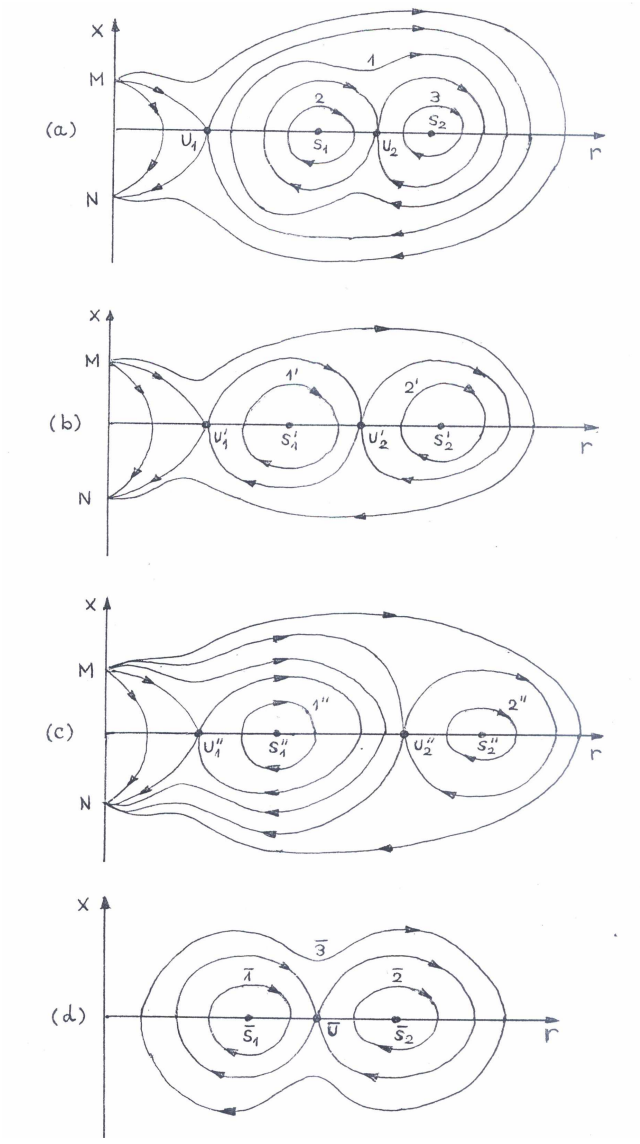

Figure 1: The phase portrait for $h < 0$, in the collisional case, for (a) $h < h_c^-$, (b) $h = h_c^-$, (c) $0 > h > h_c^-$, and in the noncollisional case (d).

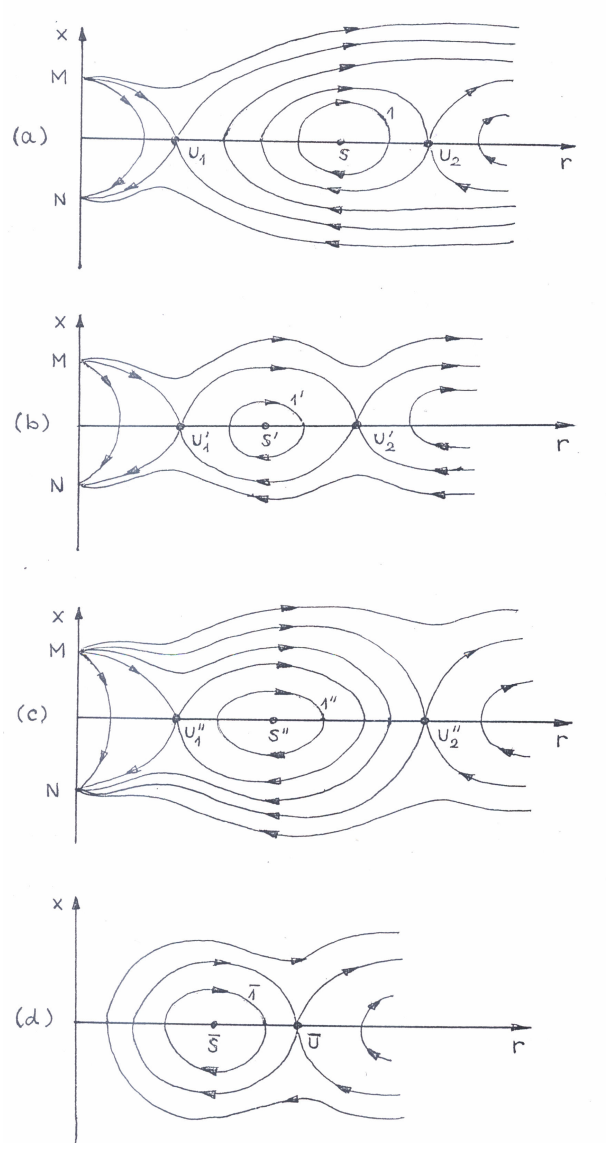

Figure 2: The phase portrait for $h \geq 0$, in the collisional case, for (a) $h < h_c^-$, (b) $h = h_c^-$, (c) $0 > h > h_c^-$, and in the noncollisional case (d).

REDUCTION OF COMPILED CATALOGUE IN THE SELECTED EXTRAGALACTIC RADIO SOURCE (ERS) FIELDS

YU.BABENKO[1], O.DANIL'TSEV[1], O.VERTYPOLOKH[1],
A.KOVALCHUK[2], YU.PROTSYUK[2], G.PINIGIN[2], A.SHULGA[2],
A.DEMENT'EVA[3], V.RYL'KOV[3], G.BOCSA[4], P.POPESCU[4]
[1])Astronomical Observatory of the Kyiv National University
Observatorna 3, 04053 Kyiv-53, Ukraine
e-mail: verto@observ.univ.kiev.ua
[2])Mykolajiv Astronomical Observatory
Observatorna 1, 54030 Mykolajiv-30, Ukraine
e-mail:yuri@mao.nikolaev.ua
[3])Main Astronomical Observatory at Pulkovo
Pulkovskoje Shosse 65/1, 196140 St-Petersburg-140, Russia
e-mail:vryl@gao.spb.ru
[4])Astronomical Institute of the Romanian Academy
Cutitul de Argint 5, 752121 Bucharest, Romania
e-mail:Gbocsa@aira.astro.ro

ABSTRACT. The work is devoted to the problem of deriving of the compiled catalogue of the positions of reference stars 12 - 15^m in the ICRF ERS vicinities for $-20° < \delta < 90°$. This research is made on the basis of the international Joint Project "Improvement of the link between optical and radio reference frames" collaboration [5]. Nikolaev Astronomical Observatory, Astronomical Observatory of Kyiv University, Main Astronomical Observatory of the Russian Academy of Sciences and Astronomical Institute of the Romanian Academy take part in compilation of the catalogue. The catalogue is created on a basis both original astrometric materials of these observatories and other known catalogues of stars in the ICRF ERS vicinities. It is planned to receive the first version of the catalogue in 2003 year.

1. INTRODUCTION

To solve the task of the maintenance and improvement of connection between radio and optical reference systems it is necessary to observe the optical counterparts of the reference ERS. To obtain their coordinates it is necessary to have secondary reference stars of 12-15 mag in ERS vicinities in Hipparcos reference system. For last decade a number of the catalogues with secondary reference stars in the ERS fields were made by different observatories (Kyiv, Nikolaev, Pulkovo, Bucharest and others). On the basis of these catalogues we intend to obtain

the compiled catalogue in the selected ERS fields in declination zone $-20^\circ < \delta < 90^\circ$.

2. OBSERVATIONS

Short description of individual catalogues is presented below. Four catalogues were obtained with the telescopes-astrographs and 3 others were obtained with CCD meridian circles.

Kyiv PIRS (Photographic Intermediate Reference Stars) Catalogue. The observations were carried out in 1989-1993 with the astrograph of the Kyiv university (D=200 mm, F=4126 mm) for 116 ERS fields. Tycho-2 catalogue was used as basic for the reduction of stars of 12-15 mag. Accuracy is about 80-100 mas in both coordinates for a single observation.

ERLcat (Extragalactic Reference Frame Link Catalogue). The observations were carried out in 1976-1994 by joint efforts of Hamburg Astronomical observatory and USNO for 398 fields with ERS [1,4]. The Northern Hemisphere was covered with the 23-cm zone astrograph located at Hamburg Observatory. The Southern Hemisphere was covered with the USNO Twin Astrograph at the Black Birch Astrometric Observatory in New Zealand. The reduction is performed for 89422 stars in an interval 12-15 mag with use of Hipparcos catalogue as basic. Accuracy is about 55 mas in both coordinates for a single observation.

Pulkovo. The observations of the stars of 10-16 mag in the vicinities of 36 ERS were made in 1991-1995 using the Pulkovo Normal Astrograph [6]. In order to reduce to Hipparcos frame the Tycho catalogue was used.

Bucharest. The observations of the 188 ERS fields were made with the Double Astrograph (D=380 mm, F=6000 mm) in 1991-2000. As the reference catalogue Tycho-2 was used.

CAMC. The number of catalogues (CAMC 1-11) are obtained with the Carlsberg Automatic Meridian Circle (D=178 mm, F=2665 mm) during the period from May 1984 to May 1998 [3]. The numbers of catalogues (CAMC 1-11) are contained 18000 reference stars in the fields of radio sources.

AMC1B. The CCD observations were made with the Nikolaev Axial meridian circle (D=180 mm, F=2480 mm) for 14403 stars in the vicinities of ERS. The observational epochs of 198 ERS fields were 1996-1998.

MAC1. The observations have been made with the Kyiv meridian axial circle (D=180 mm, F=2.3 m) for 256 fields of ERS in 2001-2002 [2]. Accuracy for stars 12-14 mag is about 50-100 mas in both coordinates for a single observation.

From the analysis of observed date it follows, that there are enough crossed fields for compilation of the summary catalogue, especially taking into account that in the catalogues for each field with ERS there are, as a rule, some plates or some observations. It's planning that the first version of the summary catalogue of stars in the fields with ERS for $-20^\circ < \delta < 90^\circ$ will be received in the first half-year of 2003.

3. REFERENCES

1. de Vegt, C., at al. 2001, AJ, 121, 2815.
2. V.Telnyuk-Adamchuk, et al. 2002, A&A, 386, 1153.
3. Carlsberg Meridian Catalogues La Palma Numbers 1-11. CD-ROM version. 1999.
4. http://ad.usno.navy.mil/erlcat/ERLcat.gz
5. N.Maigurova, et al. 2001, In "Extention and Connection of reference Frames using CCD ground-based Technique", G.Pinigin (ed.), Atoll, Nikolaev, P.52.
6. V.P.Ryl'kov, at al. 2001, In "Extension and Connection of reference Frames using CCD ground-based Technique", G.Pinigin (ed.), Atoll, Nikolaev, P.79.

KINEMATICS OF NEARBY AND DISTANT STARS

E. DROBITKO, V. VITYAZEV
The Sobolev Astronomical Institute of St.-Petersburg State University
198504, St.Petersburg, Petrodvoretz, Universitetsky pr., 28, Russia
e-mail: siggy@dorms.spbu.ru

ABSTRACT. The proper motions analysis of the main sequence stars and of the luminosity class III stars listed in the catalogue HIPPARCOS is presented. A new method based on representation of proper motions in coordinate systems whose poles are associated with each of the principal galactic axes is proposed. This method yields complete separation of all parameters of the Ogorodnikov-Milne model. The solutions for stars of different spectral classes are obtained. It was found that with respect to parallaxes the main sequence is splitted into two zones (distant and nearby stars) with rather sharp border at B-V = 0.5. It is shown that the Parenago's discontinuity may be connected with this effect.

1. INTRODUCTION

In 1950, Parenago [1] pointed out that parameters of the Solar motion and the dispersion of the stellar velocities show a certain dependence on spectral type with a sudden change at the F type. Later on this effect was named the *Parenago's discontinuity.*

The purpose of the present paper is looking at the Parenago's discontinuity from the standpoint of the newest astrometric data. The knowledge of parallaxes in HIPPARCOS catalogue gives us a possibility to separate the giants and dwarfs of the same spectral class and to localize them in 3D space. From 118 218 stars of HIPPARCOS catalogue we selected the stars which meet the following criteria: 1)only the single stars belonging to the 1.8^m-wide strips centered around the main sequence and the luminocity class III were used. The empirical lines of the main sequence and the luminocity class III have been taken according to [2]; 2)the only stars with the error of the parallax no more than 3σ, have been retained; 3)the fast stars with tangential velocities more than 80 km/sec have been excluded.

Samples of stars of the main sequence and of the giant stars were binned for different color indexes. For each bin we used the three-dimensional Ogorodnokov-Milne model [4] to get the kinematic parameters of thus formed star groups. This model was supplemented by the terms describing motion of the Sun with respect to chosen centroids. Such approach allows to determine the following parameters: U, V, W – the velocity components of the Solar motion in Galactic coordinate system; $M^+_{ij},\ i, j = 1, 2, 3$ – the elements of a matrix of local deformation of a velocity field; $\omega_i,\ i = 1, 2, 3$ – the components of the angular rate of rigid rotation of a stellar system with respect to the axes of the galactic trihedron.

The equations of conditions are defined by:

$$\mu_l \cos b = \sum_{i=1} L_i \ f_i(l, b, r), \tag{1}$$

$$\mu_b = \sum_{i=1} L'_i \ f'_i(l, b, r), \tag{2}$$

where L_i, L'_i are the described parameters; l, b, r are the galactic coordinates of a star with the proper motions $\mu_l \cos b$ and μ_b; $f_i(l, b, r)$, $f'_i(l, b, r)$ are known functions which determine the contribution of kinematic effects to the proper motions.

The unknown parameters of the model were derived from the least squares solution of the equation (1). The equation (2) was not used since for low latitude stars where the majority of the stars are concentrated it does not provide a reliable solution. The equation (1) allows us to obtain only 5 of 11 parameters of the Ogorodnikov-Milne model. To derive the remaining parameters the rotation algorithm proposed by V. V. Vityazev [3] was used.

2. RESULTS

In general, modern observational data confirm the results obtained by Parenago more than half a century ago. Still, from our solutions it follows that the Parenago's discontinuity is more complex phenomenon than it was thought before. The range of color index where the abrupt change of the kinematic parameters exists may be specified as $(0.3 < B - V < 0.75)$. More precisely our results may be formulated as follows: the parameters of the Ogorodnikov-Milne model may be derived from the proper motions of the main sequence stars rather reliably only for stars with $B - V < 0.5$. For the remaining segment of the main sequence $(B - V > 0.5)$ the reliability of determination of these parameters sharply falls down. This circumstance is tightly connected with distribution of stars of the main sequence in space. Namely, the stars with $(B - V > 0.5)$ being dwarfs are visible only at close distances (up to 100 pc). From theoretical reasons it follows, that within the limits of a volume with the radius 300 pc the Oort parameters should be determined correctly irrespective to distances. The found inconsistency means that the kinematics of the nearby stars does not follow the model of the Galaxy's flat rotation. Equally it is not compatible with more general Ogorodnikov-Milne model. Our analysis shows that the Parenago's discontinuity exists only for stars of the main sequence. It does not exist (or is too weak) for the giants of the luminocity class III, which have an uniform distribution in space at distances more than 100 pc. We see that the distance factor plays an important role in the study of the Parenago's discontinuity. In our opinion, the transition from the spectral types (color indexes) of the main sequence stars to their distances from the Sun may reduce the problem of the Parenago's discontinuity to pure kinematic nature. In this direction we are going to continue our activity.

The authors thank the RFFI (grant N 02-02-16570) and the Leading Scientific School program (grant 00-15-96775) for support.

3. REFERENCES

[1] Parenago P. P., Astronomicheskij Zhurnal (USSR), 27, 150, 1950.
[2] Michalas and Binney. Galactic Astronomy, – W.H.Freeman and Co, San Francisco, 1981.
[3] Vityazev V. V., Ph.D. thesis, 1999.
[4] Du Mont B. *Astron. Astrophys.*, 61, pp. 127-132, 1977.

PROBLEMS TO CONSTRUCT THE RADIO CELESTIAL REFERENCE FRAME USING VERA

M. FUJISHITA
Kyushu Tokai University
9-1-1, Toroku, Kumamoto, 862-8652, JAPAN
e-mail: mfuji@ktmail.ktokai-u.ac.jp

ABSTRACT. VERA, now under construction, is a Japanese differential VLBI network to measure the relative position of Galactic masers. Its target accuracy is 10 micro-arc-seconds on condition that an angular separation between the target and the reference sources is below 2 degrees. Because of this limit, VERA requires many reference sources. Required accuracy on the position of reference sources is around one micro-arc-second, because almost all of 10 micro-arc-seconds error is due to atmospheric effects. If one can use these reference sources to construct a radio reference frame, it may be possible to get a new one with accuracy of one micro-arc-second. However, it needs about 10000 sources of which positions and brightness distributions must be known to calculate source structure effects with accuracy of one micro-arc-second level. Survey of new VLBI sources and dense VLBI data on the u-v plane are indispensable.

1. OUTLINE OF VERA

VERA (VLBI Exploration of Radio Astrometry), a Japanese domestic D-VLBI (Differential or Delta Very Long Baseline Interferometer) network to measure the relative position of Galactic masers from some reference radio sources like quasars, is under construction at four sites in Japan. The 4 sites are Mizusawa (Iwate prefecture), Ogasawara (Tokyo Metropolis), Iriki (Kagoshima prefecture) and Ishigaki-jima (Okinawa prefecture). And its maximum baseline length is 2300 km. Each station has 20 m diameter antenna with two receivers that enable to make two beams simultaneously. Its target accuracy is 10 micro-arc-seconds on condition that the angular separation between the target source and the reference source is below 2 degrees.

Because of this angular limit, VERA requires many reference sources of which positions and brightness distributions (structures) are known precisely. Required accuracy on the position of reference sources is around one micro-arc-second, because almost all of 10 micro-arc-seconds error is due to atmospheric effects of the Earth. Although the reference sources used by VERA are limited around Galactic plane, they must be almost ideal sources for an accurate new celestial radio reference frame.

2. PROBLEMS ON NEW REFERENCE FRAME

Sensitivity of VERA is around 0.1 Jy. Sasao estimated that total number of radio sources over this intensity is about 5000 in the whole sky, and required number of reference sources

for VERA is 3000 (Sasao, 1999). However, this estimation of required number is based on the idea that there is one reference source in the circle centered at the target source with 2 degrees radius. In case of a reference frame, each reference source must be observed with at least another reference source to keep its precise position. On condition that each radio reference source is at the apex of equilateral triangles with 2 degrees sides, the number of sources is about 10000. Therefore the sensitivity of VERA must be improved. And, at present, there are only 2000 sources detected by VLBI. Therefore it needs active survey to increase number of known sources that can be detected by VLBI.

Usually, point like radio sources are selected as the reference points for geodetic and astrometric observations with current VLBI (including current D-VLBI). However, almost all radio sources are requested to be the reference sources for VERA, because there is not so enough number of sources as the reference of VERA. If the reference source is not point-like but has some structure, it needs structure correction to determine precise position of radio source (for example, Thomas, 1980 and Fujishita, 1983). Usually this correction is calculated from its map observed by VLBI (for example, Fey and Charlot, 1997).

Making maps from VLBI data is somewhat tricky technique. If VLBI observation can gain enough data in the u-v plane, a clear map is obtained only by direct inverse Fourier transformation. However, in case of VLBI, only a few Fourier components are observed and have no phase information. Direct inverse Fourier transformation is impossible. Therefore radio maps are made with a priori information, for example, radio brightness is not minus. This process is mathematically understood that one possible map is selected among many possible maps. There are many other maps that do not conflict with observed data. And there are various a priori assumptions, various mapping algorithms and various parameters which mapping software needs. Stability of the map using such variations is also in question. Dense VLBI data on the u-v plane is indispensable.

3. CONCLUDING REMARKS AND ACKNOWLEDGEMENTS

VERA is a powerful system to construct an accurate radio reference frame. However, it needs 10000 radio sources from the limit of its view. This needs almost all radio sources must be used as the reference sources. Therefore, survey of new VLBI sources, dense VLBI network to make a detail map of the reference sources, stable algorithm to draw a map free from used parameters are indispensable.

The author wishes to thank Michiko Mizuguchi and Motosuji Fujishita who have read the manuscript.

4. REFERENCES

Fey, A. L. and Charlot, P.: 1997, *IERS Technical Note*, 23, III-25
Fujishita, M.: 1983, *Pub. Int. Latitude obs. Mizusawa*, 17, 13
Sasao, T.: 1999, *Proceedings of 1998 Japanese VLBI symposium*, 180, text in Japanese
Thomas, J. B.: 1980, *JPL Publication 80-84*

HIPPARCOS: SEARCH FOR THE STELLAR GROUPS

E. KAZAKEVICH, V. ORLOV, V. VITYAZEV
Sobolev Astronomical Institute of St-Petersburg State University
198504, St-Petersburg, Petrodvoretz, Universitetsky pr., 28, Russia
e-mail: elen_0630@pisem.net

ABSTRACT. The local overdensities technique was applied to identify stellar groups of different scales in phase space. The stars from HIPPARCOS with known radial velocities within 125 pc from the Sun were under investigation. 11 groups in the coordinate space and 5 moving groups in the velocity space have been found. The estimation of the statistical significance of detected groups has been done. The distribution in the velocity space of the identified in the coordinate space cluster members was analyzed.

1. DESCRIPTION OF THE METHOD

In our study we applied local overdensities technique to the stars from Hipparcos with observed radial velocities within 125 pc (N=9324) in coordinate space and to the stars from this sample with heliocentric velocities less than 100 km/s (N=8785).

Let us consider two heliocentric orthonormal frames: (X,Y,Z) and (U,V,W). Axes X,U are toward the galactic center, Y,V in the direction of galactic rotation, Z,W-toward the north galactic pole.

The local overdensities technique is based on calculations of the mutual distances between the stars. We compute the number of stars around every star from our sample within sphere of radius r and compare the results with those that expected in case of random distribution. Varying the meaning of r we can identify the groups of different scales.

We obtained the star density function within 125 pc from the Sun approximated with polinom of 4-th degree for the estimation of the expected number of stars in (X,Y,Z). An expected number of stars in the velocity space was computed for the superposition of three gaussians.

2. RESULTS

The identified clusters in coordinate space are shown on Fig. 1. The detected moving groups are on Fig.2.

Besides well known clusters - Hyades, UMa, Coma, Pleiades - with probability 95% seven new clusters I-VII were detected. But analysis of the distribution of the stars from new clusters in the velocity space showed that velocities of stars are essentially different and there is only small groupings. Four new clusters in coordinate space are likely the fluctuations in the star

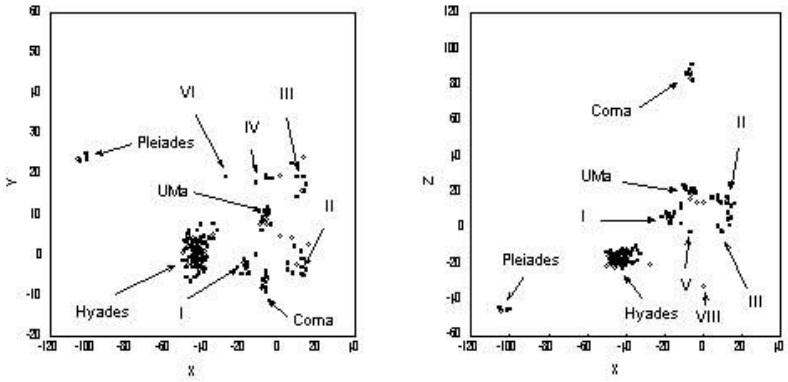

Figure 1: Star clusters in coordinate space detected using local overdensities technique with

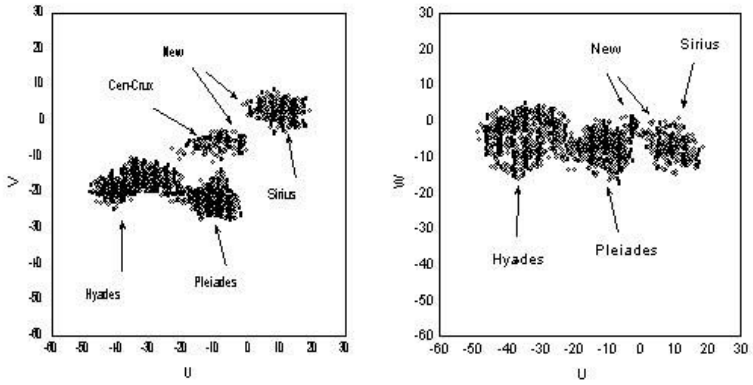

Figure 2: Moving groups detected using local overdensities technique with r=5km/s in velocity space within 100 km/s.

distribution but some of them are the poor clusters because they contain kinematically connected stars.

The analysis of the membership of the identified clusters had been carried out. There is a predominance of high luminosity stars in Hyades and UMa. On the contrary the new clusters consist on the whole of low luminosity stars.

The Monte-Carlo method was used to estimate the influence of random errors in parallaxes on the results obtained .

It must be noticed that the stars from our sample are on the whole the giants and high luminosity stars. And for the investigation of the phase space distribution of faint stars Tycho2 data complemented with the radial velocities data must be used.

TYCHO2: THE WAVELET SEARCH FOR STELLAR GROUPS

E. KAZAKEVICH, V. VITYAZEV
Sobolev Astronomical Institute of St-Petersburg State University
198504, St-Petersburg, Petrodvoretz, Universitetsky pr., 28, Russia
e-mail: elen_0630@pisem.net

ABSTRACT. The wavelet analysis was applied for identifying of the inhomogenities in the star distribution on the celestial sphere. The so-called Mexican Hat (MHAT) wavelet transform was used. The method was tested on simulations. The wavelet coefficients maps for the stars from Tycho2 Catalogue covering the whole celestial sphere at different scales were obtained.

1. DESCRIPTION OF THE METHOD

Tycho2 Catalogue contains 2539913 stars and more than 95% of them are fainter then 9^m. *So for the first time we can investigate the distribution of faint stars on celestial sphere*(there is no parallaxes in this catalogue). We applied the wavelet transform technique that was used in cosmology (see E. Slezak et. all [1]) for our investigation.

We use the so-called Mexican hat (MHAT) wavelet to identify the inhomogeneities in the distribution on the celestial sphere of stars from Tycho2. For a given zone of celestial sphere we define pixels i, j in 1^o bins in l- and b-directions. The wavelet transform for the scale σ of the star set was then computed in each pixel (i,j) according to:

$$W(i,j,\sigma) = \sum_n (2 - \frac{((i-l)^2 + (j-b)^2)}{\sigma^2}) e^{-\frac{(i-l)^2+(j-b)^2}{2\sigma^2}} \quad (1)$$

where l, b - galactic coordinates of the star.

2. RESULTS

The method was tested on simulations. The uniform distribution of 9000 stars on celestial sphere in the stripe with a length of 180^o and a width of 10^o with three clusters at $l \in [16^o;19^o]$, $b \in [3^o;5^o]$ of 60 stars, $l \in [85^o;88^o]$, $b \in [5^o;7^o]$ of 90 stars and $l \in [150^o;154^o]$, $b \in [4^o;6^o]$ of 80 stars had been simulated. The map of wavelet coefficients obtained with σ=2 can be seen on Fig.1.

With the aim of calibration, the method was applied to the stars from the regions with known groups such as Hyades and Pleiades. It was revealed that Hyades cluster can be identified only among Tycho2 stars brighter than 8^m. Stars fainter than 8^m form another structure that differs from Hyades in l-coordinate by 10^o (see Fig.2,3).

So it can be concluded that this method reveals the known structures, and there is a hope that some new clusters can be found .

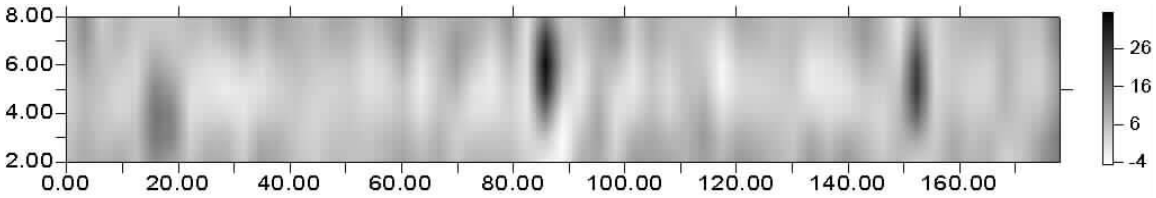

Figure 1: Map of the wavelet coefficients obtained for the stars from the simulated catalogue with $\sigma = 2$.

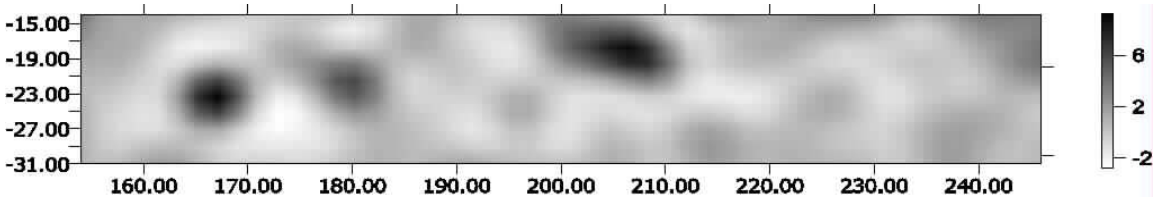

Figure 2: Map of the wavelet coefficients obtained at σ=3 for the stars from Tycho2 with V less than 8^m(in galactic coordinates).

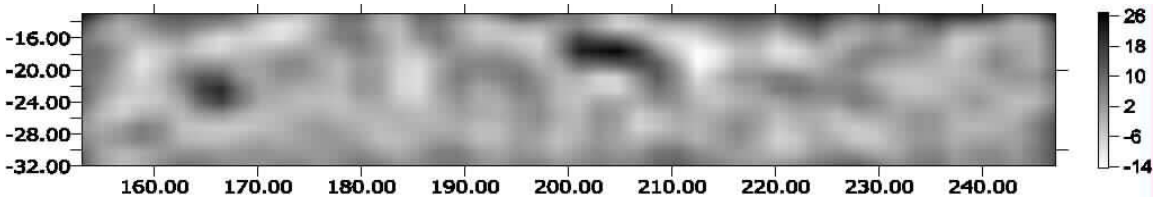

Figure 3: Map of the wavelet coefficients obtained at σ=2 for the stars from Tycho2 with V $\in$ [8^m;10^m].

The maps of wavelet coefficients for the stars from Tycho2 for the whole celestial sphere were constructed at different scales . The map of wavelet coefficients obtained for the stars from the stripe near the galactic plane with σ=1 is presented on Fig.4.

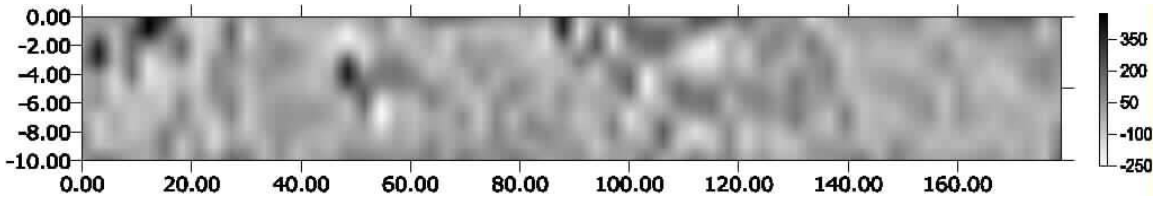

Figure 4: Map of the of the wavelet coefficients obtained at σ =1 for the stars from Tycho2.

Besides known clusters such as Pleiades and Hyades the wavelet revealed a lot of new structures among faint stars from Tycho2.

We are going to continue the research using the color indices B-V and visual magnitudes V for further studying of the membership of the detected clusters.

3. REFERENCES

[1] E.Slezak et. all, *Astron. Astrophys.*, 227, pp. 301-316, 1990.

Session II

THEORY OF EARTH ROTATION

THÉORIE DE LA ROTATION DE LA TERRE

RECENT ADVANCES IN MODELING THE LUNISOLAR PERTURBATION IN POLAR MOTION CORRESPONDING TO HIGH FREQUENCY NUTATION: REPORT ON THE DISCUSSION OF THE IAU COMMISSION 19 WG ON NUTATION

A. BRZEZIŃSKI[1] and P. M. MATHEWS[2]
[1]Space Research Centre, Polish Academy of Sciences Warsaw, Poland
e-mail: alek@cbk.waw.pl
[2]Department of Theoretical Physics, University of Madras (Guindy Campus)
Chennai, India, e-mail: sonny@eth.net

ABSTRACT. We give here a brief report on the discussion within the subgroup "Questions regarding subdiurnal nutations" of the IAU Commission 19 Working Group on Nutation. The aim was to establish a model of the polar motion corresponding to high frequency nutation excited by lunisolar perturbation, which could be included in the new IERS Conventions 2000. Such a model was needed for realization of the conventional intermediate pole (CIP) defined by Resolution B1.7 of the XXIVth IAU General Assembly in Manchester. We considered three solutions for the nonrigid Earth: by Mathews and Bretagnon (2002, 2003), by Brzeziński (2001) and Brzeziński and Capitaine (2002), and by Getino *et al.* (2001) and Escapa *et al.* (2002a,b), the last one being restricted to the diurnal component of perturbation. After clarifying several controversial points and introducing the necessary corrections, the maximum difference between these models was found to be within 0.2 microarcseconds (μas) for individual coefficients and 1 μas in the time domain, that is about 0.2% and 1% of the total effect, respectively. The remaining controversy concerning the so-called "indirect contribution" to diurnal waves from triaxiality (almost entirely from that of the core), for which the estimates differed substantially (e.g., from 1 to about 2.5 μas), was left for further research.

1. INTRODUCTION

The IAU Commission 19 Working Group on Nutation chaired by Veronique Dehant was established at the XXIV IAU General Assembly in Manchester, August 2000, as the follow-up of the former Joint IAU/IUGG WG on "Non-rigid Earth Nutation Theory". This group was divided into several subgroups aimed at solving particular problems related to the implementation of the new IAU resolutions. One subgroup, with the first author of the paper (A.B.) as the responsible person, was devoted to "questions regarding subdiurnal nutations". The aim was to establish a model of the polar motion corresponding to high frequency nutation excited by the lunisolar perturbation, for inclusion in the new IERS Conventions 2000. Such a model was needed for realization of the conventional intermediate pole (CIP) defined by Resolution B1.7 of the XXIVth IAU General Assembly (for implementation by the 1st January 2003); see IAU (2001).

The discussion within the subgroup was speeded up after the IERS Workshop on the Implementation of the New IAU Resolutions in Paris, April 2002, when Dennis McCarthy passed on to Veronique Dehant a request for "a user friendly table that could be used to model the high-frequency nutation (periods $<$ 2 days) as polar motion". Between May and July 2002 there was an intensive exchange of e-mails, and 2 circulars were issued. The second circular dated 19 July 2002, contained the proposal of the model which will be described below.

Let us give now a brief physical description of the problem. External lunisolar tidal torques exerted on the Earth cause perturbations of the angular velocity vector. The types of spherical harmonic structures in the Earth's density distribution, and the spherical harmonic components of the lunisolar potential which act on these structures to produce the equatorial component of these torques are detailed in Table 1. The main term comprising the long periodic nutation and precession involves the zonal components $U_{l,0}$ of geopotential, for $l = 1, 2, \ldots$, with the dominant contribution coming from the component of degree $l = 2$. ($U_{l,j}$ stands for the geopotential or Stokes coefficients $C_{l,j}$ and $S_{l,j}$). In addition, there are minor components associated with the departures of the mass distribution from rotational symmetry, expressed by the non-zonal terms of the geopotential: $U_{2,2}$ and $U_{l,j}$ for degrees $l > 2$ and orders $j \neq 0$. A common feature of these terms is that they have quasi-diurnal and subdiurnal periods, as seen from space. An equivalent representation, which is mandated by the recently adopted definition of the conventional intermediate pole (CIP), is obtained by treating this effect as a perturbation of the motion of the pole in the terrestrial frame, that is as polar motion. In this representation the size of perturbation remains unchanged but the periods are different, as can be seen from Table 1.

Table 1: Summary of the lunisolar perturbations responsible for the equatorial component of Earth rotation. Only those components for which the total effect reaches the level of 0.1 μas are shown. In the first column, $U_{l,j}$ stands for the Stokes coefficients $C_{l,j}$, $S_{l,j}$ of degree l and order j, and $u_{l,j}$ in the next column represents the tidal potential of degree l and order j, expressed as the series of spectral terms with coefficients $A_{l,j,s}$, $s = 1, 2, 3, \ldots$. The last column shows the sum of the absolute values af all amplitudes greater than 0.01 μas.

Geo-potential	Tidal potential	Nutation	Polar motion	Sum of all amplitudes (μas)
$U_{l,0}$ for $l = 2, 3, \ldots$	$u_{l,1}$	long periodic	retrograde diurnal	nutation $> 10^7$ + precession
$U_{3,1}$	$u_{3,0}$	prograde diurnal	long periodic	91.3
$U_{4,1}$	$u_{4,0}$			periodic 1.0 + drift 5.1 μas/yr
$U_{2,2}$	$u_{2,1}$	prograde semidiurnal	prograde diurnal	51.6
$U_{3,2}$	$u_{3,1}$			0.2
$U_{3,3}$	$u_{3,2}$	prograde terdiurnal	prograde semidiurnal	0.1
$U_{3,1}$	$u_{3,2}$	retrograde diurnal	retrograde semidiurnal	0.8
$U_{3,2}$	$u_{3,3}$	retrograde semidiurnal	retrograde terdiurnal	0.1

To our knowledge, the subdiurnal nutations, or to be more precise, the prograde semidiurnal terms associated with the triaxiality of the Earth's figure expressed by $U_{2,2}$, were considered first by Kinoshita (1977) in his nutation theory for the rigid Earth. He arrived at the conclusion that such terms "have no appreciable effect on the rotational motion of the Earth" which was true indeed given the cut-off level of $0.0001''$ that he adopted for the amplitudes . The first estimation for the nonrigid Earth was reported by Chao *et al.* (1991), and corrected later by Chao *et al.* (1996). They considered this effect as a perturbation of the pole as viewed from the terrestrial frame, and designated it as "prograde diurnal libration in polar motion". Chao *et al.* (1991) neglected the potential terms of higher degree because the lunisolar torques diminish rapidly with l. This argument was correct but overlooked an important fact that in the case of the long periodic equatorial torques associated with the $U_{3,1}$ and $U_{4,1}$ terms of geopotential,

an enhancement due to proximity to the Chandler resonance compensates the decrease of the magnitude of the torque and the corresponding polar motion is even larger than the diurnal libration; see Table 1 for the estimated magnitudes.

A more complete spectrum of the subdiurnal nutation was estimated as a part of the recent rigid Earth nutation theories, SMART97 (Bretagnon *et al.*, 1998), REN2000 (Souchay *et al.*, 1999), and RDAN97 (Roosbeek,1999); see also (Folgueira *et al.*, 2001) for comparison of these three theories.

Here we will compare the available estimates for the nonrigid Earth and describe the model which was submitted for publication in the IERS Conventions 2000.

2. MAIN POINTS OF DISCUSSION

2.1. *Solutions for the nonrigid Earth*

We considered 3 solutions for the polar motion due to lunisolar perturbation, each of them assuming a 2-layer structural model of the Earth consisting of an elastic mantle and a liquid core.

– The model developed by Brzeziński (2001) and Brzeziński and Capitaine (2002), further referred to as BC. The equation of polar motion was derived from the Liouville equation under a simple assumption that the core is not coupled to the mantle. The dissipative processes in the mantle and on the Earth were taken into account by allowing the Chandler frequency to be complex, with its parameters determined from the observations of polar motion. The external forcing was expressed by the tide-generating potential (TGP) catalogue HW95 of Hartmann and Wenzel (1995).

– The model of Mathews and Bretagnon (2002, 2003), further referred to as MB. This is based on a modification of the dynamical equations of Sasao *et al.* (1980) for the whole Earth and for the core, which take into account the coupling between the mantle and the liquid core. In addition, MB accounted for mantle anelasticity by introducing its frequency-dependent model. The TGP development RATGP95 of Roosbeek (1996) provided the forcing function in this estimation.

– The model developed by Getino *et al.* (2001) and Escapa *et al.* (2002a,b), further referred to as GFE, by applying the Hamiltonian formalism. The forcing was expressed by the perturbing potential estimated by Kinoshita (1977). So far, this theory has been confined only to the prograde quasidiurnal terms of the polar motion.

We were aware of the fact that there was one more solution for the nonrigid Earth, derived by Molodensky and Groten (2001), but we did not receive from the authors the parameters of the solution in the form enabling direct comparison with other results.

2.2. *Cut-off level*

Participants of the discussion agreed that the cut-off level 0.5 μas for the requested model of polar motion was consistent with other models submitted already for the IERS Conventions, while at the same time being sufficient for bringing out the details of the solution. After merging each pair of prograde and retrograde long periodic waves with the same period into a single elliptical wave, the model (Table 2) is found to contains 15 long periodic terms, a linear drift, and 10 prograde quasi diurnal terms representing circular waves.

2.3. *Arguments of the model*

In each term of the polar motion, the x and y coordinates of the pole are expressed as a linear combination of $\sin(arg)$ and $\cos(arg)$, where arg is an integer combination of the six astronomical arguments. Five of them are the well-known Delaunay fundamental arguments l_m, l_s, F, D, Ω which are used in the nutation theories, while the sixth one χ expresses the diurnal sidereal

Table 2: Polar motion of the nonrigid Earth due to tidal gravitation. Estimates, taken from (Mathews and Bretagnon, 2003), are based on the geopotential model JGM3, the tide generating potential RATGP95 and disregard the triaxiality of the core. Adopted cut-off level is 0.5 μas on the amplitude defined as the square root of the sin and cos coefficients of x_p or y_p, whichever is larger. The Earth's rotation angle is expressed by $\chi = \mathrm{GMST} + \pi$. The order of the tidal potential is expressed by the first digit of the Doodson number which equals the coefficient of χ.

Geo-	Tidal potential		Fundamental arguments						Period	PMx (μas)		PMy (μas)	
pot.	Doodson	deg.	χ	l_m	l_s	F	D	Ω	(days)	sin	cos	sin	cos
$U_{4,1}$	055.565	4	0	0	0	0	0	−1	6798.3837	−0.03	0.63	−0.05	−0.55
$U_{3,1}$	055.645	3	0	−1	0	1	0	2	6159.1355	1.46	0.00	−0.18	0.11
$U_{3,1}$	055.655	3	0	−1	0	1	0	1	3231.4956	−28.53	−0.23	3.42	−3.86
$U_{3,1}$	055.665	3	0	−1	0	1	0	0	2190.3501	−4.65	−0.08	0.55	−0.92
$U_{3,1}$	056.444	3	0	1	1	−1	0	0	438.35990	−0.69	0.15	−0.15	−0.68
$U_{3,1}$	056.454	3	0	1	1	−1	0	−1	411.80661	0.99	0.26	−0.25	1.04
$U_{3,1}$	056.555	3	0	0	0	1	−1	1	365.24219	1.19	0.21	−0.19	1.40
$U_{3,1}$	057.455	3	0	1	0	1	−2	1	193.55971	1.30	0.37	−0.17	2.91
$U_{3,1}$	065.545	3	0	0	0	1	0	2	27.431826	−0.05	−0.21	0.01	−1.68
$U_{3,1}$	065.555	3	0	0	0	1	0	1	27.321582	0.89	3.97	−0.11	32.39
$U_{3,1}$	065.565	3	0	0	0	1	0	0	27.212221	0.14	0.62	−0.02	5.09
$U_{3,1}$	073.655	3	0	−1	0	1	2	1	14.698136	−0.02	0.07	0.00	0.56
$U_{3,1}$	075.455	3	0	1	0	1	0	1	13.718786	−0.11	0.33	0.01	2.66
$U_{3,1}$	085.555	3	0	0	0	3	0	3	9.1071941	−0.08	0.11	0.01	0.88
$U_{3,1}$	085.565	3	0	0	0	3	0	2	9.0950103	−0.05	0.07	0.01	0.55
$U_{2,2}$	135.645	2	1	−1	0	−2	0	−1	1.1196992	−0.44	0.25	−0.25	−0.44
$U_{2,2}$	135.655	2	1	−1	0	−2	0	−2	1.1195149	−2.31	1.32	−1.32	−2.31
$U_{2,2}$	137.455	2	1	1	0	−2	−2	−2	1.1134606	−0.44	0.25	−0.25	−0.44
$U_{2,2}$	145.545	2	1	0	0	−2	0	−1	1.0759762	−2.14	1.23	−1.23	−2.14
$U_{2,2}$	145.555	2	1	0	0	−2	0	−2	1.0758059	−11.36	6.52	−6.52	−11.36
$U_{2,2}$	155.655	2	1	−1	0	0	0	0	1.0347187	0.84	−0.48	0.48	0.84
$U_{2,2}$	163.555	2	1	0	0	−2	2	−2	1.0027454	−4.76	2.73	−2.73	−4.76
$U_{2,2}$	165.555	2	1	0	0	0	0	0	0.9972696	14.27	−8.19	8.19	14.27
$U_{2,2}$	165.565	2	1	0	0	0	0	−1	0.9971233	1.93	−1.11	1.11	1.93
$U_{2,2}$	175.455	2	1	1	0	0	0	0	0.9624365	0.76	−0.43	0.43	0.76
Rate of secular polar motion (μas/yr) due to the zero frequency tide													
$U_{4,1}$	055.555	4	0	0	0	0	0	0			−3.80		−4.31

rotation of the Earth. We agreed that a proper choice for χ, which is consistent with the recent developments of the TGP, is $\chi = \mathrm{GMST} + \pi$, where GMST stands for the Greenwich mean sidereal time.

2.4. *Flattening terms in the TGP developments*

By flattening terms, we mean here the terms in the lunar/solar potential which arise from incremental acceleration of the Moon/Sun relative to the Earth because of the contribution from the Earth's flattening to the geopotential. The TGP developments used in the solutions BC and MB, that is, HW95 (downloaded from the website http://www.gik.uni-karlsruhe.de/ wenzel/hw95/) and RATGP95 (courtesy of Fabian Roosbeek), contain terms representing the flattening effect. These terms appear in the HW95 tables as $u_{3,0}$ terms, hence according to Table 1 should contribute to the long periodic part of the solution, while in RATGP95 these are the first-order degree terms which do not perturb polar motion. This inconsistency caused a systematic difference of about 0.5% in the amplitudes of the long periodic polar motion, hence reaching a detectable level for the largest waves shown in Table 2. However we found that the paper of Hartmann and Wenzel (1995) shows only degree 1 terms in the flattening contribution to the

Table 3: Comparison of the 3 solutions for polar motion of the nonrigid Earth due to tidal gravitation, derived by Brzeziński and Capitaine (2002) – BC, by Getino, Ferrándiz and Escapa (2001) – GFE, and by Mathews and Bretagnon (2003) – MB. All solutions are based on the assumption of rotational symmetry of the core.

Period	BC − MB				GFE − MB			
	PMx (μas)		PMy (μas)		PMx (μas)		PMy (μas)	
(days)	sin	cos	sin	cos	sin	cos	sin	cos
6798.3837	0.00	−0.01	0.01	0.00				
6159.1355	−0.01	0.01	0.01	−0.01				
3231.4956	0.14	−0.21	−0.04	0.06				
2190.3501	0.02	−0.03	0.00	0.01				
438.35990	−0.13	−0.05	0.05	−0.13				
411.80661	−0.05	−0.08	0.08	−0.05				
365.24219	−0.03	−0.02	0.03	−0.02				
193.55971	−0.02	−0.01	0.01	−0.02				
27.431826	0.00	0.00	0.00	0.00				
27.321582	−0.03	−0.01	0.00	−0.01				
27.212221	−0.01	0.00	0.00	0.00				
14.698136	0.00	0.00	0.00	−0.01				
13.718786	0.00	0.00	0.00	0.00				
9.1071941	0.00	0.00	0.00	0.01				
9.0950103	0.00	0.00	0.00	0.00				
$\sum$|ampl|	0.44	0.43	0.23	0.33				
1.1196992	0.00	0.00	0.00	0.00	0.00	0.00	0.00	0.00
1.1195149	−0.02	0.02	−0.02	−0.02	0.00	0.01	−0.01	0.00
1.1134606	0.00	0.00	0.00	0.00	0.00	0.00	0.00	0.00
1.0759762	−0.02	0.01	−0.01	−0.02	−0.01	0.00	0.00	−0.01
1.0758059	−0.09	0.05	−0.05	−0.09	−0.03	0.02	−0.02	−0.03
1.0347187	0.01	−0.01	0.01	0.01	0.00	0.00	0.00	0.00
1.0027454	−0.03	0.02	−0.02	−0.03	−0.01	0.01	−0.01	−0.01
0.9972696	0.10	−0.06	0.06	0.10	0.03	−0.02	0.02	0.03
0.9971233	0.02	−0.01	0.01	0.02	0.01	0.00	0.00	0.01
0.9624365	0.00	−0.01	0.01	0.00	0.00	−0.01	0.01	0.00
$\sum$|ampl|	0.29	0.19	0.19	0.29	0.09	0.07	0.07	0.09
Rate of secular polar motion (μas/yr) due to the zero frequency tide								
		0.01		0.02				

potential, in agreement with Roosbeek (1996). Therefore we omitted the $u_{3,0}$ flattening terms in the final computations.

2.5. *Indirect effect of the triaxiality*

This effect, first considered by Escapa et al. (2002) and further developed by Mathews and Bretagnon (2003), is caused by the coupling produced between the diurnal prograde and retrograde wobbles by triaxiality terms in the angular momentum of the whole Earth and of its fluid core. Its contribution to the diurnal prograde terms of the model considered here can be significant due to the FCN-related resonance in the retrograde wobbles, but is small (below 0.1 μas) if the core is rotationally symmetric. Unfortunately, there was a significant discrepancy, up to a factor of 2.5 or even more, between estimates of the indirect effect obtained by Escapa *et al.* (2002a,b) and by Mathews and Bretagnon (2003), (about 2.5 μas versus 1 μas for the largest contribution, when it is assumed that $A_c/B_c = A/B$, where A, B are principal equatorial moments of inertia of the whole Earth, and A_c, B_c are the corresponding quantities for the core alone); see (Escapa *et al.*, this volume) for further details and comparisons. This was the main controversy of the

discussion which needs to be resolved by further study.

2.6. *Assumptions about the model*

We decided to provide for the IERS Conventions 2000 the model based on the assumption that the core is rotationally symmetric ($A_c = B_c$). There were two reasons for that:
– The triaxiality of the core, which is expressed by the equatorial moments of inertia A_c, B_c, can only be estimated from the geophysical determinations of the core-mantle boundary topography. However,comparison between different geophysical models (Brzeziński and Capitaine, 2002) shows large differences which suggests that it is too early to give preference to any of them. Such opinion was shared by Veronique Dehant (private communication) who headed that time the IERS Special Bureau for the Core.
– As stated in Sec. 2.5, there is no agreed set of values for the "indirect contributions" from the core triaxiality coefficient A_c/B_c. This problem requires further study. On the other hand, when disregarding the triaxiality of the core, the three sets of coefficients become very similar as can be seen from comparison shown in Table 3.

2.7. *Comparison of different estimates*

The 3 solutions for the nonrigid Earth, computed under the assumption of rotational symmetry of the core ($A_c = B_c$), are compared in Table 3. There can be observed an almost perfect agreement between the solutions MB and GFE. A slightly larger difference is between the solutions MB and BC, up to 0.2 μas in terms of the individual amplitudes, and about 1 μas in the time domain. This difference comes almost entirely from modeling of the nonrigid Earth response, because a similar comparison done for the rigid Earth (not shown here) yielded almost perfect agreement. The largest differences are for the terms with periods 8.85 years, 438 days, 412 days, and are caused by the fact that in the MB estimation the parameters of the Chandler resonance, the period and the quality factor, were frequency-dependent while in the solution BC these parameters were kept fixed. In the case of diurnal terms, the differences are caused by other features of the models, mostly by the omission in the solution BC of the indirect effect of the triaxiality.

2.8. *Comparison with oceanic and atmospheric contributions*

At prograde diurnal frequencies, the lunisolar perturbations in polar motion are superimposed on the variations excited by the ocean tides and the atmospheric tides. From Table 4 it can be seen that the atmospheric contribution is comparable in magnitude to the lunisolar effect but its power distribution among diurnal frequencies is different. The largest term with the amplitude of about 7 μas has a period of 1 solar day corresponding to the S_1 tide. This term has no counterpart in Table 2 and the corresponding ocean tide contribution is several times

Table 4: Prograde diurnal polar motion excited by the oceanic tides (Chao *et al.*, 1996) and by the atmospheric tides (Brzeziński and Petrov, 2000). Amplitudes are in μas and periods are in days.

Fundamental arguments						Tidal	Terrestrial	Oceanic				Atmospheric			
								PMx		PMy		PMx		PMy	
χ	l_m	l_s	F	D	Ω	code	period	sin	cos	sin	cos	sin	cos	sin	cos
1	−1	0	−2	0	−2	Q_1	1.1195149	6.2	26.3	−26.3	6.2				
1	0	0	−2	0	−2	O_1	1.0758059	48.8	132.9	−132.9	48.8				
1	0	0	−2	2	−2	P_1	1.0027454	26.1	51.2	−51.2	26.1	−0.6	1.2	−1.2	−0.6
1	0	−1	0	0	0	S_1	1.0000000	−0.6	−1.2	1.2	−0.6	5.2	−4.9	4.9	5.2
1	0	0	0	0	0	K_1	0.9972696	−77.5	−151.7	151.7	−77.5	−1.4	−0.7	0.7	−1.4
1	0	1	0	0	0	ψ_1	0.9945541	−0.6	−1.2	1.2	−0.6	0.5	−0.5	0.5	0.5

smaller, therefore there exists at least a potential chance that this atmospheric wave will be detected in the observations of polar motion. In case of the oceanic perturbations the situation is more difficult. Comparison of Table 4 with Table 2 shows that the ocean tide contributions are systematically about 10 times larger and differ in phase by about 90°. It is unlikely that the model of the dominant ocean-driven polar motion is sufficiently accurate for separating this effect from the direct influence of the tidal gravitation.

3. CONCLUSIONS

We presented here a report on the discussion within the subgroup "Questions regarding subdiurnal nutations" of the IAU Commission 19 Working Group on Nutation. The aim was to establish a model of the lunisolar perturbation in polar motion corresponding to high frequency nutation, which could be included in the new IERS Conventions 2000. We considered three different solutions for the nonrigid Earth comprising the solid mantle and the liquid core. Under the assumption of the rotational symmetry of the core, the difference between these solutions was found to be no greater than 0.2 μas in terms of the individual coefficients of the harmonic development and about 1 μas in the time domain, that is about 0.2% and 1% of the total effect. The remaining controversy which requires further research, is a question how the "indirect contributions" to the diurnal waves depend on the core triaxiality coefficient A_c/B_c. There seems to be little chance that this controversy will be solved in the near future on the basis of the measurements of polar motion, because for that one needs predictions for the dominant ocean tide contribution which are good at least at the 1 μas level.

Acknowledgments. In addition to the authors of the report, the following researchers contributed to the discussion: Christian Bizouard, Pierre Bretagnon, Nicole Capitaine, Veronique Dehant, Alberto Escapa, Jose Ferrándiz, Marta Folgueira, Juan Getino, Dennis McCarthy, Fabian Roosbeek and Jean Souchay. We would like to express our thanks for their efforts and cooperation. This research and participation of A.B. in the conference had been supported by the Polish National Committee for Scientific Research (KBN) under grant No. 9 T12E 005 19. Accommodation costs of A.B. were covered by the Romanian Academy of Sciences in frame of bilateral cooperation with the Polish Academy of Sciences.

REFERENCES

Brzeziński A. (2001). Diurnal and subdiurnal terms of nutation: a simple theoretical model for a nonrigid Earth, in. *Proc. Journées 2000 Systèmes de Référence Spatio-Temporels*, edited by N. Capitaine, Paris Observatory, 243–251.

Brzeziński A. and N. Capitaine (2002). Lunisolar perturbations in Earth rotation due to the triaxial figure of the Earth: geophysical aspects, *Proc. Journées Systèmes de Référence Spatio-Temporels 2001*, edited by N. Capitaine, Paris Observatory, 51–58.

Brzeziński A. and S. Petrov (2000). High frequency atmospheric excitation of Earth rotation, *International Earth Rotation Service Technical Note 28*, edited by B. Kołaczek, H. Schuh and D. Gambis, Paris Observatory, 53–60.

Chao B. F., D. N. Dong, H. S. Liu and T. A. Herring (1991). Libration in the Earth's rotation, *Geophys. Res. Letters*, **18**, No. 11, 2007–2010.

Chao B. F., R. D. Ray, M. J. Gipson, G. D. Egbert and Ch. Ma (1996). Diurnal/semidiurnal polar motion excited by oceanic tidal angular momentum, *J. Geophys. Res.*, **101**, No. B9, 20,151–20,163.

Escapa A., J. Getino and J. M. Ferrándiz (2002a). Influence of the triaxiality of the non-rigid Earth on the J_2 forced nutations, *Proc. Journées Systèmes de Référence Spatio-Temporels 2001*, edited by N. Capitaine, Paris Observatory.

Escapa A., J. Getino and J. M. Ferrándiz (2002b). Indirect effect of the triaxiality in the Hamiltonian theory for the rigid Earth nutations, *Astronomy & Astrophysics*, **389**, 1047–1054.

Folgueira M., Ch. Bizouard and J. Souchay (2001). Diurnal and subdiurnal luni-solar nutations: comparisons and effects, *Cel. Mech. Dyn. Astr.*, **81**, 191–217.

Getino J., J. M. Ferrándiz and A. Escapa (2001). Hamiltonian theory for the non-rigid Earth: Semidiurnal terms, *Astronomy & Astrophysics*, **370**, 330–341.

Hartmann T. and H.-G. Wenzel (1995). The HW95 tidal potential catalogue, *Geoph. Res. Lett.*, **22**, 3553-3556.

IAU (2001). International Astronomical Union Information Bulletin No.88, Astronomical Society of the Pacific, CA.

Mathews P. M. and P. Bretagnon (2002). High frequency nutations, *Proc. Journées Systèmes de Référence Spatio-Temporels 2001*, edited by N. Capitaine, Paris Observatory, 28–36.

Mathews P. M. and P. Bretagnon (2003). Polar motions equivalent to high frequency nutations for a nonrigid Earth with anelastic mantle. *Astronomy & Astrophysics*, **400**, 1113–1128.

Molodensky S. M. and E. Groten (2001). Semidiurnal and long-period components in polar motion connected with the triaxiality of ellipsoid of inertia of the Earth and planets, *Studia geoph. et geod.*, **45**, 37–54.

Roosbeek F. (1996). RATGP95: a harmonic development of the tide-generating potential using an analytical method, *Geophys. J. Int.*, **126**, 197–204.

Roosbeek F. (1999). Diurnal and subdiurnal terms in RDAN97 series, *Cel. Mech. Dyn. Astron.*, **74**, 243–252.

Sasao T., S. Okubo and M. Saito (1980). A simple theory on the dynamical effects of a stratified fluid core upon nutational motion of the Earth, *Nutations and the Earth's Rotation*, edited by Fedorov, Smith and Bender, Reidel, Dordrecht, Netherlands, 165–183.

Souchay J., B. Loysel, H. Kinoshita and M. Folgueira (1999). Corrections and new developments in rigid Earth nutation theory: III. Final tables "REN-2000" including crossed-nutation and spin-orbit coupling effects, *A&A Suppl. Ser.*, **135**, 111–131.

NUTATION RESIDUALS AND PHYSICS OF THE EARTH INTERIOR

V. DEHANT, O. DE VIRON, T. VAN HOOLST
Royal Observatory of Belgium
3, Avenue Circulaire, B-1180Brussels (Belgium)
e-mail: Veronique.Dehant@oma.be; DeViron@oma.be; T.VanHoolst@oma.be;

M. FEISSEL-VERNIER,
Observatoire de Paris (DANOF-UMR8630)
61 Avenue de l'Observatoire, 75014 Paris (France)
e-mail: Martine.Feissel@obspm.fr

C. MA
Goddard Space Flight Center, Greenbelt, MD, USA

ABSTRACT. Nutations are mainly determined from Very Long Baseline Interferometry (VLBI) data. The nutations allow us to infer properties of the Earth's interior, such as the flattening of the core-mantle boundary and, with some hypotheses, the electromagnetic fields at the inner core and outer core boundaries.

We examine how far we can go now in the understanding of the Earth's interior and how VLBI observations can be used to constrain Earth's interior models.

This allows us to get the confidence intervals on the Earth's interior parameters deduced from VLBI as done for the MHB2000 model.

1. OBSERVATION

Nutations are observed by Very Long Baseline Interferometry (VLBI). From arrival time delays of radio signals at two different stations, the orientation of the Earth in space and its time variations are deduced. Nutations coefficients are derived from this time series. The possible motions of the radio-sources limit the precision at a few tens of microarcseconds.

2. THEORY

The IAU adopted nutation model is the model MHB2000A by Mathews et al. (2002), based on geophysical considerations and geophysical parameters fitted on the observations. The nutations used for this fit are not corrected for the atmospheric effects except for a constant prograde annual contribution at the level of 0.1 milliarcsecond. Yseboodt et al. (2002) have demonstrated that the atmosphere also contributes to other nutation components at an observable level. These authors have also shown that, from one atmospheric model to the other, the atmospheric contributions to nutation varies strongly. The interpretation of the nutation data in terms of the

physics of the Earth interior is therefore limited by the uncertainties on the atmospheric effects: in particular, MHB2000A erroneously interpret atmospheric effects as contribution of the Earth interior, and the inferred Earth interior parameters have an accuracy limited accordingly. Additionally, the MHB2000 nutation model is based on an Earth model, which is simplified (3 homogeneous layers, with ellipsoidal boundaries). Consequently, the Earth's interior parameters obtained from the nutation model are only valid in the limit of validity of this Earth model. In this study, we investigate how the uncertainties in the Earth interior contribution to the transfer function associated with the atmospheric contribution propagate into the Earth interior parameters.

3. STRATEGY

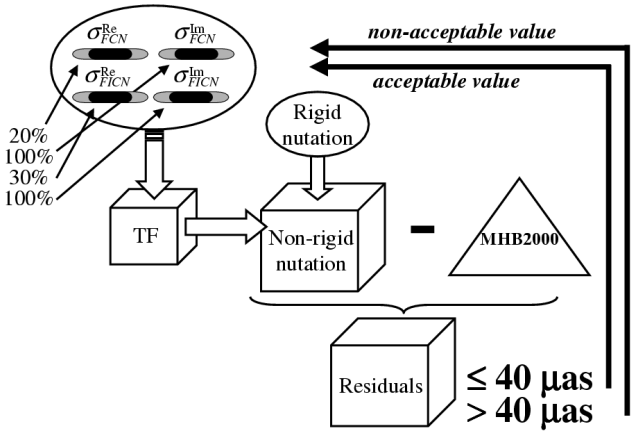

Figure 1: Strategy to test the Model of MHB2000.

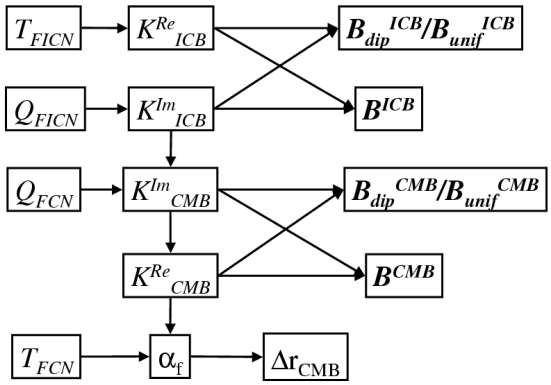

Figure 2: Parameter computational scheme

The strategy is explained by the sketch of Figure 1. It represents the different steps performed in the evaluations:

- to take values of the FCN and FICn complex freqeuncies within the interval given a priori,
- to compute the transfer function with these parameters,
- to convolve with the rigid Earth nutation in order to get the non-rigid Earth nutation,
- to compute the residuals with respect to MHB2000,
- if all residuals are smaller than 40 microarcseconds, to accept the starting value of the parameters, and
- if one of the residuals is larger than 40 microarcseconds, to reject the starting value of the parameters.

From that computation, we get acceptable ranges for the periods and damping of the Free Core Nutation (FCN) and Free Inner Core Nutation (FICN). From these values, it is possible to deduce the coupling constant involved at the Inner Core Boundary (ICB) and Core-Mantle Boundary (CMB). From the values of the coupling constants, the amplitude of the ICB magnetic field and the ratio between the dipole and uniform fields can be derived (supposed to be the only part of the field contributing to nutation in MHB2000 theory, see Buffett et al., 2002). From the value of the imaginary part of the FICN and from the damping of the FCN, one gets the real

part of the coupling constant at the CMB. As shown in Figure 2, from the two coupling constant values at the CMB, one obtains the amplitude of the magnetic field and the ratio between the dipole part and the uniform part at the CMB. From the real part of the coupling constant and the real part of the FCN, the flattening of the core can be determined.

Error intervals on the damping factors and periods can so be converted into error intervals on Earth's interior parameters. The results are represented on Figure 3.

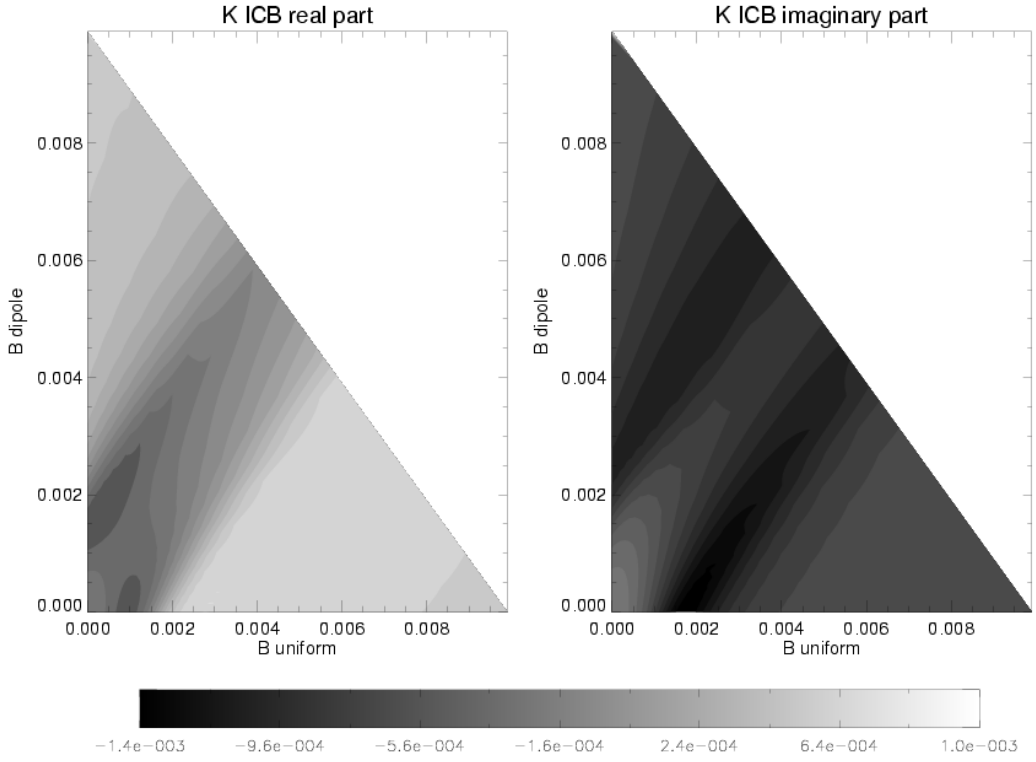

Figure 3: Interval on dipole and uniform magnetic field components

4. CONCLUSION

We have shown with this approach that the intervals given in MHB2000 on the parameters are reasonable if we take 40 microarcseconds uncertainty on the nutation amplitudes, and in the limit of validity of the model used.

5. REFERENCES

Buffett, B.A., Mathews P.M., and Herring T.A., 2002, "Modeling of nutation-precession: effects of electromagnetic coupling", *J. Geophys. Res.*, 107(B4), 10.1029/2001JB000056.

Mathews, P.M., Herring, T.A., and Buffett, B.A., 2002, "Modeling of nutation-precession: new nutation series for nonrigid Earth, and insights into the Earth's interior", *J. Geophys. Res.*, 107(B4), 10.1029/2001JB000390.

Yseboodt, M., de Viron, O., Chin, T.M., and Dehant, V., 2002, "Atmospheric excitation of the Earth nutation: Comparison of different atmospheric models", *J. Geophys. Res.*, 107(B2), 10.1029/2000JB000042.

VARIATIONAL APPROACH TO THE ROTATIONAL DYNAMICS OF A THREE-LAYER EARTH MODEL: FLUID OUTER CORE INTERACTIONS

A. ESCAPA[1], J. GETINO[2] and J. M. FERRÁNDIZ[1]
[1] Dpto. Matemática Aplicada. Escuela Politécnica Superior.
Universidad de Alicante. E-03080 Alicante. Spain
E-mail: Alberto.Escapa@ua.es
[2] Grupo de Mecánica Celeste. Facultad de Ciencias
Universidad de Valladolid. E-47005 Valladolid. Spain

ABSTRACT. By means of the Hamiltonian theory of the rotation of the non–rigid Earth, we have obtained explicit expressions of the torques exerted by the fluid on the solid layers of a two and three–layer Earth models as functions of the canonical Andoyer variables. When rewriting these formulae in terms of the components of angular velocities and symmetry axes of the layers, the transformated expressions are the same as those derived by other authors using different methods. Anyway, here the derivation is obtained in a much more simple way without the concurrence of Hydrodynamics equations.

1. INTRODUCTION

The determination of the rotational motion of a celestial body around its barycenter is one of the most important problems in Celestial Mechanics. This relevance is stressed if the celestial body is the Earth. The reason is clear: the accurate knowledge of Earth rotation is fundamental to tackle the definitions and realizations of space and time reference systems.

The Earth rotation problem can be studied by applying different approaches. One of them is based on the application of the Variational Principles of Mechanics, that is to say, the establishment and resolution of the problem is performed in the context of Lagrangian (Lagrange equations) or Hamiltonian (canonical equations) frameworks. At the beginning of the XXth century this line was followed by Poincaré (1910) and Andoyer (1923) when dealing with the rotational motion of non-rigid and rigid Earth models. Later, there have been other investigations sharing this approach such as the works of Kinoshita (1977), Moritz (1982), Getino and Ferrándiz (2001), etc. In the last years the rotational motion of a more sophisticated Earth model composed of three layers (mantle, fluid outer core and inner core) is also being investigated under this variational perspective by means of a Hamiltonian theory (e.g. Escapa et al. 2001) or with the help of Poincaré equations (Escapa et al. 2002).

A fact that must be underlined is that the resolution of the Earth rotation problem by means of the Variational Principles of Mechanics is not only interesting from an academic point of view but also from a practical one. Let us remember that the Hamiltonian theory of the rotation of the rigid Earth (Kinoshita 1977, Souchay et al. 1999) is probably the most complete and precise

theory for this kind of Earth model available nowadays. Likewise, the Hamiltonian theory by Getino and Ferrándiz (2000) provides competitive rotational models for the non–rigid Earth. On the other hand, the variational approach presents some advantages with respect to other treatments based on the Vectorial Mechanics (e.g. Sasao et al. 1980, Mathews et al. 1991, 2002). In particular, the explicit computation of the torques exerted by the fluid on the solid layers is avoided.

In this note we focus our attention in obtaining the interactions among the fluid and the solid layers. Anyway, let us recall (Escapa et al. 2001, 2002) that in the variational context it is not necessary to know the explicit functional expression of these torques, since the equations of motion are derived from the Hamiltonian or Lagrangian of the system. However, it is interesting to have the expressions of the torques with a twofold aim: first, to gain some kinematical and geometrical insight into the interactional mechanism among the fluid and the solid layers. Second, to compare them with the expressions used in the vectorial approach which are obtained by means of a cumbersome procedure involving Hydrodynamics equations.

2. VECTORIAL MECHANICS APPROACH

The Vectorial Mechanics approach is based on the general equation of angular momentum conservation of a system

$$\frac{d\boldsymbol{L}}{dt} = \boldsymbol{N}, \tag{1}$$

where $\boldsymbol{L}$ is the angular momentum of the system and $\boldsymbol{N}$ the torque acting on it. Next, we sketch the basic features of the way in which eq. (1) is applied to solve Earth rotation problems. Specifically, we will consider the line followed by Sasao et al. (1980) and its generalizations. Anyway, let us point out that there are other approaches (e.g. Wahr 1981) starting basically from (1) that we will not treat in this note.

To model the rotational motion of the Earth it is considered one equation of the form (1) for each layer of the Earth. Besides it is necessary to perform some additional considerations that allows to tackle this complicated problem (see Kinoshita and Sasao 1989). One of the most important simplification is to assume that the field of velocities of each layer is composed of a dominant rigid–rotation term. So the angular momentum (rotational) of a layer has the form

$$\boldsymbol{L}_i = \Pi_i \boldsymbol{\varpi}_i, \tag{2}$$

being Π_i the tensor of inertia of the layer and $\boldsymbol{\varpi}_i$ its associated angular velocity (rigid–rotation term) with respect to an inertial frame. This one is decomposed as

$$\boldsymbol{\varpi}_i = \boldsymbol{\omega}_m + \boldsymbol{\omega}_i. \tag{3}$$

$\boldsymbol{\omega}_m$ is the associated angular velocity to the mantle. There are other possibilities to make this decomposition, see Mathews et al. 1991, but these ones do not change the fundamental idea of the method. In this way the equation (1) is written as

$$\frac{d\boldsymbol{L}_i}{dt} + \boldsymbol{\omega}_m \wedge \boldsymbol{L}_i = \boldsymbol{N}_{i\,out} + \boldsymbol{N}_{i\,int}. \tag{4}$$

The subscript i refers to the different layers (mantle, fluid outer core,...). We have described the evolution of $\boldsymbol{L}_i$ with respect to a frame (Tisserand frame) evolving with the angular velocity $\boldsymbol{\omega}_m$. In addition, we have split out the torque acting on the layer in two parts: $\boldsymbol{N}_{i\,out}$ is the torque due to the interactions produced outside the Earth and $\boldsymbol{N}_{i\,int}$ is the torque produced inside

the Earth. The equation referring to the variation of the angular momentum of the mantle is substituted by one describing the behaviour of the whole Earth. Namely

$$\frac{d\boldsymbol{L}}{dt} + \boldsymbol{\omega}_m \wedge \boldsymbol{L} = \boldsymbol{N}_{out}, \tag{5}$$

with $\boldsymbol{L} = \sum \boldsymbol{L}_i$, $\boldsymbol{N}_{out} = \sum \boldsymbol{N}_{i\,out}$. To simplify the terminology we also refer to this equation as the equation of a layer (the whole Earth). The internal torques do not appear in the above formula because of Newton's action–reaction principle. Finally, to determine the rotational motion of the Earth we have to add to the dynamical eqs. (4) and (5) a new set of relations that involve the variables characterizing the Earth orientation, such as the case of the Euler angles. These relationships mix the time derivatives of Euler angles with the components of the angular velocities of each layer (see Escapa et al. 2002) and with (4) and (5) form the fundamental system of differential equations whose solutions provide the rotational motion of the Earth (precession, nutation and length of day).

In this framework it is possible to study the rotational motion of different Earth models. First, we have to fix the number of layers of our model, that is to say to consider a one–layer, two–layer or three–layer Earth model. Second, we have to provide analytical expressions for the quantities entering in eqs. (4) and (5). Depending on the physical characteristics of the model it will be necessary to consider different expressions for the tensors of inertia and for the external and internal torques. For example, the external torques could take into account the gravitational perturbations of moon, sun, etc. Some of the internal torques can be due to dissipative processes happening in the interior of the Earth, the interactions of the fluid with the solid layers (pressure torques), etc. Other characteristics of the Earth model, such as the elasticity of the layers, can also be fitted in this scheme by performing some approximations (Sasao et al. 1980).

The explicit expressions of the torques or tensor of inertia of each layer are derived following different methods. For instance, the torques of gravitational origin (internal and external) are obtained through a potential function; the dissipative torques are linear combinations of the components of the angular velocities of the layers (Sasao et al. 1980). In the case of the pressure torques the derivation of explicit expressions is more complicated. These expressions come from the equations of fluid motion following a cumbersome procedure (Sasao et al. 1980), specially in the case of a three–layer Earth model (Mathews et al. 1991).

The next step in the development of this approach would be to solve the differential equations of motion. The procedure followed is to use the so–called transfer function method, which essentially consists in taking advantage of the solution produced for a rigid Earth model. In this way it is not necessary to work with the explicit expressions of the gravitational potential of moon, sun and planets, although the method also presents some limitations (Escapa et al. 2002). This stage of the theory is out of the scope of this paper and will not be considered.

3. VARIATIONAL APPROACH

The Variational approach is based on consider the extremals of the variational problem

$$\delta \int_{t_1}^{t_2} F\, dt = 0, \tag{6}$$

where F is a function depending on the system. Starting from this standpoint several methods have been developed to treat the Earth rotation problem (Poincaré 1910, Moritz 1982, etc). The main approximations performed in the Vectorial approach (e.g. rigid–rotation field of velocities) are also assumed in these methods. We focus our attention on the Hamiltonian formalism due to Getino and Ferrándiz, giving a brief outline of the fundamentals of the method.

In this context the equations of motion of a system with n degrees of freedom are derived with the help of the Hamilton canonical equations

$$\frac{dp_i}{dt} = -\frac{\partial H}{\partial q_i} + Q_{q_i};\ \frac{dq_i}{dt} = \frac{\partial H}{\partial p_i} - Q_{p_i};\ i = 1, \ldots, n. \tag{7}$$

p_i, q_i are the canonical variables, momenta and coordinates, that describe the dynamical behaviour of the system. H is the Hamiltonian function: it is a sum of the kinetic, T, and potential, V, energies of the system and Q_{ξ_i} are the generalized forces, necessary to model the dissipative or non-conservative processes. When studying the rotational motion of a system there are several possibilities to chose the canonical variables. One of the most useful is to employ the Andoyer canonical set (or some variation of this set, Getino 1995a, b, Escapa et al. 2001) because of its simplicity and the direct geometrical interpretation of its canonical momenta in terms of the components of the (rotational) angular momentum (Kinoshita 1977). In this way we associate one Andoyer set, composed of six canonical variables, to each layer of the Earth.

By so doing the equations of the rotational motion are established specifying the analytical expressions of T, V and Q_{ξ_i}, which depend on the physical characteristic of the Earth model. So, T is the sum of the (rotational) kinetic energy of each layer, this one can be computed through the equation

$$T_i = \frac{1}{2} < \Pi_i^{-1} \boldsymbol{L}_i, \boldsymbol{L}_i > . \tag{8}$$

$<,>$ stands for the scalar product in the real tridimensional space and Π_i^{-1} is the inverse of the tensor of inertia of the layer. V is the potential energy arising from the gravitational interactions of internal or external origin. This is derived from a potential function expressed in terms of the canonical variables by means of the Wigner's theorem. The generalized forces Q_{ξ_i} are obtained from the dissipative torques (González and Getino 1997).

To solve the equations of motion the Hamiltonian formalism exploits the powerful canonical perturbations methods. These ones present a great advantage with respect to the transfer function method, since the non–linear terms of the differential equations can be also studied with this formalism. This is not the case for the transfer function method, which is intrinsically a linear procedure. There are other advantages of the Hamiltonian formalism (Escapa et al. 2002) that we do not analyze in this work.

4. VARIATIONAL DERIVATION OF FLUID INTERACTIONS

In the previous sections we have described the way in which the different mechanics characterizing the Earth models are taken into account in the Vectorial and Hamiltonian approaches. Anyway, there is one interaction that is explicitly worked out by means of the Hydrodynamics equations in the Vectorial treatment and that, apparently, does not appear in the Hamiltonian formalism. We are referring to the fluid interaction (pressure torque). Where are this effect taken into account in the Hamiltonian formalism?

This effect is included in the Hamiltonian of the system through the kinetic energy of the fluid layer (Moritz 1982, Getino 1995a). In this way to derive the equations of motion of the system we do not need to employ the fluid motion equations to obtain its interactions; we have only to construct the kinetic energy of the system, which is a simple task. This is a great advantage of the Hamiltonian formalism, shared with other variational approaches, with respect to the Vectorial Mechanics method. Anyway, using the Hamiltonian formalism we can obtain the explicit expressions of these interactions. By so doing, we can compare these ones with the expressions employed in the Vectorial approach. With this aim we are going to compute the interaction fluid torques for a two and three–layer Earth models. Besides, due to the fact that these interactions are included through the kinetic energy we can consider simple Earth models where the solid

layers are rigid and there is no gravitational interactions nor dissipative processes. This fact will simplify the exposition and the computations without changing the basic features of the method.

Two–layer Earth model

We will consider the free rotation of an Earth model composed of two layers: a rigid axial–symmetrical mantle that encloses a fluid core. The Hamiltonian of the system is

$$H = T_m + T_f = \frac{1}{2} < \Pi_m^{-1} \boldsymbol{L}_m, \boldsymbol{L}_m > + \frac{1}{2} < \Pi_f^{-1} \boldsymbol{L}_f, \boldsymbol{L}_f > . \tag{9}$$

To derive the form of the fluid interactions we write eq. (4) as

$$\boldsymbol{N}_{m\ int} = \frac{d\boldsymbol{L}_m}{dt} + \boldsymbol{\omega}_m \wedge \boldsymbol{L}_m. \tag{10}$$

In this situation $\boldsymbol{N}_{m\ int}$ is the torque due to the interaction of the fluid with the mantle ($\boldsymbol{N}_{m\ int} = -\boldsymbol{N}_{f\ int}$). To obtain the expression of the left hand side of eq. (10) we have to write the right hand side in terms of the elements of the Hamiltonian formalism, which are the known data. Besides, it is expedient to recall that the time derivative of a function of the canonical variables can be computed through the Poisson bracket

$$\frac{df}{dt} = \{f, H\} + \frac{\partial f}{\partial t} = \sum_{i=1}^{n} \left(\frac{\partial H}{\partial q_i} \frac{\partial f}{\partial p_i} - \frac{\partial H}{\partial p_i} \frac{\partial f}{\partial q_i} \right) + \frac{\partial f}{\partial t}, \tag{11}$$

being H the Hamiltonian of the system and p_i, q_i the canonical variables.

To compute the former formulae we have to specify a canonical set. As usual, we employ the Andoyer variables (Getino 1995a, b), in addition to take advantage of the geometrical meaning of this set we will express $\boldsymbol{\omega}_m$ and $\boldsymbol{L}_m$ in terms of the the angular momentum of the system $\boldsymbol{L}$ and of the fluid $\boldsymbol{L}_f$

$$\boldsymbol{L}_m = \boldsymbol{L} - \boldsymbol{L}_f;\ \boldsymbol{\omega}_m = \Pi_m^{-1} \left(\boldsymbol{L} - \boldsymbol{L}_f \right). \tag{12}$$

So, the components of $\boldsymbol{N}_{m\ int}$ in the Tisserand frame will be given by

$$(N_{m\,int})_j = \left\{ (L)_j - (L_f)_j , H \right\} + \sum_{l,k,p=1}^{3} \varepsilon_{jlk} \left(\Pi_m^{-1} \right)_{lp} \left[(L)_p - (L_f)_p \right] \left[(L)_k - (L_f)_k \right], \ j = 1, 2, 3. \tag{13}$$

ε_{jkl} is the alternating symbol; j, k, l denotes the components in the Tisserand frame. Taking into account the relationships between the Andoyer variables with the components of the angular momentum and the form of the tensors of inertia of the mantle and the fluid (Getino 1995b), we obtain that the expression for the fluid interaction that turns out to be

$$\boldsymbol{N}_{m\ int} = -\boldsymbol{N}_{f\,int} = \boldsymbol{L}_f \wedge \left(\Pi_f^{-1} \boldsymbol{L}_f \right) = \boldsymbol{L}_f \wedge \left(\boldsymbol{\omega}_m + \boldsymbol{\omega}_f \right). \tag{14}$$

This expression is the same as that obtained by Sasao et al. (1980) by using the fluid motion equation. The same expression is also derived by Moritz (1982) using a variational approach based on Poincaré equations.

Three–layer Earth model

Next, let us consider a model composed of three layers: a rigid axial–symmetrical mantle, a fluid outer core and a rigid axial–symmetrical inner core. The Hamiltonian of the system that is equal to the kinetic energy of the layers is

$$H = T_m + T_f + T_s = \frac{1}{2} < \Pi_m^{-1} \boldsymbol{L}_m, \boldsymbol{L}_m > + \frac{1}{2} < \Pi_f^{-1} \boldsymbol{L}_f, \boldsymbol{L}_f > + \frac{1}{2} < \Pi_s^{-1} \boldsymbol{L}_s, \boldsymbol{L}_s >, \tag{15}$$

where the subscript s refers to the rigid inner core. For this model the fluid interacts both with the mantle and with the inner core, so we have to compute two torques. To do this we follow a similar procedure to the previous one considering the equations

$$\boldsymbol{N}_{m\,int} = \frac{d\boldsymbol{L}_m}{dt} + \boldsymbol{\omega}_m \wedge \boldsymbol{L}_m;\; \boldsymbol{N}_{s\,int} = \frac{d\boldsymbol{L}_s}{dt} + \boldsymbol{\omega}_m \wedge \boldsymbol{L}_s. \tag{16}$$

Therefore, the total torque acting on the fluid is $\boldsymbol{N}_{f\,int} = -\boldsymbol{N}_{m\,int} - \boldsymbol{N}_{s\,int}$. To write easily the former expressions in terms of the Andoyer set for a three–layer Earth model we will put

$$\boldsymbol{L}_m = \boldsymbol{L} - \boldsymbol{L}_f - \boldsymbol{L}_s;\; \boldsymbol{\omega}_m = \Pi_m^{-1}\left(\boldsymbol{L} - \boldsymbol{L}_f - \boldsymbol{L}\right). \tag{17}$$

In this way the components of the interaction torques in the Tisserand frame are

$$\begin{aligned}
\left(N_{m\,int}\right)_j &= \left\{\left(L\right)_j - \left(L_f\right)_j - \left(L_s\right)_j, H\right\} + \\
&+ \sum_{l,k,p=1}^{3} \varepsilon_{jlk} \left(\Pi_m^{-1}\right)_{lp} \left[\left(L\right)_p - \left(L_f\right)_p - \left(L_s\right)_p\right] \left[\left(L\right)_k - \left(L_f\right)_k - \left(L_s\right)_k\right], \\
\left(N_{s\,int}\right)_j &= \left\{\left(L_s\right)_j, H\right\} + \sum_{l,k,p=1}^{3} \varepsilon_{slk} \left(\Pi_m^{-1}\right)_{lp} \left[\left(L\right)_p - \left(L_f\right)_p - \left(L_s\right)_p\right] \left(L_s\right)_k .
\end{aligned} \tag{18}$$

The right hand side of these equations are computed by expressing $\boldsymbol{L}$, $\boldsymbol{L}_f$, $\boldsymbol{L}_s$, Π_m, Π_f and Π_s in terms of the Andoyer canonical set (Escapa et al. 2001). After doing some algebra we obtain the torque acting on the fluid

$$\boldsymbol{N}_{m\;int} + \boldsymbol{N}_{s\,int} = -\boldsymbol{N}_{f\;int} = \boldsymbol{L}_f \wedge \left(\Pi_f^{-1}\boldsymbol{L}_f\right) = \boldsymbol{L}_f \wedge \left(\boldsymbol{\omega}_m + \boldsymbol{\omega}_f\right). \tag{19}$$

The expression related with the inner core is complicated. Anyway, if we only retain first order terms we get the simplified equations

$$\begin{aligned}
\left(N_{s\,int}\right)_1 &= \Omega A_s \delta \left[\left(\omega_m\right)_2 + \left(\omega_f\right)_2 - \left(\Omega k_s\right)_2\right], \\
\left(N_{s\,int}\right)_2 &= -\Omega A_s \delta \left[\left(\omega_m\right)_1 + \left(\omega_f\right)_1 - \left(\Omega k_s\right)_1\right], \\
\left(N_{s\,int}\right)_3 &= 0.
\end{aligned} \tag{20}$$

$\left(k_s\right)_1$ and $\left(k_s\right)_2$ are the x and y components of the symmetry axis of the inner core on the Tisserand frame, Ω is the mean angular velocity of the Earth, A_s is the equatorial inertia moment of the inner core and δ is an adimensional parameter proportional to the dynamical ellipticity of the inner core (Escapa et al. 2001).

If we had employed the method used by Mathews et al. 1991 we would have obtained the same expressions as in (19) and (20). However, here the procedure has been much more simple, since we have only used the kinetic energy of the system. Finally, let us underline the fact that with the Hamiltonian formalism, or other variational method, it is not necessary to compute the expressions of the pressure torques to construct the equations of motion of the system, since these equations are directly derived from the Hamiltonian of the system. This is a great advantage with respect to the Vectorial Mechanics approaches.

5. ACKNOWLEDGMENTS

This work has been partially supported by Spanish Projects I+D+I, AYA2000-1787 and AYA2001-0787, Spanish Project ESP2001-4533-PE and *Junta de Castilla y León*, Project No. VA072/02.

6. REFERENCES

Andoyer, M. H. , *Cours de Mécanique Céléste*, 2 vols., Gauthier–Villar, Paris, 1923.

Escapa, A., Getino, J. and Ferrándiz, J. M., *J. Geophys. Res.*, 106, 11387-11397, 2001.

Escapa, A., Getino, J. and Ferrándiz, J. M., *Proceedings of the Journées 2001*, ed. N. Capitaine, Observatorie de Paris, 239–245, 2002.

Getino, J., *Geophys. J. Int.*, 120, 693–705, 1995a.

Getino, J., *Geophys. J. Int.*, 122, 803–814, 1995b.

Getino, J., and J. M. Ferrándiz, *Proceedings of IAU Colloquium 180*, eds. K. J. Johnston, D. D. McCarthy, B. J. Luzum, and G. H. Kaplan, 236-241, U.S. Nav. Obs., Washington, D.C., 2000.

Getino, J., and J. M. Ferrándiz, *Mon. Not. R. Astr.Soc.*, 322, 785–799, 2001.

González, A. B. and Getino, J., *Celest. Mech.*, 68, 139–149, 1997.

Kinoshita, H., *Celest. Mech.*, 15, 277–326, 1977.

Kinoshita, H. and Sasao, T., *Reference Frames in Astronomy and Geophysics*, eds. J. Kovalesvsky, I. I. Mueller and B. Kolaczek. Dordrecht, Kluwer, 173–211, 1989.

Mathews, P. M., B. A. Buffet, T. A. Herring, and I. I. Shapiro, *J. Geophys. Res.*, 96, 8219-8242, 1991.

Mathews, P. M., B. A. Buffet, T. A. Herring, *J. Geophys. Res.*, 107, 10.1029/2001JB000390, 2002.

Moritz, H., *Bull. Géod.*, 56, 364–380, 1982.

Poincaré, H., *Bull. Astron.*, 27, 321–356, 1910.

Sasao, T., S. Okubo, and M. Saito, *Proceedings of IAU Symposium 78*, eds. E. P. Federov, M. L. Smith, and P. L. Bender, 165–183, D. Reidel, Norwell, Mass., 1980.

Souchay, J., Losley, B., Kinoshita, H. and Folgueira, M., *Astron. Astrophys. Suppl. Ser.*, 135, 111–131, 1999.

Wahr, J. M., *Geophys. J. R. Astron. Soc.*, 64, 705–727, 1981.

VARIABLE PROCESSES IN POLAR MOTION AND LENGTH OF DAY

C. BIZOUARD, S. LAMBERT
SYRTE/UMR8630-CNRS, Observatoire de Paris
61 avenue de l'Observatoire 75014 Paris - FRANCE
e-mail: christian.bizouard@obspm.fr

ABSTRACT. Seasonal terms in the Earth rotation parameters (polar motion and length of day) are broad band processes. This denotes variability of their amplitudes in phase, probably associated with the underlying geophysical process. We show that the patterns of variability in the seasonal terms of the observed polar motion and lenght of day are well correlated with those found in the combined atmospheric-oceanic excitation. This result confirms the reliability of the oceanic angular momentum time series. However correlation between atmospheric-oceanic and observed excitation seems to be spoiled episodically by El Niño and La Niña events.

1. INTRODUCTION

The "fluid layers" of the Earth, the atmosphere, the oceans and the underground water present variable masse distributions, and for this reason exchange angular momentum with the solid Earth. It results considerable effect on the Earth's rotation, currently deduced from the estimates of the Atmospheric Angular Momentum (AAM) and Oceanic Angular Momentum (OAM) changes.

Whereas AAM series are routinely determined since 10 years, OAM series remain still sparse, and production of Hydrological Angular Momentum (HAM) has just started. The first OAM time series date back 1998. Longest official series spans over 1985-1998 (Ponte et al., 1998, 1999, 2000 ; Johnson, 1999).

As shown by recent studies (Brzezinski and Nastula (2000), Gross (2000)) the combined forcing of atmosphere and oceans better matches the observed polar motion (PM), especially the Chandler term. Mean effects of prominent harmonics are investigated in former studies, but spectral peaks reveal broad band processes associated with variable amplitudes and phases. We wonder to which extend pattern of variability in seasonal terms of the polar motion and lenght of day can be accounted for those found in the combined atmospheric-oceanic excitation.

2. GEOPHYSICAL AND GEODETIC EXCITATION FUNCTIONS

Easiest investigation of the atmoshperic/oceanic/hydrological effects on the Earth rotation is to compare the so-called geophysical excitation functions, to the "observed" excitation, which can be inferred from Earth Orientation Parameters (EOP). Geophysical excitation function are less-dimensional forms of the Atmospheric Angular Momentum (AAM) and Oceanic Angular Momentum (OAM).

Let be p the complex-valued coordinate of the Celestial Ephemeris Pole (CEP) in the terrestrial reference frame ($p = x - iy$) and ΔLOD the excess of length-of-day proportional to the time derivative of $UT1 - TAI$ (Universal time - Temps Atomique International). It can be shown (Barnes et al. 1983) that for processes at scales longer than a few days :

$$\begin{aligned} \chi_G &= p + \frac{i}{\sigma_{\rm cw}} \frac{{\rm d}p}{{\rm d}t} \\ \chi_{G,3} &= \frac{\Delta LOD}{LOD} = -\frac{d(UT1 - TAI)}{dt} \end{aligned} \tag{1}$$

where $\sigma_{\rm cw} = \frac{1}{433}(1 + \frac{i}{2Q})$ is the complex-valued frequency of the Chandler Wobble, known as a damping process of frequency of 0.8435 cycles per year and quality factor Q=170 according to Wilson and Vicente (1990), and LOD is the nominal duration of the mean solar day (86400 s). The quantities χ_G and $\chi_{G,3}$ are the so-called geodetical excitation functions to be compared with the geophysical ones coming from the atmosphere χ_A and from the oceans χ_O.

Our basic data are the following :

- The AAM time series (1948-2001) are those of the NCEP-NCAR Reanalysis project, sampled at 0.25 day (Special Bureau for Atmosphere of the IERS : ftp://ftp.aer.com/pub/collaborations/sba/).
- Our OAM series (1985.0 - 1997.95, sampled at 5 days intervals) has been obtained by completing the Ponte's series (1985.0 - 1996.3, sampled at 5 days intervals) with the last years of the Johnsons series (1996.3-1997.95, sampled at 3 days intervals) (Special Bureau for Oceans of the IERS : http://euler.jpl.nasa.gov/sbo/). This complemention is the weak point of our study, in the sense that both oceanic series are unconsistent for some seasonal terms on their overlapping interval.
- The Polar motion-length (from 1958.0 to 2000.0) of the IERS combined series C04, sampled at 1 day, comprehending fluctuations from 6 days (Earth Orientation Center : http://hpiers.obspm.fr/eop-pc/).

We derived Geodetic (G), atmospheric (A) and oceanic (O) excitations sampled at 5 days and spanning 1985.0-1997.95. The effect of zonal tides is removed from UT1 and oceanic tidal effects are removed from PM (9.12, 9.13, 13.63, 0.52, 13.66, 27.56 days) (Gross, 1998).

3. MEAN SEASONAL EFFECTS AND TREND

Seasonal terms and trend (annual, semi-annual and ter-annual) are the most prominent features of the excitation functions. They have been estimated by a least-squares fit on the whole data span 1985-1998.

For this purpose any equatorial excitation function is modelled as the sum of circular and linear terms :

$$\begin{aligned} \chi_1 &= \textstyle\sum_i \quad A_i^{(ip)} \cos(\omega_i t) - A_i^{(op)} \sin(\omega_i t) + at + b \\ \chi_2 &= \textstyle\sum_i \quad A_i^{(ip)} \sin(\omega_i t) + A_i^{(op)} \cos(\omega_i t) + ct + d \end{aligned} \tag{2}$$

where $A^{(ip)i}$ is called the "in-phase" amplitude and $A^{(op)i}$ the "out-of-phase" amplitude with respect to the reference epoch J2000.0 (1 january 2000, 12h UTC). The ω_j, j=1,2,3 are the frequencies associated with the following circular periodic terms : annual prograde and retrograde

terms (-1,1 cpy), semi-annual prograde and retrograde terms (2, -2 cpy), ter-annual prograde and retrograde (3, -3 cpy).

The axial excitations are modeled by :

$$\chi_3 = \sum_i B_i^{(ip)} \cos(\omega_i t) + B_i^{(op)} \sin(\omega_i t) + et + f \tag{3}$$

For equatorial components, adding OAM brings significant improvement of the balance between geodetic and geophysical excitations, except for the semi-annual (both prograde and retrograde) oscillation. The prograde annual term of the atmospheric excitation exhibits too much power with respect to the observed excitation, but the oceanic forcing reduces the relative offset from 30% to 10%. The annual retrograde amplitude undergoes even better change : from 90% to 16%. In all cases the phases are considerably closer to those of the geodetic excitation. This effect of OAM contribution is particularly significant for 1 cpy, -3 cpy, and 3 cpy. These results confirm the influence of the oceanic angular momentum variations on polar motion.

For axial component the OAM does not have significant effect.

4. TIME EVOLUTION OF THE COHERENCE

We have computed the mean coherence function associated with two frequency bands over a sliding window of 2 years. The frequency bands are the "seasonal" ones from -4 cpy to 4 cpy, and the "overall" one including all components from -36 cpy to 36 cpy. Results are displayed in Fig. 1 and Fig. 2 for both axial and equatorial components. The bottom graphics shows that the oceans globally improve the overall coherence, except for some limited periods. In the upper graphics are displayed both the coherence in seasonal band between χ_{A+O} and χ_G and the Southern Oscillation Index (SOI), which quantify the global pressure inhomogeneity over south pacific. The agreement at seasonal frequencies seems to be blurred during the strong minima and maxima of the SOI, that corresponds respectively to El Niño and La Niña events. This is striking for axial and equatorial excitations at the beginning of the year 1987 (maximum of El Niño) and beginning of the year 1989 (maximum of La Niña).

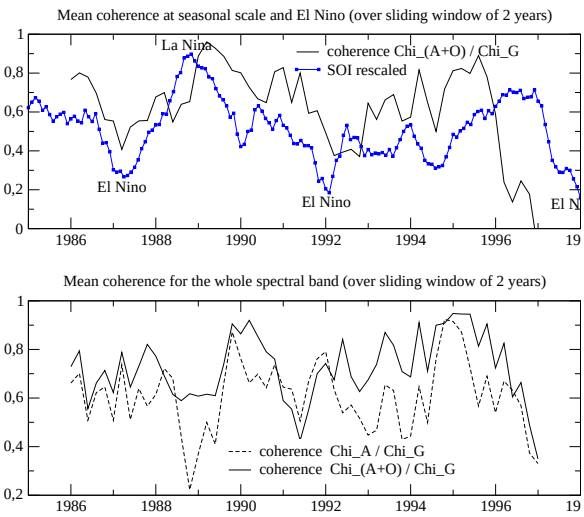

Figure 1: Mean coherence between equatorial excitation functions

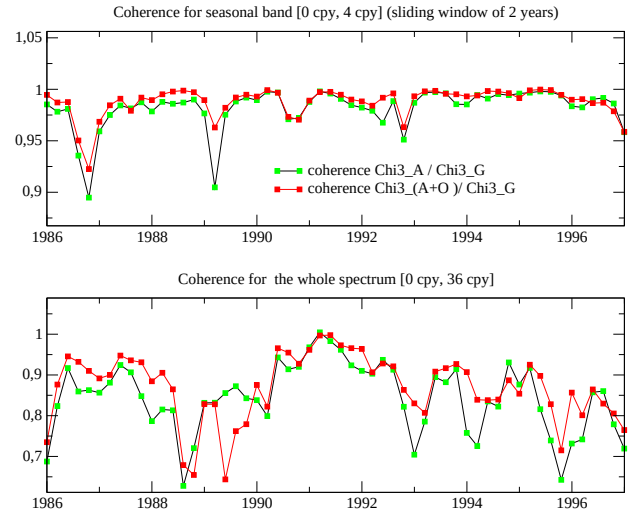

Figure 2: axial excitation functions over 2-year sliding windows

The bottom graphics gives the coherence between χ_G and χ_A or χ_{A+O} over the whole spectrum, the upper ones are restricted to the seasonal bands [-4 cpy, 4 cpy], and shows the rescaled SOI.

5. LEAST-SQUARES ESTIMATION BY SLIDING WINDOW

Time local features in the seasonal band can be determined by least-squares estimations of in-phase and out-of-phase terms restricted to smaller sliding windows.

This procedure has been applied to the excitation functions for the periods of which the amplitude is greater than 4 mas (*i.e.* at least 2 times the rms of the spectrum). The amplitudes are estimated from the residuals, *i.e.* the original signal where the mean periodic effects and the trends have been removed. The model used for least-squares estimation is given by Equations (3) and (3) where the trend is not estimated. The sliding window length is 2 years and the window is shifted by 0.5 year.

Polar motion. For the seasonal components of the equivalent polar motion ($p(\sigma) = \chi(\sigma)/(1 - \sigma/\sigma_{CW})$) results of the least-squares analysis are plotted on Figure 3. The formal error on the estimates is about 4 mas for the annual term, and is below 0.5 mas for the other terms.

Globally the time variations of the amplitude of the seasonal terms on the observed polar motion are well explained by the combined action of the atmosphere and the oceans. Adding the contribution of the oceans makes the value closer to the observation (see Figure 3) and the similarity of the shape of the curve is very strong. The best improvements are encountered for the prograde semi-annual (in-phase and out-of-phase), the prograde annual (out-of-phase) and the prograde ter-annual (out-of-phase) terms for which the correlation grows up very significantly and is then very close to 1.

Nevertheless, for the retrograde annual (out-of-phase), the retrograde semi-annual (in-phase), the prograde ter-annual (in-phase) and the retrograde ter-annual (in-phase) terms, the correlation was close to 1 with the atmospheric effect alone. Adding the oceans does not bring anything or deteriorates the value of the correlation.

For the other seasonal terms, the correlation is made better, but still remains below 0.5 : prograde and retrograde annual terms (in-phase), retrograde semi-annual (out-of-phase) and retrograde ter-annual (out-of-phase) terms.

The ratios of the associated standard deviations are also closer to 1, except for the retrograde semi-annual (out-of-phase) and the retrograde annual (in-phase) terms for which they are deteriorated. Except for the prograde annual component and the ter-annual (out-of-phase) components, the ratios remain around 0.6 even if they are improved by the addition of the oceans.

These small inconsistencies in correlation and standard deviation for seasonal terms are reflected in time domain when the geophysical equivalent polar motion does not agree with the observed polar motion. For example : during the years 1988-1990 in the in-phase terms for +1 and -1 cpy, and around 1994 on the same plots, or 1988-1990 in the out-of-phase term for 3 cpy. On several spans, neither the atmospheric contribution nor the oceanic one are sufficient to explain the observed polar motion. It is the case during the year 1994 on the out-of-phase term for 1 cpy where the addition of the oceanic contribution does not bring anything. The amplitude in the fluid layers is too much important compared to the polar motion, and this result had already been noticed using the wavelet method. The same remark can be done for the out-of-phase term at -2 cpy : around 1993, the polar motion is higher than the predicted effect of the fluid layers and just after 1994, the phenomenon is inverted.

Lenght-of-day. The variability of the seasonal terms is identical in shape both in length-of-day and axial atmospheric excitation. Oceans do not bring significant improvement. However the power of the atmospheric excitation is significantly lower than that on observed in the LOD.

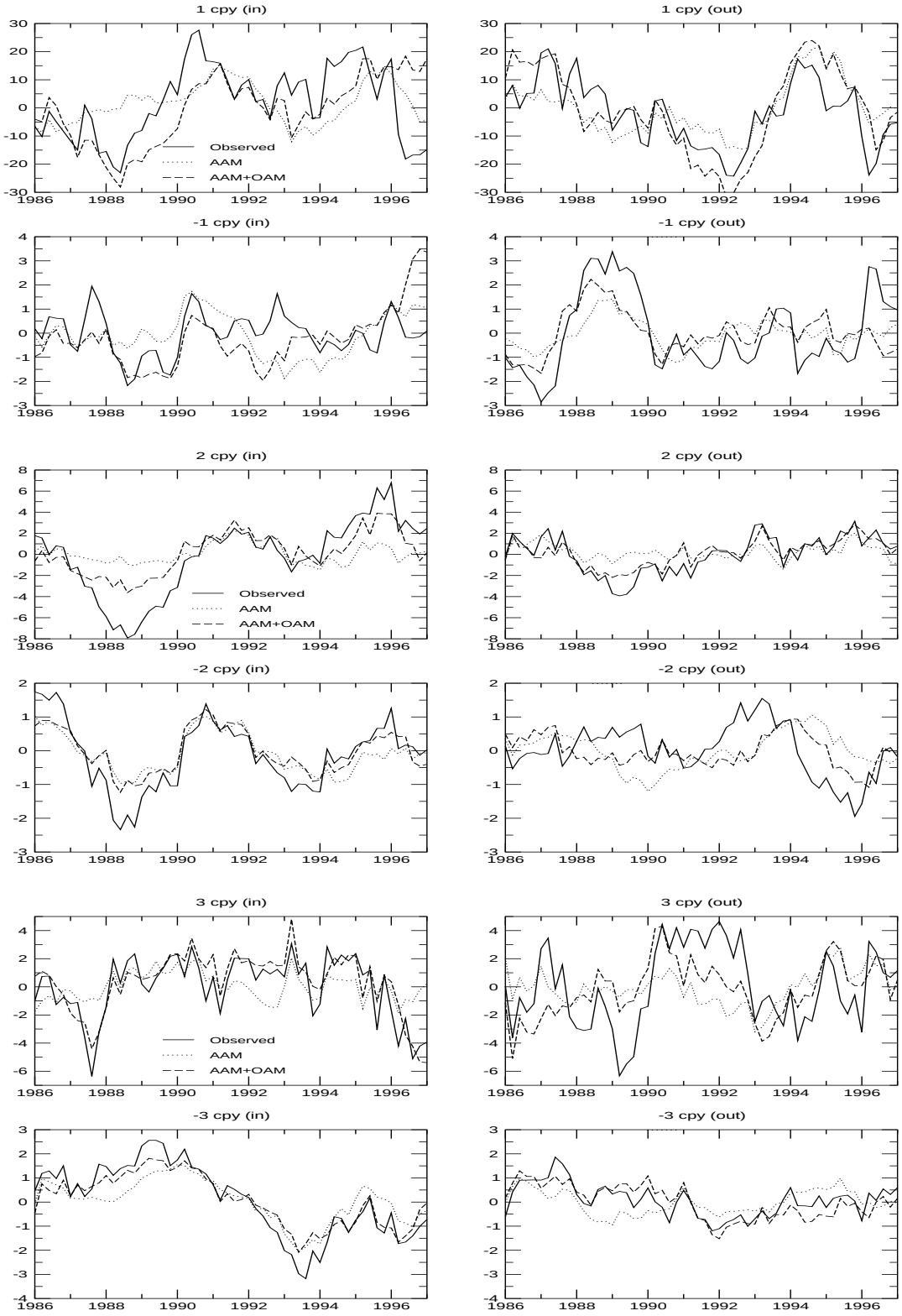

Figure 3: Time variability of prograde and retrograde seasonal terms in the polar motion (full line), the atmosphere (dotted line) and the fluid layers (dashed line) using least-squares estimates and a sliding window. In-phase and out-of-phase terms are defined by Expression (3). The quantity plotted is the equivalent polar motion computed from the excitation.

6. CONCLUSION

Combined atmospheric and oceanic forcing almost well explain the time variability of prominent periodic terms in polar motion. This is a postive test for the reliability of the OAM series. Oceans take a minor part in the axial excitation. Moreover coherence seems to be decreased when El Niño and La Niña present their maximum of activity. This is probably due to the mismodeling of the oceanic and atmospheric circulation during such events.

7. REFERENCES

Barnes R.T.H., Hide R., White A.A., and Wilson C.A., 1983 : Atmospheric angular momentum fluctuations, length-of-day changes and polar motion, *Proc. R. Soc. London*, **A 387**, 31–73.

Brzeziński and Nastula, 2000 : Investigations of the oceanic excitation of non-seasonal polar motion, to be published in *Proceedings COSPAR'2000 Scientific Meeting*, Advances in Space Research.

Gross R., 1998 : Effects of long-period ocean tides on the Earth's polar motion, *progress in oceanography*,vol. **40**, No. 1-4, 385-397.

Gross R., 2000 : The excitation of the Chandler Wobble, *Geophys. Res. Let.*, Vol. **27**, 15, 2329-2332.

Johnson et al., 1999 : *J. Geophys. Res.*, vol. 104, pp. 25183-25195.

Ponte R.M., D. Stammer and J. Marshall, 1998 : Oceanic signals in observed motions of the Earth's pole of rotation, *Nature*, vol. **391**, 476-479.

Ponte R.M. and D. Stammer, 1999 : Role of ocean currents and bottom pressure variability on seasinal polar motion, *J. Geophys. Res.*, vol. **104**, 23393-23409.

Ponte R.P. and D. Stammer, 2000 : Global and regional axial ocean angular momentum signals and length-of-day variations (1985-1996), *J. Geophys. Res.*, vol. **105**, 17161-17171.

Wilson C. R. and Vicente R. O., 1990 : Maximum likelihood estimates of polar motion parameters, *Variations in Earth Rotation, Geophys. Mono. Ser.*, 59, edited by D. D. McCarthy and W. E. Carter, 151-155, AGU, Washington, D.C.

POLAR MOTION PREDICTION BY DIFFERENT METHODS IN POLAR COORDINATES SYSTEM

W. KOSEK
Space Research Centre
PAS, Warsaw, POLAND

1. INTRODUCTION

Prediction errors for a few days in the future of the pole coordinate data determined from the new space techniques is several times greater than their determination errors, which are of the order of 0.1 mas. The current prediction method of polar motion data carried out in the IERS Rapid Service/Prediction Center is the least-squares extrapolation of a Chandler circle, annual and semiannual ellipses and a bias fit to the last 1 year of the combined pole coordinate data (McCarthy and Luzum 1991, IERS 2000). Previously, the length of polar motion data from which this extrapolation model was computed was equal to three years however this increase caused an increase of the mean polar motion prediction errors especially during the time of El Niño events (Kosek et al. 2001a,b). Any improvements made to the polar motion forecast using the autocovariance prediction procedures (Kosek et al. 1998, 2000) were not effective especially in the time of the El Niño event in 1997/98. In this paper, the autocovariance and least-squares prediction were applied to the pole coordinate data transformed into polar motion radius and angular distance (Kosek 2002).

2. DATA

The analysis used the USNO pole coordinate data in the years 1973.0 to 2002.7 with a sampling interval of 1 day (USNO 2002), the IERS EOPC01 pole coordinate data in the years 1846.0 to 2000.0 with the sampling interval of 0.05 years and the IERS EOPC04 pole coordinate data in the years 1962.0 to 2002.7 with the sampling interval of 1 day (IERS 2002). Additionally, the monthly sea surface temperature anomalies Nino 1+2 and Nino 4 in the years 1976.0 to 2002.7 from the Climate Prediction Center (NOAA 2002) were used.

3. THE IERS LEAST SQUARES PREDICTION ERRORS

The distances between polar motion data and their least-squares predictions at different starting prediction epochs from 1 to 50 days in the future are shown in Figure 1. The polar motion data from which the extrapolation model of the Chandler circle, annual and semiannual ellipses and a bias was computed was equal to one and three years. The increase of the length of polar motion data going into the least-squares extrapolation model increases the polar prediction errors (Kosek et al. 2001b). The reasons for these increased errors are irregular short period oscillations of pole coordinate data (Kosek and Kolaczek 1995, Kosek 2000) as well as the phase and amplitude variations of the annual oscillation (Kosek et. al. 2000, 2001a,b). The amplitude

and phase variations of the Chandler and annual oscillations computed by the least-squares method in one year and three year time intervals for the USNO x pole coordinate data are shown in Figure 2. The amplitude variations of these oscillations computed from the y pole coordinate are very similar (Kosek et. al. 2001a,b).

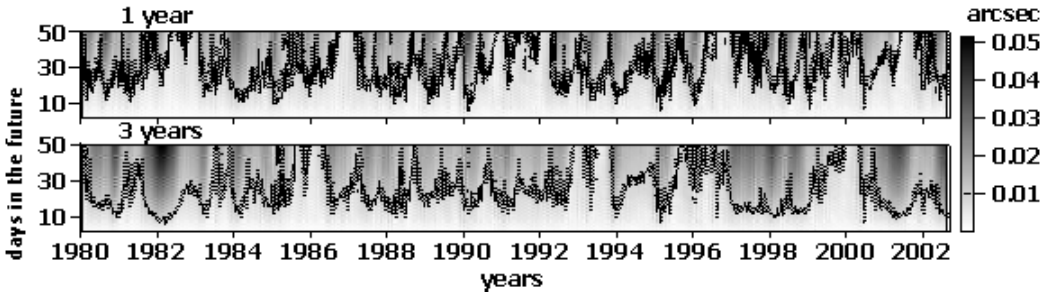

Figure 1: The distances between polar motion data and their least-squares predictions computed at different starting prediction epochs for the time span of polar motion data going into the least-squares extrapolation model equal to one and three years (contour lines at 0.01 arcsec).

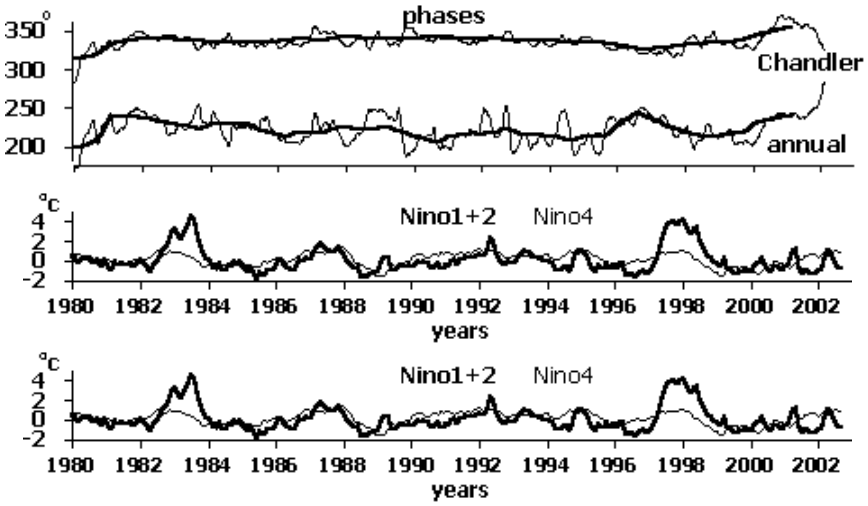

Figure 2: The amplitude and phase variations of the Chandler and annual oscillations computed by the least-squares method in the one (thin line) and three (heavy line) year time intervals and the Nino 1+2 (heavy line) and Nino 4 (thin line) data.

The amplitudes and phases of the Chandler and annual oscillations become smoother when the interval of data going into the least-squares extrapolation model becomes longer. The phases computed by the least-squares using the three year intervals are smoother for the Chandler than the annual oscillation. This means that poor accuracy of the least-squares polar motion predictions are caused by irregular variations of the annual oscillation phases. The two biggest maxima of the annual oscillation phase and amplitude preceded the two biggest El Niño events in 1982/83 and 1997/98 by about 1.5 and 0.5 years, respectively. The increase of the phase and amplitude of the annual oscillation in the year 2000 suggests that another El Niño is expected in the end of this year. The Nino 4 index corresponding to the sea surface temperature difference in the central Pacific has already begun to increase.

4. TRANSORMATION OF POLE COORDINATE DATA BETWEEN CARTESIAN AND POLAR COORDINATE SYSTEM

In order to transform pole coordinate data from the Cartesian to the polar coordinate system in which the polar radius is stationary we must refer the pole coordinate data to the mean pole positions. The radius and angular distance are computed by the following formulae:

$$R_t = \sqrt{(x_t - x_t^m)^2 + (y_t - y_t^m)^2}, \quad t = 1, 2, ..., n \tag{1}$$

$$L_t = \sqrt{(x_t - x_{t-1})^2 + (y_t - y_{t-1})^2}, \quad t = 1, 2, ..., n \tag{2}$$

where: x_t, y_t are the pole coordinates data and x_t^m, y_t^m are the mean pole coordinates data.

The transformation from the polar into the Cartesian coordinate system is carried out when the first predictions of the radius R_{n+1} and angular distance L_{n+1} are known. Time-frequency amplitude spectra computed by the Fourier transform band pass filter (FTBPF) of the complex-valued pole coordinate data show that the amplitudes of oscillations with positive periods are bigger than the amplitudes of oscillations with the negative ones which indicates that oscillations in polar motion are mostly counterclockwise (Kosek 1995). Assuming, that polar motion is counterclockwise, the coordinates of the first prediction point are computed by the linear intersection formulae (Fig. 3) :

$$\begin{Bmatrix} x_{n+1} \\ y_{n+1} \end{Bmatrix} = \frac{\begin{Bmatrix} x_n \\ y_n \end{Bmatrix} \left(\frac{R_{n+1}^2 + R_n^2 - L_{n+1}^2}{4P} \right) + \begin{Bmatrix} -y_n \\ x_n \end{Bmatrix} + \begin{Bmatrix} x_n^m \\ y_n^m \end{Bmatrix} \left(\frac{R_{n+1}^2 + R_n^2 - R_{n+1}^2}{4P} \right) + \begin{Bmatrix} y_n^m \\ -x_n^m \end{Bmatrix}}{2R_{n+1}^2 + 2R_n^2 - L_{n+1}^2 - R_{n+1}^2/4P} \tag{3}$$

where P is the area of the triangle shown in Figure 3.

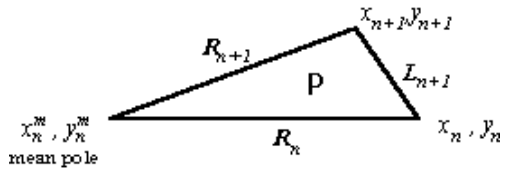

Figure 3: Linear intersection - computation of the first prediction point from the prediction of the radius and angular distance

5. PREDICTIONS OF THE MEAN POLE, RADIUS AND ANGULAR DISTANCE

In order to compute predictions of the radius and angular distance the autocovariance (Kosek 1993, 1997) and least-squares prediction methods were applied. It has been shown that the autocovariance prediction of the model pole coordinate data similar to the observed polar motion data does not predict these data as accurately as the forecast computed from the predictions of the radius and angular distance (Kosek 2002).

One of the problems in polar motion prediction through transformation of pole coordinates into a polar coordinate system is the determination of the mean pole and its prediction. The mean pole coordinate data were computed by the Ormsby (Ormsby 1961) and Butterworth (Otnes and Enochson 1972) low pass filters (LPF) with the cutoff period of 18 and 7 years, respectively. The Ormsby LPF cuts off the beginning and the end of time series outputs due

to filter length by 3 years, so in order to have the mean pole positions at the end of time series they must be predicted. Three-year least-squares predictions of the mean pole computed at different starting prediction epochs are shown in Figure 4. The agreement between the mean pole coordinates and their predictions is good and of the order of the differences between outputs of the different LPFs. The systematic difference between the mean pole and its prediction will produce an oscillation with a period approximately equal to one year in the computed polar motion radius (eq. 1). The radius and angular distance computed from the EOPC01 extended by the EOPC04 pole coordinate data are shown in Figure 5. The reason for longer period variations in the polar motion radius is the variable amplitude of the Chandler oscillation (Schuh et al. 2001). Time-frequency amplitude spectra computed by the FTBPF of the polar motion radius and angular distance show that the beat period of the Chandler and annual oscillations is not constant. Since 1960s the oscillation with a period equal to about 3 years can be seen as a beat period between the semiannual and semi-Chandler oscillations (Kosek and Kolaczek 1997).

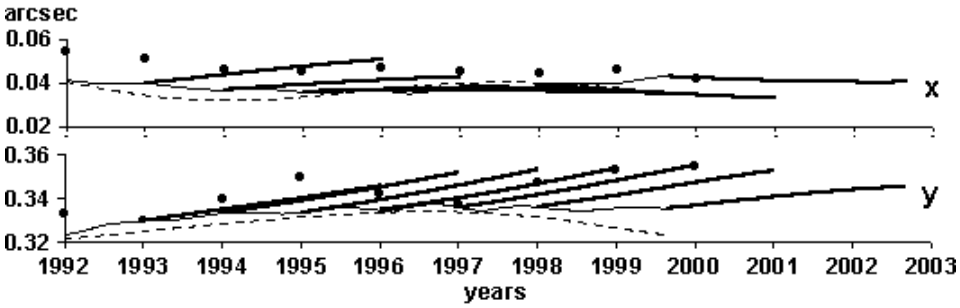

Figure 4: Three-year least-squares predictions computed at different starting prediction epochs (heavy line) of the mean pole computed by the Ormsby LPF (thin line) and the mean pole computed by the Butterworth LPF (dashed line) and by the IERS (dots) (IERS 2002).

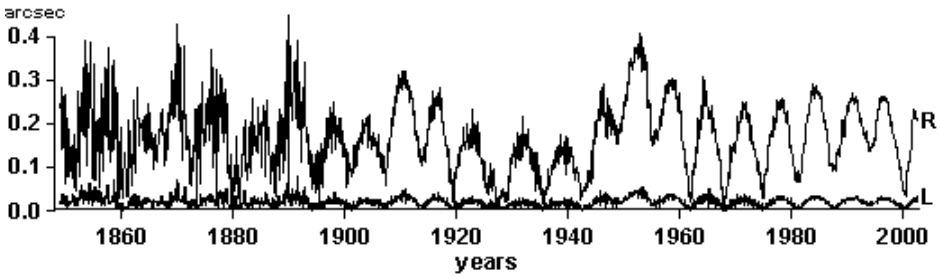

Figure 5: The radius and angular distance computed from the IERS C01 pole coordinate data.

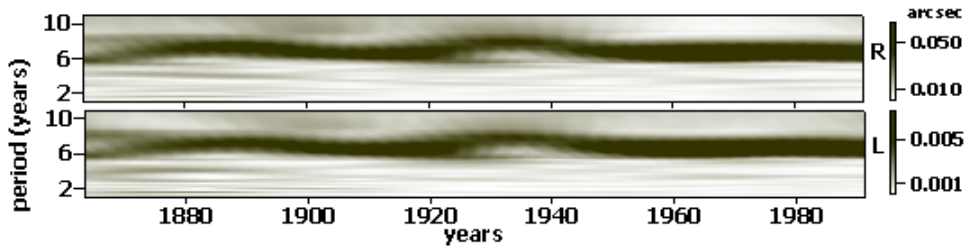

Figure 6: Time-frequency FTBPF amplitude spectra of the polar motion radius and angular distance.

The beat period of the Chandler and annual oscillations computed from the minima and maxima of the polar motion radius and angular distance is shown in Figure 7. The beat period of the Chandler and annual oscillation can be also computed from the least-square phase variations $\Delta\varphi$ of the Chandler and annual oscillations shown in Figure 2. The change of the period ΔT of the Chandler or annual oscillations can be computed from the change of the their least-squares phase variations $\Delta\varphi$ according to the formula:

$$2t\pi/T + \varphi + \Delta\varphi = 2t\pi/(T + \Delta T) + \varphi = const \tag{4}$$

The beat period of the Chandler and annual oscillation can be computed from variable periods of these oscillations according to the following formula:

$$1/T_{beat} = 1/(T_{An} + \Delta T_{An}) - 1/(T_{Ch} + \Delta T_{Ch}) \tag{5}$$

Since the Chandler phase is not fixed in time a robust method (Priestley 1981) was applied to eliminate its drift before the change of the Chandler period ΔT_{ch} was computed.

One-year autocovarince and least-squares predictions of polar motion radius and angular distance computed at different starting prediction epochs agree well with the future data (Fig. 7). In the least-squares prediction the beat period was equal to 6.1 years in the extrapolation model and this model shows a good agreement with the future data only from 1995 to 1998. Outside this time interval, this beat period does not have an appropriate value in the extrapolation model.

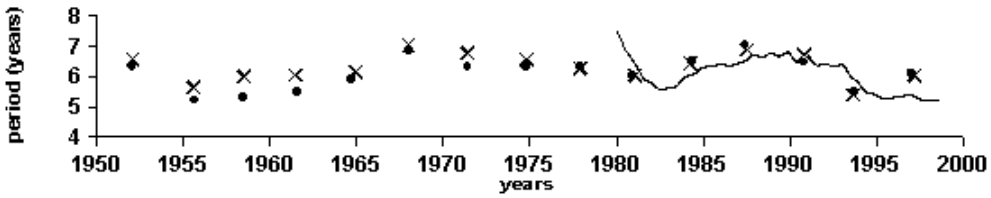

Figure 7: The beat period of the Chandler and annual oscillations computed from the smoothed minima and maxima of the polar motion radius (crosses) and angular distance (dots) and computed from the least-squares phase variations $\Delta\varphi$ of the Chandler and annual oscillations

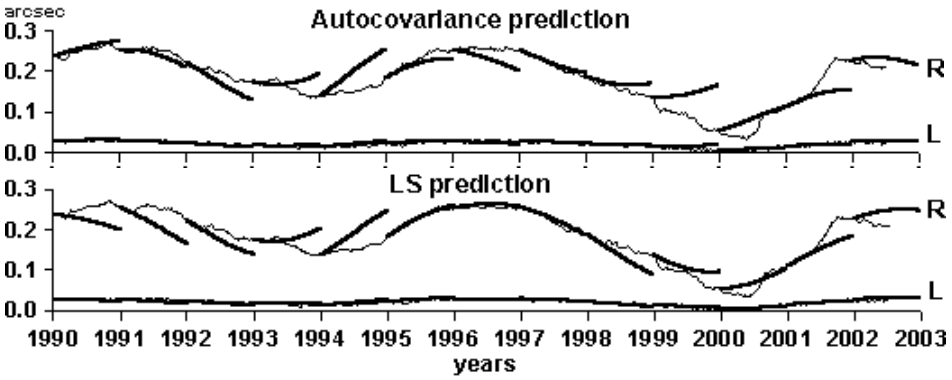

Figure 8: One-year autocovarince and least-squares predictions (heavy lines) of polar motion radius and angular distance (thin lines) computed at different starting prediction epochs.

The distances between the pole coordinate data and their autocovariance predictions computed at different starting prediction epochs are shown in Figure 9. The prediction errors depend

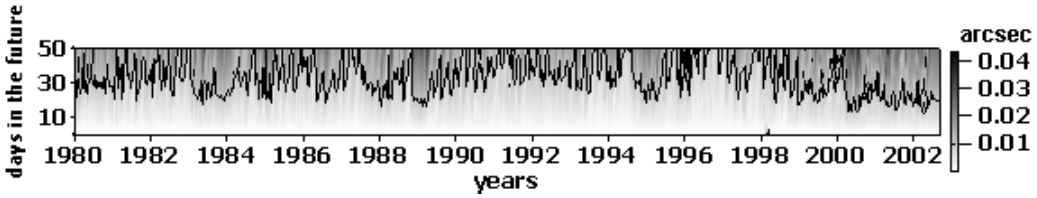

Figure 9: The distances between polar motion data and their autocovariance predictions computed at different starting prediction epochs (contour line at 0.01 arcsec).

on starting prediction epochs but they are not as big as the predictions carried out by the IERS Rapid Service/Prediction Center (Fig. 1) especially for short prediction times.

5. CONCLUSIONS

Polar motion least-squares prediction errors depend on irregular phase and amplitude variations of the annual oscillation that had maximum values before the El Niño events in 1982/83 and 1997/98. The increase of the annual oscillation phase and amplitude in 2000 indicates that another El Niño is expected in the end of this year.

Transformation of pole coordinate data from the Cartesian to a polar coordinate system transforms the Chandler and annual as well as the semi-Chandler and the semiannual frequencies into their beat frequencies which helps to solve the frequency resolution problems. Accuracy of polar motion prediction by the method of autocovariance through the transformation to polar coordinate system depends on predicting accurately the mean pole, radius and angular distance. The period of the most energetic oscillation in polar motion radius and angular distance representing the beat period of the Chandler and annual oscillations is variable mainly due to variable phase or period of the annual oscillation.

The error of the autocovariance prediction for a few days in the future is less than the prediction error of the current polar motion forecast carried out by the IERS Rapid Service/Prediction Center.

Acknowledgments. This paper was supported by the Polish Committee of Scientific Research project No 8 T12E 005 20 under the leadership of Dr. W. Kosek. The author thank Brian J. Luzum for his comments that improved the manuscript.

6. REFERENCES

IERS 2000, IERS Annual Report 2000, http://www.iers.org/iers/publications/reports/2000/.

IERS 2002, The Earth Orientation Parameters, http://hpiers.obspm.fr/eop-pc/.

Kosek W. 1993, The Autocovariance Prediction of the Earth Rotation Parameters. Proc. 7th International Symposium "Geodesy and Physics of the Earth" IAG Symposium No. 112, Potsdam, Germany, Oct. 5-10, 1992. H. Montag and Ch. Reigber (eds.), Springer Verlag, 443-446.

Kosek W., 1995, Time Variable Band Pass Filter Spectra of Real and Complex-Valued Polar Motion Series, Artificial Satellites, Planetary Geodesy, No 24, Vol. 30 No 1, 27-43.

Kosek W. and Kolaczek B., 1995, Irregular Short Period Variations of Polar Motion. Proc. Journées 1995 "Systèmes de Référence Spatio-Temporels", Warsaw, Poland, Sep. 18-20, 117-120.

Kosek W., 1997, Autocovariance Prediction of Short Period Earth Rotation Parameters, Artificial Satellites, Journal of Planetary Geodesy, Vol. 32, No. 2, 75-85.
Kosek W. and Kolaczek B., 1997, Semi-Chandler and Semiannual Oscillations of Polar Motion. Geophysical Research Letters, Vol. 24, No 17, 2235-2238.
Kosek W., McCarthy D.D., Luzum B. 1998, Possible Improvement of Earth Orientation Forecast Using Autocovariance Prediction Procedures, Journal of Geodesy, 72, 189-199.
Kosek W., 2000, Irregular short period variations in Earth rotation, IERS Technical Note 28, 61-64.
Kosek W., D.D. McCarthy and B.J. Luzum, 2000, Prediction of complex-valued polar motion using the combination of autocovariance prediction and a least-squares extrapolation, paper presented at the EGS General Assembly, 2000, Nice, France, 24-29 April, 2000.
Kosek W., McCarthy D.D., and Luzum B.J., 2001a, El Niño impact on polar motion prediction errors, Studia Geophysica et Geodaetica, 45, 347-361.
Kosek W., McCarthy D.D., and Luzum B.J., 2001b, Variations of annual oscillation parameters, El Niño and their influence on polar motion prediction errors, submitted to Proc. Journées 2001 "Systèmes de Référence Spatio-Temporels", Brussels, Belgium, 24-26 September 2001.
Kosek W., 2002, Autocovariance prediction of complex-valued polar motion time series, Advances of Space Research, Vol. 30, No. 2, 375-380.
McCarthy D.D. and Luzum B.J. 1991, Prediction of Earth Orientation, Bull. Géod., 65, 18-21.
NOAA 2002. Climate Prediction Center - Data: Current Monthly Atmospheric and SST index values, http://www.cpc.ncep.noaa.gov/data/indices/
Ormsby J.F.A., 1961. "Design of Numerical Filters with Application to Missile Data Processing", J. Assoc. Compt. Mach., 8, 440-466.
Otnes R.K. and Enochson L., 1972, Digital Time Series Analysis, John Wiley and Sons Inc., New York.
Priestley M.B. 1981, Spectral Analysis and Time Series, Academic Press, London, 1981.
Schuh H., Nagel S., Seitz T., 2001, Linear Drift and Periodic Variations Observed in Long Time Series of Polar Motion. Journal of Geodesy, 74, 701-710.
USNO 2002, The Earth orientation parameters - finals.all

PRECISE ANALYSIS OF EOP SERIES: AN ATTEMPT TO DISTINGUISH CHAOTIC AND NON-STATIONARY PROCESSES.

O. KUDLAY
Main Astronomical Observatory of National Academy of Sciences of Ukraine
03680, Golosiiv, Kyiv-127, UKRAINE
e-mail: Kudlay@mao.kiev.ua

ABSTRACT. Recently some authors applying independent mathematical techniques - Lyapunov exponents and Volterra-Wiener-Korenberg (VWK) predictor - have detected chaotic properties in EOP and AAM series. Using extreme VWK robustness and sensitivity we processed short (less than 1 per cent data length fitted for the classic Lyapunov method) and variable EOP and AAM series to perform time decomposition of chaotic signal. Method validation and verification are discussed also.

Last two years were reported about results of new approach to Earth Orientation Parameters (EOP) series analysis [1], [2],[3]. The new interpretation of EOP data with nonlinear dynamics techniques as a chaotic values had a definite success. But usually applied methods such as Lyapunov exponents and correlation integral having strong restriction - data length can not be shorter than 10000 points, and weak sensibility gave only definite confidence results for limited number of series. Two years ago we applied to EOP series recently developed in system analysis Volterra-Wiener-Korenberg (VWK) method further study of which showed its unic properties [4]. VWK provided reliable detection of chaotic signal in contaminated by noise and distorted by other processes data. But the main property that makes it most powerful for the real series analysis is the possibility to process small number of points data. For its mathematical foundations please refer to [5], [6].

In chaotic data analysis VWK works as one-step-ahead predictor that consider a system as a close-loop version of black box when output y_n feeds back as delayed input . Discrete Volterra-Wiener-Korenberg form of degree d and memory k is constructed to calculate the predicted time series y_n^{calc}:

$$\begin{aligned} y_n^{calc} = \quad & a_0 + a_1 y_{n-1} + a_2 y_{n-2} + \ldots + a_k y_{n-k} + \\ & a_{k+1} y_{n-1}^2 + \ldots + a_{k+2} y_{n-1} y_{n-2} + a_{M-1} y_{n-k}^d \end{aligned} \tag{1}$$

where all distinct combinations of $(y_{n-1}, y_{n-2}, \ldots, y_{n-k})$ up to degree d is composed.

Prognosis quality are estimated as normalized error squared

$$\varepsilon^2(k,d) = \sum_{n-1}^{N} (y_n^{calc}(k,d) - y_n)^2 / \sum_{n-1}^{N} (y_n - \bar{y})^2$$

Predictions are performed until optimal degree d and memory k minimizes information criterium C(r)

$$C(r) = \log \varepsilon(r) + r/N \tag{2}$$

where r- number of polynomial terms of truncated Volterra expansion for a certain pair {k,d}.

Srandard Fisher criterium serves to reject the hypothesis that nonlinear model is not better that linear one as one-step-ahead predictor. For the simulated chaotic system it is easy to choose what model is better due to the large difference - some orders of value, between them. Another situation arises when real EOP data are processed , because both curves becomes fluctuative, not so distant one from other and their prediction level is much closer to zero . Fisher criterium vary over the signifince level, but conclusion about models superiority becomes marginal [4] .

To find the origin of distortions we performed a study of method constraints and tested it on large diversity of simulated models as chaotic and stochastic ones. First of all we looked for shortest data length the method can reliably process. As it was occured VWK do not have practically such a constraint - even about 20-30 points can be enough if the system is more or less simple. If so, then what about reliability of Fisher criterium on such short time span? Most crucial moment here is the whitness of prognosis residuals. To verify it one used Pirson criterium compared with carefully simulated white noise signal . Realibility was confirmed with full confidence.

Tne next step - simulation stochastic signals . We applyed theory of probability theorem as generator of arbitrary complex stochastic signal x(r).If random value r has constant distribution on the [0,1] span then the relation between it and random value x(r) with dencity function f(t) is:

$$r = \int_{-\infty}^{x(r)} f(t)dt \tag{3}$$

Solving the function equation one can provide process x(r) stationary or not depending on are the Gaussian function f(t) has stationary or not parameters. An analysis of large diversity of series generated such a way displayed that prediction power of both linear and nonolinear models are low and practically equal one to another but at the same time much more fluctuative.

Last step - series generation which contain strong harmonics contaminated by noise. Here we found main restriction of the method - it fails when beating processes are in data, may be due to their proportionality to linear correlation function involved in computing of Volterra form coefficients.

So after short summary of above mentioned results it was chosen the optimal way for Volterra-Wiener-Korenberg method application. First of all - to return to tradional nonlinear analysis processing -preliminary data filtration and work in spectral bands . And second - to perform VWK on short time span of about hundred points which moves along the series. In fact we provide such a way temporal evolution of chaotic signal in the spectral domain.For the analysis we have taken the same frequency bands for all series: low frequency band with periods T more than 2 years, high frequency band - seasonal oscillations with T less than 100 days, and Chandler band - 2 months wide near 1.2 year value. After that innovation the analysis results changed drastically.

IPMS polar motion leaves no doubts in chaotic behaviour in all frequency domains. The picture is held for EOP C01 series to the exclusion of low frequency band . From our point of view chaotic signal disappearance here could happen due to the plate motion exclusion from the series. The hypothsis must be verified in the future investigation.

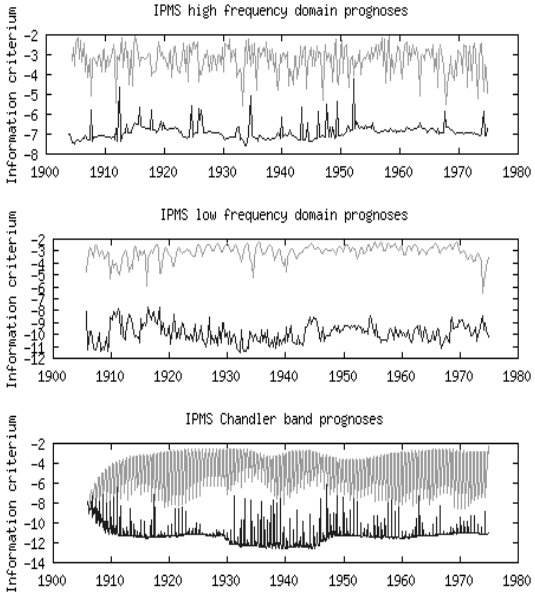

Figure 1: IPMS polar motion prediction by VWK . Frequency bands from up downward:high,low,Chandler. Everywhere polar motion is recognized as confidently chaotic. Vertical axes scale is logarithmical so results presented here about 100 times more confident then in [4]

SPACE 2002 polar motion, LOD and Atmospheric Angular Momentum (AAM) x,y preassure terms showed chaoticity with big confidence also. Fisher criterium was 1000 times stronger than theoretical value for the level 99 % for all series.

CONCLUSIONS

1. Volterra-Wiener-Korenberg is the first technique that enabled to compute temporal evolution of chaotic processes with good resolution.

2. The analysis results in definite spectral bands assures that polar motion, LOD and some components of AAM are chaotic values.

3. Disapearance of low frequency chaotic signal in EOP C01 and SPACE 2002 series were happened may be due to plate motion exclusion during data preprocessing.

4. To be the explicit parameter chaoticity of polar motion, LOD and some AAM components must be approved by careful investigation of possible perturbations which mathematical preprocessing procedures can do in chaotical series. Classical astrometry and new technique observations are not direct mesuarements of EOP. Polar motion, length of day and AAM components are the result of big number mathematical procedures and reduction application. And as preliminary study revealed [4] some of them inevitably distort chaotic values

References

[1] Kudlay O., *Nonlinear effects detection in EOP series. Journees 2000, Observatoire de Paris, 2000.*

[2] Frede V.,Mazzega P., *Detectability of deterministic non-linear processes in Earth rotation time-series. Embedding ,Geophys.J.Int, 137,551-564, 1999.*

[3] Frede V., Mazzega P., *Detectability of deterministic non-linear processes in Earth rotation time-series. Dynamics ,Geophys.J.Int, 137,565-579, 1999.*

[4] Kudlay O., *Earth orientation parameters irregularity effect on rotational eigenmodes modelling , Journees 2001, Royal observatory of Belgium , 2001.*

[5] Barahona M., Chi-Sang Poon, *Detection of non-linear dynamics in short, noisy time series, Nature, 381, 215-217, 1996.*

[6] V.Volterra, *Theory of functional and Intergo-Differential Equations, Dover, New York, 1953.*

FREE MOTION OF ELASTIC BODIES WITH RESPECT TO AN INERTIAL AND BODY-FIXED FRAME. APPLICATION TO THE EARTH

J. SOUCHAY[1] and M. FOLGUEIRA[2]

[1] SYRTE - Observatoire de Paris
61 avenue de l'Observatoire
E-mail: Jean.Souchay@obspm.fr

[2] Instituto de Astronomía y Geodesia (UCM-CSIC), Facultad de Ciencias Matemáticas
Universidad Complutense de Madrid, 28040 Madrid. Spain
E-mail: martafl@iagmat1.mat.ucm.es

ABSTRACT

The free motion of an elastic body can be obtained from that of a rigid one with the same parameters, but by taking into account the variations of the components of the tensor of inertia with respect to the time.

We show how this way of computation, constructed either from the classical equations for the angular momentum or from Hamiltonian theory as well, leads to some interesting contributions to the polar motion, depending on the elasticity and the triaxial form of the body (for instance the Earth), to be added to some classical ones, as the presence of the Chandler wobble.

1. INTRODUCTION.

The torque-free rotational motion, sometimes called the *Euler-Poinsot problem*, of a body corresponds to that in which the torque exerted by the Sun and the Moon is neglected. The formulation of the corresponding equations of such problem for elastic body can be expressed into two different ways:

- In terms of the rectangular components of the angular velocity vector, by considering the classical Liouville equations, and
- In terms of Andoyer's variables (L, G, H) and its canonically conjugate variables (l, g, h), by using Hamiltonian mechanics.

Motivated by Kubo's procedure (1991), which applied Hamiltonian mechanics to the problem of the free motion of the elastic Earth, we undertake an extension of his study considering an axially body instead of a body with rotational symmetry.

2. EXTENSION OF KUBO'S PROCEDURE: VARIATIONAL EQUATIONS.

In this section, we will generalize the equations of the torque-free rotational motion of a rigid body in terms of the Andoyer variables as discussed in (Souchay *et al.*, 2002), to the case of a deformable body. The Hamiltonian for the free rotation (which is equal to the kinetic energy) in this case has the form (Kubo, 1991):

$$\begin{aligned} \mathcal{K} &= \frac{1}{2\,ABC}\Big\{\Big[\,BC\sin^2 l \,+\, AC\cos^2 l\Big]\,(G^2-L^2) \,+\, ABL^2 \\ &- CF(G^2-L^2)\sin 2l \,-\, 2L\sqrt{G^2-L^2}\,\Big[\,BE\sin l \,+\, AD\cos l\Big]\,\Big\} \end{aligned} \tag{1}$$

where, A, B and C are the moments of inertia and D, E and F are the products of inertia of an non-rigid body with respect to the Tisserand axes ($A = A_0 + \Delta A$, $B = B_0 + \Delta B$ and $C = C_0 + \Delta C$, with (A_0, B_0, C_0) corresponding to a rigid axially body).

If the elastic body rotates about an axis which deviates from the axis of symmetry of the body, then centrifugal forces tend to distort it and therefore this distorsion originates variations in the tensor of inertia. This effect is known as *rotational deformation*, which is the only one to take into account in the study of the torque-free rotational motion of an elastic body. Periodic variations in the tensor arising from rotational deformation are given by (Kubo, 1991; Souchay & Folgueira, 2002):

$$\begin{aligned} \Delta A &= \Delta B = \Delta C = 0 \\ D &= \beta\, C_0 \sin J^\star \,\cos l^\star \,=\, \beta\, C_0 \sin J^\star \,\cos(l+\delta) \\ E &= \alpha\, C_0 \sin J^\star \,\sin l^\star \,=\, \alpha\, C_0 \sin J^\star \,\sin(l+\delta) \\ F &= 0 \end{aligned} \tag{2}$$

where the following notations were adopted:

$$\alpha = \frac{k}{k_s}\frac{C_0 - A_0}{A_0} \quad \text{and} \quad \beta = \frac{k}{k_s}\frac{C_0 - A_0}{B_0} \tag{3}$$

with, k is a *Love number*, k_s is the *secular Love number* equals to $\frac{3\kappa^2(C_0-A_0)}{a^5\Omega^2}$ (κ^2 denotes the gravitational constant and a is the Earth's equatorial radius). Following (Kubo, 1991; p.171), D and E should be considered only as functions of time. So, we have denoted J and l in the above expression as $J^\star$ and $l^\star$. Numerically, they are equal to J and and l, respectively. δ represents a time lag between the rotational axis and the pole of the equatorial bulge due to the centrifugal force, then, $l^\star$ should be equal to $l + \delta$ ($\delta > 0$).

When these last expressions are substituted in the general expression of the Hamiltonian (1) one obtains, neglecting terms of second and higher order:

$$\begin{aligned} \mathcal{K} &= \frac{1}{2\,A_0B_0C_0}\Big\{\big[B_0C_0\sin^2 l \,+\, A_0C_0\cos^2 l\big]\,(G^2-L^2) \,+\, A_0B_0L^2 \\ &- 2L\,\sqrt{G^2-L^2}\,\Big[\,\alpha B_0C_0\sin J^\star\,\sin l^\star\,\sin l \,+\, \beta A_0C_0\sin J^\star\,\cos l^\star\,\cos l\Big]\Big\} \end{aligned} \tag{4}$$

Adopting the following notations:

$$\bar{A} \;=\; \frac{A_0+B_0}{2} \qquad \text{and} \qquad \varepsilon = \frac{A_0-B_0}{A_0+B_0} \tag{5}$$

the Hamiltonian (4) can be then rewrite as, in terms of $\bar{A}$ and ε:

$$\mathcal{K} \;=\; \mathcal{K}^R \,-\, \frac{L}{\bar{A}}\sqrt{G^2-L^2}\sin J^\star \Big[\,\alpha(1-\varepsilon)\sin l^\star\,\sin l \,+\, \beta(1+\varepsilon)\cos l^\star\,\cos l\Big] \tag{6}$$

where $\mathcal{K}^R$ is the Hamiltonian of the torque-free motion for a rigid body with a triaxial form (Souchay *et al.*, 2002).

Variational equations:

Once we have obtained the Hamiltonian corresponding to the torque-free rotational motion of an elastic body in terms of Andoyer variables (L, G, H, l, g, h), we can use the general Hamilton's equations of motion to establish the variational equations of the problem considered here (Kinoshita, 1977):

$$\begin{aligned} \frac{d}{dt}(L,G,H) &= -\frac{\partial \mathcal{K}}{\partial(l,g,h)} \\ \frac{d}{dt}(l,g,h) &= \frac{\partial \mathcal{K}}{\partial(L,G,H)} \end{aligned} \tag{7}$$

which express the time variations of Andoyer variables in function of partial derivatives of the Hamiltonian. Thus, the substitution of the Hamiltonian (6) in the previous expressions gives us the following expressions for the temporal variations of Andoyer variables and the angle J:

$$\begin{aligned} \frac{dL}{dt} &= \frac{\varepsilon}{\bar{A}}\,G^2\sin^2 J\sin 2l \,+\, \frac{GL}{\bar{A}}\sin J\sin J^\star\,[\rho\sin\delta \,+\, \tau\sin(2l+\delta)] \\ \frac{dG}{dt} &= 0 \\ \frac{dH}{dt} &= 0 \\ \frac{dl}{dt} &= -\frac{L}{\bar{A}}\left(\frac{C_0-\bar{A}}{C_0}\right) - \frac{\varepsilon}{\bar{A}}\,L\cos 2l \,+\, \frac{L}{\bar{A}}\,[\rho\cos\delta \,-\, \tau\cos(2l+\delta)] \\ \frac{dg}{dt} &= \frac{G}{\bar{A}} \,+\, \frac{\varepsilon}{\bar{A}}\,G\cos 2l \,-\, \frac{L}{\bar{A}}\,[\rho\cos\delta \,-\, \tau\cos(2l+\delta)] \\ \frac{dh}{dt} &= 0 \\ \frac{dJ}{dt} &= -\frac{\varepsilon}{\bar{A}}\,G\sin J\sin 2l \,-\, \frac{L}{\bar{A}}\sin J^\star\,[\rho\sin\delta \,+\, \tau\sin(2l+\delta)] \end{aligned} \tag{8}$$

where,

$$\rho \;=\; \frac{1}{2}\left[\alpha(1-\varepsilon) \,+\, \beta(1+\varepsilon)\right] \qquad \text{and} \qquad \tau = \frac{1}{2}\left[\alpha(1-\varepsilon) \,-\, \beta(1+\varepsilon)\right] \tag{9}$$

To integrate this system of first order differential equations, we have used a fifth-order adaptative stepsize Runge-Kutta-Fehlberg algorithm.

3. CONCLUSIONS AND APLICATIONS.

It should be worthy of noticing that this numerical approach provides not only a check on some classical results from the analytical methods but it is particulary useful and effective in obtaining the solution in a not so complicated way as that carried out using different approaches.

As the solution of this problem has a direct dependence with the principal moments of inertia of the body, the torque-free rotational motion will therefore provide an useful material relating to the behaviour of the body under a large-scale, and it may hence be of great interesting connection with the investigation of slow changes in the figure of the Earth and any other celestial bodies.

7. REFERENCES

Kinoshita, H.: 1977, "Theory of the rotation of the rigid Earth". *Celes. Mech.* **15**, 277-326.

Kubo, Y.: 1991, "Solution to the rotation of the elastic Earth by method of rigid dynamics". *Celes. Mech.* **50**, 165-187.

Lambeck, K.: 1980, "The Earth's variable rotation". *Cambridge University Press.*

Moritz, H. and Mueller, I.I.: 1987, "Earth rotation: Theory and Observation". *The Ungar Publishing Company*, New York.

Munk, W.H. and MacDonald, G.J.F.: 1975, "The rotation of the Earth: A geophysical discussion". *Cambridge University Press.*

Souchay, J., Folgueira, M. and Bouquillon, S.: 2002, "Effects of the triaxiality on the rotation of celestial bodies: application to the Earth, Mars and Eros". *(submitted to Earth, Moon and Planets).*

Souchay, J. and Folgueira, M.: 2002, "Solution to the torque-free rotational motion of an elastic body by a numerical integration method". *(in preparation).*

THEORY OF NUTATION OF THE NON-RIGID EARTH WITH THE ATMOSPHERE

V.E. ZHAROV, S.L. PASYNOK
Sternberg State Astronomical Institute
119992, Universitetskij pr.,13,Moscow,Russia
e-mail: zharov@sai.msu.ru

ABSTRACT. The nutation series ZP2002 based on geophysical theory of the non-rigid Earth with the atmosphere was obtained. The modeling of precession and nutations is based on a fit to the VLBI observational data. A brief description of the series is presented.
The series ZP2002 was obtained by convolution of the rigid Earth nutation series with the transfer function. The resonance parameters and frequencies of the transfer function are determined by the Earth structure. They were calculated by taking into account physical limitations related to the Earth's inner structure parameters. Another important step is an incorporation of additional effects in order to create a more accurate theory. In particular, we investigate the role of the atmosphere as well as viscosity of the liquid core on nutation. The wrms errors of residuals in $\Delta\varepsilon$ is 0.29 mas, and in $\sin\varepsilon_0\Delta\psi$ is 0.20 mas (the FCN model is not included in ZP2002 series).

1. INTRODUCTION. The IAU Resolution B1.6 (2000) states that beginning on 1 January 2003, the IAU 1976 Precession Model and IAU 1980 Theory of Nutation will be replaced by the precession-nutation model IAU 2000A (MHB2000, based on the transfer functions of Mathews, Herring and Buffett(2000)). Besides this, the IAU recommends to continue of theoretical developments of non-rigid Earth nutation series for more accurate account of some processes which are difficult to model.
In this paper account of the atmosphere, viscosity of the fluid outer core (FOC) with radial distribution and non-isotropic heating of the FOC are discussed. The solid inner core (SIC) and electro-magnetic coupling were taken into account according Mathews et.al.(1998). The mantle non-elasticity (frequency-dependent number k and others) was taken into account according Wahr and Bergen (1986). For ocean corrections the model of Huang et. al. (2001) was used.

2. THE ATMOSPHERE EFFECTS ON NUTATION. There are two methods of account of the atmosphere: angular momentum and torque approaches. The torque approach was developed in many papers (see e.g. de Viron and Dehant (1998), Bizouard, de Viron and Dehant (1999)).

We used the angular momentum approach that has been applied for modeling of the atmospheric effects on nutation in papers of Sasao and Wahr (1981), Zharov and Gambis (1996),

Bizouard et al. (1998). It allows to avoid direct calculation of the friction torques. Besides, angular momentum approach allows to describe the rotation of the atmosphere by the dynamical equation and add it to system of other equations.

The atmosphere moments of inertia are very small ($\cong 1.4{\cdot}10^{32}\mathrm{kg}{\cdot}\mathrm{m}^2$) compared with the moments of inertia of the whole Earth. Thus the ratio of moments of inertia of the atmosphere C_a and whole Earth C is equal $C_a/C \approx 1.8 \cdot 10^{-6}$. However, statement, that rotation of the atmosphere does not influence on nutation, is not true at that level of accuracy, which is required from the nutation theory now.

Rotation of the atmosphere as whole layer relative to the mantle is necessary to take into account due to possibility of the tides resonant strengthening. Such amplification of amplitudes of some nutation terms can be caused by new Earth's normal modes connected with the free rotation of the atmosphere relative to the mantle, if the frequencies of these modes lay in diurnal frequency band.

The dynamical equations for the Earth with the atmosphere can be written as

$$\frac{\partial \overline{H}}{\partial t} + \overline{\Omega} \otimes \overline{H} = \overline{L}, \quad \frac{\partial \overline{H}_f}{\partial t} - \overline{\omega}_f \otimes \overline{H}_f = 0$$

$$\frac{\partial \overline{H}_s}{\partial t} + \overline{\Omega} \otimes \overline{H}_s = \overline{L}_s, \quad \frac{\partial \overline{H}_a}{\partial t} + \overline{\Omega} \otimes \overline{H}_a = \overline{L}_a$$

where $\overline{H}, \overline{H}_f, \overline{H}_s, \overline{H}_a$ are the angular moments of whole Earth with the atmosphere, the FOC, the SIC and the atmosphere, $\overline{L}, \overline{L}_s, \overline{L}_a$ are the torque acting on the Earth with atmosphere, on the SIC and on the atmosphere.

For description of the Earth's rotation and motion of the layers six coordinate systems are entered. Every coordinate system has beginning in the Earth's center of mass. First Cartesian coordinate system is the inertial system, second coordinate system rotates in the inertial space with the constant angular velocity Ω_0. The axes of the terrestial coordinate system $\overline{i}_1, \overline{i}_2, \overline{i}_3$ are the Tisserand mantle axes. The axes of other coordinate systems are the Tisserand FOC, SIC and the atmosphere axes.

It is supposed that the instantaneous angular velocity vector of the Earth Ω is connected with angular velocity vectors of the FOC $\overline{\Omega}_f$, SIC $\overline{\Omega}_s$, and atmosphere $\overline{\Omega}_a$ by equations

$$\overline{\Omega} = \overline{\Omega}_0 + \overline{\omega} \equiv \Omega_0 \left(\overline{i}_3 + \overline{m}\right),$$

$$\overline{\Omega}_f = \overline{\Omega} + \overline{\omega}_f \equiv \Omega_0 \left(\overline{i}_3 + \overline{m} + \overline{m}_f\right),$$

$$\overline{\Omega}_s = \overline{\Omega} + \overline{\omega}_s \equiv \Omega_0 \left(\overline{i}_3 + \overline{m} + \overline{m}_s\right),$$

$$\overline{\Omega}_a = \overline{\Omega} + \overline{\omega}_a \equiv \Omega_0 \left(\overline{i}_3 + \overline{m} + \overline{m}_a\right).$$

The dimensionless vectors $\overline{m}, \overline{m}_f, \overline{m}_s, \overline{m}_a$ characterize the layers' velocities variations.

If we consider that the atmosphere is in state of hydrostatic equilibrium and connect coordinate system with the Tisserand axis then torque can be expressed through the atmospheric excitation functions χ:

$$\tilde{L}_a = L_{a1} + iL_{a2} = iUeA\left(\chi_1^p + i\chi_2^p\right)$$

where A is the Earth's principle equatorial moment of inertia, e is the dynamical ellipticity of the Earth, U is parameter depending on topography, $\chi_{1,2}^P$ are the pressure term components. We did not use the hypothesis of inverted barometer here. The contribution of atmospheric winds in torque in the Tisserand axes system is equal zero.

Table 1: The largest terms in parameter U.

j(degree)	m(order)	$U_{j,m}$
2	-1	($0.508 \cdot 10^{-9}$, $-0.116 \cdot 10^{-7}$)
2	0	($0.101 \cdot 10^{-7}$, $-0.173 \cdot 10^{-11}$)
4	-2	($-0.532 \cdot 10^{-9}$, $-0.581 \cdot 10^{-10}$)
4	-1	($-0.314 \cdot 10^{-9}$, $0.718 \cdot 10^{-8}$)

Parameter U is the proportional coefficient between atmospheric torque and the atmospheric excitation function. It is appeared because of we used angular momentum approach. Parameter U can be calculated analytically only for ellipsoidal surface of the Earth. In order to take into account the topography we used the spherical harmonic coefficients of the pressure field and topography of the Earth, and U is sum of terms depending from degree and order of them. The most important terms of U are shown in the Table 1.

For calculation of U we used complex spherical decomposition of the pressure field and topography, so order of harmonic can be negative.

Note that value of coefficient U_{20} exactly corresponds the ellipsoidal Earth's surface and imaginary part of coefficient $U_{2,-1}$ approximately equal to real part of $U_{2,0}$ but with opposite sign.

Effect of the atmosphere on nutation consists not only in corrections for some nutation terms but in appearance of new normal modes, frequencies of which are equal to

$$\sigma_{PFAN} \approx -1 + \left(U/\Omega_0^2\right) e_a \quad , \quad \sigma_{AW} \approx \left(1 - U/\Omega_0^2\right) e_a$$

where σ_{AW} is the Atmosphere Wobble frequency and σ_{PFAN} is the Prograde Free Atmosphere Nutation frequency. Value of U is changed during year and is complex quantity. It means that the frequencies of the normal modes depend on time, and topography not only determines the frequencies but determine dissipation of energy too. The frequencies σ_{PFAN}, σ_{AW} are proportional the dynamical ellipticity of the atmosphere e_a. As our calculation shown, ellipticity e_a was variable with period of one year.

The Bizouard et al. (1998) amplitudes of the atmospheric excitation function were used for numerical calculation effect of the atmosphere.

3. VISCOSITY AND ELECTROMAGNETIC COUPLING. Role of viscosity of the fluid core was discussed in Sasao et al. (1980), Getino and Ferrandiz (1997). It was proposed that viscosity did not depend on radial distance and had very small value in these works. But on base of experiments (Brazhkin and Lyapin, 2000) more complicated model of viscosity was proposed. We used this model and incorporated the electro-magnetic torque in the nutation theory too.

In order to take into account viscosity of the liquid core, we used radial distribution of viscosity which was proposed on base of experiments and measurements of the viscosity of melted iron under a high pressure by Brazhkin and Lyapin (2000).

Viscosity is increased exponentially in the thin layer near the SOC according this results. This conclusion allows to simplify solution of hydrodynamical equations in order to determine the velocity as function of radius and calculate the viscous torque. The torque depends on parameter W and proportional to difference of angular velocities of the FOC and SIC that are characterized by non-dimensional vectors $\overline{m}_f, \overline{m}_s$:

$$\overline{L}_f^{(\eta)} = -\Omega_0^2 W \left(\overline{m}_f - \overline{m}_s\right).$$

Here $\overline{L}_f$ is the torque acting on the FOC from the SIC. One can show that for distribution of viscosity shown on Fig.1 the torque acting on the FOC from the mantle is significantly less then Γ_f and

$$W \equiv \eta_s \frac{8\pi r_s^4}{3\delta r \Omega_0}$$

where η_s is viscosity on the FOC – SIC boundary; $\delta r = 100$ km is thickness of the layer of high viscosity; r_s is radius of the Earth's solid inner core.

The electromagnetic coupling was incorporated into our model in accordance with Mathews et al. (1998). Then

$$S_{22} = e_f - i\frac{W}{A_f} + S_{22}^{(e)}, \quad S_{23} = i\frac{W}{A_f} + S_{23}^{(e)},$$

$$S_{32} = i\frac{W}{A_s} + S_{32}^{(e)}, \quad S_{33} = -i\frac{W}{A_s} + S_{33}^{(e)},$$

where $S_{ij}^{(e)}$ is term depending on electromagnetic coupling.

4. THE SYSTEM OF EQUATIONS. Forced nutations can be found from equation:

$$Mx = y$$

where:

$$M =$$

$$\begin{pmatrix}
\sigma(1+\kappa)+\kappa-e & (1+\sigma)(\frac{A_f}{A}+\xi) & (1+\sigma)(\frac{A_s}{A}+\zeta) & (1+\sigma)\alpha_3 e_s \frac{A_s}{A} & (1+\sigma)\frac{A_a}{A} & (1+\sigma)\frac{A_a}{A} e_a (1+\kappa') \\
\sigma\left(1+\gamma\left(1-\frac{U_f}{\Omega_0^2}\right)\right) & 1+\sigma(1+\beta)+S_{22}-\frac{U_f}{\Omega_0^2} & \sigma\delta\left(1-\frac{U_f}{\Omega_0^2}\right)+S_{23} & -\sigma\alpha_1 e_s \frac{A_s}{A} & 0 & \sigma\left(\frac{\xi}{\tau}+h_f-\frac{U_f}{\Omega_0^2}\right)\frac{A_a}{A_f} e_a \\
\sigma(1+\theta)-e_s\alpha_3-\theta\frac{U_s}{\Omega_0^2} & \sigma\chi+\alpha_1 e_s+S_{32}-\chi\frac{U_s}{\Omega_0^2} & \sigma\nu+1+\sigma+S_{32}-\nu\frac{U_s}{\Omega_0^2} & (1+\sigma-\alpha_2)e_s & 0 & \left(\sigma-\frac{U_s}{\Omega_0^2}\right)(\frac{\zeta}{\tau}+h_s)\frac{A_a}{A_s} e_a \\
0 & 0 & 1 & \sigma & 0 & 0 \\
\sigma-e_a & 0 & 0 & 0 & 1+\sigma & (1+\sigma)\sigma+\left(1+\sigma-\frac{U}{\Omega_0^2}\right) e_a \\
0 & 0 & 0 & 0 & 1 & \sigma
\end{pmatrix}$$

$$x = \begin{pmatrix} \widetilde{m} \\ \widetilde{m_f} \\ \widetilde{m_s} \\ \widetilde{n_s} \\ \widetilde{m_a} \\ \widetilde{n_a} \end{pmatrix}, \qquad y = \begin{pmatrix} (\kappa - e + \sigma\kappa)\widetilde{\phi} - (1+\sigma)(1+\kappa')\frac{\widetilde{c_3^a}}{A} \\ \sigma\gamma\widetilde{\phi}\left(1-\frac{U_f}{\Omega_0^2}\right) - \sigma\left(\frac{\xi}{\tau}+h_f-\frac{U_f}{\Omega_0^2}\right)\frac{\widetilde{c_3^a}}{A_f} \\ \left(\sigma\theta-\alpha_3 e_s-\theta\frac{U_s}{\Omega_0^2}\right)\widetilde{\phi} - \left(\sigma-\frac{U_s}{\Omega_0^2}\right)(\zeta/\tau+h_s)\frac{\widetilde{c_3^a}}{A_s} \\ 0 \\ -\left(1+\sigma-\frac{U}{\Omega_0^2}\right)\frac{\widetilde{c_3^a}}{A_a} \\ 0 \end{pmatrix}.$$

The parameters A, A_f, A_s, A_a are the equatorial moments of inertia, e, e_f, e_s, e_a are the dynamical ellipticities of the whole Earth, the FOC, the SIC and the atmosphere, σ is the frequency of harmonics of the tidal potential $\widetilde{\phi}$. Other greek symbols are the compliancies representing the deformations of the Earth and the core. From this equation the transfer function was obtained. Forced nutations of the Earth without effects of the mantle anelasticity and oceans were obtained by multiplication of the transfer function on the rigid Earth nutation series RDAN97.

The mantle anelasticity corrections were estimated according formulae from Wahr and Bergen (1986) for QMU model with the $\alpha = 0.15$. For ocean corrections the model Huang et. al. (2001) was used. The final nutation amplitudes were estimated as the nutation of the Earth without effects of the mantle anelasticity and oceans plus mantle anelasticity corrections and ocean corrections.

The frequencies of the resonance modes were obtained from equation:

$$Mx = 0. \tag{1}$$

5. THE NEGATIVE IMAGINARY PART OF THE RESONANCE FREQUENCY PROBLEM AND NON-ISOTROPIC HEATING EFFECT. The CW resonance frequency is:

$$\sigma_{CW} = \frac{A}{A_m}(e - k) + \Delta \tag{2}$$

where Δ is small factor. Frequency σ_{CW} is obtained as solution of equation (1). Imaginary part of the Δ arises from the electro-magnetic coupling in the MHB2000 theory. The eigenfrequency of CW of the Earth differs from those in (2) because frequency dependence of the k leads to the correction to k. This correction can be calculated according formulae from Wahr and Bergen (1986); it is complex value and arises from the anelastic dissipation in mantle.

Sign of the imaginary part of the Δ is negative in the MHB2000 theory. It means that Δ can not arise from the electro-magnetic forces because electro-magnetic forces can not leads to the generation of the energy. The correction to the imaginary part of the k is positive and large. Therefore resulting imaginary part of the CW frequency is correct and positive. But it can not explain the negative sign of the imaginary part of Δ. For explanation of negative sign of the imaginary part of Δ it is necessary to find process that can provide energy for it.

At first we built model with the super-rotation of the SIC. It was proposed that the SIC has non-zero mean angular velocity relative to the mantle. This hypothesis is based on results of work Song and Richards (1996) (see also Whaler and Holme 1996; Vidale et al., 2000). As our calculations shown it was possible to fit theoretical and observed nutations with rms error of 0.24 mas. It is possible to get positive parts of the normal mode frequencies, but differential rotation of the SIC has to be very large $\sim 15^0/\text{day}$ (the velocity of the differential rotation of the SIC was estimated as $0.15^0/year$ in the latter paper). So this model was rejected.

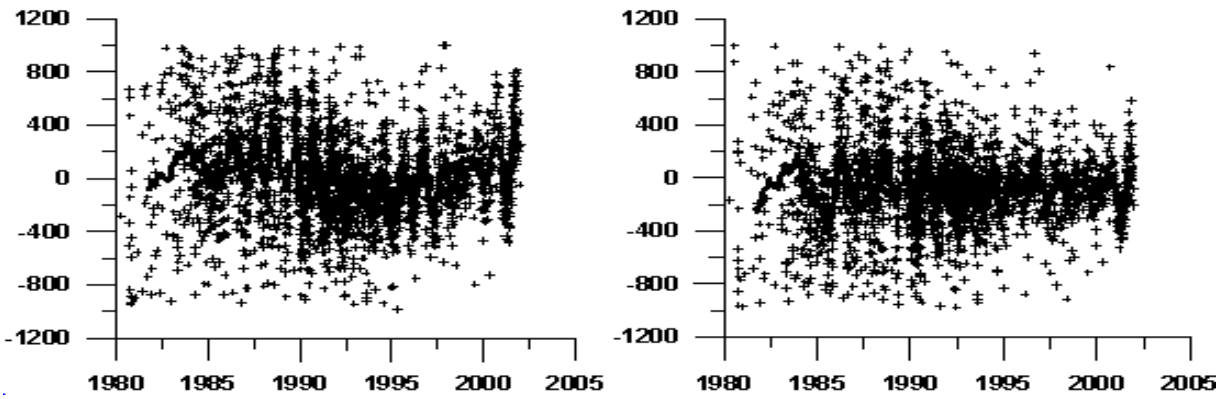

Figure 1: Comparison with the VLBI observations. The corrections $d\varepsilon$ to the theoretical nutation angle ε (in μas) for ZP2002 without FCN (left) and MHB2000 without FCN (right). The solid line is the running average.

Model that is suggested can explain the negative sign of the imaginary part of Δ. It was based on assumption that there are sources of heat in the Earth's deep interior. This situation is similar to the atmospheric excitation owing to absorption of solar energy. If we use the excitation functions formalism then we can write:

$$\tilde{L}^h_f = iU_f e_f A_f \left(\chi^p_{1f} + i\chi^p_{2f}\right) \quad \tilde{L}^h_s = iU_s e_s A_s \left(\chi^p_{1s} + i\chi^p_{2s}\right)$$

where the excitation functions $\widetilde{\chi}^p_f$ and $\widetilde{\chi}^s_f$ can be expressed through the components of the inertia tensors fluctuations $\widetilde{c}^f_3 + A_f e_f \widetilde{n}_f$ and $\widetilde{c}^s_3 + A_s e_s \widetilde{n}_s$. The U_f and U_s are considered as complex constants which has to be determined from the fitting procedure.

6. THE NUMERICAL RESULTS. The package OCCAM5.0 was used for comparison our series ZP2002 with VLBI observations and with the MHB2000 theory. The VLBI observations from 1980 to 2002 were processed and corrections to nutation angles for the theories MHB2000 and ZP2002 were obtained. On Fig.1 we show corrections $d\varepsilon$ for the nutation angle ε.

The wrms errors are 0.29 mas for $\Delta\varepsilon$ and 0.20 mas for $sin\varepsilon_0\Delta\psi$ for the ZP2002 theory without FCN. The same quantities for the MHB2000 theory without FCN are 0.22 and 0.17 mas. It is interesting that if we assume that ZP2002 corrections arise from FCN than wrms errors will be 0.17 mas in $\Delta\varepsilon$ and 0.18 mas in $sin\varepsilon_0\Delta\psi$. The same quantities for the MHB2000 theory with FCN are 0.19 and 0.12 mas.

It is preliminary result because the non-linear terms in gravitational torques are not included in our theory. The final conclusions and comparison of theories will be made when these terms will be took into account.

This work was supported by grant 01-02-16529 of the RFBR.

7. REFERENCES

Brazhkin, V. V., and Lyapin, A.G.,2000, *Journal "Uspehi phizicheskih nauk"* 170, 5, 535-551(in russian).

Getino, J., and Ferrandiz, J.M., 1997,*Geophys. J. Int.*, 130, 326-334.

IAU Resolutions 2000,24th General Assembly,Manchester, August, 2000.

Mathews, P.M., Herring, T.A., Buffet, B.A.,2002,*J. Geophys. Res.*,(in press).

Mathews, P.M., Buffet,B.A., Herring,T.A., Fessel M.,1998, In: *Proc. of Journées 1998, Systèmes de référence spatio-temporels*, Paris, 86-91.

Bizouard, Ch., de Viron, O., and Dehant, V., 1999, In: *Proc. of Journées 1999, Systèmes de référence spatio-temporels*, Dresden, Allemagne,157-166.

Bizouard Ch., Brzezinski, A., PETROV, S.,1998, *Journal of Geodesy*, 72, 561-577.

Huang,C.L.,Jin,W.J.,Liao,X.H.,2001, *Geophys.J.Int.* ,146, 126-133.

de Viron, O., and Dehant, V., 1998, In: *Proc. of Journées, Systèmes de référence spatio-temporels*, Paris,146-147.

Sasao, T.S., Okubo and Saito, M., 1980, In: *Proc. of IAU Symposium on Nutation and Earth's Rotation*, 78, 165-183.

Sasao, T.S., and Wahr, J.M., 1981,*J. R. Astr. Soc.*, 64,729-746.

Song, X., and Richards, P.G., 1996, *Nature*, 382, 221.

Vidale, J.E., Dodge, D.A., and Earle, P.S.,2000, *Nature*, 405, 445 - 448.

Wahr, J., and Bergen, Z.,1986,*Geophys. J. R. Astron. Soc.*,87,633-688.

Whaler, K. A., and Holme, R., 1996, *Nature*, 382, 205.

Zharov, V.E., and Gambis, 1996, *Journal of Geodesy*, 70, 321-326.

MARTIAN ROTATION INFLUENCE ON ECCENTRIC TRAJECTORIES OF ORBITERS

V. MIOC and M. STAVINSCHI
Astronomical Institute of the Romanian Academy
Str. Cuţitul de Argint 5, RO-752121 Bucharest, Romania
e-mail: vmioc@aira.astro.ro, magda@aira.astro.ro

ABSTRACT. The modelling of perturbing effects is of particular importance in the theoretical study of a spacecraft motion, in view of a better knowledge of the future trajectory.

This paper deals with the influence of Mars' rotation on the dynamics of an orbiter via the rotation and oblateness of its atmosphere (considered separately from the general atmospheric drag). For the density distribution, we have adopted the nominal density profile proposed by Sehnal, valid within the height range 100−1000 km.

Starting from the Newton-Euler equations, we have estimated analytically the variations of the orbital elements over one nodal period. These changes were determined to first order in the magnitude of the perturbing factors and to second order in eccentricity.

1. INTRODUCTION

While studying theoretically the motion of a spacecraft, of first importance is the modelling of as much perturbing effects as possible. Better known the influence of the various perturbing factors is, and better known the future trajectory of the cosmic vehicle will be.

Among the effects that act on the motion of a planetary orbiter, the planet's rotation was less studied. Its influence can be tackled from many standpoints, considering for instance: the even zonal harmonics of the planetary gravitational potential, the relativistic effect of the quadrupole momentum, the Lense-Thirring effect, the atmospheric rotation and/or oblateness (due, obviously, to the planet's rotation).

We approach here the last situation for the concrete case of Mars. The motion of an orbiter in the Martian atmosphere was first studied analytically by Sehnal and Pospišilová (1988). Using the data provided by Moroz et al. (1988), they modelled the density distribution by the law

$$\rho = \exp(a_{j1} + a_{j2}/h), \qquad j = \overline{1,3}, \tag{1}$$

where the numerical value of the density ρ results in kg/m^3 for the altitude h, expressed in km, above Mars' surface. The constants a_{j1}, a_{j2} are separately determined for the minimal ($j = 1$), nominal ($j = 2$) and maximal ($j = 3$) density profiles. In the nominal model, used by us for numerical estimates, Sehnal (1990) gave $a_{21} = -37.936$, $a_{22} = 2376.1$. Expression (1) is valid for the altitude range 100 km $\leq h \leq$ 1000 km.

The quoted papers did not consider the atmospheric rotation and oblateness. Further analytic approaches took into account these effects (e.g., Mioc et al. 1991, 1992), but imbedded in the general atmospheric drag effect, or went deeper in the Martian atmospheric drag problem,

but without considering rotation and oblateness (e.g., Mioc and Radu 1991b). In this paper we are interested in the way in which the *separate* influence of the rotation and oblateness of Mars' atmosphere affects the motion of an orbiter. Such a study was performed by Mioc and Stavinschi (2001), but only for initially circular orbits. Here we resume this problem for eccentric orbits, using expansions to second order in eccentricity. We determine the changes of five independent orbital parameters over one nodal period under the following hypotheses:

(i) the atmosphere rotates with the same angular velocity ω_M as Mars, and is oblate (the surfaces of equal density having the same oblateness ε as the planet);

(ii) the initial orbits lies entirely in the height range 100−1000 km above Mars' surface;

(iii) the perturbations are estimated to first order in the magnitude of the perturbing factors and to second order in eccentricity.

2. BASIC EQUATIONS

We start from the Newton-Euler equations written with respect to the argument of latitude (u):

$$\begin{aligned} p' &= 2(\gamma/\mu)r^3T, \\ \Omega' &= (\gamma/\mu)r^3BN/(pD), \\ i' &= (\gamma/\mu)r^3AN/p, \\ q' &= (\gamma/\mu)\{r^3kBCN/(pD) + r^2T[r(q+A)/p + A] + r^2BR\}, \\ k' &= (\gamma/\mu)\{-r^3qBCN/(pD) + r^2T[r(k+B)/p + B] - r^2AR\}, \\ t' &= \gamma r^2/\sqrt{\mu p}, \end{aligned} \tag{2}$$

where $' = d/du$, p = semilatus rectum, Ω = longitude of the ascending node, i = inclination, r = planetocentric radius vector, μ = Mars' gravitational parameter, $q = e\cos\omega$, $k = e\sin\omega$ (e = eccentricity, ω = argument of periastron), $(A, B) = (\cos, \sin)u$, $(C, D) = (\cos, \sin)i$, $\gamma = (1 - r^2C\dot{\Omega}/\sqrt{\mu p})^{-1}$, (R, T, N) = radial, transverse, and binormal components of the perturbing acceleration, respectively.

Considering only the influence of Mars' atmospheric rotation (oblateness entailed) on the orbiter motion, and expanding the orbit equation

$$r = p/(1 + Aq + Bk) \tag{3}$$

to second order in q and k (hence in eccentricity), the perturbing acceleration components read (cf. Mioc and Radu 1991a):

$$\begin{aligned} R &= 0, \\ T &= \rho\delta\sqrt{\mu p}C[1 - ABqk + (1 - A^2)q^2/2 + A^2k^2/2]\omega_M, \\ N &= -\rho\delta\sqrt{\mu p}D[1 - ABqk + (1 - A^2)q^2/2 + A^2k^2/2]A\omega_M, \end{aligned} \tag{4}$$

where δ is the drag parameter of the orbiter.

Let us retain the first five equations (2) and consider, as usual, that the perturbations of the orbital elements over one revolution are small, such that the parameters $\{y_i\}_{i=\overline{1,5}} = \{p, \Omega, i, q, k\}$ may be considered constant (and equal to their initial values) in the right-hand side of the motion equations. These ones may then be integrated separately, and the variations of the orbital elements over one nodal period can be deduced from

$$\Delta y_i = \int_0^{2\pi} y'du, \qquad i = \overline{1,5}. \tag{5}$$

The integrals will be estimated by successive approximations, with $\gamma \approx 1$, observing hypothesis (iii).

Replacing (4) in (2), and using the same expansions of r, the integrands in (5) are

$$\begin{aligned}
p' &= \rho pLC[2-6Aq-6Bk+(1+11A^2)q^2+(12-11A^2)k^2+22ABqk], \\
\Omega' &= -\rho LAB[1-3Aq-3Bk+(1+11A^2)q^2/2+(12-11A^2)k^2/2 \\
&\quad +11ABqk], \\
i' &= -\rho LDA^2[1-3Aq-3Bk+(1+11A^2)q^2/2+(12-11A^2)k^2/2 \\
&\quad +11ABqk], \\
q' &= \rho LC[2A+(1-5A^2)q-6ABk+2A(4A^2-1)q^2+A(12-11A^2)k^2 \\
&\quad +B(19A^2-3)qk], \\
k' &= \rho LC[2B-4ABq+(5A^2-4)k+B(1+5A^2)q^2+2B(3-4A^2)k^2 \\
&\quad +A(10-13A^2)qk],
\end{aligned} \tag{6}$$

where we abridged $L = \gamma\delta\omega_M p^{5/2}/\sqrt{\mu}$.

It is clear that equations (6) can be brought to the very concentrated form

$$y_i' = \rho \sum_{t=0}^{4} (G_{it}A^t + H_{it}A^tB), \qquad i = \overline{1,5}, \tag{7}$$

in which the coefficients G_{it}, H_{it} depend on μ, ω_M, δ, and the initial values of p, i, q, k.

3. VARIATIONS OF THE ORBITAL ELEMENTS

Let us now express the density (1) in terms of quantities considered constant over one nodal period, and of u (via A and B). To this end, we use

$$h = r - R_M(1 - \varepsilon \sin^2\varphi), \tag{8}$$

where R_M = mean equatorial Martian radius, φ = latitude. With $\sin\varphi = DB$, and expanding r and the exponential in (1) to second order in q and k, the expression of the density can be brought to the concentrated form

$$\rho = \sum_{j=0}^{6} (R_jA^j + S_jA^jB), \tag{9}$$

in which the coefficients R_j, S_j depend on a_{21}, a_{22}, ε, R_M, and the initial values of p, i, q, k.

By (7) and (9), equations (5) become

$$\Delta y_i = \int_0^{2\pi} \left[\left(\sum_{j=0}^{6} R_jA^j \right) \left(\sum_{t=0}^{4} G_{it}A^t \right) + \left(\sum_{j=0}^{6} S_jA^jB \right) \left(\sum_{t=0}^{4} H_{it}A^tB \right) \right] du, \qquad i = \overline{1,5}, \tag{10}$$

where we used $\int_0^{2\pi} KA^nBdu = 0$ (K = constant, $n \in \mathbf{N}$).

Denoting $U_{ik} = \sum_{j+t=k} R_jG_{it}$, $V_{ik} = \sum_{j+t=k} S_jH_{it}$, $j = \overline{0,6}$, $k = \overline{0,10}$, $X_{ik} = U_{ik} + V_{ik} - V_{i,k-2}$, $k = \overline{0,12}$, $i = \overline{1,5}$ (where we have artificially introduced $U_{i,11} = U_{i,12} = V_{i,11} = V_{i,12} = V_{i,-2} = V_{i,-1} = 0$), performing the calculations in the integrand of (10), then performing the integrations, we obtain the expressions of the variations of the orbital elements over one nodal period in the general form

$$\Delta y_i = \pi \left(2X_{i0} + X_{i2} + \frac{3}{4}X_{i4} + \frac{5}{8}X_{i6} + \frac{35}{64}X_{i8} + \frac{63}{128}X_{i,10} + \frac{429}{1024}X_{i,12} \right). \tag{11}$$

Of course, this expression can be particularized to each considered orbital element, by assigning the corresponding numerical value to the index i.

4. CONCLUDING REMARKS

4.1. Integrating the motion equations (6), we have obtained analytical expressions (with a second-order accuracy in eccentricity) for the variations of five orbital parameters caused by Mars' rotation over one nodal period of the orbiter. Expressions for such changes can be obtained for any other orbital element (semimajor axis, eccentricity, argument of periastron, etc.).

4.2. The choice of u as independent variable allows the study of the perturbations for very low eccentric orbits (even circular). This becomes impossible if one of the anomalies is taken as independent variable (the anomalistic period being considered as the basic time interval).

4.3. The final formulae (11) can serve as a departure point for the study of the evolution of such elements over large time intervals, via either averaging-type methods or numerical integration.

4.4. Integrating (5) between u_0 (initial) and u (current), instead of 0 and 2π, the results can subsequently be used to determine the perturbations of the nodal period itself.

5. REFERENCES

Mioc, V., Radu, E.: 1991a, *Bull. Astron. Inst. Czechosl.* **42**, 298.

Mioc, V., Radu, E.: 1991b, *Bull. Astron. Inst. Czechosl.* **42**, 395.

Mioc, V., Blaga, C., Radu, E.: 1991, *Europhys. Lett.* **16**, 327.

Mioc, V., Blaga, C., Radu, E.: 1992, *Rev. Mex. Astron. Astrofis.* **24**, 15.

Mioc, V., Stavinschi, M.: 2001, communication held at *Journées 2001: Systèmes de référence spatio-temporels*, 24-26 September 2001, Bruxelles, Belgium.

Moroz, V. I., Izakov, M. N., Linkin, V. M.: 1988, *Inst. Kosm. Issled. AN SSSR*, Preprint No. 1449.

Sehnal, L.: 1990, *Bull. Astron. Inst. Czechosl.* **41**, 107.

Sehnal, L., Pospišilová, L.: 1988, *Astron. Inst. Czechosl. Acad. Sci*, Preprint No. 75.

GRAVITATIONAL POTENTIAL, INERTIA AND EARTH ROTATION

G. BOURDA
SYRTE - UMR8630/CNRS, Observatoire de Paris
61 avenue de l'Observatoire - 75014 Paris, FRANCE
e-mail: Geraldine.Bourda@obspm.fr

INTRODUCTION

Several satellite missions, devoted to the study of the Earth gravity field, have been launched (like CHAMP, recently). This year, GRACE (Gravity Recovery and Climate Experiment) will allow us to obtain a more precise geoid. But the most important is that they will supply the temporal variations of the geopotential coefficients (called Stokes coefficients).
In the poster, we show how the Earth gravitational potential is linked to the Earth rotation parameters. Indeed, through the Earth inertia coefficients, we can connect the variation of LOD and Polar Motion with the temporal variations of the Stokes coefficients. We also consider the nutations, that are related to the gravitational geopotential coefficients.
We discuss the possibility of using the Stokes coefficients in order to improve our knowledge of the Earth rotation.

1. LENGTH-OF-DAY

The excess in the length-of-day can be related to the instantaneous Earth rotation rate $\omega = \Omega\ (1 + m_3)$, where Ω is the mean Earth speed of rotation. Indeed, we have :

$$\Delta(LOD) = LOD - LOD_{mean} = k\ \frac{2\pi}{\omega} - k\ \frac{2\pi}{\Omega} \simeq -k\ \frac{2\pi}{\Omega}\ m_3 \tag{1}$$

where k is the conversion factor from sidereal to mean solar days. That involves :

$$-\frac{\Delta(LOD)}{LOD_{mean}} = m_3 \tag{2}$$

By the way of the Liouville's equations, m_3 (third component of the Earth instantaneous rotation vector) is linked with L_3, third component of the external torque, with c_{33}, time-dependant difference to the constant part C of the third principal moment of Earth inertia and with h_3, third component of the relative angular momentum of the system. In this case, not considering the external perturbations, we have :

$$\frac{\Delta(LOD)}{LOD_{mean}} = \frac{c_{33}}{C} + \frac{h_3}{C\ \Omega} \tag{3}$$

Furthermore, the variable part c_{33} of the Earth inertia tensor depends on the temporal variation of the Stockes coefficient C_{20} of degree 2 and order 0 (Gross, 2000) :

$$c_{33}(t) = \frac{1}{3}\ \Delta Tr(I) - \frac{2}{3}\ M\ {R_e}^2\ \Delta C_{20}(t) \tag{4}$$

where $\Delta Tr(I)$ is the time-dependent difference to the constant part of the inertia tensor trace, M is the mass of the Earth and R_e is its mean equatorial radius. Due to the conditions (fluid

atmospheric and oceanic layers parts of our system), we can consider that there is conservation of the volume and the mass of our system under deformations. For this reason, according to (Rochester and Smylie, 1974), we have : $\Delta Tr(I) = 0$. Finally, according to the equations (3) and (4), but also considering surface loading and rotationnal deformation (Barnes et al., 1983) (factor 0.7), we obtain :

$$\frac{\Delta(LOD)}{LOD_{moyen}} = -0.7 \ \frac{2}{3 \ C} \ M \ {R_e}^2 \ \Delta C_{20} + \frac{h_3}{C \ \Omega} \tag{5}$$

2. POLAR MOTION

According to (Gross, 1992), we can connect the polar motion $p = x - iy$ with the motion of the instantaneous rotation axis $m = m_1 + i \ m_2$: $m = p - i/\Omega \ \dot{p}$. Considering (Gross, 2000), this brings to link the polar motion to the temporal variations of some Stockes coefficients :

$$\begin{cases} p + i \ \frac{\dot{p}}{\sigma_r} = \chi \\ \chi = \frac{1}{\Omega \ (C-A)}(\Omega \ c + h) = \frac{1}{\Omega \ (C-A)} \left(-M \ {R_e}^2 \ \Omega \ (C_{21} + i \ S_{21}) + 1.43 \ h \right) \end{cases}$$

where $C_{21} \equiv \Delta C_{21}$, $S_{21} \equiv \Delta S_{21}$, $c = c_{13} + i \ c_{23}$, and the coefficient 1.43 comes from (Barnes et al., 1983).

3. NUTATIONS

Some authors have derived the nutations of the Earth rotation axis using the harmonic coefficients of the gravity geopotential (Melchior,1973; Bretagnon, 1997; Brezinski and Capitaine, 2001).
The most important Stokes coefficient for such a phenomenon is C_{20}, but we can see that the other zonal coefficients act on the nutations. It would be then interesting to have their temporal variations, even if they are diurnal in the Earth.

DISCUSSION

We have provided the equations linking the temporal variations of the geopotential coefficients with the Earth rotation parameters (variation of LOD, polar motion and nutations). With the new gravity missions, we will be able to determine variations of Stokes coefficients, and to isolate the total variations of the solid Earth moment of inertia, what is totally new.
This is a new method, so comparing our results with those already known will be interesting, but a study of the precision needed for such a work is necesary and will be done.

REFERENCES

Barnes R., Hide R., White A., Wilson C., 1983, *Proc. R. Soc.* pp 31-73

Bretagnon P., Rocher P., Simon J., 1997, *Astron. Astrophys.*pp 305-317

Brzeziński A., Capitaine N., 2001, *Proceedings Journées 2001 Systèmes de Références spatio-temporels* pp 51-58, N. Capitaine (ed.), Observatoire de Paris

Gross R., 1992, *Geophys. J. Int.* pp 162-170

Gross R., 2000, *Gravity, Geoid and Geodynamics 2000*, IAG Symposium 123

Lambeck K., 1988, "Geophysical geodesy : The slow deformations of the Earth", Oxford Science Publications

Melchior P., 1973, "Physique et dynamique planétaires : Géodynamique", Vol. 4, Vander

Rochester M., Smylie D., 1974, *J. Geophys. Res.*pp 4948-4951

QUASI-SEMMIDIURNAL NUTATIONS INDUCED BY THE INDIRECT EFFECT OF THE TRIAXIALITY OF THE EARTH: RIGID AND NON-RIGID MODELS

A. ESCAPA[1], J. M. FERRÁNDIZ[1] and J. GETINO[2]
[1] Dpto. Matemática Aplicada. Escuela Politécnica Superior.
Universidad de Alicante. E-03080 Alicante. Spain
e-mail: Alberto.Escapa@ua.es
[2] Grupo de Mecánica Celeste. Facultad de Ciencias
Universidad de Valladolid. E-47005 Valladolid. Spain

ABSTRACT. In this work we compute the numerical nutation amplitudes due to the indirect effect of the triaxialy of the Earth (Escapa et al. 2002a, 2002b) for different rigid and non-rigid Earth models. In some cases we found contributions larger than 1 μas that should be incorporated in IERS Conventions.

1. INTRODUCTION

The triaxiality of the Earth is the main source of the high frequency variations in Earth rotation, contributing to the diurnal and subdiurnal nutation series in two ways. First, through a direct effect due to the apparence of the non-zonal harmonics C_{nm}, S_{nm}. This effect is the most studied in rigid and non-rigid models (see, for example, Souchay et al. 1999 and Getino et al. 2001). Second, through an indirect effect due to the fact that the response of the Earth to the external interactions depends on the Earth itself and, therefore, on the triaxiality. As far as we know, this effect has not been studied in a systematic way by other theories different from the Hamiltonian one. In this context, the nature of the indirect effect is clear. It is originated because the solution of the unperturbed problem in the triaxial case is different from the axial-symmetrical case, since the expressions of the kinetic energy are also different in these cases. So, it affects to all the terms of the potential when constructing the generating function. However, the part proportional to the J_2 coefficient provides the most significative contribution.

2. RIGID AND NON-RIGID EARTH MODELS

The indirect effect of the triaxiality on the rigid Earth nutations was recently computed by Escapa et al. 2002a by expressing the disturbing potential in terms of the action-angle variables for the torque free-motion of the triaxial Earth, since this canonical set does not coincide with the canonical Andoyer variables. Numerically, the most remarkable fact is that the indirect effect produces new quasi semidiurnal contributions to the nutation series. Some terms are within the truncation level adopted by REN–2000 (Souchay et al. 1999), that does not consider this effect.

In the case of a two-layer Earth model premiliminary estimations of the indirect effect of

the triaxiality were given by Escapa et al. 2002b. The contributions to the nutations, which have also quasi semidiurnal period, are proportional both to the triaxiality of the whole Earth and to the triaxiality of the fluid core, the part relative to the core providing the main of the contribution.

3. NUMERICAL REPRESENTATION

The main difficulty in evaluating the indirect effect arises when considering a non-rigid Earth model because there is a large uncertainty in the values of the equatorial moment of inertia of the core (Brzezinski and Capitaine 2002). Due to this fact, we have computed the contribution of the indirect effect for the quite different models. These are characterized by the value of $2d_c = 1 - A_c/B_c$ that is a measure of the triaxiality of the core. The values are: 0 (symmetrical core, SC), $4.922\,10^{-6}$ (Morelli and Dziewonski 1987, MD), $9.088\,10^{-6}$ (Defraigne et al. 1996, DDW), $11.015\,10^{-6}$ (triaxiality of the core equals to that of the total Earth, TE). The values of MD and DDW models are taken from Brzezinski and Capitaine (2002).

In Table 1 we have displayed the contribution in terms of the polar motion, hence the periods are now quasi diurnal. The contribution is specially important, about 12% of the direct effect, for the term of period .9973 but in the case of Model SC that does not provide any contribution. However, it seems quite improbable that d_c is exactly equal to 0. We believe that the value deduced from DDW is more realistic since this is the most updated model. Therefore, in our opinion it is necessary the inclusion of this effect (Model DDW) in IERS conventions in order to avoid an unnecessary bias.

Table 1: Polar Motion for different Earth models: X-component (μas)

Arguments						Period	Model SC		Model MD		Model DDW		Model TE		Rigid Earth	
Φ	l_M	l_S	F	D	Ω	(days)	sin	cos	sin	cos	sin	cos	sin	cos	sin	cos
1	-1	0	-2	0	-2	1.1196	.018	-.010	.021	-.012	.024	-.014	.025	-.014	.014	-.008
1	0	0	-2	0	-1	1.0760	.016	-.009	.021	-.012	.025	-.014	.026	-.015	.013	-.007
1	0	0	-2	0	-2	1.0758	.084	-.048	.109	-.063	.131	-.075	.141	-.081	.069	-.040
1	-1	0	0	0	0	1.0347	-.006	.003	-.010	.006	-.013	.007	-.014	.008	-.005	.003
1	0	-1	-2	2	-2	1.0055	.002	-.001	.006	-.004	.010	-.006	.012	-.007	.002	-.001
1	0	0	-2	2	-2	1.0028	.025	-.014	.134	-.077	.227	-.130	.270	-.155	.028	-.016
1	0	0	0	0	1	.9974	.000	-.000	.021	-.012	.038	-.022	.047	-.027	.002	-.001
1	0	0	0	0	0	.9973	0	0	-1.113	.639	-2.055	1.180	-2.491	1.430	-.083	.048
1	0	0	0	0	-1	.9971	.001	-.001	-.160	.092	-.297	.170	-.360	.206	-.011	.006
1	0	1	0	0	0	.9946	-.005	.003	.043	-.024	.083	-.048	.102	-.058	-.001	.000
1	0	0	2	-2	2	.9919	-.003	.001	.009	-.005	.019	-.011	.023	-.013	-.001	.001

4. ACKNOWLEDGMENTS

This work has been partially supported by Spanish Projects I+D+I, AYA2000-1787 and AYA2001-0787, Spanish Project ESP2001-4533-PE and *Junta de Castilla y León*, Project No. VA072/02.

5. REFERENCES

Brzezinski, A. and Capitaine, N., *Proceedings of the Journées 2001*, Ed. N. Capitaine, Observatorie de Paris, pp. 243–251, 2002

Escapa, A., Getino, J. and Ferrándiz, J. M., *Astron. Astrophys.*, 389, 1047-1054, 2002a

Escapa, A., Getino, J. and Ferrándiz, J. M., *Proceedings of the Journées 2001*, Ed. N. Capitaine, Observatorie de Paris, pp. 275–281, 2002b

Getino, J., Ferrándiz, J. M. and Escapa, A., *Astron. Astrophys.*, 370, 330-341, 2001.

Souchay, J., Losley, B., Kinoshita, H. and Folgueira, M., *Astron. Astrophys. Suppl. Ser.,* 135, 111-131, 1999

VARIATIONS OF THE INTENSITY OF SIBERIAN ANTICYCLONE AND EARTH ROTATION.

A. KORSUN(1), G. KURBASOVA(2),
(1) Main Astronomical Observatory, Ukrainian Academy of Sciences,
Kiev-127,03680, Ukraine
e-mail: akorsun@mao.kiev.ua
(2) Crimea Astrophysical Observatory,
p/o Nauchny, Crimea, 98677,Ukraine,
e-mail: gsk@crao.crimea.ua

ABSTRACT. For the research of time variations, displacement of the centre of the Siberian anticyclone and parameters of orientation of the Earth were used data for the period 1891-1967 years. At the decision of a problem of revealing of the connected variations in the compared data the effect of coherence of fluctuations in the system composed of the Earth and the Moon was taken into account. Variations in change of dynamic parameters of the system composed of the Earth and the Moon which may play a role of the trigger mechanism in change of amplitude and displacement of the centre of the Siberian anticyclone are revealed.

1. INTRODUCTION

It is known that the origin, evolution and intensity of atmospheric cyclones and anticyclones are connected with the season of the year by the various geophysical phenomena. The atmosphere is dynamical shell of our planet in which various physical processes differently proceed. It has high sensitivity charge of a mechanical pressure i.e. relation of force to the area. The tidal pressure created by forces of the attraction of the Moon and the Sun, definitely influence background atmospheric processes changing speeds of distribution of the centres of anticyclones. The tides create essential sign-variable (they may either strengthen or slow down processes in the atmosphere) the additive to a background field of pressure. Therefore it is rather useful to study the low of the time changes of the connection tides and the atmospheric phenomena as they may act in a role of the trigger mechanism at the origin of cyclones and anticyclones. At a final stage of origin of cyclones and anticyclones enough extremely weak push which may appear a tidal pressure and gravitational interaction in system the Earth—the Moon.

Unstable processes occurbing in an atmosphere results in the reorganization of spectral structure of waves which reasons are not always clear. This reorganization is expressed in change of one dominant waves by other in their merge and splitting.

The analysis of the data for 77 years (1891-1967) about anomalies intensities and displacement of the centre of the Siberian anticyclone shows that this anticyclone reaches the greatest force in January that will be coincide with the maximum al speed and the position of the Earth in the perihelion. The redistribution of energy in the connected system the Earth—the Moon causes the consented variations in the mobile shell of the Earth and the parameters of orientation of the Earth.

Our article is devoted to a problem of the revealing of the connected variation in the system the Earth— the Moon. We pay main attention to global period of the variation centred at a period close to 4.4 years in following phenomena: Earth rotation, integrated seismic energy, ENSO phenomenon and the variation of the distance between of the centers of the Earth and the Moon.

2. THE DATA AND THE METHOD OF THE ANALYSIS

For the analysis the mean-annual data of the polar coordinates of the Earth (as $z = \sqrt{x^2 + y^2}$), changes of the duration of day (ΔD), integrated seismic energy (E), index of the Southern fluctuation (I) and the data about minimal ($\rho_{\min}$) and maximal distance ($\rho_{\max}$) between the centers of the Earth and the Moon were used. Parameters of the Siberian anticyclone: displacements of the centre on a longitude (S_λ), on a latitude (S_φ), and anomalies of the intensity (S_α)[2]. The method of two-channel spectral analysis was used [1]. This method finds out compares the fluctuations of identical frequency in the series of the initial data located in two channels. The results of the analysis are given in Table 1.

The degree of similarity of the fluctuation with the identical period (column 3) is determined by size of square of the module cogerence (column 4). The relative displacement of the compared fluctuations are given in column 6.

The analysis of the results of a comparison shows that at the data there is a variation with the common component centred at a period close to 4.4 years. This fluctuation is found out both in geodynamic and the geophysical data that may specify the common source of its generation. Such source may be gravitational interaction in system the Earth—the Moon. Periodic power exchange processes generated it include all mobile shells of the Earth and its atmosphere. In is possible to show that if as own frequencies of system the Earth—the Moon to accept average frequency Chandler fluctuation ($\omega_1 = 0.839c/y$) and frequency of fluctuation of a line of sites of a lunar orbit ($\omega_2 = 1.054c/y$) interaction the Earth and the Moon on a degree of transfer of energy will cause the change of chandler fluctuation with the period $P = 4.65$ year ($2\pi/(\omega_2 - \omega_1)$).

3. CONCLUSIONS

1.In complicated processes of change of parameters of the Siberian anticyclone there are the determined fluctuations generated by power exchange processes in system the Earth–the Moon.

2.The global period of variation of different geophysical processes and variation of the distance between the Earth and the Moon is the period close to 4.4 years.

3.Redistribution of energy in fluctuations of close frequency creates the conditions for occurrence of trigger effect. The determined geodynamic processes may serve in a role of the trigger mechanism.

4.For a prediction of extreme atmospheric and other geophysical deviations it is necessary to take into account influence of the determined gravitational interaction, at least, the Earth and the Moon.

4. REFERENCE

1. G.Kurbasova, A.Korsun' et al. *Statistical interrelation of ten years variations of the mean-annual data on change of some geodynamic, geophysical parameters.* Astron. Journal in russian v.74, 1,139-145.
2. A.Sorkina. *The specified data on intensity and positions of the centers of action of an atmosphere in northern hemisphere.* The Works GOIN, 114, 1972.

I – channel	II – channel	P , year	Squared coherence %	Phase Coherence Shift ,year.
ρ_{min}	Z	21.79	92	5.23
		8.39	87	1.15
		4.38	76	1.53
		4.10	82	1.27
	ΔD	12.49	60	3.59
		4.45	81	-1.62
	I	8.68	76	1.94
		5.54	79	0.81
		4.43	96	0.66
	E	4.43	88	0.17
		3.07	55	-0.21
	S_λ	20.48	62	-2.46
		4.34	89	0.18
	S_φ	4.36	99	0.63
		3.51	91	-1.56
	S_a	4.38	89	1.73
		3.86	81	0.11
ρ_{max}	Z	27.68	81	8.83
		8.75	93	0.08
		4.34	68	0.17
	ΔD	9.43	70	3.2
		4.39	78	0.75
	I	8.26	86	1.95
		4.45	77	-1.27
		3.78	79	-0.26
	E	22.76	65	-11.33
		4.45	89	-1.95
		3.66	63	0.31
	S_λ	19.32	67	0.28
		7.94	81	1.03
		4.47	79	-1.63
	S_φ	7.16	89	1.09
		4.39	96	-1.22
	S_a	7.42	64	2.30
		4.18	68	-0.74

MARTIAN PRECESSION AND NUTATION

Y. XIA, C. ZHANG
Department of Astronomy, Nanjing University
22 Hankou Road, Nanjing 210093, P.R.China
yfxia@nju.edu.cn, czzhang@nju.edu.cn

ABSTRACT. In this paper, the recent progress on studies of Martian precession is reviewed. The research work on Mars nutation is divides into three aspects: the rigid Mars nutation series, the Martian internal structure model constructed by the physical parameters which are determined from the space exploration, the Mars normal mode and the non-rigid Mars transfer function. They are discussed respectively.

1. INTRODUCTION

Mars is a terrestrial planet. It shows Earth-like properties in many aspects. The motion of Mars pole in space depends directly on Martian precession and nutation. Martian precession and nutation, on the one hand, can be modeled by theory, on the other hand, are restrained by the observational data acquired from the space exploration. The comparison between the observational data and the theoretical results on the motion of Mars' pole is an important means for checking the Martian internal structure. It also provides the basis for improving the theory of Martian precession and nutation.

2. MARTIAN PRECESSION

By analogy with the Earth, Martian precession is composed of the "lunisolar" precession and the planetary precession. The "lunisolar" precession for Mars can be determined with the Earth-based methods or the space-based methods.

The first attempt to calculate Martian "lunisolar' precession rate was made by Struve (in 1898). Hilton (1991) took the effects of various sources into account in calculating the precession rate. He obtained the value as (-7".296 ± 0".021)/y. Folkner et al. found the observational value from the Mars Pathfinder spacecraft. Their value was (-7".576± 0".053)/y.

Bouquillon and Souchay (1999) obtained the Martian planetary precession as $\chi = 1".74571$ / y. The value of geodesic precession is obtained as $p_g = 0".0067547$ / y.

3. RIGID MARS NUTATION SERIES

The rigid Mars nutation theory is the basis of constructing the non-rigid Mars nutation theory. At present, like the rigid Earth, the methods of deriving the rigid Mars nutation series

can be divided into three categories: the torque approach, the Hamiltonian approach and the tidal potential approach. Different author used different approach respectively.

Roosbeek's theory of rigid Mars' nutation (1999) was based on the calculation of torque produced by the Sun, Phobos and Deimos. The rigid Mars nutation series for the angular momentum axis were computed. Finally, the nutation series including six fundamental arguments of astronomical parameters were obtained. With the 0.1 mas truncation level, 24 waves in longitude and 10 waves in obliquity were found.

4. MARTIAN INTERNAL STRUCTURE MODELS

The study of the space exploration may acquire the physical shape, the mean density and gravitational field of Mars. When the mean density and the polar moment-of-inertia coefficient of Mars were known, Martian internal structure models can be constructed.

The basic structure of Mars model is similar to the Earth's. It includes a shell, an elastic mantle and a core. At present, the distribution law of Martian rheological parameters in the planetary interior are not known exactly. The value of C/MR^2 is also not determined reliably. Hence, some simplified assumption for Mars has to be made. The initial values of central density, central rigidity, rigidity of the core and radius of the core are adopted. With solving the Emden equation and taking the boundary condition into account, the Martian parametric model is constructed (e.g. Zhang, 1994). Different observational values and various approaches will lead to different Mars internal structure models.

5. NORNAL MODE AND TRANSFER FUNCTION OF MARS ROTATION

Normal mode expansion theory shows that a hydrostatic, unstressed, elastic, rotating planet with a solid mantle and a liquid core is subject to three oscillatory modes: the tilt over mode (TOM), the Chandler wobble (CW) and the nearly "diurnal" free wobble (NDFW). If the core of Mars is a fluid core, Mars is also subject to these modes.

	Cause of formation	Period
TOM	The motion of Martian mean axis of rotation about its instantaneous rotation axis	identical to the rotating period of Mars
CW	Free wobble of instantaneous rotation axis with respect to the body-fixed reference frame axis	191-225 days *)
NDFW	The result of spheroidal liquid core	near the rotating period of Mars

*) The Eulerian period for rigid Mars is about 178.7 days

The value of CW period depends on the Mars dynamical flattening and Love number, also on the core radius and the polar principle moment of inertia. The NDFW corresponds to the free core nutation (FCN) if it is observed in inertial space. The FCN period ranges about from -330 to -220 days. The FCN period is extremely useful in determining the size of Mars core.

The TOM, the CW and the NDFW are three natural modes of oscillation of Mars. The forced nutation components of Mars are the driven oscillations of the planetary motion. The ratio between theoretically the rigid Mars nutation amplitudes and actually the observed nutation amplitudes should be a result of the resonance between the driven oscillations and the nature modes of oscillation of the planet. Theoretical nutations for a non-rigid model of Mars are computed from a convolution of rigid Mars nutations with transfer functions accounting for geophysical parameters influencing the Mars response. Hilton (1992) used the normal mode expansion method on the basis of the rigid Mars nutation model. He considered some disturbing

effect in his modelling and derived the non-rigid Mars nutation series, which were in keeping with the motion of the actual Mars pole.

6. CONCLUDING REMARKS

From the preceding review it is obvious that a lot of factors are uncertainties in the studies of Martian precession and nutation as well as the free wobble, such as, the polar moment-of-inertia coefficient C/MR^2 , the distribution of the rheological parameters in the Mars interior, the size and property of Mars core and Mars Love number of the second degree et cetera. At present, various authors derived different non-rigid Mars' nutation models by using different approaches. The recognized Mars precession-nutation model does not exist yet. The space exploration is undoubtedly the most effective means in order to clarify these uncertain factors. The results of the space exploration not only include the effects of the Sun, the Mars satellites and the other planets on Mars, but also represent the physical activities in the interior of Mars. Therefore, they reflect the comprehensive phenomenon of various objective factors.

REFERENCES

Bouquillon, S., Souchay, J., *Astron. J.*, 1999, 345:282
Hilton J L. *Astron. J.*, 1991, 102(4):1510
Hilton J L. *Astron. J.*, 1992, 103(2):619
Roosbeek F. *Celest. Mech. Dyn. Astr.*, 1999, 75:287
Zhang C Z. *Earth, Moon and Planets*, 1994, 64:117

COMPARATIVE ANALYSIS OF THE NEW NUTATION SERIES

V.E. ZHAROV, S.L. PASYNOK
Sternberg State Astronomical Institute
119992, Universitetskij pr.,13,Moscow,Russia
e-mail: zharov@sai.msu.ru

J.GETINO
Grupo de Mecánica Celeste
Facultad de Ciencias. 47005 Valladolid, Spain.
e-mail: getino@hp9000.uva.es

ABSTRACT. Different approaches can be used for construction of the nutation series. For comparative analysis we took series that were based on empirical, semi-analytical and on the Hamiltonian analytical theories. For the VLBI data set covering the period from 1982 to the 2002, the angles $\Delta\varepsilon$ and $\sin\varepsilon_0\Delta\psi$ were calculated on base of each nutation theories.

1. INTRODUCTION. The comparison with the VLBI observations for modern nutation series (MHB2000(Mathews et.al. (2002)),GF99(Getino and Ferrandiz(2000)),Huang et. al. (2001) and preliminary ZP2002 series(Zharov and Pasynok (2002))) were made. For data processing we used the IVS *.ngs files for VLBI observations from 1980 to 2002. The package OCCAM5.0 (Titov and Zarraoa(2001)) was used for calculation of corrections for each theory.

As results the files with corrections to the nutation angles $\Delta\varepsilon$ and $\sin\varepsilon_0\Delta\psi$ for each theory were obtained.

2. NUMERICAL RESULTS AND RESUME. The corrections for the angle $d\varepsilon$ are shown at Fig.1. The wrms errors are shown in Table 1. The corrections to the IAU 1980 precession rates are shown in Table 2.

Main factors which determine the wrms errors of the theories at sub-milliarcsecond level of accuracy are the non-linear terms in the gravitational torque and the FCN model. Therefore, the theories can be divided on three groups. The best accuracy was achieved in the theories which include the FCN model as well as non-linear terms (MHB2000 with FCN); the second group includes the theories in which the non-linear terms are taken into account but not the FCN model (MHB2000 without FCN and GF99), and the third group contains the theories which not include both the FCN model and the non-linear terms.
The small linear drift of the IERS observations series compared with the VLBI observations

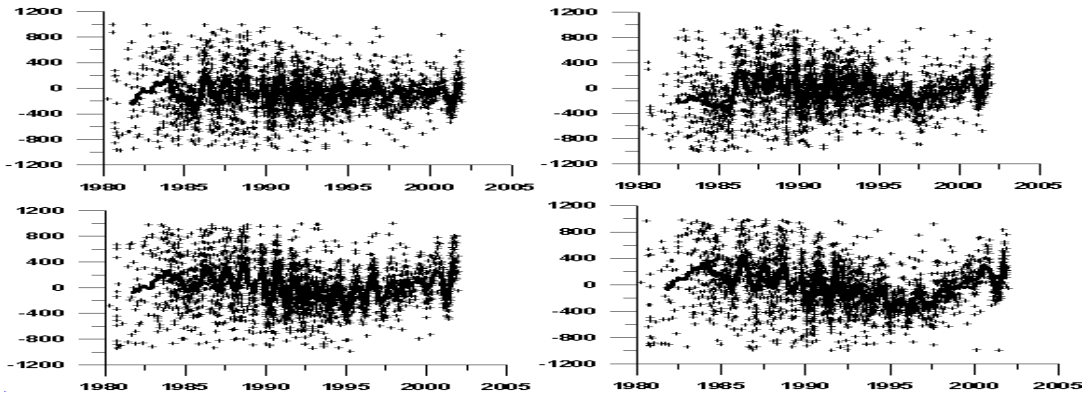

Figure 1: Corrections $d\varepsilon$ to the theoretical nutation angle ε for the nutation theories: MHB2000 without FCN (left upper), GF99(right upper), preliminary ZP2002 theory without FCN (left bottom), Huang et. al. 2001 (right bottom). The solid line is the running average.

Table 1: The wrms errors for the nutation series.

	MHB2000 with FCN	**ZP 2002 with FCN**	**MHB2000 without FCN**	**GF99**	**ZP 2002 without FCN**	**Huang et. al. 2001**
$d\varepsilon(\mu as)$	186	173	218	232	287	288
$d\psi(\mu as)$	291	447	430	434	508	560
$\sin\varepsilon_0 d\psi(\mu as)$	116	178	171	173	202	223

Table 2: Corrections to the IAU1980 precession rates for the nutation series.

	MHB2000	**GF99**	**ZP 2002**	**Huang et. al. 2001**
$d\varepsilon(arc\sec/c)$	-0.0252	-0.024	-0.023	-0.028
$d\psi(arc\sec/c)$	-0.2997	-0.304	-0.309	0.300

series was detected. Therefore VLBI observations series for fitting process can be recommended.

This work was supported by grant 01-02-16529 of the RFBR.

3. REFERENCES

Huang, C.L., Jin, W.J., Liao, X.H., 2001, *Geophys.J.Int.* ,146, 126-133.
Getino, J., Ferrandiz, J.M.,2000, *Proceedings of IAU Colloquium 180* , 236-241.
Mathews, P.M., Herring, T.A., Buffet, B.A., 2002, *J. Geophys. Res.*, (in press).
Titov, O., Zarraoa, N., OCCAM5.0: Users Guide.
Zharov, V.E., Pasynok, S.L., 2002, (this issue).

Session III

SPACE AND GROUND-BASED ASTROMETRY

ASTROMÉTRIE AU SOL ET DANS L'ESPACE

ALL-SKY SURVEY MISSIONS AND OPTICAL INTERFEROMETERS: COMPLEMENTARY TOOLS IN BUILDING REFERENCE FRAMES

G. DAIGNE
Observatoire de Bordeaux
2, rue de l'Observatoire 33270-Floirac, France
e-mail: daigne@observ.u-bordeaux.fr

ABSTRACT. With several space astrometry missions planned for being launched during the next 10 years, celestial reference frames in the optical range should have their accuracy boosted by several orders of magnitude. The potential of all-sky survey missions in building reference frames is compared with that of space interferometers. With their unique capability in quasar imaging, large ground-based interferometers will contribute also to the extension of the International Celestial Reference Frame (ICRF) into the optical/near-IR range.

1. INTRODUCTION

The International Celestial Reference Frame (ICRF) is the primary realization of the International Celestial Reference System (ICRS). It is based on the most accurate positions of compact radio-loud quasars, measured through VLBI observing in the centimeter wavelength range (Arias et al. 1995). In the optical range, the ICRS realization had to be a two-step procedure, firstly with an accurate sphere of stellar objects, the Hipparcos sphere Great Circle solution, and then with the linking of this sphere to the extragalactic frame (Kovalevsky et al. 1997).

The actual frame for astrometric measurements in the optical range is the Hipparcos Stellar Reference Frame (HCRF), with about 100 000 objects. As this name tells us, a frame needs celestial objects and a building tool, i.e. a measuring instrument with accurate methods in its data analysis.

Much denser frames should be materialized for any positioning of celestial objects observed with modern large telescopes (that is with small fields), and large telescopes are needed for positioning extragalactic compact sources (QSOs). Densification and improvement of the optical frame is one of the objectives of future all-sky survey missions. DIVA[1] was supposed to measure the astrometric parameters of all objects up to a magnitude 15 (for a K0 star), that is about 40 millions stars. FAME[2] was supposed to observe the same amount of stars, with improved accuracy mainly due to a longer mission duration (5 years for FAME versus 2 for DIVA). [3]

[1] http://www.ari.uni-heidelberg.de/diva/

[2] http://www.usno.navy.mil/FAME/

[3] This contribution has been prepared while the chances of having a post-Hipparcos astrometry mission launched before GAIA were not meagre. DIVA was then asking for some ESA support. Furthermore a cooperative venture between DIVA and FAME could have been considered. In February 2003, DIVA has been stopped.

Waiting for the next all-sky survey mission, astronomers are left with astrometric catalogs realized with ground-based observations. The most accurate extension catalog with all-sky coverage is supposed to be the USNO CCD Astrograph Catalog (Zacharias et al 2000) with more than 50 millions stars. A preliminary release of UCAC2 has been issued in May 2003. It is covering the all declination range up to about +50 degrees.

An all-sky survey mission is a mass production method providing a systematic census of astrometric parameters for a (large) bulk of celestial objects, whose size is mainly dependent on the aperture size of the telescope. The observing conditions are set at once and cannot be adjusted on purpose. A more versatile instrument for space astrometry is a long baseline steered optical interferometer: (i) fainter objects can be observed with small apertures, the exposure duration being a free parameter, (ii) higher precision in angular measurement can be achieved due to the length of the baseline (as compare to the aperture size of a telescope).

This contribution is mainly an outlook to the intricate relation between optical interferometry and reference frames, with two main questions: what could bring optical interferometers in this field, and conversely, what would be needed as spatial reference frame for optical interferometers to work properly ? Basic principle of measuring tools are first recalled in Sect.2 and Sect.3.

2. ALL-SKY SURVEYS

In the Hipparcos concept, objects from two widely separated fields of view are simultaneously observed with a single telescope. The separation angle between the two fields is along the scan direction of a spinning spacecraft. The DIVA and FAME projects strictly obeyed this concept, with a CCD focal plane assembly and charge transfer along the scan direction (TDI mode). The GAIA mission (see *http://astro.esa.int/gaia/*) partly followed this concept in its 2000 design. Due to the large entrance pupils, two independent telescopes tied on a rigid mount were viewing two widely separated fields. In the 2002 GAIA revised design, the two fields are superposed in an intermediary image plane of a telescope assembly, the two entrance pupils viewing fields at wide angle. The result is a common focal plane for the two superpimposed fields.

A CCD cell in the TDI observing mode is simply modelled as a linear (1-D) detector nearly perpendicular to the scan direction. Furthermore, effects of uncontrolled variations in the spacecraft attitude are strongly reduced for angular measurements between objects in one and the other field. Observing quasi simultaneously different objects in two fields well apart acts precisely as replacing poorly constrained attitude parameters with a fixed basic angle, built in the instrument. The net result is much more accurate measurements in the scan direction, remaining uncertainties in the spin axis direction producing only second order effects.

Objects are observed many times, with different scanning directions. For simple objects, estimating the astrometric parameters is an over-determined problem. The first reduction step of along scan strips, in so-called Great Circle provisionary frames, could take their initial solution from Hipparcos (HCRF) in case of a DIVA/FAME type of mission, and eventually from such a mission with sub-mas accuracy in case of GAIA.

All-sky surveys, and particularly a series of all-sky survey missions, are powerful tools for building celestial reference frames, as long as they are realizations of the ICRS. GAIA will observe and measure the position of several millions extragalactic objects, QSOs and galaxies, for a new realization of the ICRS in the optical range. With a smaller mission, like DIVA, only a few extragalactic objects might be observed, but a link with sub-mas accuracy per each quasar is still possible with ground-based technics such as large optical interferometers in the near-IR, as discussed in the last Section.

3. OPTICAL INTERFEROMETERS

In long-baseline optical interferometry with dilute apertures, the measured quantity is an optical path difference, given by the scalar product $\vec{B} \cdot \vec{\Theta}$, where $\vec{B}$ is the baseline vector and $\vec{\Theta}$ the source direction. Astrometry with a single baseline interferometer appears to be an under-determined problem with a single measurements and three unknown if the baseline length is measured independently. The problem can only be solved with the observation of several sources and a set of baseline directions. For ground-based observations, Earth rotation makes the baseline to change, as seen from the direction of the sources. With enough sources, their relative direction together with baseline orientations can be determined in the same reference system.

In space, baseline orientation or precise attitude control of a spacecraft is much more of a problem. The Space Interferometry Mission (SIM) (see *http://planetquest.jpl.nasa.gov/SIM/*) brings an answer with two auxiliary (or guide) interferometers and a main (or science) one sharing the same baseline. The guide interferometers will observe two different sources well apart the main target for attitude control of the interferometer baseline.

High precisions can be reached in small angle measurements, even with not so accurate positioning of the guide stars in a celestial reference frame. They need only to be fixed during a whole observing sequence of several stars with a set of baseline orientations. A local solution will be found for the relative directions of sources. This mode of observation has been labelled the Gridless Narrow Angle Astrometry mode. It will be used by SIM for the detection of exoplanetary system through the displacement of their central star, which is the driving scientific program for SIM. 'Basic' requirements for narrow-angle astrometry (less than 1 degree) are 3 μas per measurement.

Although not really design for, SIM will be able to build a whole celestial frame, step by step, with measurement of angular distances up to 15 degrees. Such a frame, the 'astrometric grid', will be further used during the 5 years mission for accurate baseline calibration. It will be materialized with the position (and astrometric parameters) of about 3000 stars in the V magnitude range 11-12. With a baseline orientation under control, objects as faint as V=18-19 can also be observed with the science interferometer, and the 'astrometric grid' can be positioned in the inertial system (ICRS). 'Basic' requirements for global astrometry are 30 μas in each object position uncertainty.

By analogy with the basic angle setup of all-sky survey missions, an astrometric space interferometer will greatly benefit from a dual-field system, with simultaneous observation of two sources at a certain angle. The measured quantity will be the projection of the separation angle between the two sources ($\vec{\Delta}\Theta$) onto the interferometer baseline. Attitude control is still needed, but becomes much less stringent when the two vectors, $\vec{B}$ and $\vec{\Delta}\Theta$ are nearly aligned. Such a setup has been proposed in the OSIRIS project which should be mounted on the Russian segment of the International Space Station (ISS) (Tokovinin et al. 1999). This dual-field optical interferometer had been designed for wide-angle measurements and a precision of 20-30 μas per measurement.

Optical space-based interferometry will probably reach very high precision in angular measurements, all the more these are small angles. But, in trying to build a celestial reference frame by its own, it may suffer from the lack of closure relations and of the lack of redondancies. Space interferometry appears to be a complementary tool in astrometry, and not so much a primary one. The effect of baseline uncertainty is proportional to the measured angle, and the benefit of an all-sky mission being launched before SIM may have to be reconsidered for not too small angular measurements with the space interferometer.

4. DISCUSSION

Much denser frames than HCRF have to be considered for ground-based observations with large telescopes, and much more accurate frames have to be considered for space interferometry. With both needs, the most useful magnitude range for a celestial reference frame is probably V=11-16. On the faint edge, the mean on-sky density is about a thousand stars per square degree. On the bright edge, optical interferometry and fringe tracking is possible with small apertures.

Such a magnitude extension of HCRF requires a post-Hipparcos survey mission. With detailed imaging of the near-IR counterpart of quasars (Daigne et al. 2003), large ground-based interferometers will greatly contribute to building an optical/near-IR reference frame with about the same accuracy as that of the ICRF.

5. REFERENCES

Arias, E. F., P. Charlot, M. Feissel and J.-F. Lestrade, 1996, The extragalactic reference system of the International Earth Rotation Service, ICRS. *Astron. Astrophys.* 303, 604–608.

Daigne, G., P. Charlot, C. Ducourant and J.-F. Lestrade, 2003, Potential of the VLTI for linking stellar frames to ICRF. *Astrophysics and Space Sciences* (in press).

Kovalevsky, J., L. Lindegren, M. A. C. Perryman, et al., 1997, The HIPPARCOS catalogue as a realisation of the extragalactic reference system. *Astron. Astrophys.* 323, 620–633.

Mignard, F., 2002, Observations of QSOs and reference Frame with GAIA. in *GAIA: A European Space Project*, O. Bienaymé and C. Turon eds, EAS Pub. Series, 2, pp. 327–339.

Tokovinin, A., M. A. Smirnov, A. A. Boyarchuk et al., 1999, OSIRIS: the spatial interferometer for astrometry. in *Atelier GAIA*, M. Froeschlé and F. Mignard eds, Observatoire de la Côte d'Azur, pp. 195–198.

Zacharias, N., S. E. Urban, M. I. Zacharias et al., 2000, The first USNO CCD Astrograph Catalog. *Astrophys. J.* 120:2131-2147.

SPACE ASTROMETRY MISSIONS : PRINCIPLES AND OBJECTIVES

F. MIGNARD, J. KOVALEVSKY
OCA/CERGA,
Avenue Copernic, 06130 Grasse (France)
e-mail: francois.mignard@obs-azur.fr
e-mail: jean.kovalevsky@obs-azur.fr

ABSTRACT. The objectives of space astrometry are the same as those of ground-based astrometry: to measure relative positions in a small field of view or/and to determine positions in a consistent full-sky reference frame (global astrometry). Three space techniques exist, and we present the principles of each, with a description of one realisation :

- The spaceborne classical small field imaging (HST);
- Michelson interferometry (SIM), optimised for small field astrometry, but which can also be used to build a global reference frame;
- Hipparcos type, two fields of view astrometry (GAIA, and DIVA and FAME, if they are re-endorsed). Specifically designed for global astrometry, but can also obtain good results within small fields.

In conclusion, a selection among the very large number of astronomical and astrophysical objectives of SIM and GAIA is presented.

1. INTRODUCTION

The objectives of space astrometry are, in principle, the same as those of ground based astrometry: to determine the apparent positions of celestial bodies and derive from them astrophysically important parameters such as distances, proper motions, movements within double and multiple star systems. There is no universal ground-based astrometric instrument. Different types are built and used for specific objectives: transit instruments and Schmidt telescopes for star position catalogues (global astrometry), long focus telescopes for parallaxes and double stars (small field astrometry), speckle and Michelson interferometry for stellar diameters and close binaries (analysis of structures). A description of these instruments can be found in Kovalevsky (2002). The final objective of all the observations collected by these instruments is to contribute essentially to stellar and galactic physics, planetary detection and fundamental physics, the latter including the realisation of a non-rotating kinematical frame.

So while highly specialised instruments are possible on the ground, where the cost of building and operating is reasonable, this is not possible in the case of the expensive space research where one must design more versatile instruments. In the latter case, one has an additional incentive, which is a dramatic increase of precision. But even this is not sufficient and it is necessary, in

order to convince the space organisations, to devise a multi-purpose satellite. Three solutions are possible:

1. To give some astrometric capabilities to a general purpose satellite. This is the case of the Hubble Space Telescope (HST);

2. To design a mission capable to obtain results in all the fields mentioned above. The example is the Space Interferometry Mission (SIM);

3. To add to a satellite dedicated primarily to astrometry as many other functions as possible that enhance the astrophysical value of the observations. This is the policy underlying the design of GAIA.

We shall present, in the following sections these three missions. They illustrate the principles on which space astrometry is based, and why, considering their respective limitations, they are complementary rather than competing.

2. THE HUBBLE SPACE TELESCOPE

The HST is a multi-purpose pointing telescope in optical wavelengths. The $14'$ circular field of view is divided into eight segments, each dedicated to a specific scientific instrument (Hall, 1991). Among these, the three outer ones constitute the Fine Guidance Sensors (FGS), two of which are used to guide the telescope. The third is available for astrometry (Fig. 1). The position of a point in the field of view makes use of two star selectors which are actually two beam deflectors of fixed lengths a and b rotating in order to bring the light from an object anywhere in the FGS field of view into the $3''$ square aperture of the detector assembly. The star selector positions are referred to a fixed direction ZX by angles θ_A and θ_B so that, in the focal plane of the instrument, the coordinates of the center of the detected field S are given by

$$\begin{aligned} x &= a\cos\theta_A + b\cos\theta_B, \\ y &= a\sin\theta_A + b\sin\theta_B. \end{aligned}$$

The relative position of S' is then defined by $\Delta\theta_A$ and $\Delta\theta_B$. The image around S is sent through transmitting optics to a beam splitter towards two Koester interferometric prisms controlling the motion of the image until it is centered. The precision in position for 4 or 5 stars observed during 20 minutes is of the order 4 mas. It is also possible to measure double stars through the analysis of the transfer function. The general design, the modes of operation and calibration are described in Duncombe et al., (1991).

There is another small field astrometric capability of the HST. The central $2\farcm7 \times 2\farcm7$ field of view is reflected and sent to the Wide-Field / Planetary Camera ensemble (WC/PC). The beam can be folded into two systems of four 800×800 CCDs. The Wide-Field configuration provides a view of the full field, while the Planetary Camera configuration registers a $1\farcm1 \times 1\farcm1$ field of view. More details are given in Seidelmann (1991).

3. THE SPACE INTERFEROMETRY MISSION

The Space Interferometry Mission (SIM) will be the first space-based interferometer designed for precision astrometry, operating in the optical band with a 10-m baseline. SIM is an approved NASA project, which should be launched around 2009 on a trailing solar orbit slowly drifting at about 0.1 AU per year. SIM will serve also as a technology precursor for future missions such as the Terrestrial Planet Finder. The stellar interferometer comprises two siderostats with

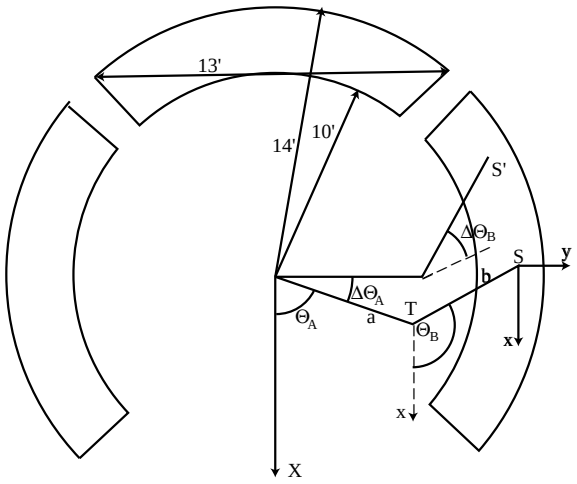

Figure 1: HST: the three segments of the FGS and the positioning of the star selectors .

equal apertures of 30 cm collecting the light with a separation of 10 meters. Each pod has two steerable mirrors which are the collectors of two guide interferometers directed towards bright stars and are used to determine the orientation in space of the baseline during the observation period. This allows measuring the relative positions of sources separated in the sky by 15°. The collected light is directed towards delay lines and a beam combiner. The principle is illustrated in Figure 2.

The basic measurement consists in adjusting the delay line so that the resulting optical path delay is closest to zero. In this configuration the instrument observes the white-light fringe. Therefore the observation equation for a single star is given by,

$$d = \mathbf{B} \cdot \mathbf{s} + \mathbf{C} \tag{1}$$

where $\mathbf{B}$ is the baseline vector and $\mathbf{s}$ the unit vector in the stellar direction. The constant delay C is a fixed instrument offset which must be calibrated to carry out absolute astrometry. On the other hand relative positions of stars are obtained from the change in the internal delay between the two sources as,

$$\delta d = \mathbf{B} \cdot (\mathbf{s_2} - \mathbf{s_1}) \tag{2}$$

which is independent of the instrument constant bias to first order. One must note that the instrument is sensitive only to the component of the relative displacement parallel to the baseline, hence several baselines have to be used. The microarcsecond accuracy translates immediately into a requirement in the fringe delay sensor $\sigma_d \simeq B\sigma_\theta \simeq 50$pm, or equivalently better than 10^{-4} in phase, imposing very severe constraints on the internal metrology, stability and calibration.

The accurate positioning of the collecting mirrors with respect to the beam combiner will be performed by infrared stabilised interferometers with an absolute accuracy of 1 μm per meter and the nulling technology is demonstrated to have a sensitivity of 10^{-4} in 5 minutes.

During its five years of operation SIM will cover the sky in a series of overlapping 'tiles', each 15 degress in diameter, with an average of 6 stars per tile. In total, the grid will comprise approximately 1300 metal-poor K-giant stars at R = 12 which should be observed with an uncertainty of 4 μas in wide angle astrometry (3 μas for parallaxes and 2 μas/yr for proper motions). Fainter objects, down to magnitude $\sim$ 20, like extragalactic sources to tie the grid

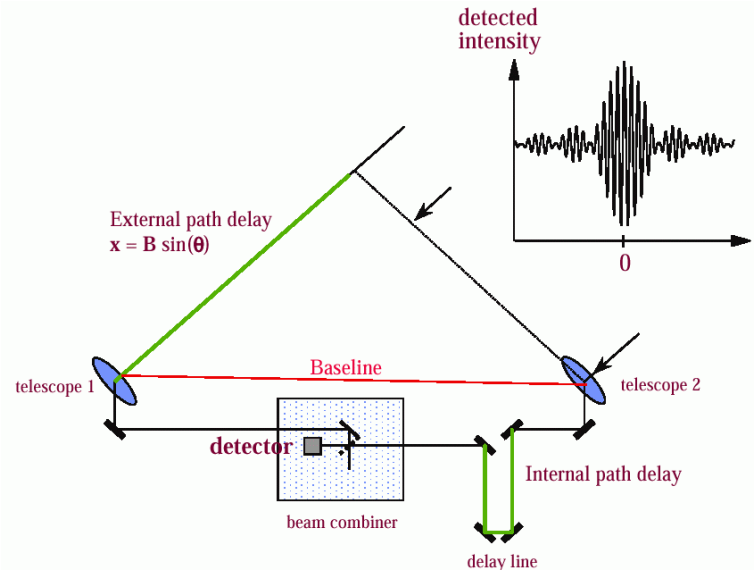

Figure 2: Principle of SIM astrometric measurements

to the ICRF, will also be included in this reference grid. This will need an integration time of 1 second for stars of magnitude smaller than 10, 200 s at magnitude 15, and more than four hours for the faintest objects, which will be observed only in exceptional circumstances.

SIM will have a single-measurement precision of 1 microarcsecond in a frame defined by nearby reference stars (field $< 1°$), enabling searches for planets with masses as small as a few earth masses around the nearest stars (typically 250 F, G, K stars within 10 pc). This will be complemented by a broad survey of planetary systems over a sample of $\sim$ 2000 stars within 25 pc. In addition, the interferometer can be used in amplitude mode, providing imaging potentiality with a uniform $u - v$ coverage. This will allow measuring diameters and shapes of stars and imaging symbiotic stars. More information can be found at http://sim.jpl.nasa.gov.

4. GAIA

4.1 Overall principles

Following the success of Hipparcos, the GAIA project has been approved in October 2000 as an ambitious experiment to probe with accurate astrometry and photometry a very large numbers of stars of our Galaxy. GAIA, which could be understood as an acronym for *Global Astrometric Instrument for Astrophysics*, is an ESA mission to be launched around 2010 as a cornerstone of the next generation in the science program. In opposition to HST and SIM, which are pointing instruments observing a preselected list of objects, GAIA is a scanning satellite that surveys in a systematic way, and repeatedly, the whole sky, linking together without regional errors widely separated sources. This has also the advantage of minimising the dead time and making use of almost all photons reaching the instrument. The disadvantage is, of course, that it cannot observe an interesting object when it is not coincident in time with the scanning law or to adapt the time allocation to the source brightness or astrophysics interest. The two principles are really complementary and do not compete with each other.

The principle is the one of Hipparcos, which has been described in many occasions. The

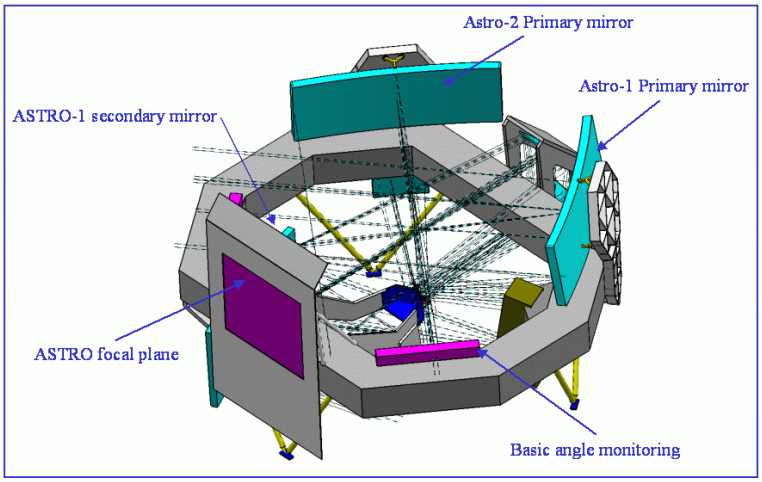

Figure 3: The GAIA payload with its two astrometric instruments separated by the 106° basic angle.

most detailed one can be found in Perryman et al. (1989). The reduction procedure was also described in many places. See, for instance, Kovalevsky et al. (1992) and Lindegren et al. (1992). The same principle was adopted for two other space missions: DIVA (Germany) and FAME (United States). Unfortunately both missions have stopped and it is not clear whether there is a chance for them to be re-activated.

4.2 The GAIA Payload

GAIA scans the sky according to a predefined pattern in which the axis of rotation (perpendicular to the two viewing directions) is kept at fixed angle from the Sun, describing a precessional motion about the Solar direction at a slightly variable rate so modulated as to ensure a constant motion of the rotation axis on the sky. The choice of the angle is a trade-off between the size of the Sun-shield, the parallax accuracy and its variation with ecliptic latitude, the interest of observing at small angle from the Sun for the space curvature determination and for the discovery of minor planet orbiting inside the orbit of the Earth.

In the case of GAIA, the two fields of view are separated by 106° with a Sun aspect angle of 50° (Hipparcos had 43°). The satellite rotates around an axis perpendicular to the plane of the two optical axes in 6 hours (Hipparcos, 2.2 hours). A description of the first design of the satellite is given in ESA (2000). Since then, the size was somewhat reduced so that, now, the astrometric instrumentation consists of two telescopes with a rectangular entrance pupil whose dimensions are 1.4×0.5 m^2 with a 46.7 meter equivalent focal length. The common focal plane covers two fields of view of $0.^\circ66 \times 0.^\circ66$ filled with some 180 CCDs operating in drift scanning mode. The pixel size will be $10 \times 30\,\mu$m^2 or equivalently 44×133 mas^2, allowing a good sampling of the diffraction pattern of about 100 mas along-scan.

The first two columns of the mosaic are sky-mappers which detect images above some given threshold and determine their positions and speeds in the focal plane. Then the image crosses the astrometric CCDs and the five broad bands photometers, but only small pixel windows around the predicted path are read and transmitted to the ground after some on-board treatment. The size of this widow is enlarged if an extended source or a multiple star system is recognised as such by the sky mappers.

A third instrument is placed midway between the two astrometric telescopes and dedicated

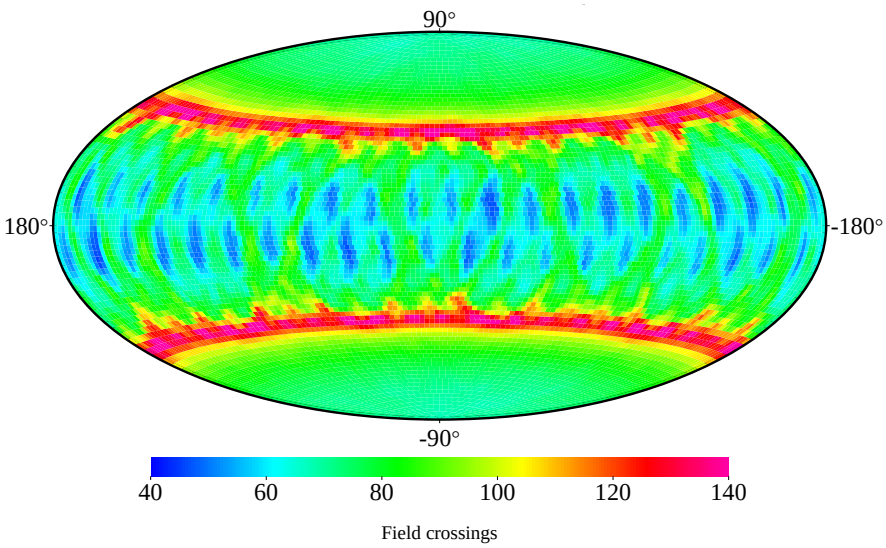

Figure 4: Number of observations in the astrometric fields of GAIA for a 5-year mission. Diagram plotted in ecliptic coordinates for the new design.

to the spectroscopy and the measurement of radial velocities, together with medium-band photometry over 11 bands of about 20-30 nm of width. The telescope is of smaller size (0.5×0.5 m^2) with a focal length of 2.1 m and a total field of view (spectroscopy + photometry) of $2\overset{\circ}{.}0 \times 4\overset{\circ}{.}8$. The image quality allows the use of 10μm^2 pixels within the photometric field corresponding to a spatial resolution of 1 arcsec.

The spectrometer is based on a slitless spectrograph whose resolution should be $R = 12\,000$, or equivalently 0.036 nm/pixel in the spectro CCD. GAIA spectra will cover the range 849 – 875 nm, centered on the near-IR Ca II triplet. This is the strongest spectral feature in the red/near-IR spectrum of the cool stars, visible even in the very metal-poor stars of the Halo. This will enable GAIA to measure radial velocities on virtually all GAIA targets. The main limitation will come from the sensitivity (not many photons are expected in each pixel with the dispersed light for stars fainter than V = 17) and from the crowding leading to overlapping spectra. In total the number of spectral targets should be around 10^8 implying, as in astrometry and photometry, a fully automatic data treatment.

4.3 Orbit and operation

GAIA is intended to be placed on a Lissajous orbit around the Lagrange point $L2$ of the Earth-Sun system in such a way that it avoids eclipses of the Sun by the Earth and can be operated in a very stable thermal and radiative environment. After the launch it will take five months to reach $L2$ when the observations will start, in principle for five years in the nominal mission. The sustained science data rate is about 1 Mbit per second which should be returned to the single ground station with a high gain antenna in daily 8-hour transmission sessions (meaning a data rate transmission of at least 3 Mbit/s and an on-board storage capacity for a few days).

The number of observations and their time distribution are two essential factors to achieve the scientific objectives. A large number of field crossings increases the photon statistics and the astrometric accuracy. But the distribution of these observations during the mission is just as important (i) to obtain a smooth sampling of the parallactic ellipse over the years, (ii) to be

sensitive to the tiniest proper motion displacement, (iii) to study the orbit of astrometric binaries or (iv) to investigate the periodic output of variable stars of every type. A scanning mission like GAIA has a strong dependance of the total number of observations with the ecliptic latitude as illustrated in Fig.4. On the average, the number of crossings of the two astrometric fields is ~ 80, while it is 100 for the spectro field and 150 for the medium band photometer. The ecliptic region is under-observed compared to the average, while the number of field crossings is larger by a factor two at the ecliptic latitude 40°. A typical sequence of astrometric observations is a crossing in the first field, followed by a crossing of the second field 106 minutes later, and possibly a second pair five hours later. Then one must wait between 2 to 6 weeks for a new sequence of observations to happen. Over five years the number of different epochs at which observations are carried out is between 25 and 45, for all the fields, with a very distinctive pattern showing two well delimited region : below 30 degrees of ecliptic latitude with the smaller number and above 40 degrees for the larger. The transition is very steep.

4.4 Astrometric Accuracy

Compared to Hipparcos there are several components that account for the improved performance :

- The much larger optics provide a smaller diffraction pattern, so a better astrometric definition of the image center.
- This larger collecting area yields many more photon per unit of time.
- Going from a photoelectric detector to a CCD has a major impact on the detection efficiency and sensitivity.
- Detector arrays replacing a single sensitive surface permits to record many stars at a time.

A straight combination of these factors indicates an overall efficiency factor as large as 1400 relative to Hipparcos, yielding an accuracy of about 11 μas at $V = 15$.

A much more refined approach during study phase has confirmed this simple-minded estimate. The expected accuracies of positions and parallaxes for a 5 year mission, range from 4 μas for stars up to magnitude 12, degrading to 11 μas at magnitude 15, 27 μas at magnitude 17, and 160 μas for magnitude 20. The accuracy of yearly proper motions should be about three quarters of these numbers in $\mu\mathrm{as\,yr}^{-1}$. As for Hipparcos, GAIA will also provide relative positions and magnitudes of the components of double stars.

The numbers quoted above were recently confirmed by a laboratory experiment simulating the observations at the CCD pixel level. It was shown that the centroid of the image of a point-like object could be determined with an accuracy of one hundredth of a pixel, that is 0.3 mas at the CCD level. This is, in a much more disturbed environment, 1.2 times the theoretical estimate computed in exactly the same way as for the evaluation of the mission performances.

5. ASTROPHYSICAL OBJECTIVES

As stressed in the Sect.1 all these space missions have a wide range observing capabilities beyond the primary purpose. The true objectives of astrometric missions is to provide data for the description and the understanding of various features in our Galaxy, as well as in the extragalactic neighbourhood. In the case of GAIA, they are described in a very detailed manner in ESA (2000). The headlines can be summarised as follows:

- Recalibrate the galactic and extragalactic distance scale (Cepheides, RR Lyrae);

- Define and build an optical inertial reference frame;
- Determine absolute luminosities of a wide range of spectral types;
- Detailed structure of an extended to more dimensions HR diagram;
- Study in details the structure, content and kinematics of the Galaxy;
- Determine the age of globular clusters;
- Detect companion stars, brown dwarfs and giant planets;
- Determine stellar masses;
- Map the interstellar matter;
- Contribute to fundamental physics (General Relativity tests);
- Determine orbits, masses and taxonomy of asteroids.

SIM will be able to perform, but only by sampling the objects, some of the above tasks that GAIA will do over a very large number of stars. For instance, it is contemplated to construct a reference frame with few tens or hundreds extragalactic objects with an accuracy of 4 μas instead of two tenths of a μas with hundreds of thousands objects expected from GAIA (Mignard, 1998, 2002). But there are a series of specific objectives of SIM that are not accessible to GAIA, particularly, but not only, in the extragalactic environment. Among them, one can mention:

- Distance of nearby galaxies using rotational parallaxes;
- Detection of motions of active galactic nuclei (AGN) and bright knots in galaxies;
- Kinematics and dynamics of nearby galaxies;
- Structure of the central parts of some galaxies;
- Search for terrestrial type planets around neighbouring solar type stars;
- Structure of spectroscopic binaries and particularly of symbiotic stars;
- Search for microlensing effects.

So, in conclusion, SIM and GAIA have essentially different objectives and are therefore remarkably complementary. Their launch dates are now very similar and both are planned for a 5-year mission and they need to process all astrometric observations to draw the full benefit of their capabilities.

REFERENCES

Duncombe, R.L, Jefferys, W.H., Shelus, P.J. et al., 1991, Advan. Space Res., **11-2**, 87-96

ESA, 2000, *GAIA, Composition, Formation and Evolution of the Galaxy, Concept and Technology Study Report*, ESA-SCI(2000)4, European Space Agency, Paris

Hall, D.N.B. (Ed.), 1982, *The Space Telescope Observatory*, NASA CP 22-44

Kovalevsky, J., 2002, *Modern Astrometry*, 2nd edition, Springer Verlag, Heidelberg

Kovalevsky, J., Falin, J.-L., Pieplu, J.L. et al., 1992, Astron & Astroph., **258**, 7-17

Lindegren, L., Høg, E., van Leeuwen, F. et al., 1992, Astron & Astroph., **258**, 18-30

Mignard F., 1998, in *Journées 1998, Systèmes de référence spatio-temporels*, ed N. Capitaine, Observatoire de Paris, 10-17

Mignard F., 2002, in *GAIA : A European Space Project*, ed O. Bienaymé, C. Turon, EDP, 327-339

Perryman, M.A.C., Hassan, H. et al., 1989, *The Hipparcos Mission, Pre-launch Status*, vol. 1, ESA SP-1111, European Space Agency, Paris

Seidelmann, P.K., 1991, Advan. Space Res., **11-2**, 103-111

THE IAU WORKING GROUP "THE FUTURE DEVELOPMENT OF GROUND-BASED ASTROMETRY"

M. STAVINSCHI
Astronomical Institute of the Romanian Academy
Str. Cutitul de Argint 5, RO-752121 Bucharest, Romania
e-mail: magda@aira.astro.ro

ABSTRACT. The "Space and Ground Based Astrometry" section of the international colloquium JOURNES 2002 is dedicated to the main problems of IAU WG "The Future Development of Ground-Based Astrometry". This paper shortly reviews the group's activity and the present situation in order to open the debates concerning future programmes.

The third section of the colloquium JOURNES 2002 is dedicated to space and ground-based astrometry. Naturally, this is not about a competition between the two, but the establishment of the measure in which ground-based astrometry can complete space one or can still work independently, in clearly set programs.

The recent performances of the space missions, the astrometric ones included, such as Hipparcos were those which began to doubt the present and especially the future of the ground-based programs, of the astrometric ones in particular. Actually, this has been the main reason why the XXIVth IAU General Assembly has decided to set up a working group within Division I Fundamental Astronomy "The Future Development of Ground - Based Astrometry", according to the following :

"The post-Hipparcos era has brought an element of uncertainty as to the goals and future programs for all of ground-based astrometry. In order to identify such programs and make assessment of the whole situation including available instrumentation, a new WG on "The Future Development of Ground-Based Astrometry" headed by Magda Stavinschi (Romania) and Jean Kovalevsky (France) has been established. The main objective of this WG is to identify scientifically important programs that can be realized using ground-based astrometric or related observations, and to study what kind of modifications, upgrades or additions to the existing instruments should be performed in order to provide useful astronomical information with necessary accuracy, keeping in mind what the future astrometric satellites will contribute."

The working group began to function from the middle of 2001, when its site http://www.astro.ro/wg.html was set up.

On 10 November of the same year its first reunion took place, as a Joint Discussion - Astron-

omy with Telescopes, within the international reunion JENAM 2001. The main conclusions were drawn on the basis of the interventions of several participants, from among which we would like to mention J.-E. Arlot, W. Thuillot, C. Delmas, H. Rovithis-Livaniou, A. Riffeser, N. Bochkarev, M. Andrade, A. Irbah, M.B. Ignatyev (Stavinschi M., Kovalevsky J., 2001).

Jean Kovalevsky, who led the debates, managed to select the most topical fields for the researches made by means of small telescopes, both for the benefit of some theoretical studies and of the space missions that are to be launched in the following decade, such as DIVA or GAIA. They refer to:

- double star observations (with CCDs or speckle interferometry) for orbital elements and stellar masses;
- dynamics in the Solar system: observation of minor planets and natural satellites;
- solar diameter and shape;
- stellar diameters with speckle interferometry or occultations by the Moon;
- study of crowded fields: determination of proper motions within clusters for dynamical studies or search of microlensing events;
- radial velocities of stars: this is the most needed kinematic parameter for stellar dynamics and double star mass determination;
- proper motions of young stars and associations to establish connection with star formation regions. Observations should be coupled with a reduction of old plates;
- position of radiosource optical counterparts All programs need coordination within some well-defined networks, such as the observations of occultations of stars by minor planets, Earth grazing asteroids, mutual events of Galilean satellites, light curves of variable stars or rotating minor planets, etc. They are programs of long duration, even if intermediate results must generally be released as they go along. These results concern long period variable stars, minor planet monitoring, double. A number of fields was then reviewed, in keeping with the above criteria. Another effect of this characteristic is also the homogeneity of the data and the possibility to detect some long periods in the dynamics of the bodies in the solar system.

After the joint discussion of 2001, the working group continued to function and a part of the programs discussed last year were set to work. We shall mention the largest of them, that of the PHEMU 2003 campaign, which covers a period of about 14 months, from October 2002 until the end of 2003. IIt is carried out under aegis of IMCCE (Institut de Mcanique Cleste et Calcul des phmerides). As we also showed at JENAM 2001, by means of this campaign J.-E. Arlot brings a proof on the importance of continuous observations of large and small satellites in the Solar system. All the photometric or astrometric programmes during this campaign may be performed on small telescopes. In addition, the observation of mutual events between Galilean satellites of Jupiter is a major input to the dynamical study of these satellites. Even a 30cm telescope is enough to observe them. To collect a sufficient number of such observations, they must be programmed in many observatories all around the world.

Naturally, the debates of this WG reunion will also bring forth other problems or programs which will become working topics of the following period for the astrometry researchers who are still working with small instruments.

REFERENCES

Kovalevsky, J.: 2002, Modern Astrometry, 2nd edition, A&A Library, Springer-Verlag.

Arlot, J.-E., Stavinschi, M.: 1996, Eds.: Atelier de travail PHESAT'95, Ann. Physique 21, 1-1.

Stavinschi, M, Kovalevsky, J,: European Astronomy with Small Telescopes, the EAS Newsletter, Issue 22, December 2001., p.8.

JD3 European Astronomy with Small Telescopes, Abstracts of Contributed Talks and Posters presented at the JENAM 2001, Astronomische Gesellschaft, Abstract Series No.18, 2001, pp.111.

http:/www.astro.ro/wg.html

http://www.astro.ro/journees2002.html

http://www.bdl.fr/Phemu03/

OBSERVATIONS WITH THE REAL INSTITUTO Y OBSERVATORIO DE LA ARMADA CCD TRANSIT CIRCLE IN ARGENTINA

J.L. MUIÑOS, F. BELIZÓN, M. VALLEJO
Real Instituto y Observatorio de la Armada en San Fernando.
Plaza de las Marinas S/N 11110, San Fernando (Spain)
e-mail: ppmu@roa.es

C. MALLAMACI, J.A. PÉREZ
Observatorio Astronómico Félix Aguilar.
Av. Benavidez 8175W, San Juan (R. Argentina)
e-mail: ccmalla@unsj.edu.ar

ABSTRACT

The Real Instituto y Observatorio de la Armada (ROA) meridian circle was moved to the Estación de Altura Carlos Ulrrico Cesco in the República Argentina in 1996. Until november 1999 the observations were carry out with a moving slit micrometer. In spring 2001 the result of these observations has been published, forming the first Hispano-Argentinian Meridian Catalogue (HAMC). In december 1999 was installed a SpectraSource CCD camera of 1552x1024 pixels of 9 μ. The CCD camera observe in drift scan mode. A survey of the south hemisphere is being observed from $+3^{o}$ to -60^{o} of declination.

In this contribution its presented a description of the telescope and the automatic control system, the results of observations carried out with the slit micrometer, and the observational and preliminary reduction techniques with the CCD camera, the present state of the south hemisphere survey and the future possibilities.

1. INTRODUCTION

The transit circle of the Real Instituto y Observatorio de la Armada (Spain) ROA was built in 1948 by Grubb Parsons. It has an aperture of 18 cm and a focal length of 266 cm. In the early 90's it was fully automated and provided with a moving slit photoelectric micrometer to observe the stars and a automatic system based in six CCD CCTV cameras to read the circle.

In 1996 June was moved to Argentina to the Carlos U. Cesco Observatory (CUC) in the east slopes of the Andes at to 69^{o} W of longitude, 31^{o} S of latitude and 2330 m of altitude. The Observatorio Astronómico Félix Aguilar (OAFA) of the Universidad Nacional de San Juan owns the CUC. Both institutions the ROA and the CU share the management of the instrument.

Since 1997 October to 1999 september was observing regularly a program of stars, planets, satellites and minor planets. The results of these observations were published in the Hispano-

Argentinean Meridian catalogue 2001.

In 1999 December the photoelectric micrometer the CMASF was removed and was installed in it a CCD camera of 1552x1024 pixels of 9 μ observing in drift scan mode. Since then the telescope is observing a program to produce a survey of stars from $+3^o$ to -60^o degrees in declination and between 7.5 and 16.0 of visual magnitude. In pararell with the observations for the survey are carried out observations of Pluto, Neptune and Triton when they transit by the CUC meridian during night-time. Also some special observational programs are developed in collaboration with other South Americans institutions.

2. PHOTOELECTRIC OBSERVATIONS

During the period 1997 october to 1999 september the CMASF observed with its photoelectric micrometer a program of stars, and Solar System objects. With these observations were computed the positions for the Hispano-Argentinian Meridian Catalogue 2001 (HAMC). This catalogue was published in 2001 in CD-ROM format. It is composed with the positions (RA and declination J2000), proper motions and magnitudes of 6192 stars with declinations between $+40^o$and -90^o and brighter than 15.5V, and 923 positions and magnitudes of 92 objects of the Solar System. The catalogue also contains 886 mean observed positions of the FK5 stars used to transfer the instrumental system to the ICRF.

The men error of a catalogue position in the zenith is 0".08 in right ascension and declination. The mean error in proper motions is typically in the range of 0".004 per year.

3. CCD OBSERVATIONS

The CCD camera is positioned in the transit telescope in order to get that the longer side of the photo sensitive area of the CCD chip is pararell to the local meridian. Having in account the size of the CCD approximately 14x9 mm and the focal length of the objective, when observing in drift scan mode a strip of sky of 18' in declination and with a length of until 2.7 hours in right ascension is observed. The length in right ascension is limited for software storage reasons.

At the end of 1999 after the installation in the CMASF of the CCD camera began a regular program of observations os stars south of $+3^o$ degrees. Occasionally observations of Pluto, Neptune, Triton and some short special observational programs are carried out.

3.1. Regular observations

The regular program consist in observing the band of the sky from $+3^o$ to -60^o in declination in order to publish a survey containing right ascension, declination and magnitude of the stars in the band brighter than 16 V. The observations are carried out automatically even the selection of the strips to be observed every night. In the morning all the strips of the previous night are pre-reduced automatically to refer them to the ICRF using Tycho2 stars as references. The identification of the strips and the result of the pre-reduction are store in a log file. After that a program search the log file and find the strips not observed or bad observed (big errors or limit magnitude below 14.5 V) and select the strips to be observed having in account some priorities choose conventionally.

In order to remove atmospheric fluctuations he strips are overlapped 8' with the two adjacent strips in declination. Using the stars in the common zones of several consecutive strips over and below the strip in question is possible to compute a calibration function (D. Evans, 2002) to remove the fluctuations.The expected precision of a star position in the survey would be below 50 mas in both coordinates.

The magnitudes produces with the CMASF are not in a photoelectric standard system as there is not any filter in front of the CCD camera window. They are referred approximately to the V band using the Tycho2 reference stars magnitudes.

In general no proper motions will be computed, but at present a joint project with Dr. C. Abad from the CIDA (Venezuela) is in progress to remeasure the *Carte du Ciel* plates of San Fernando zone ($-3^o$to -9^odegrees). The positions of the stars in those plates and those of the survey will be used to produce proper motions.

Figure 1 is a plot of the status of the survey observations on last september.

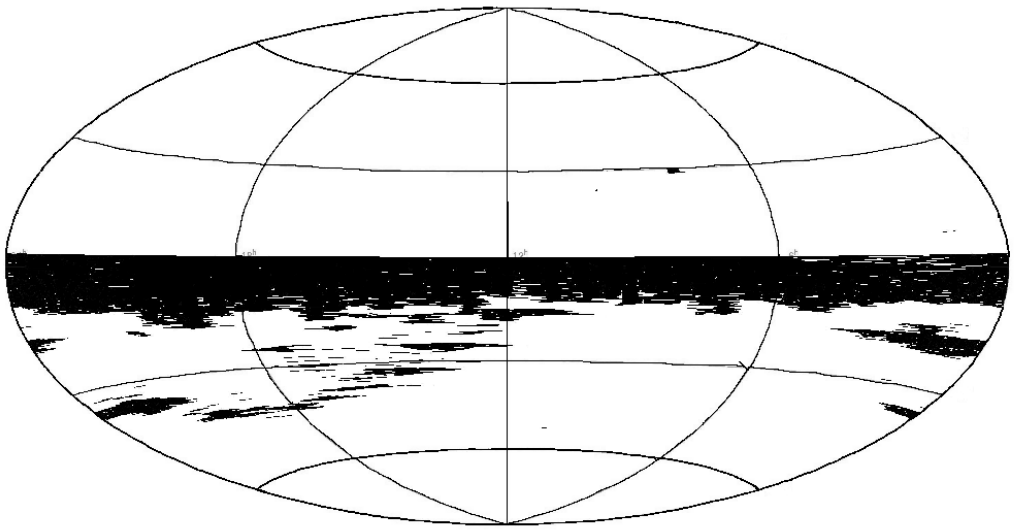

Figure 1: Status of the survey observations on september 2002

3. 2 Planet observations

In pararell with the survey observations a program to observe Neptune, its satellite Triton and Pluto started in 2001. The three objects are observed every five days when they transit through the CUC meridian during night-time. Neptune and Triton are observed in the same strip.

To observe enough Tycho2 reference stars to reduce the planet observation a strip of 10 minutes centred in the planet are observed. In this way a minimum of 10-11 references stars are identified in every strip.

To correct for the atmospheric fluctuations, the slow right ascension motion of the planet is taken in account. The observed strips of Neptune and Pluto are divided in set of three, four or five of them depending of the time interval in which they are been observed. All the stars sorroundind the planet common to all the strips of a particular set are considered. For these stars are computed average of its coordinates and the differences between these averages and

the coordinates in every strip of the set. Using these differences, corrections to the R.A. and declination are computed to remove the fluctuations from the planet coordinates.

3.3 Other ocasional programs

Sometime official institutions request to the Management Committee of the CMASF to observe with this instrument some zones of the south hemisphere to use them in joint research with the CMASF team.

In 2001 one of these special program was carry out to research in collaboration with Dr. Texeira from Valinhos Observatory (Brazil). The matter of the research was to find for stars with big proper motions in areas of X-ray sources to try to search for young stars.

The second special program was developed in spring 2002. It was requested by Dress. Orellana from La Plata observatory (Argentina) collaborating also Dr. Texeira. A zone of 1.5 x 1.5 degrees surrounding NGC2516 was observed to compute proper motions taking as first epoch positions those measured in an old plate observed in La Plata on 1914. Figure 2 is a plot draws with the positions computed from the CMASF observations. In it is possible to appreciate the cluster near the center.

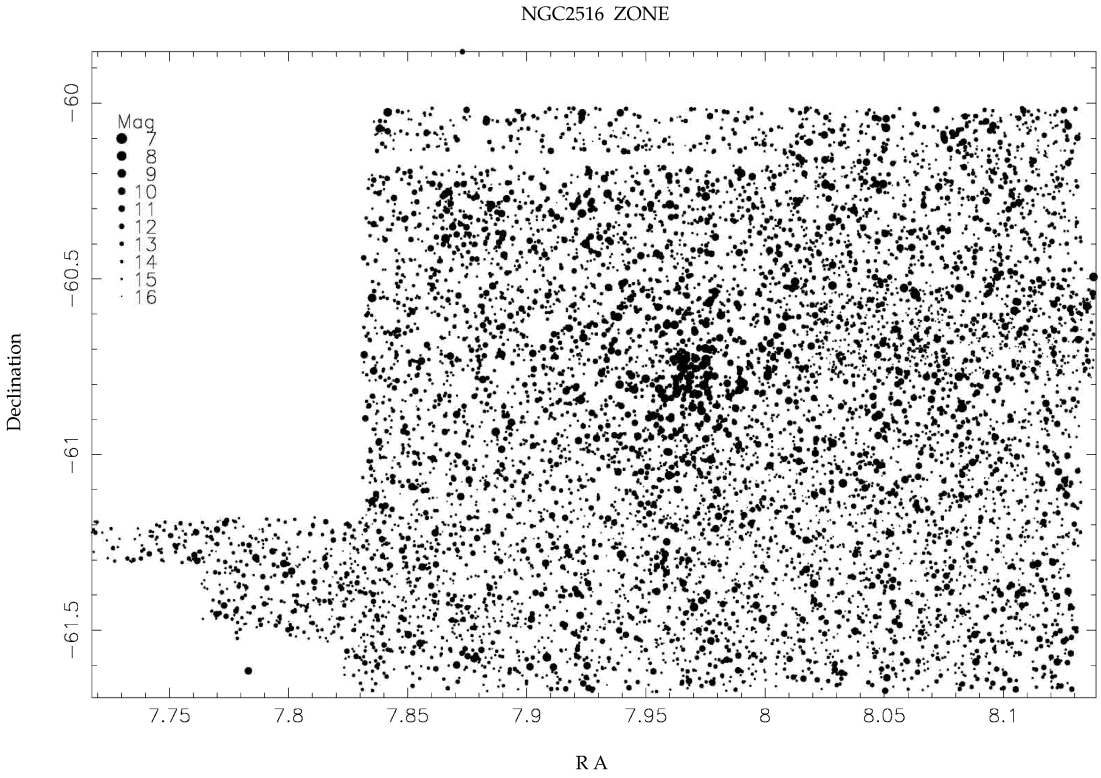

Figure 2: CMASF observations surrounding NGC2516

4 CONCLUSIONS

The CCD observations with the CMASF are expected to be published at least 10 years before the first results of GAIA or SIM will be published. So they will permit to extend the

Hipparcos frame to magnitude 16 in the south hemisphere and the survey positions compared with those from the UCAC will be possible to investigate for systematic errors in both surveys, supplying very good positions to be used for the astronomical community.

Also the comparison of those positions with new measures of existing *Carte du Ciel* plates will produce proper motions with a high degree of precision for faint stars.

Precise positions of Solar System objects are expected to be useful to study the Solar System dynamics.

Short and inexpensive observational programs combined with new measures of old photographic plates will serve to research for young stars or to identify clusters components.

So even if the launch of GAIA and SIM will be produced in the expected respective years and both two will reach their predict orbits, the observations with small and medium astrometric instrument will be very important to the astronomical research in the inter-period.

5. REFERENCES

Evans D. W., (2001). Astronomische Nachrichten, 322-347.

Evans D. W., Irwin M. J., Helmer L. (2002). A & A submitted.

Helmer L., Morrison L. V., (1985). Vistas Astronomy, 28, 505.

Hispano Argentinian Maridian Catalogue (2001), Real Instituto y Observatorio de la Armada, San Fernando (Spain).

SOLAR DIAMETER OBSERVATIONS ON THE MAXIMUM OF CYCLE 23

A. H. ANDREI [1,*] J. L. PENNA [2],
E. REIS NETO [2], E. G. JILINSKI [3,4],
S. C. BOSCARDIN [2,5], C. DELMAS [6],
F. MORAND [6], F. LACLARE [6]

1- GEA-Observatório do Valongo/UFRJ-Observatório Nacional/MCT, Brasil
R. Gal. José Cristino, 77, Rio de Janeiro, Brasil
2- Observatório Nacional/MCT, Brasil
3- Lboratório Nacional de Computação Científica/MCT, Brasil
4- Observatory of Pulkova, Russia
5- Observatório do Valongo/UFRJ, Brasil
6- CERGA/Observatoire de la Côte d'Azur, France
*e-mail: oat1@on.br

ABSTRACT.

The Réseau de Suivi au Sol du Rayon Solaire numbers four stations, in France, Brasil, Turkey and Algeria. Though formally established in 2002, the common works of those groups was started as early as ten years before, particularly involving the CERGA and the ON.

The method and instruments used by this network are introduced. Results of solar semi-diameter variation campaigns are presented for the years corresponding to the peak of the solar activity cycle 23. The outcome shows that the average value for a session of measurements is obtained with accuracy better than few tenths of arc second, what enables to establish a positive correlation with the sunspots count to a level of certainty better than 0.99.

1. THE RÉSEAU DE SUIVI AU SOL DU RAYON SOLAIRE

The principle of measurement of the solar diameter with astrolabe derived instruments is based on the time difference of the upper and lower limb summit transit by an instrumentally defined zenith distance. Several prior experiments had shown that the astrometry of such type of measurement was accurate to the level of some tenths of arc second, and remained coherent on the scale of years (Andrei et al., 2000). As early as 1975 solar diameter observations with a modified Danjon astrolabe were started at the CERGA (Laclare et al., 1996). In 1989, the same group introduced the CCD acquisition of the solar images, followed in 1996 by the fully digitized treatment of the observations, and automation of the analysis. It is interesting to remark that, even though the different modes of observation, which lead to the diminution of the results dispersion by a factor of 10, there is no discontinuity on the measured values. Figure 1 shows the CERGA measurements made with the series of modified astrolabes.

Since then several solar astrolabes stations (eg., Brasil, Spain, Chili, Turkey) confirmed the variations observed by Laclare at CERGA. Presently, the Réseau de Suivi au Sol du Rayon Solaire (R2S3) was established, by the groups of the CERGA/Observatoire de la Côte d'Azur (France), Observatório Nacional (Brasil), Tubitak National Observatory (Turkey), and CRAAG/Observatoire d'Alger (Algeria). At the CERGA there is a prototype, DORAYSOL, of the second generation instrument that will be at work among the R2S3 groups. The new in-

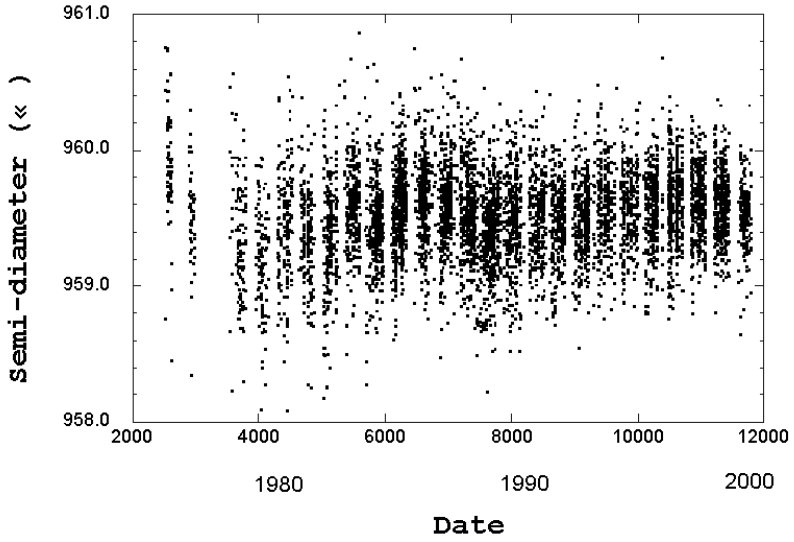

Figure 1: Solar Astrolabes CERGA series (values corrected to zenith conditions).

struments are characterized by a highly stable frontal prism of variable angle, multi-wavelength capability, tele-commanded pointing and image acquisition, and a telescope replacing the objective lense of the classical astrolabe. The combination of the characteristics enable to obtain a much larger number of independent measurements (up to 40/day), and enhanced accuracy (at the level of 0".1). A seeing monitor will work at the CERGA station, which will also harbor test measurements for the SODISM instrument on board the solar satellite PICARD. Table 1 schematizes the instruments of the Network

Réseau de Suivi au Sol du Rayon Solaire R2S3
(Christian Delmas, **Astrométrie et Métrologie Solaires**, septembre 2002)

Sites	**Calern**	**Rio de Janeiro**	**Tamanrasset**	**Antalya** (Turquie)
Instrument de Référence	AstroSol de FL 11 Prismes fixes Série Visuelle **1975-2002** 7000 mesures, **σ = 0.28"**	AstroSol de AHA **PV1** (prototype Calern 1986) Série CCD **1997-2002** 14000 mesures, **σ = 0.40"**	DORAYSOL 2 Télescope + CCD **2003** Prisme Variable **PV3**	AstroSol de FC et OG 3 Prismes fixes Série CCD **1999-2002** 1500 mesures, **σ = 0.30"**
2ème Instrument	DORAYSOL 1 Télescope + CCD Prisme Variable **PV2** (prototype CNRS 1989) Série CCD **1999-2002** 6000 mesures, **σ = 0.24"**	Type DORAYSOL Télescope + CCD **2003** Prisme Variable **PV3** (*à l'étude*)		DORAYSOL 3 **2004 ?** Prisme Variable **PV3**
3ème Instrument	MISOLFA Paramètres et profils de turbulence atmosphérique **2003** Observations simultanées avec DORAYSOL 1			

Table 1: Instruments of the Réseau de Suivi au Sol du Rayon Solaire - R2S3 Network.

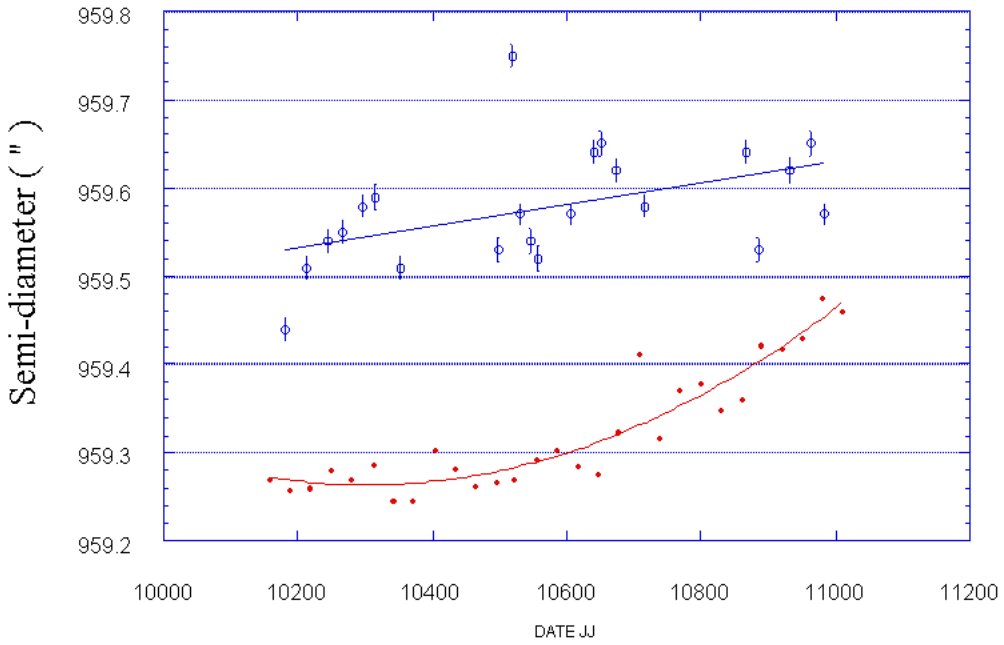

Figure 2: The semi-diameter measurements (corrected to zenith conditions) from the CERGA solar astrolabe are shown by the upper curve. The bottom curve shows the sunspot count number.

2. COMPARISON WITH THE SOLAR ACTIVITY

The very different atmospheric conditions and the different helio latitudes of the measured solar diameter, give a complementary nature to the results from the four stations. From the Rio de Janeiro station, the observations can be carried out all year around.

During the rise and maximum of the solar activity cycle 23, a positive correlation between the solar diameter variation and the sunspot count number was verified. Figure 2 compares the measured diameter, obtained by the CERGA solar astrolabe, and the sunspot count number, for the period from 1996.5 to 1998.5, which corresponds to the rise of cycle 23. Emilio et al. (2000) found similar agreement analyzing MDI SOHO observations.

The correlation close to the maximum of the cycle (from 1998 to 2000) is shown in Figures 3, for the Rio de Janeiro observations. In this case, the Mann-Whitney non-parametric correlation test does not distinguish between the two normalized distributions even to the level of 99%.

3. CONCLUSION

The results from solar semi-diameter variation monitoring programs are increasingly being used to derive constraints on solar models (Pap et al., 2001; Rozelot et al., 2002, Reis Neto et al., 2002). Important advances on the reliability of the measures have been obtained by DORAYSOL like, second generation instruments. Also the use of frontal prism of variable angle increased the quantity of possible measures by one order of magnitude.

A next important step has been done by the establishment of the Réseau de Suivi au Sol du Rayon Solaire network, which groups four stations, that had already long term forms of cooperation. The R2S3 network, aims to common measurements, similar equipment facilities, and interchange of methods.

Here we present results from the R2S3 observations, showing a statistically significant positive correlation between the increasing on the measured semi-diameter and the increasing on the sunspot count number, during the rise and maximum of the solar activity cycle 23.

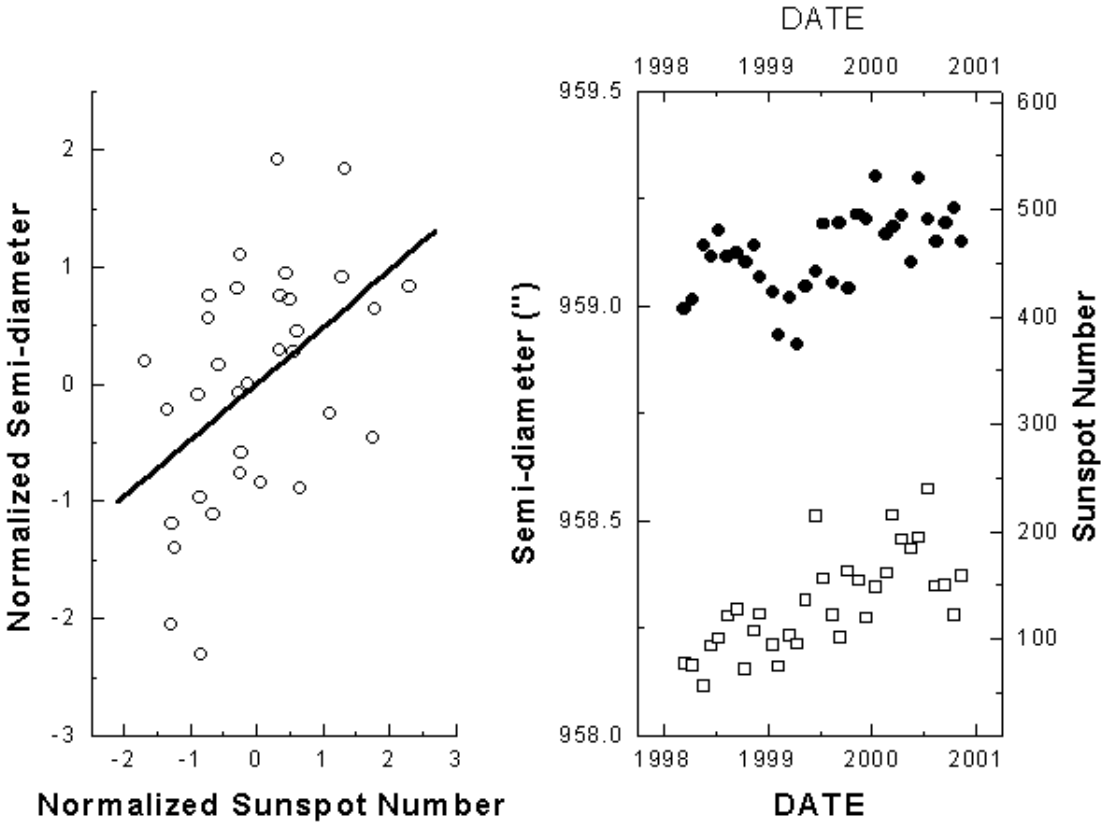

Figure 3: Rio de Janeiro station monthly average for the measured solar semi-diameter and the monthly average for the sunspot count number. On the left the direct comparison, where the linear correlation is verified at 3σ. On the right the time evolution of the average values (filled circles for semi-diameter values and open squares for sunspot numbers).

4. REFERENCES

Andrei, A.H., Laclare, F., Penna, J.L., Jilinski, E.G., Puliaev, S.P. & Delmas, C., 2000, IAU Coll.178, "Polar Motion: Historical and Scientific Problems", ed. S. Dick, D. McCarthy and B. Luzum

Emilio, M., Kuhn, J. R., Bush, R. I. & Scherrer, P., 20008, ApJ, 543, 1007

Laclare, F., Delmas, C., Coin, J. P. & Irbah, A., 1996, Sol.Phys., 166, 211

Lefebvre, S. & Rozelot, J.-P., 2002, "Latitudinal variations: from the observations to the theory", SF2A-2002: Semaine de l'Astrophysique Française, ed. F. Combes and D. Barret, 79

Pap, J., Rozelot, J. P., Godier, S. & Varadi, F., 2001, A&a, 372, 1005

Reis Neto, E., Andrei, A.H., Penna, J.L., Jilinski, E.G. & Puliaev, S.P., "Observed Variations of the Solar Diameter in 1998/2000", to appear in Sol.Phys

OBSERVATIONS OF PLUTO IN BUCHAREST DURING 1932 AND 1967-1975: PRECISE POSITIONS AND MAGNITUDES

G. BOCŞA
Astronomical Institute of the Romanian Academy
Str. Cuţitul de Argint 5, RO-752121 Bucharest, Romania
e-mail: gbocsa@aira.astro.ro

ABSTRACT. The observations of Pluto obtained in 1932 and during 1967-1975, performed at the Astronomical Observatory of Bucharest with the 380/6000 mm astrograph are presented. Both Turner's (constants) and Schlesinger's (dependencies) methods were used for the computation of the normal coordinates of the object.

1. PRECISE POSITIONS

Pluto was observed in 1932 by G. Demetrescu on plates of 13×18 cm, with a 52 minutes exposure, and also in the period 1967−1975 by C. Cristescu on plates of 24×24 cm, with exposures ranging between 20 minutes and one hour. To determine more precise positions, we tried to take into consideration as many reference stars as possible, and we have used the PPM catalogue J2000.0, referring all the determinations to the epoch 2000.0. The most difficult problem was the identification of the planet (by superposition of two plates) on the plates obtained in 1932, because all observations were made in the same month and the planet did not have a significant proper motion.

The values $(O-C)_\alpha$ and $(O-C)_\delta$ were calculated by M. Svechnikov from the Institute of Applied Astronomy in Sankt Petersburg, on the basis of the precise positions obtained in Bucharest, which we integrated in Pluto's orbit (Table 1).

2. DETERMINATION OF MAGNITUDE

We have also determined the photographic magnitude of Pluto at the observatory level, as against the photographic magnitude of 9 stars situated in the neighbourhood of the planet. We used the machine for coordinates measurements, with which we measured twice the diameter for each star, as well as for Pluto. By means of a graphic program, where we introduced for each plate the diameter in abscissa and the photographic magnitude of the stars in ordinate, we obtained a straight line ($M = m \times d_P + n$) and the values m and n. Introducing in the straight line equation the value of Pluto's diameter we obtained the value of its photographic magnitude. To check the parameters m and n for several cases, we resorted to Gauss' method, obtaining values very close to those of the two parameters. The results obtained are approximate because of the imprecision, especially of the measurement of Pluto's diameter. We give the graph for 7 January 1932 (Fig. 1).

No	Data + UT			$\alpha_{2000.0}$			$\delta_{2000.0}$			$(O-C)_\alpha$	$(O-C)_\delta$	M
				h	m	s	°	'	"			
1	1932	01	07.950165	7	35	54.645	22	08	56.50	+0.008	+0.05	13.1
2	1932	01	15.914949	7	35	11.033	22	11	06.97	.012	- .08	13.1
3	1932	01	29.888239	7	33	56.211	22	14	48.39	.011	.24	13.1
4	1967	05	15.806346	11	42	20.067	18	25	55.35	- .099	- .28	12.3
5	1967	06	03.874135	11	41	57.156	18	19	57.85	- .074	- .32	12.3
6	1967	06	07.825795	11	41	57.635	18	18	06.59	- .058	- .92	12.2
7	1968	02	22.835410	11	57	53.882	17	17	54.38	- .116	- .40	11.5
8	1968	03	21.855089	11	55	14.951	17	38	06.11	- .073	.20	11.5
9	1968	04	18.824871	11	52	41.305	17	50	09.77	- .032	- .08	11.4
10	1968	04	22.812544	11	52	22.639	17	50	59.67	- .033	- .62	11.5
11	1973	03	29.877944	12	39	31.497	14	15	14.59	.027	.87	11.5
12	1974	03	18.863596	12	49	44.763	13	20	33.36	.009	- .15	11.5
13	1974	03	21.848487	12	49	27.560	13	22	44.22	- .015	- .94	11.6
14	1975	04	03.840961	12	57	21.330	12	42	48.00	- .003	- .57	12.3
15	1975	04	07.856013	12	56	57.352	12	45	11.84	.068	- .33	12.3
16	1975	04	14.787035	12	56	16.030	12	48	52.49	- .024	- .47	12.5
17	1975	05	05.798947	12	54	20.626	12	56	00.18	.099	.13	12.4
18	1975	05	08.789367	12	54	06.121	12	56	28.57	- .008	.07	12.4
19	1975	05	12.801994	12	53	47.693	12	56	53.50	- .017	.20	12.4

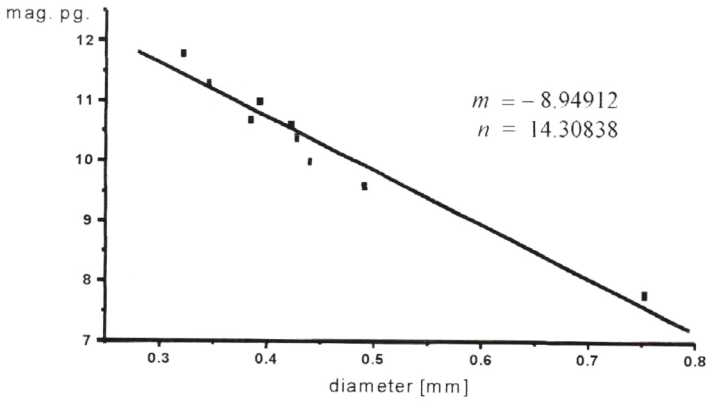

Fig. 1. Diameter-magnitude diagram

More details can be found in Bocşa's (2001) paper.

3. REFERENCE

Bocşa, G.: 2001, *Rom. Astron. J.* **11**, 77.

AN IMPROVED STAR CATALOGUE FOR ONDŘEJOV PZT

C. RON, J. VONDRÁK
Astronomical Institute, Academy of Sciences of the Czech Republic
Boční II 1401, 141 31 Praha 4, Czech Republic
e-mail: ron@ig.cas.cz, vondrak@ig.cas.cz

ABSTRACT. The observations of 305 stars made in the period from 1973 to 2002 with the PZT at Ondřejov Observatory were combined with the positions of the same stars in the catalogues AGK2, AGK3 and HIPPARCOS in order to obtain their mean positions and proper motions. The modified algorithm of Vondrák (1980) and Ron & Vondrák (1985) has been used for the adjustment. More than 77000 individual star transits in 2561 nights have been observed within the period in question with the PZT.

1. INTRODUCTION

Regular observations with the PZT at Ondřejov (Carl Zeiss Jena, $f = 3780$ mm, $D = 250$ mm) have been made since 1973 up to now. The observed stars lie in the narrow declination belt between 49°35' and 50°15'. The observations were performed in 3 different observing programmes:

- 192 stars divided into 15 unequally spaced groups were observed in the interval 1973–1978.0;
- In 1978, 113 stars were added and 8 stars excluded, which led to the observing programme consisting of 297 stars in 15 groups. The positions of the new stars were taken from AGK3 catalogue (Dieckvoss & Heckmann, 1975);
- Since 1979 224 stars divided into 16 equally spaced groups (1.5 hour) are observed. These stars were selected from the 297 stars observed in 1978.

Several star catalogues were derived from the observations done by Ondřejov PZT but only some of them were used as working catalogues for the PZT. In 1973–1978 the catalogue **PZT75** was used; the star positions were taken from the SAO catalogue and were improved from the first two years of observations (Webrová & Weber, 1976). In 1979 the catalogue **PZT75a** was used that was basically PZT75 with the positions of new 113 stars improved by using the PZT observations in 1978. In 1980–1984 the catalogue **PZT78** was used. The star positions were derived from the observations 1973–1978 in combination with the AGK2 and AGK3 positions (Vondrák, 1980). Since 1985 the catalogue **PZT83** has been used. The star positions were derived from the observations 1973–1983 in combination with AGK2 and AGK3 positions, using an analogous method as for PZT78 (Ron & Vondrák, 1985). The catalogue **PZT86**, consisting of 224 PZT stars, was derived from PZT observations in 1973–1986. This catalogue was never used for PZT adjustment, due to insufficient accuracy in proper motions (Vondrák, 1988). The

catalogue **PZT89**, consisting of 305 PZT stars, was based on combination of PZT observations with AGK2/3 positions (Ron, 1992). This catalogue was used neither since we decided not to change the working catalogue, expecting the new HIPPARCOS catalogue . HIPPARCOS catalogue was used for the re-reduction of the optical astrometry observations in the HIPPARCOS reference frame (Vondrák et al. 1998). We found the inadequacy of proper motions of about 1/5 of the stars, therefore the corrections of proper motions were derived from the residuals.

2. METHOD OF SOLUTION

The present analysis uses a slightly modified method which was already used for the improvements of the catalogues PZT78, PZT83 and PZT86. The determination of positions and proper motions is divided into two steps.

In step one, only the corrections of star positions are determined in the short intervals (one or two years long). The problem is solvable on the assumption that:

- the observed quantity (i.e., latitude φ or clock correction UT0–UTC) is constant during one night;
- the error in the star's position is constant during the interval in question.

The unknowns to be found from the adjustment by the method of least squares, independently in each interval of observations, are M values of observed quantities $\bar{x}_j$ (latitude or clock correction) for each night, and N corrections of each star's catalogue position a_i (declination or right ascension). The observation equation then reads

$$v_{ij} = \bar{x}_j - a_i - x_{ij},$$

where v_{ij} and x_{ij} denote the residual after adjustment and observed value for the i-th star in the j-th night respectively. The standard least-squares method leads to the system of $M + N$ linear equations whose matrix is singular. An additional constraint has to be imposed of the form $\sum a_i = 0$ applied to a subset or all adjusted star positions. All of the observed quantities have the weight equal to one. The algorithm is applied to each of the intervals.

In step two, the corrections of the star positions, obtained in step one for the particular one or two year intervals, are combined and adjusted in order to derive the new improved positions and proper motions in the epoch J2000.0. In order to obtain proper motions with better precision, PZT observations can be combined with the AGK2/3 or HIPPARCOS catalogue positions of the stars, used as fictitious observations. The observation equation for the i-th star observed in the k-th PZT interval reads

$$v_{ik} = \Delta x_i + \Delta\mu_i(t_{ik} - 2000) - \Delta_k - a_{ik},$$

where a_{ik} is the result from the preceding step and Δ_k is an additional constant shift of the PZT results for the k-th interval. The observation equation for the i-th star in AGK2/3 catalogue or in the HIPPARCOS catalogue (experiment b and c, see below) is

$$v_{ik} = \Delta x_i + \Delta\mu_i(t_{ik} - 2000) + l_{ik},$$

where l_{ik} is the difference PZT83 – AGK2/3 or HIPPARCOS at the mean epoch of the catalogues. The shifts Δ_k were identically put equal to zero in case of fictitious observations to bring the resulting positions and proper motions to the system of the reference catalogue. The input values a_{ik} are taken with the weights derived from the standard deviations of particular stars which lead to weights ranging from 1 to 50. These values roughly correspond to the number

k	Interval	N	m_α [s]	m_δ [″]	M	n
1	1973/74	197	±0.0127	±0.142	156	4432
2	1975/76	192	±0.0128	±0.144	167	4130
3	1977	197	±0.0130	±0.131	104	2333
4	1978	296	±0.0127	±0.133	107	3869
5	1979	224	±0.0128	±0.132	108	3057
6	1980	224	±0.0136	±0.135	97	2638
7	1981	224	±0.0128	±0.126	114	2870
8	1982	224	±0.0140	±0.132	138	3956
9	1983	224	±0.0130	±0.133	144	4189
10	1984	224	±0.0129	±0.135	149	4024
11	1985	224	±0.0134	±0.149	122	3452
12	1986	224	±0.0134	±0.157	133	3830
13	1987	224	±0.0135	±0.149	123	3610
14	1988	224	±0.0135	±0.140	112	3433
15	1989	224	±0.0134	±0.133	130	4004
16	1990	224	±0.0144	±0.148	135	4367
17	1991	224	±0.0144	±0.152	111	4168
18	1992	224	±0.0146	±0.147	70	2654
19	1993	224	±0.0168	±0.175	49	1736
20	1994	224	±0.0182	±0.178	49	1755
21	1995/96	224	±0.0175	±0.179	50	1883
22	1997/98	224	±0.0180	±0.179	77	2792
23	1999/00	224	±0.0208	±0.214	46	1524
24	2001/02	224	±0.0220	±0.217	69	2390
1-24	1973/2002	305	±0.0144	±0.150	2560	77096

Table 1: The survey of PZT observations obtained from the adjustment in step one. N – the number of different stars observed in the interval, m_α, m_δ – standard errors of a single observation in right ascension and declination, M is the number of observing nights in the interval and n – number of star transits observed in the interval.

of observations of the i-th star in the k-th interval. The weights of the fictitious observations l_{ik} taken from AGK2/3 were set to 1 and 2, respectively (see, Vondrák, 1980). The weight of fictitious observation taken from HIPPARCOS catalog was set to the value of the average number of observation of one star (250) and moreover, this value leads to the smallest average standard errors. The observational equations lead to the system of $2N+K$ linear equations. For more information on the solution of normal equations see Vondrák (1980) and Ron & Vondrák (1985).

3. THE OBSERVED DATA USED IN THE ADJUSTMENT AND THE RESULTS

From the reduction of PZT observation we can get the values φ and UT0–UTC, separately for each star transit. We have re-reduced all PZT observations obtained in 1973-2002, using the single catalogue, PZT83. The detection of the outliers has been done before the adjustment – the observation was excluded in case its difference from the 'floating' median (the L1 norm applied to the interval of 15 days before and after the moment of observation in question) was greater

catalogue	m_α [s]	m_{μ_α} [s/cy]	m_δ ["]	m_{μ_δ} ["/cy]	t_0
PZT83	±0.0019	±0.0240	±0.020	±0.260	1978.8
PZT86	±0.0015	±0.0510	±0.017	±0.570	1981.6
PZT01a	±0.0015	±0.0089	±0.016	±0.095	1984.8
PZT01b	±0.0015	±0.0081	±0.016	±0.085	1984.0
PZT01c	±0.0013	±0.0089	±0.013	±0.088	1986.2

Table 2: The average standard errors of the catalogues PZT83, PZT86 and PZT01a,b,c in position m_α, m_δ and proper motion m_{μ_α}, m_{μ_δ}.

than 0.8″ and 0.08s for φ and UT0–UTC, respectively. If applied, the fictitious observations were taken from the AGK2/3 catalogue (Dieckvoss & Heckmann, 1975) and HIPPARCOS catalogue (ESA, 1997) (in the experiments b and c, see below).

In step one we divided the period of the PZT observations into 24 intervals, one or two years long. The constraint $\sum a_i = 0$ was applied to all observed stars ($i = 1, .., 305$).

The global statistics of the observations in different intervals is displayed in Tab. 1. It should be noted that the progressive decrease of the accuracy after 1992 is caused by the considerable limitation of observations.

In step two the combination of the corrections for each of 24 intervals was performed. We have done 3 experiments:

- Only the PZT observations were used (PZT01a), processed similarly as in Vondrák (1988);
- PZT observations were combined with AGK2 and AGK3 positions (PZT01b), processed similarly as in Ron & Vondrák (1985);
- PZT observations were combined with the HIPPARCOS positions (PZT01c). Only 282 stars from the HIPPARCOS catalogue were observed in Ondřejov PZT. Further 17 stars which were detected as suspicious in Vondrák et al. (1998) were rejected which led to 265 stars that were constrained by $\sum a_{ij} = 0$, leading to the catalogue linked to the HIPPARCOS reference frame.

The resulting standard errors of the three experiments and the comparison with the previous catalogues PZT83 and PZT86 are shown in Tab. 2. The accuracy of these catalogues at any epoch t can be described by a standard error m_t calculated from the formula

$$m_t^2 = m_0^2 + m_\mu^2 (t - t_0)^2,$$

where standard errors m_0 and m_μ and the mean epoch of the catalogue t_0 are given in Tab. 2 (m_0 means m_α or m_δ and analogously for m_μ). These errors are graphically compared in Fig. 1. It is evident that the precision of all the catalogues PZT01a,b,c is superior to that of PZT83 and PZT86 in longer time span.

4. CONCLUSIONS

The new PZT01 catalogue using more than 77000 transits in the period 1973–2002 gives the positions and proper motions of 305 stars with significantly better precision than each of the previous PZT catalogues. The standard errors of proper motions are comparable to those of the Hipparcos Catalogue. For the stars that were observed during the whole period the mean errors

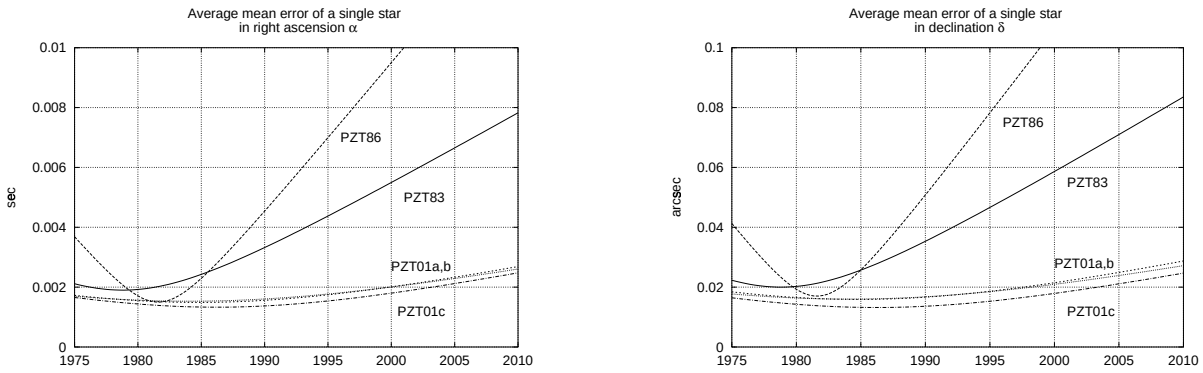

Figure 1: Comparison of the average mean errors in right ascension m_α and declination m_δ of a single star in the cataogues PZT83, PZT86 and PZT01a,b,c in the interval 1975–2010.

do not exceed ± 0.003s and $\pm 0.03''$ in right ascension and declination, respectively, in the interval 35 years long. Adding the fictitious observations from AGK2/3 catalogues to the adjustment does not bring any longer an obvious improvement as it does in our previous solutions (PZT83, PZT89). The next processing of the PZT observations will be used to improve the new Earth Orientation Catalogue (Vondrák & Ron, 2003).

Acknowledgements. We appreciate the support by the grant No. 3205 awarded by the Grant Agency of the Academy of Sciences of the Czech Republic (ASCR). Our participation in the Journées was supported within the frame of bilateral cooperation between the ASCR and Rumanian Academy of Sciences.

5. REFERENCES

Dieckvoss W., Heckmann O. (1975) AGK 3. Star catalogue of positions and proper motions north of -2.5 deg. declination. Hamburg-Bergedorf, Hamburger Sternwarte.

ESA (1997), The Hipparcos and Tycho Catalogues, ESA SP-1200.

Ron C. (1992) The determination of the tidal variations of the plumb line and the nearly diurnal free wobble from the PZT observations. In: H. Montag and Ch. Reigber (eds.) *Proc. IAG symp. 112 Geodesy and Physics of the Earth*, Potsdam, Springer Verlag, 421– 424.

Ron C., Vondrák J. (1985) Mean positions and proper motions of 305 stars obtained from combination of PZT observations at Ondřejov with AGK positions. *Bull. Astron. Inst. Czechosl.*, **36**, 289–300.

Vondrák J. (1980) The determination of mean positions and proper motions of 304 stars from PZT observations at Ondřejov, *Bull. Astron. Inst. Czechosl.*, **31**, 89–101.

Vondrák J. (1988) Mean positions and proper motions of 224 stars based on PZT observations at Ondřejov in 1973–1986, *Bull. Astron. Inst. Czechosl.*, **39**, 152–164.

Vondrák J., Ron C. (2003) An improved optical reference frame for long-term Earth rotation studies. In: N. Capitaine (ed.) *Journées 2002 Systèmes de référence Spatio-temporels*, Observatoire de Paris, this volume.

Vondrák J., Pešek I., Ron C., Čepek A. (1998) Earth orientation parameters 1899.7–1992.0 in the ICRS based on the HIPPARCOS reference frame. *Publ. Astron. Inst. Acad. Sci. Czech R.* **87**, 56 pp.

Webrová L., Weber R. (1976) Der Sternkatalog des photographischen Zenitteleskop in Ondřejov *Wiss. Z. Techn. Univers. Dresden* **25**, 919–921.

PROPER MOTION SURVEY IN THE BORDEAUX M2000 ZONE

C. DUCOURANT[(1)], R.-W. ARGYLE[(2)], J.-F. LE CAMPION[(1)], G. DAIGNE[(1)], J.-P. PÉRIÉ[(1)], M. RAPAPORT[(1)], C. SOUBIRAN[(1)]

(1) Observatoire de Bordeaux, France
(2) Institute of Astronomy, Cambridge, UK

ABSTRACT. We started in 1997 the astrometric project of re-measurement of the Bordeaux Carte du Ciel zone ($11° < \delta < 18°$) with the Bordeaux automated CCD meridian circle. These recent observations should be combined with the Carte du Ciel plate measurements scanned at APM (Cambridge) in order to produce an astrometric catalogue of positions and proper motions in the Hipparcos Reference Frame for all stars detected on the plates. The positional catalogue M2000 has been published in June 2001 (Rapaport et al. 2001) including 2.3 million stars down to the magnitude limit $V = 15.4$. The median internal standard error in position is 35 mas in the magnitude range $11 < V < 15$. The 563 Carte du Ciel plates have been automatically scanned at the cambridge APM automated plate measuring machine. The combination of the M2000 astrometric catalogue with these first epoch measurements and other available astrometric sources is underway. The resulting proper motion catalogue should be ready by the end of 2002. We present here the Carte du Ciel plates reductions and preliminary results for the proper motion derivation.

LIMITED POSSIBILITIES OF THE GROUND-BASED OPTICAL ASTROMETRY INSTRUMENTATION

G. PINIGIN
Nikolaev Astronomical Observatory
Observatorna 1, Nikolaev, 54030 UKRAINE
e-mail: pinigin@mao.nikolaev.ua

ABSTRACT. A general overview of various types of ground-based telescopes for astrometric programs is presented. Also the limiting accuracy in positional determination with corresponding instruments is shown. Technical possibilities of modern ground-based optical astrometry can provide an accuracy of astrometric parameters about 20-30 mas for significant number of stars up to 18-23 mag. Taking into account expected accuracy of optical interferometers at a level 0.1-0.01 mas, it is possible to hope that ground-based optical astrometry will be necessary as observational base for preparation and maintenance of selected astrometric programs, especially before the future space projects. As to the means of control and research of solar system bodies and near-Earth space objects the progress in the new direction such as near-Earth astronomy has confirmed efficiency of significant number of small telescopes equipped with the modern instrument set together with the large telescopes.

1. INTRODUCTION.

The positional astronomy is in the state of active development. The most impressive facts and steady tendencies of this period are the following:
- On the base of impressing results of space experiment Hipparcos the leading role of space astrometry was ratified as an independent and predominant direction in astronomy, especially, for establishment and maintenance of the ICRF reference coordinate system;
- Future projects of astrometrical satellites of the 21-st century such as DIVA, OSIRIS, SIM, GAIA promise to increase accuracy up to microarcsecond level for tens and hundreds of millions of celestial objects with brightness from 16 to 20 magnitudes;
- The role of ground-based astrometrical researches is undergoing substantial changes. Dominant factors in this process are the following: selection of scientific tasks, solved by ground-based means; formation of new directions (such as near-Earth astronomy, creation of virtual telescopes and virtual astronomical observatories etc); introduction of new generation of ground-based observational techniques with wider possibilities; use of standards in recording, processing and storing of observational data; use of mobile telescopes, differential methods of measurements, etc.

2. PROBLEMS AND LIMITS OF GROUND-BASED ASTROMETRY INSTRUMENTATION

Analysis of observational programs, carried out with telescopes of small and large sizes, shows that majority of them has astrometrical tasks. Let's consider the most known telescopes from the position of their participation in the astrometrical programs.

2.1 *Possibilities of automatic meridian telescope (AMT)*

The latest technical achievements are used to equip modern ground-based AMT:
- CCD sensors with high sensitivity, devices with an active cell (APS);
- automatic control of observations;
- reduction and storage of observational data with high-effective computing means;
- information networks and CD-ROM.

Six most modernized and active AMT are shown in Table 1.
Theyare mentioned on the sites (http://www.ast.cam.ac.uk/ ˜ dwe/AstSurv and http://www.uni-sw.gwdg.de/˜hessman/MONET/links.html) Certainly, it is possible to name some additional meridian telescopes with moderate possibilities.

Table 1. Automatic meridian telescopes

AMT	**Location**	**Current Programs**	**CCD, FOV**	**Declination zone [^{o}], mag.**	**Catalogs Accuracy (mas)**	**Position: CCD active since**
AMC D180, F2480	Nikolaev, Ukraine, +47^o, 52m	Selected fields, ERS, solar system objects	1040x1160, 16mkm, 1.″33/pix, 23′x26′	-20÷+90 9^m-16^m	30-40 V,R $\pm 0.05^m$	1996-
MC D190, F2370	Bordeaux, France, +45^o, 75m	Meridian-2000 Survey, catal. 2.3 mln., position and p.m. stars	1024x1024, 19mkm, 1.″65/pix, 28′x28′	-20÷+70 9^m-16^m	30-50 V $\pm 0.05^m$	1997-
FASTT D200, F2000	USNO, Flagstaff, +35^o, 2230m	Selected fields for SDSS, solar system objects, ERS	2048x2048, 15mkm, 1.″55/pix, 51′x51′	-2÷+2 $18.^m3$(V)	40 U,B,V $\pm 0.03^m$	1996-
CAMC D178, F2665	La Palma, Canaries, +29^o, 2100m	star survey, Schmidt plates, solar system objects	2060x2048, 9mkm, 0.″70/pix, 25′x25′	-30÷+90 7^m-17^m 0.2 mln	30-50 U,B,V $\pm 0.05^m$	1997-
SFAMC D176, F2664	El Leoncito Argentine, -31^o, 2330m	star survey in zone 060, s.s.objects, selec. fields	1552x1024, 9mkm, 0.″70/pix, 18′x12′	-60÷+38 7^m-16^m 0.7mln	50 B,V	1999-
Valinhos MC D190, F2590	San Paulo, Brasil, -23^o, 850m	Selected fields, s.s. objects, Radiostars, ERS (QSO)	512x512, 19mkm, 1.″51/pix, 13′x13′	-77÷+30 8^m-16^m	50 V $\pm 0.05^m$	1996-

2.2*General features of modern AMT:*

- The full account of instrumental errors up to the level from 10 to 5 mas can be achieved in different ways, for example:

a) by using telescope with special design for reduction of weight and thermal deformations such as horizontal Axial Meridian Circle (AMC) of Nikolaev Observatory;

b) by using perfect inspection and recording of all instrumental parameters with accuracy of linear measurements up to 0.01mkm.

- The accuracy of CCD coordinate measurements of celestial objects is possible up to 1-2 % of pixel. It allows us to measure their coordinates, including faint objects, at the level of instrumental accuracy. Really CCD micrometer of FASTT can register of celestial objects up to 18.3 mag.

- Automatic computer control of the AMT makes possible to carry out determination of parameters and properties of instrumental orientation, preparation and conduction of observations, reduction and storage of observational data. Therefore, productivity of automatic meridian telescopes (AMT) with drift-scan mode CCD is very high, for example more than 9000 stars per hour can be observed with FASTT.

2.3*Refraction problems*

The influence of atmosphere is still important and main problem for ground-based astrometry. For differential measurements with sufficient number of reference stars in CCD frame, it is possible to take into account the influence of such anomalous refractions as diurnal and annual ones. High-mountain location of the majority of AMT is a positive factor. Abnormal refraction inside domain is taken into account with the help of automatic meteostation. It is more difficult to remove influence of refraction, caused by atmospheric turbulence of high frequency (up to 20 kHz), which has dominant value. Calculated data for AMT with the generalized parameters such as field of view $30'30'$, exposition 100 seconds show an accuracy up to 20 mas of positional measurements of stars in the range of 9-16 mag [1]. Optimistic estimations show that the achievement of accuracy 10 mas is possible under condition of observation in visible range of waves with the help of the two-colour techniques [2,3]. High precision of HC reference system allows to observe with AMT only in differential mode, that is widely spread now. On the other hand, it is possible to observe CCD strips in drift-scan mode until several hours in right ascention to register sufficient number of reference stars.

AMT programs include ten or hundred thousands celestial objects up to 16^m - 18^m and provide positional accuracy of 30-40 mas for the support and improvement of reference frames, observations of the solar system objects such as asteroids, planets, satellites, selected celestial objects.

2.4 *CCD astrographs in ground-based astrometry*

Many telescopes equipped with CCD cameras participate in the solution of various tasks in differential astrometry (widespread diameter of optics is 0.5 - 3 meters), and some large telescopes with small fields, as well (Table 2). [4-8].

Table 2. Selected CCD astrographs, participating in the solution of astrometric tasks

Telescope (Dm, Fm)	**Location**	CCD, FOV	**Mag, spectral Bandpas**	**Current Program**	**Declination zone** (^{o})	**Number of stars (mln)**	**Position error (mas)**	**Position: active since**
SLOAN telescope (D 2.5m)	Apache Point observatory, USA	mosaic 22 CCD 2048x400, [2.^{o}2]	10÷23 U, B, V, R, J	SDSS positions, photometry	(North Galactic Zone), 10^4 (π)	100	30	1998- [4]
Astrometric Reflector (D 61$''$)	USNO, Flagstaff USA	CCD	10÷21	positions, proper motions	-30^o± +90^o	100	20	1998-
Astrometric Reflector (D 0,9m) UCAC Telescope (D 0.2m, F 2m)	CTIO, Chile USNO, USA	CCD 4096x4096 [9mkm] 0.$''$9/pix [61$'$x61$'$]	7÷16 9÷14	UCAC (USNO CCD Astrograph Catalog)	-90^o±+2^o ±+90^o	40	20÷70	1997-2003, 60 mln stars; 2000 - first version UCAC-1 (S), 27 mln stars, -90^o± -6^o ; [5, 6]
RTT150 (D 1.5m, F 11.6m)	Antalia Turkey-Russia, 37^o	ST-8 1530x1020 9x9 mkm 0.$''$16/pix [4$'$x3$'$]	20 U, B, V, R, J	positions, photometry ERS, solar system objects	-40^o±+90^o		20-30	1999- [7]
VST (D 2.65m) (Italy)	ESO, Cerro Paranal, Chile	mosaic 32 CCD, 16K x 16K [15mkm] [1,^{o} 5]	25 U, B, V, R, J	positions, photometry	southern hemis-phere		20-30	2001- [8]
SUBARU (D8.3m, F15m)	Mauna Kea, Hawaii, USA	mosaic of 10 CCD, 2048x4096, [15mkm] 0.$''$2/pix	Up to 26,6 (V) U, B, V, R, J	deep survey, double stars, asteroids with 40a.u. and more			10	2000- [9]

The majority of CCD astrographs have wide possibilities: number of objects up to 21-23 mag achieves in some programs up to 100 millions, expected positional accuracy is 20-30 mas. Let's note also that the majority of the given telescopes have the unique designs and equipment such as adaptive optics, single wide-field CCD and their mosaics, possibility of CCD cameras using in several modes (drift-scan, stare-mode, driving-mode and combined one).
The real results confirming the expected accuracy 20-30 mas are quite achievable (UCAC-1 is already compiled with accuracy 20-70 mas). Considering possibilities and accuracy restrictions of the mentioned types of ground-based astrometrical telescopes, one can note that they are determined by technical means, atmospheric conditions, and methodical features. Taking into account all factors, the optimistic estimation of positional accuracy in narrow fields is about 10 mas. [5]

2.5 *Telescopes for the near-Earth space and observation solar system bodies.*

Significant increase of interest in research of near-Earth space and solar system (space debries - artificial celestial bodies, comet-asteroid hazard - NEO, minor planets, trans-neptunian objects) was accompanied by active use of CCD optical means. Moreover, manufacture of high quality telescopes, equipped with modern CCD cameras and computers of rather low cost, is adjusted now. In accordance with data of reviews, the number of instruments, working in the specified direction, exceeds 300 (see fig. 1) [10-16]. The majority of robotic telescopes, working in the automatic mode, have the mirror sizes from 0.2 to 1 meters and more.

Fig. 1 Number (N) of telescopes for observation of NEO and solar system objects with different mirror diameters (D)

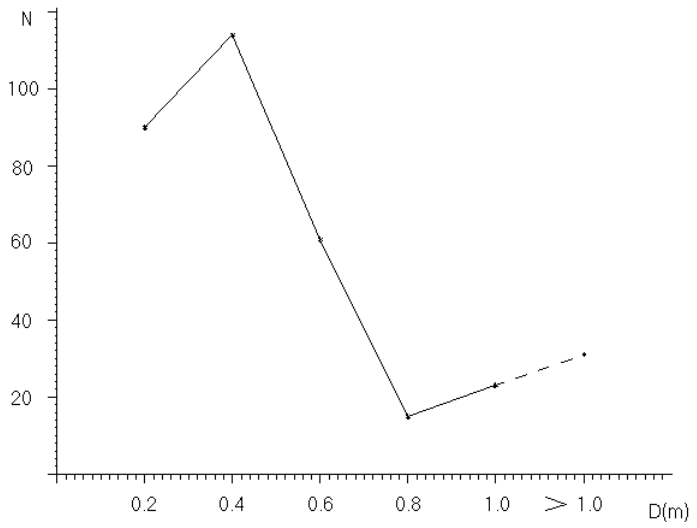

Selected telescopes with diameter more than 100 m, working in the Space Watch system , carrying out observations of space debries, numbered minor planets, and trans-neptunian objects, are given in Table 3.

Table 3. The selected optical telescopes, observing objects in the near-Earth and Solar system space

Telescope, Aperture D, Focal lengh F (m)	Organisation, location	Program	CCD, FOV	Accuracy of single observ.	Limit. mag.	Remarks, additional data from:
USA, 695 MPC, D 3.8m	Kit Peak, USNO	NMP Obsev.	CCD	$\pm 0.''15$		[10]
USA, 807 MPC, D4.0m, F14.4m	Cerro Tololo, USNO	NMP Obsev.	CCD $37'$x$37'$, $0.''27$/pix,	$\pm 0.''17$		[10]
Australia, 413 MPC, D1.2, 3.6, 1.0m	Siding Spring, USNO	NMP Obsev.		$\pm 0.''10$		[10]
Japan, D1.5m	CRL	NEO, space debris	CCD, FOV $0.^o28$	$\pm 0.''10$	$18.^m7$	[14,15]
USA, D3.0	NASA	NEO, space debris	CCD, FOV $0.^o30$		$21.^m5$	[14,15]
Russia, Ukraine, D1.0	RAS, CRAO	NEO, NMP	CCD, $12'$x$12'$		19^m	[14,15]
Ukraine,121 MPS, D0.7	AO Kharkiv university	NEO, NMP	CCD, $10'$x$8'$		18^m	[10]
USA, 691 MPC Spacewatch telescop, D0.91 F4.6	Spacewatch	NEO, NMP	CCD, $32'$x$32'$	$\pm 0.''20$		[10]
USA, SOR 3.5 3.5 f/1.5	AB Kirtland, New-Mexiko	Near-earth objects	CCD			[16]
USA, 701 MPC D1.0, F2.2, LINEAR telescope	Sokorro, New-Mexiko, Linkoln Lab.	NEO, space debris, NMP	robotics, CCD, $32'$x$32'$	$\pm 0.''51$	$15.^m5$	[10,16]

While estimating possibilities of telescopes (Fig. 1, Table 3), it is necessary to note that the telescopes of rather small sizes (D = 0.4m-0.6m), equipped with modern equipment, have found their niche in topical direction of near-Earth astronomy such as observations of solar system bodies and near-Earth objects, allowing to observe objects up to 18-20 mag with high accuracy.

The majority of instruments of professional and amateurs observatories participates in observations of the numbered minor planets. The estimation of their results based on materials of MPC is the range about $\pm 0.''1 - \pm 0.''5$[10]. Alongside with this, the observations of NEO, exoplanets, trans-neptunian objects, educational programs, world-sky patrol and all-sky survey, service observations under the various astronomical and applied programs are carried out with the large ground-based telescope [12].

3. INTERFEROMETRY COMPLEXES FOR GROUND-BASED OPTICAL ASTROMETRY

New possibility of accuracy increase in positional astronomy has recently appeared on the base of optical interferometry application for the solution of astrophysical tasks.

Table 4. Interferometry complexes for ground-based optical astrometry

Telescopes (D, F)	**Location**	**Base number and lengh (m)**	**Program, Declination zone (^{o})**	**Mag., spectral band-pass**	**Position accuracy (mas)**	**Position**
MARK-III Interferometr (D0.08m)	Mt. Wilson, USA	3, 3-31m	astrometric, double stars, $+15^o$- $+65^o$	5	6-10, 2 (double stars)	1986-92 [17]
NPOI - I (D 0.5m) NPOI - II (D 0.5m)	USNO, Flagstaff, USA	4, 19-38m 6, 2-437m	astrometric, $-30^o \div +90^o$ imaging, double stars	10, 0.45÷ 0.85mkm	1 0.5	active since 1998, $[18-21]$
VLTI (D 8.2m)	ESO, Cerro Paranal, Chile	4, 130m 8, 8-202m	imaging, micro-arc-second astrometry	18-20, 0.45÷1.2 mkm	1-0.01	active since 2003, $[22-24]$
KIIA (D 10m)	Mauna Kea, Hawaii, USA	2, 85 6, 165	imaging, solar system objects	19-21, 1.5÷5 mkm	3-0.03	active since 2002, Since 2005 for 6 bases

At the beginning of 1990es, on the base of MARK-III in USNO, more perfect interferometry complex NPOI (Navy Prototype Optical Interferometer) was created. NPOI-I, intended for the solution of astrometric tasks, consists of four tubes with mirror diameters of 0.5 meters and variable base of 19-38 meters, vacuum delay lines (DL), laser measuring system for the control of DL, necessary optical and mechanical systems, and recording devices. Interferometer is completely automated. Observations of stars up to 10 mag were begun in 1996 with NPOI-I on the program of creation of co-ordinate system of bright stars with mas accuracy [18]. IAU congress in Kyoto (1997) was informed about positional accuracy of stars with NPOI at the level of 1 mas for both co-ordinates [19]. As a whole, ground-based optical interferometer NPOI as one of the largest long-based interferometers is the most developed instrument for precise wide field observations (under thorough account of atmosphere influence, base metrology control and other instrumental parameters) [20,21].

The development of optical fibre communication lines has resulted in creation of interferometry complexes, including large telescopes with diameters of mirrors up to 8 meters and bases up to 200 meters (KIIA, VLTI etc.) [22,23]. Though the main tasks of such complexes lie in the field of astrophysical researches (while forming the images of the observed objects), the unique possibilities are opened in the field of positional determinations for ground-based astrometry such as search and research of faint satellites of planets, new objects of solar system, new planetary systems in vicinities of the nearest stars, detection of microlensing objects, study of single stars, double, and multiple star systems etc.

VLTI includes four telescopes with mirrors of 8.2 meters and a base of 57-130 meters. There is a possibility to include in its structure two telescopes with mirrors of 1.8 meters to increase the base up to 202 meters. The precise measuring system VLTI - PRIMA (Phase-Referenced Imaging and Microarcsecond Astrometry) makes it possible to measure relative angular positions of stars up to 18 mag with accuracy of 10 microarcseconds at angular distances up to $10''$ and interferometry time about 30 minutes. Such accuracy allows to find out planets like Jupiter on distance up to 240 parsec from the central star, like Uranium up to 44 parsec, and planets with mass ten times larger than Earth, on the distance up to 1.5 parsec from the central star [24].
Six large telescopes, located on Hawaii (Mauna Kea), in one of the best astroclimate places on the Earth, including Keck I and Keck II, form a unique interferometry complex with fifteen variable bases from 85 to 165 meters. In a differential mode, it is possible to achieve an accuracy of 30 mas for objects up to 21 mag under exposition about one hour. Among main scientific tasks of Keck interferometer, it is necessary to note the study of new planetary systems in vicinities of one hundred nearest stars under the program NASA- TOPS (Towards Other Planetary systems). Marking importance of scientific potential of such huge interferometry complex for astrophysics of the 21st century, its high angular resolution at a microarcsec level will allow us to solve astrometric tasks at the same time as well.

While estimating the possibilities of ground-based optical interferometers, it is possible to speak about limited accuracy of positional determinations about 1 mas for wide angular distances, and with the use of large interferometers with the narrow field, the limit can be removed up to 0.1-0.01 mas [24,25].

4. CONCLUSIONS

• Technical possibilities of modern ground-based optical astrometry can provide an accuracy of astrometric parameters about 20-30 mas for significant number of stars up to 18-23 mag.
• Taking into account accuracy of optical interferometers at the level 0.1-0.01 mas, it is possible to hope that ground-based optical astrometry will be necessary as an observational base for preparation and maintenance of solution of the selected astrometric programs, especially before the future space projects.
• As to the means of control and research of solar system bodies and near-Earth space objects, it is possible to say that the progress in a new direction - near-Earth astronomy has confirmed efficiency of significant number of small telescopes, equipped with the modern instrument set, along with the large telescopes.
• Also we should note that the modern level of computer facilities, telecommunications, and computer science allows us to carry out association of the distributed astronomical resources (digital archives, databases etc.), containing billions of objects on the whole celestial sphere with high resolution, virtually in all ranges of waves from gamma-rays to radio. This source of information can be available basically to any researcher by means of "the virtual telescope", equivalent to some physical telescope located on the Earth or in space. Interactive archives can be considered as astronomical virtual observatory for the solution of a number of astronomical tasks, including astrometrical ones. It is possible to expect a usage of virtual telescopes in ground-based astrometry in the future. Also, large perspectives will be proposed by Extremely Large Telescopes (ELT) [26].

In conclusion, it is to be noted that many researches of modern ground-based optical astrometry are made with the space means and meathods in all-spectral range. Astrometry over all-spectral range will be assential part of all astrometry [25,27-29]

5. REFERENCES

1. Stone R.C., Dahn C.C. 1995. Astronomical and Astrophisical Objectives of Sub-Milliarcsecond Optical Astrometry. Dordrecht. Kluwer, 3.
2. Pan X.P., Kulkarni H., Shao M., Colavita M.M. 1995. Astronomical and Astrophisical Objectives of Sub-Milliarcsecond Optical Astrometry. Dordrecht. Kluwer, pp.13-18.
3. Zacharias N., 1996. Publications of the Astronomical Society of the Pacific. V.108, 1135.
4. Gunn J.E., Knapp R.R., 1993, Sky Surveys, V.43, 267.
5. Zacharias N., 1997. Astrometric quality of the USNO CCD astrograph (UCA), AJ,V.113, N5, pp.1925-1932.
6. Zacharias N., Rafferty T.J., Urban T.J., Zacharias M.I., Wycoff G.L., 2000, The UCAC as Input Catalog for FAME, Towards models and Constants for Sub-microarcsecond Astrometry, Ed. by K.J. Johnston, D.D.McCarthy, B.J.Luzum, G.H.Kaplan, USNO, USA, 80.
7. Sakhibullin NA., Aslan Z. et al, 2002, First observational Programs at the telescope AZT-22 in Turkey, in: Proceedings of the international conference "International Collaboration in Astronomy: State and Perspectivs", May25-June2, Moscow, Astronomical&Asrtrophysical Transactions(in print).
8. Arnaboldi, Capaccioli m., Mancini D., Rafanelli P., Scaramella R., Sedmak G., Vettolani G.P. 1998, VLT Survey Telescope, Messenger N93, Sept., pp.30-35.
9. Subaru Telescope, 1997, Prospect, NAO of Japan, Kyoto, IAU 23.
10. Bykov O.P., Ismailov I.S., L'vov V.N. and Sumzina N.K., 2001, Accuracy of positional observations of numbered minor Planets during 2000, In."Near-Earth astronomy of the XXI century", Proceedings of Conference, Zvenigorod, 2001, May 21-25, Moscow, Geos, 199; private communications from O.P.Bykov in 2001,2002.
11. Bykov O.P., L'vov V.N., 2000, Astrometric Accuracyof the Koiper Belt asteroids observations with the large ground-based telescopes, SPIE's international Symposium on "Astronomical Telescopes and Instrumentation 2000".
12. Abalakin V.K., Bykov O.P., L'vov V.N., 2000, Role of the large ground-based telescopes in miner planets research, SPIE's international Symposium on "Astronomical Telescopes and Instrumentation 2000".
13. http://www.ast.cam.ac.uk/˜dwe/AstSurv, http://www.uni-sw.gwdg.de/˜hessman/MONET/links.html.
14. Technical Report on Space Debris, Text of the Report adopted by the Scientific and Technical Subcommittee of the United Nation Committee on the Peacefull uses of Outer Space, United Nations, New York,1999, pp.1-43.
15. Rykhlova L. et al, 2001, In " Extention and Connection of reference Frames using CCD ground-based Technique", G.Pinigin (ed), Atoll, Nikolaev, pp.161-170; private communications in 2000-2002.
16. Agapov V.M., 2001, In:"Near-Earth astronomy of the XXI century", Proceedings of Conference, Zvenigorod, 2001, May 21-25, Moscow, Geos; private communications in 2001.
17. Shao M., Colavita M.M., Hines B.E.,Hershey J.L, Hughes J.A., Hitter D.J., Kaplan G.H., Johnston K.J., Mazurkewich D., Simon R.S., Pan X.P. The Mark III stellar interferometer. Astron. Astroph., 1988, V.193, pp.357-371.
18. Weiler K.W., Johnston K.J., Mozurkewich D. et all., 1991. The NRL/USNO Optical Interferometer Project (OIP), In Proceedings of ESO conference on "High-resolution Imaging by Interferometry II", 15-18 Oct.1991,Carching, Germany, ed. by J.M.Beckers and F.Makle, pp.757-763.
19. Hutter D.F.,Elias N.M., Hummel C.A. 1998, First astrometric results from the NPOI, In

Proceedings of ESO conference 1998, Garching, Germany.
20. Hutter D.F., 2000, The Accuracy of Ground-based Optical Interferometer Observation, In: "Towards models and Constants for Sub-microarcsecond Astrometry", Ed. by K.J. Johnston, D.D.McCarthy, B.J.Luzum, G.H.Kaplan, USNO, USA, 47.
21. Hummel C.A., 2000, The Practice of Interferometry with NPOI, In: SPIE's international Symposium on "Astronomical Telescopes and Instrumentation 2000".
22. Mariotti M. J., Coude de Foristo V., Perrin G., Zhao Peigion, Lena P., 1996, Interferometric Connection of large Ground-based telescopes, Astron. Astrophys. Suppl. Ser. 116, 381.
23. Beckers J.M., 1997, Techniques for High angular resolution , In: "Instrumentation for large Telescopes", ed. by J.M.Rodriguez Espinosa, A. Herrero and F. Sanchez, Instituto de Astrophysica de Canaries, Tenerife, Spain, pp. 1-33.
24. Delplanske F., Leveque S., Kervella P., Glindemann A., d'Arcio L., 2000, Phase-referenced imaging and micro-arcsecond astrometry with the VLTI. In: SPIE's international Symposium on "Astronomical Telescopes and Instrumentation 2000".
25. Kovalevsky J., 1999. The next decade: a new boost to Astrometry?, In: Journees 1999 and IX Lohrmann-Kolloquium, Dresden 13-15 Sept. pp.103-110.
26. Proceedings of SPIE's international conference on "Astronomical Telescopes and Instrumentation 2000", - "Future Giant Telescopes", 22-28 August 2002, Hawaii, USA.
27. Gnedin Yu.N., 2000, Astrometry in non-optical spectral range. In Proceedings of Conference: "Astrometry, Geodynamics and Celestial Mechanics before XXI Century", 19-23 June 2000, IAA RAS, Petersburg (russian).
28. Vityazev, V.V., 2001, In."Astrometry and Celestial Mechanics", Petersburg, 2001, pp.93-101 (russian).
29. Seidelman P.K., 1997, Astrometry in the Future, In: "Celestial Mechanics and Dynamical Astronomy", 66, pp.97-106.

PRELIMINARY TESTS FOR CCD OBSERVATIONS OF MUTUAL PHENOMENA IN BUCHAREST

R. POPESCU, P. POPESCU, P. PARASCHIV
Astronomical Institute of the Romanian Academy
Str. Cuţitul de Argint 5, RO-752121
e-mail: pradu@aira.astro.ro, petre@aira.astro.ro, paras@aira.astro.ro

ABSTRACT. In the next observation campaign of mutual phenomena of Jupiter satellites, a Meade telescope with CCD will be used beside the other instruments already in function at Bucharest Observatory.The installation of the instrument began with different tests performed with the CCD camera. That includes laboratory tests, observations of stars and of planetary satellites. Different image acquisition and data storage software were used.

1.INTRODUCTION

1.1 Observations with small instruments

The occultation of Galilean satellites is easy to observe even with small telescopes (whose diameter is under 20"), because they are bright enough (mv ¡ 5), and the light flux acquired by the instrument during the event is sufficient for detection.

On the other hand, rapid observations performed with small instruments and sensitive CCD cameras avoid the image degradation due to atmospheric turbulence.In our case, the used telescope is a 10" f/10 Meade LX50. It is very bright despite its small aperture.

1.2 Characteristics of the used CCD

The CCD camera adapted to telescope for this purpose is a Mintron MTV12V1-Ex, acquired from Lechner TV. The chip is a 1/2" - line transfer SONY with 795x596 picture elements, very sensitive: 0.01 lux typical and 0.0001 lux in star light mode(126 frames added in 2.5 seconds).

Because of the great transfer rate of images, it is possible to build up the light curve of observed phenomenon, even in a short period of time (60 -100seconds).

1.3 The acquisition system

As we can see in figure 1, the whole system consist in:

- Telescope + CCD camera + computer;
- Time signals (UTC) obtained by time GPS receiver;

- PCI frame grabber +software
- Time acquisition card (CHRONO) +software ;

  Fig.1: The acquisition system

1.4 Filters used in observations

For long exposures, greater than 1second of time, it is necessary to be used filters, in order to avoid saturation. In our case, the presence of filter vas not necessary, because of short exposure times. With MTV12V1-Ex, at 0.04 seconds exposure time, both Jupiter and satellites can be easily detected.

However, in next future, we intend to introduce R filters to decrease the brightness of the sky.

1.5 Accurate timing of observation

The technical notes recommend that the observation be correctly related to the UT. The accepted error cans be estimated at 0.1- 0.2 seconds of time. That task is easy to accomplish, by correlating the computer intern clock with accurate UTC time signals received from a GPS. The correlation is done through a time acquisition card. The accuracy of acquired time signal is less than 1 ms.

2. OBSERVATIONS

2.1 The acquisition software

There have been used different software packages. Because the frame grabber is designed upon the BT878 chipset, all of them have to be compatible with VFW driver

2.2 The reduction software

Because the main goal of this kind of observations is the modeling of light curve, we tried some photometry software packages.

Preliminary studies were performed with Iris(Buil 2002), that seems to be good enough for our purposes.

References

[1] Buil, C., 2002: www.astrosurf.com/buil/us/iris/iris/htm,

[2] BT848 info sheet,

[3] PHEMU, 2002: Notes techniques1,3,

[4] MintronTV, 2002: MTV12V1-Technical notes

[5] VFW-development kit

CONDITIONS OF POSSIBLE PROGRAMS USING SMALL AND MEDIUM SIZE GROUND-BASED ASTROMETRIC INSTRUMENTS

J. KOVALEVSKY
OCA/CERGA,
Avenue Copernic, 06130 Grasse (France)
e-mail: kovalevsky@obs-azur.fr

ABSTRACT. The post-Hipparcos era has brought some uncertainty on the future of ground based astrometry. However, the discussions that were initiated by the IAU Working Group on future development of ground-based astrometry, showed that there are a number of fields that will not be satisfactorily covered by space astrometry. The instruments that could be used are shortly described. Then the complementarity of ground-based and space astrometry is discussed. The papers presented at this very session confirm the point of view that, with minor modifications and improvement of existing instruments, many sound scientific programs can be undertaken. The principal domains in which major scientific inputs are expected from ground-based astrometry concern the dynamics of minor planets and satellites, the shape of the Sun, double stars, kinematics within stellar clusters, and radiosource optical counterparts. In addition, the use of some small telescopes for monitoring long period irregular variable stars could be a useful reconversion of astrometric activity. Most of these programs require international cooperation to ensure sky coverage and extension in time. Some possible projects in these fields have been presented, but the Working Group cannot manage such programs. Its objective is to help organizing them and to encourage people to join them. An important point concerning these programs is that all the participants should have a reward in their work in terms of publications.

1. WHAT IS THE PROBLEM ?

In face of the remarkable progress already achieved and even more fantastic progress in astrometry that is expected, what is it reasonable to anticipate in terms of useful contributions of ground-based astrometry in the next ten-twenty years? More generally, what contribution to astronomy can still bring small and medium-size instruments in collecting fundamental data and providing new observational results? What techniques will remain competitive? These questions arose many years ago, when it became certain that astrometry from space will be carried out. At that time, there were worries in some people's minds and diverging views (Tucker and Teleki, 1978). Later, when the achievements of Hipparcos and the Hubble Space Telescope were well established, it appeared that there was still room for Earth-based astrometry in many domains of research (Kovalevsky, 1991).

But now that an additional jump of two or three orders of magnitude in accuracy is expected from SIM and GAIA (see Mignard and Kovalevsky in this volume), the same questions are

again in the minds of many directors of observatories who want to participate to the scientific adventure but cannot afford installing new expensive instruments. But, as this will be shown, there is a large amount of observations that will not be done by large telescopes or space missions, and that are very important, provided that some simple not expensive arrangements are made. First answers were given recently by Stavinschi (2001) giving several reasons for continuing work on ground. In this context, the IAU, during its XXI-st General Assembly in 2000, created a Working Group to consider this problem and propose programs and any other action to help observatories to enter efficiently in the new environment. This paper describes the present state of the thoughts in the Working Group.

2. THE IAU WORKING GROUP

The IAU Working Group on future developments in ground-based astrometry was established by the IAU under the co-chairmanship of M. Stavinschi and J. Kovalevsky with the three following main objectives

1. To identify scientifically important observations that can be made with astrometric or other astronomical instruments, and that can provide data of interest to the study of the Solar System, stars, or the Galaxy, and that cannot be performed as well by space techniques.

2. To suggest possible modifications, upgrading, or additions to these instruments that would allow them to perform such observations and provide useful information with adequate accuracy, keeping in mind what future space missions will contribute to.

3. To promote the organization of international cooperative undertakings with the objective to perform observing programs, that would correspond to the above description.

The Working Group exchanged views by correspondence, and some of its members met twice. There was also an open joint discussion at the JENAM 2001 meeting in Dresden. Although the conclusions will be finalized for the 2003 IAU General Assembly in Sydney, it is already possible to give the main features of what will be presented there.

3. THE INSTRUMENTS

Let us first see what techniques are now available for ground-based observations and could be used in order to play its part in the general progress of astronomy.

The most striking advance in astrometric techniques is the outbreak of CCDs into all branches of astronomy. The dimensions of CCD chips, which were for a long time limited to 800×800, have raised to much larger dimensions. Systems with 4096×4096 pixels are now available. The read-out capabilities are also being extended with the availability of very fast compact data processors and computers. This trend is extended by arranging CCDs in mosaics. They have a very high sensitivity, so they are, in practice, the closest to a perfect detector in astronomy. In addition, the possibility to control the speed of charge transfer adds a new flexibility to their use (scan mode).

Another striking example of the progress that is now currently available at the focus of 1 meter class telescopes is speckle interferometry. The theory of speckles (Korf, 1973) shows that each individual speckle, which is a distorted interferometric pattern contains all the angular information that tha telescope could provide if it were in a perfect environment. The pattern changes with a period of a few hundredth of a second, so that the successive views are uncorrelated. A speckle interferometer consists essentially of an electronic receiver at the focus of a

telescope with a focal extension giving focal ratios of 300-500, which registers in a few milliseconds on a CCD, all the details of the image consisting of speckles. The successive images are combined by a computer. Then, the autocorrelation function is determined or, if one works in the Fourier space, its Fourier transform. The result is added to analogous results obtained in successive CCD frames, the final analysis being done on the mean of the computed functions. Images of double stars are obtained with sub-milliarcsecond accuracies. See also, Kovalevsky (2002).

Although photometers are essentially used for the determination of the apparent brightness of stars, they have also important astrometric applications for instance for the observation of eclipses and occultations. It could be a good use of small telescopes to be dedicated to single or, better, multi-channel photometry because, in addition to astrometric applications, there are plenty of important programs related to variable stars. And, for completeness, let us mention specific instruments for special objectives like the solar astrolabe or CORAVEL-type spectroscopic instruments. However, they are rather expensive and difficult to calibrate.

4. SPACE AND GROUND-BASED ASTROMETRY COMPLEMENTARITY

The role of the ground-based astrometry in the future must be considered in the light of the expected results of the space astrometry missions. Potential accuracies and high magnitudes that will be reached are such that there is no way to compete with them from the ground. Hence, the role of ground-based astrometry is to complement these observations in those domains where they do not contribute at all, or at least insufficiently.

One may list the main deficiencies of space astrometry missions as follows:

1. *They are not flexible.* In the case of Hipparcos and GAIA, once the scanning law is initialized, one may know in advance when a given spot on the sky will be observed. At any other time, this spot will not be observed. In the case of SIM or the HST, there are possibilities to observe a phenomenon at any time, but the flexibility is still very limited.

2. *They are not designed for monitoring.* Even for a steerable instrument like HST or SIM, the large number of users does not permit systematic continuous observations of a given body.

3. *They have a limited lifetime.* Even if a variable feature has a sufficiently dense observation record, other means must be deployed to continue the observations after the end of the mission.

4. *They cannot observe every type of object.* The Sun is an example (though the projected satellite COROT will determine its shape and diameter), but it is also the case of very crowded portions of the sky in which even GAIA will not be able to separate or identify stars. Astrometric positions of comets, large planets and their faint satellites are also out of the reach of the projected space astrometry missions.

On the contrary, ground-based astrometry programs may be set to monitor, if necessary indefinitely, an evolving feature at any given periodicity. They have the flexibility to observe transient phenomena and all types of suddenly appearing objects such as novæ, bursts, comets, etc... These considerations lead to the following open list of objectives for ground-based astrometry. Let us consider them in the next sections.

5. THE SOLAR SYSTEM

The main objective of astrometric observations of bodies in the Solar system is to provide

data for the improvement of our knowledge and understanding of the dynamical behavior of its components. Several types of programs contribute to this goal, all of which cannot be properly accomplished by space missions.

5.1.*Minor planets*

The most important objectives for astrometric position determination are the following:

- Observations of minor planets used to determine planetary masses. This requires the observation of both the perturbing and the perturbed planets during long intervals of time, so that the effect on the orbits become sizeable. The largest is the time interval, the better are the uncertainties of the determination.
- Observations of identified minor planets whose orbits have interesting features for Celestial Mechanics such as chaotic behavior, resonant orbits, etc...
- Systematic observations of Earth's grazing objects for which it is necessary to update frequently the orbits.
- Observation of objects of special interest such as comets or objectives of space probes.
- Bulk observation of newly discovered objects in order to determine a sufficiently good orbit so as to recognize them at further oppositions.
- If a sufficiently large telescope is available, the positions of objects in the Kuiper belt are necessary to determine or improve their orbits.

The common characteristics of these observations is that they have either to be carried out during a long time, or in special occasions. Both requirements do not fit in space astrometric programs, even if, occasionally, they may produce useful data.

Another important activity is the observation of the occultation of stars by a minor planet. One needs several photometers spread in latitude and coupled with accurate time determinations. The goal is to determine the length of several planetary arcs from the duration of the occultation. Very accurate ephemerides of the planet are required to forecast the geographic position of the photometers, and this means preliminary accurate astrometric observations of the planet.

5.2. *Satellites*

The main objective of the observations of natural satellites is to improve their orbits. In addition to the specific interest for Celestial Mechanics (resonances, high inclinations or eccentricities), many are objectives of planetary space probes, which require very accurate ephemerides. There are two types of observations:

1. Photometric observations of occultations, eclipses and mutual events of the quasi-equatorial satellites of Jupiter and Saturn.
2. CCD observations of the relative positions of satellites with a mask to dim the high luminosity of the planet.

None of these observations is expected to be performed from space.

5.3.*Solar diameter and shape*

The observations of solar diameter by solar astrolabes have shown variations that are not well understood and are unpredictable. It is therefore essential to continue to have an organized

net of instruments in both northern and southern hemispheres to monitor them throughout the years.

6. STARS

Space astrometry missions are optimized for the determination of positions, proper motions, and parllaxes of stars. Now that SIM, and especially GAIA are approved missions, there is no sense to have ground-based observing programs to obtain these parameters. The exception may be using a very large specialized instruments like the 61-inch Flagstaff astrometric telescope for faint stars, but even there, the Hipparcos accuracy is very difficult to reach. So, one should forget about such ground-based stellar astrometry programs. On the other hand, GAIA also collects photometric and double star data, but these observations are limited to the life-time of the mission, and this may not be sufficient. In this case, ground-based observations are necessary to complement them.

1. *Double stars.* For separated double stars, the determination of the orbital elements is, in general, impossible using only four or five years of observations. During the mission, Hipparcos and GAIA provide very good values of the separation, of the position angle, and of the magnitudes for large classes of binaries. But whenever the time span is too short, it is necessary to complete them with observations made over a longer time. Even if they are not as precise, the time factor plays such a role, that the contribution of the latter is comparable in weight and provides the necessary diversity of equations of condition.

   For close binaries, speckle interferometry is the ideal technique, as shown by the excellent results obtained by several groups (Mason et al., 2002). However, the large number of such stars and their potential for mass determination call for more instruments devoted to speckle interferometry.

   It is to be noted that astrometric observations alone do not permit the actual determination of the masses, but only some conditions on masses. In addition, one must determine the absolute motion of each component together with the parallax. For such a program, a long focus telescope is necessary. Another issue is to measure the radial velocity of each component. In this case, one needs a high dispersion spectrograph, but not necessarily a large telescope: there are still very many bright double stars with good orbits, but with unknown masses.

2. *Stellar diameters.* The apparent dimension of stars is another parameter that is known for a very limited number of stars. If the most efficient technique is stellar interferometry, either fromthe ground, or with SIM, one may also use speckle interferometry. But the most accessible method to small telescopes is the photometric observation of occultations by the dark limb of the Moon. It is to be noted that to get astrophysically significant results, it is advisable to observe them in three different colors, including near infra-red.

3. *Variable stars.* The GAIA mission will provide individual multi-color data for variable stars. As i was the case for Hipparcos, this is sufficient to describe fully the periodic variables (Cepheids, eclipsing binaries, RR Lyræ, etc..). But long periodic, semi-periodic, and irregular variables, novæ, burst stars must be observed either systematically or when they are active. This is again a perfect objective or ground-based small or medium-size instruments.

4. *Stellar systems.* As said above, it is a domain in which space astrometry cannot be challenged. There is, however, one exception: in very densely crowded fields, the GAIA

images will overlap, and will not be properly separated. Confusion will arise when the same field is projected on different reference great circles. So, using CCD speckle images on long focus instruments, it may be possible to recognize individual stars and determine proper motions within globular clusters or other highly populated areas of the Galaxy.

5. *Miscellaneous.* Identification of the optical counterparts of objects that are observed in other wavelengths: radio, microwave, and infra-red sources.

7. ORGANIZATION OF PROGRAMS

Most of the programs sketched above have in common the property that they can be performed with a part- time use of small or medium size telescopes that exist in many observatories, and are not very actively operated. They should be supplied with one or a mosaic of CCDs and/or a photometer with a few filters. This rather light and cheap equipment is sufficient to participate in several such programs.

Some of them could be undertaken in a single observatory, but in other cases, cooperation between several teams in different observatories will considerably increase their efficiency. This is already the case of the observation of the mutual events of Jupiter and Saturn satellites. Organized by J.-E. Arlot and his team, this program lasts since more than twelve years and is very successful. It is a model hat could be followed in many other instances. The IAU working Group encourages such cooperations and will support as much as possible atronomers who would wish to organize them.

An important point, however, is that all participants to a cooperative program should be rewarded by being associated to publications and, whenever feasible, to publish personalized papers. These programs, making use of small or medium size instrument, provide in addition a very good opportunity to introduce students and young astronomers to astronomical observations.

8. REFERENCES

Korf, D., 1973, J. Optical Soc. of America, **63**, 971-980

Kovalevsky, J., 1991, Astrophysics and Space Science, **177**, 457-464

Kovalevsky, J., 2002, *Modern Astrometry*, 2nd edition, Springer Verlag, Heidelberg, Berlin

Mason, B.D., Hartkopf, W.I., Urban, S.E. et al., Astron. Journal, **124**, 2254-2272

Stavinschi, M., 2001, in *Journées 2000 Systèmes de référence spatio-temporels*, N. Capitaine (Ed.), 48-52

Tucker, R.H. and Teleki, G., 1978, in *Modern Astrometry*, IAU Colloquium 48, F.V. Prochazka and R.H. Tucker (Eds.), Vienna University Publication, Vienna, 545-556

RADIO STRUCTURE EFFECTS ON THE OPTICAL AND RADIO REPRESENTATIONS OF THE ICRF

A. H. ANDREI [1,*] D.N. da SILVA NETO [2], M. ASSAFIN [1,3], R. VIEIRA MARTINS [1]

1- GEA-Observatório do Valongo/UFRJ- Observatório Nacional/MCT
R. Gal. José Cristino, 77, Rio de Janeiro, Brasil
2- Observatório Nacional/MCT
3- Observatório do Valongo/UFRJ

*e-mail: oat1@on.br

ABSTRACT.

Silva Neto et al. (SNAAVM: 2002) show that comparing the ICRF Ext1 sources standard radio position (Ma et al., 1998) against their optical counterpart position (ZZHJVW: Zacharias et al., 1999; USNO A2.0: Monet et al., 1998), a systematic pattern appears, which depends on the radio structure index (Fey and Charlot, 2000). The optical to radio offsets produce a distribution suggestive of a coincidence of the optical and radio centroids worse for the radio extended than for the radio compact sources. On average, the coincidence between the optical and radio centroids is found 7.9 ± 1.1 mas smaller for the compact than for the extended sources.

Such an effect is reasonably large, and certainly much too large to be due to errors on the VLBI radio position. On the other hand, it is too small to be accounted to the errors on the optical position, which moreover should be independent from the radio structure. Thus, other than a true pattern of centroids non-coincidence, the remaining explanation is of a hazard result. This paper summarizes the several statistical tests used to discard the hazard explanation.

1. STATISTICAL TESTS

The main data set used in SNAAVM analysis comprises 234 ICRF sources, with measured radio structure index, for which ZZHJVW determined the optical counterpart position, at the level of 50mas. There are 127 compact sources and 107 extended sources. Most of them (177) lie in the northern sky, while the division between defining (94) and non-defining (140) is more even. The method used for the analysis is to compare the averages of the optical and radio arclength difference distributions (Li and Jin, 1995) for the extended and compact sources subsets. As an optically independent sample, there are 288 ICRF sources in the A2.0 catalogue, to a 220mas precision level, for which the radio structure index is known. Again, most of them are northern sources and the defining to non-defining sources proportion is even enough. One third of this sample does not belong in the ZZHJVW sample. Finally, the RORF (Johnston et al., 1995) radio positions list, although highly redundant with the ICRF positions, is also used, as the only choice for a radio to radio positions comparison.

On Tables 2, 3, and 4 of SNAAVM, the arclength method is applied for the distributions produced by the ZZHJVW and A2.0 lists, without or with different weighting schemes, giving allways rise to larger averages for the extended sources subsamples. Even the simple root square

differences indicate the same tendency. In the tests below, the radio to optical residuals are juggled with to verify that those results are never seen as a chance outcome.

Sky location from ZZHJVW - The optical minus radio offsets from compact sources were assigned to the extended sources, and vice-versa. **The extended to compact sources difference remains.** E-C = 10.5 ± 1.4mas (11.3 ± 1.4mas, removing 2.5σ tails)

Sky location at random - The true offsets from the compact and extended sources populations were assigned to ICRF positions draw at random. **The extended to compact sources difference remains.** E-C = 7.8 ± 1.2mas (8.8 ± 1.0mas, removing 2.5σ tails)

Fake data (Gaussian) - Fake offsets drawn from a Gaussian distribution, with same mean and standard deviation as the real offsets distribution, were assigned to the actual compact and extended sources. **The extended to compact sources difference vanishes.** E-C = 0.3 ± 0.9mas (0.1 ± 0.6mas, removing 2.5σ tails)

Fake data (Random) - Fake random offsets, varying between ±10 and ±30 mas, were assigned to the actual compact and extended sources. **The extended to compact sources difference shows up.** E-C = 7.5 ± 0.9mas (8.2 ± 0.6mas, removing 2.5σ tails)

Changing categories - Standard arc length procedures applied to the defining and non-defining sources, instead of to the compact sources and extended sources. **The difference vanishes.** ND-D = 1.0 ± 0.9mas

Segregation (Non-Defining Sources) - Standard arc length procedures applied for the non-defining sources only (66 compact sources and 74 extended sources). **The extended to compact sources difference remains.** E-C = 7.3 ± 1.8mas

Segregation (Defining Sources) - Standard arc length procedures applied for the defining sources only (limited in scope, since there are 61 compact sources, but only 33 extended sources). **The extended to compact sources difference remains.** E-C = 7.3 ± 3.2mas

The same tests applied to the USNO A2.0 sources distribution show equivalent results.

Optical to optical - Standard arc length procedures applied, using the ZZHJVW and the USNO A2.0 positions. **The difference vanishes.** E-C = 2.6 ± 3.8mas

Radio to radio - Standard arc length procedures applied, using the ICRF and the RORF positions **The difference vanishes.** E-C = 0.6 ± 1.1mas

3. REFERENCES

Fey, A.L. & Charlot, P., 2000, ApJS, 128, 17

Johnston, K.J., Fey, A.L., Zacharias, N., Russel, J.L., Ma, C., de Vegt, C., Reynolds, J.E., Jauncey, D.L., Archinal, B.A., Carter, M.S., Corbin, T.E., Eubanks, T.M., Florkowski, D.R., Hall, D.M., McCarthy, D.D., McCulloch, P.M., King, E.A., Nicolson, G. & Shaffer, D.B., 1995, AJ, 110, 880

Li, J.L. & Jin, W.J., 1995, A&A, 303, 276

Ma, C., Arias, E. F., Eubanks, T. M., Fey, A. L., Gontier, A.-M., Jacobs, C. S., Sovers, O. J., Archinal, B. A. & Charlot, P., 1998, AJ, 116, 516

Monet, D. G., Bird, A., Canzian, B., Dahn, C., Guetter, H., Harris, H., Henden, A., Levine, S., Luginbuhl, C. Monet, A.K.B., Rhodes, A., Riepe, B., Sell, S., Stone, R., Vrba, F. & Walker, R., 1998, USNO-A2.0 (Washington: US Naval Obs.)

da Silva Neto, D.N., Andrei, A.H., Vieira Martins, R. & Assafin, M., 2002, AJ, 124, 612

Zacharias, N., Zacharias, M.I., Hall D.M., Johnston, K.J., de Veget, C. & Winter, L., 1999, AJ, 118, 2511

KYIV MERIDIAN AXIAL TELESCOPE OBSERVATIONAL PROGRAMS: FIRST RESULTS

Yu. BABENKO[1], P. LAZORENKO[2], O. VERTYPOLOKH[1], V. KARBOVSKY[2], V. ANDRUK[2], S. KASJAN[1], M. BUROMSKY[1], O. DENISYUK[2]

[1])Astronomical Observatory of the Kyiv National University
Observatorna 3, 04053 Kyiv-53, Ukraine
e-mail: babenko@observ.univ.kiev.ua
[2])Main Astronomical Observatory, National Academy of Sciences of Ukraine
Zabolotnogo 27, 03680 Kyiv-127, Ukraine
e-mail:laz@mao.kiev.ua

ABSTRACT. We present first results of the modernization of the meridian axial circle (MAC) in Kyiv which was accomplished by means of a new CCD micrometer installation. The micrometer was designed by the Observatory of the National Academy of Sciences, the Kyiv University Observatory, and in collaboration with the Mykolaiv Observatory. The MAC (Scoryk et al., 1989) is a meridian refractor (D=180 mm, F=2.3 m) located 10 km from the centre of Kyiv (Ukraine). Now the instrument is used for observations of star fields in the direction of ICRF objects and for the equatorial zone astrometric survey.

1. THE INSTRUMENT DESCRIPTION

The new micrometer is based on a front-illuminated CCD Silar ISD017AP with 1040x1160 pixels. At a 16 mkm pixel size and a scale of $1.394''$ per pixel, the CCD covers a $24.2'$ wide strip in declination. The exposure, or the time interval during which equatorial stars cross a matrix, is about 108 sec. The electric signal from the CCD after amplification is conversed to a 12-bit digital form. The dark current is 6 e^-/pk/sec, and the readout noise 20 e^-. A two-stage thermo-battery ensures cooling of the chip to 40^0 below the ambient air temperature. Electronics supports scan mode of observations.

To standardize instrumental photometric system, a glass filter with a passband of 480-580 nm reproducing a Johnson V filter is used. The brightest images detected with no pixel saturation correspond to stars of 11 mag (V), and the limiting magnitude is about 16 mag (V). At $0^0 < \delta < 30^0$ where the CCD scan distortion is small, the star images are of symmetric Gaussian shape with FWHM= 2.5 pk.

2. OBSERVING PROGRAMS

Since March 2001 we have started the program of observations of star fields with extragalactic radio-sources being the objects of the ICRF. The observational list includes 209 ICRF sources

located in declination zone of $0^0 < \delta < 30^0$ and taken from the catalogue GAOUA 99 C 03 (Molotaj, 2000). The purpose of the program is to determine positions, proper motions, magnitudes and V-R colours of faint stars in the direction of radio-sources.

A catalogue of measured astrometric and photometric data for stars to approximately 16 mag (V) will be built in 2003. Reduction to the ICRF system is made differentially, using the Tycho-2 stars as reference. About 900 strip scans of the sky each of 24.2(declinations)x46.5′ (right ascensions) size (1040x2000pk) have already been obtained, thus most of the fields have a 4-5 fold coverage.

The second observing program of the MAC is aimed at densification of the Hipparcos-Tycho reference frame and its extension to fainter magnitudes in the equatorial zone. Also, the program will provide invaluable information on astronomical events registered during observations and which may be interesting for related studies. The program will continue for a lengthy period of time and is intended to be an astrometric survey of the sky for declinations initially restricted by $0+5^0$, with a 4-fold center-to-edge overlapping of scans.

In this stage of the project, we focused largely on obtaining the observational data. Also, we permorfed a tentative analysis of the accuracy of observations with the MAC that gave satisfactory results. Computed internal errors of one observation in right ascensions and in declination as a function of magnitude are given in the table. These estimates are slightly better than those reported in (Telnyuk-Adamchuk et al., 2002) due to the improved technique of reduction.

V	σ_α	σ_δ	V	σ_α	σ_δ
10^m	$0.071''$	$0.049''$	14	0.097	0.142
11	0.052	0.047	15	0.130	0.182
12	0.039	0.069	16	0.256	0.298
13	0.078	0.075			

First observations of stars, and error estimates obtained with a CCD micrometer, allow us to conclude that the MAC may be efficiently used in a number of observing projects, in particular, to link the radio and optical reference frames. A large astrometric survey of the equatorial zone in the two photometric passbands will provide extensive astrometric and photometric data that may serve as a source of information when studying non-stationary events and moving objects. The accuracy of a single position measurement for 11-14 mag stars is $0.05 - 0.10''$, and the accuracy of photometry is 0.03-0.06 mag. At 4-5 fold overlapping of strips, the errors of the catalogue data are expected to be $0.02 - 0.05''$ for positions and 0.02-0.03 mag for magnitudes.

3. REFERENCES

Molotaj O. 2000, in *IVS 2000 General Meeting (Koetzting)*, ed. N.Vandenberg, K.Baver, NASA, Hanover, 338.

Scoryk K., Lazorenko P., et al. 1989, *Kinemat. Phys. Celest. Bodies*, 2, 79.

Telnyuk-Adamchuk V., et al. 2002, *Astron. Astrophys.*, 386, 1153.

STATISTICAL METHODS IN APPLICATION TO ASTROMETRY

M. BOUGEARD (1) (2)
(1) Université LYON.1-IGD, UFR Mathematique, 69622 Villeurbanne Cedex, France
(2) Observatoire de Paris: UMR8630, 61 av. de l'Observatoire, 75014 Paris, France
e-mail: bougeard@hpopa.obspm.fr

ABSTRACT

Various important problems in astrometry require algorithmic solutions and statistical modeling. As a matter of fact, it is known that efficient methods for small-scale problems do not necesseraly translate into efficient methods in the large-scale setting and conversely. In this contribution, we present various recent statistical methods that can be exploited when solving estimation problems. They will be examplified in different astrometrical situations.

EXPLORATORY MULTIVARIATE DATA and PROJECTION PURSUIT METHODS

Exploratory Multivariate Analysis is usually based on the hope that a part of the data is redundant. Several statistical methods could be performed and acted efficiently in this context. Introduced by Friedman and Tukey (1974), the "Projection pursuit techniques" intend to select low-dimensional orthogonal projections of the data under modeling, in order to reduce dimensionality for computational purposes. Several methods belong to such approach.

Recall that, in the family of Principal Components Methods, the index of interestingness of a selected projection is the *proportion of variance related to the projected data.* These techniques are said *essentially algebraic "second order"* methods since they are based on the *Singular Value Decomposition* (SVD) of a specific data matrix, as stated by Jones and Sibson (1987, J. Royal Stat. Soc., vol 150-1, p1-36).

In astrometry, such tools may be quite relevant in data analysis, depending on the context. To examplify each approach, we present below, different fields in which they have been applied and can work efficiently in the future.

- APPLICATION 1) *Least Squares Fit Under Multicollinearity* Observations of minor planets are of importance to determine corrections to astronomical parameters between reference frames. Due to collinearities, a direct least squares fit is potentially misleading. Based on Hipparcos minor planet data, *principal component regressions* were successfully performed. The main references are:

  Bec-Borsenberger A., Bange J.F, Bougeard M.L., 1995, Hipparcos minor planets, *Astr. Astroph, 304,p176-181*

  Bange J., Bec-Borsenberger A., Bougeard M.L., Caquineau C., 1996, Lien entre referentiel dynamique et ICRS-Hipparcos, in:*Journées Systèmes de Référence spatio-temporels 1996*

  Bougeard M.L., Bange J., Bec-Borsenberger A., 1999, Singular Statistical Analysis of astrometric measurements with application to Hipparcos Minor Planet Observations, Pulkovo ed

- APPLICATION 2) *SMART and Projection Pursuit Regression, PPR, to estimate how approximated is the use of a linear model*

  For details on this nonparametric method, for which computational efficient procedures are now available, and for an example of application to ground-based astrometrical observations, we refer to:

  Bougeard M.L., 1990, L'ajustement statistique par Directions Revelatrices. Applications en astrometrie, *Journées JRS 1990, Paris-Observatory ed.*

- APPLICATION 3) *Singular Spectrum Analysis SSA and Application to Polar Motion series*

  In the context of SSA modeling, the PCA method is adapted to lessen the effects of possible irrelevant noises in order to separate the signal into "interpretable" components. In this context, the matrix under consideration is a M-lag covariance matrix. The most difficulty is that the consistency of the selected model mainly depends on the choice of the tuning parameter M.

  For application to the determination of episodic terms in the 1999-2000 Polar motion series, the reader is referred, for instance, to the paper below and the references therein.

  Bougeard M.L., Rouveyrollis N., Gambis D., 2001, EOP-SSA deteremination of episodic terms in the 1999-2000 Polar Motion, *Journées JRS 2001, Bruxelles-Observatory ed.*

A UNIVERSAL COMPUTER PROGRAM FOR HIGH PRECISION POSITION DETERMINATION OF MINOR PLANETS ON CCD-FRAMES

R. LANGHANS
Lohrmann-Observatory Dresden
Mommsenstrasse 13, 01067 Dresden, Germany
e-mail: langhans@astro.geo.tu-dresden.de

ABSTRACT. The necessity as well as the possibility of the development of a universal computer program for high precision position determination of minor planets on CCD-frames and the concepts of realization are discussed. In Dresden we started with the development of such a universal astrometric tool. The present status of this project is reviewed. Details such as special correction methods for projection errors are presented.

1. NECESSITY

In the past a lot of programs for processing astronomical pictures have been developed. Most of these applications were designed only for special observation equipment and do not give best results when using another. Others are very hard to handle or too interactive.

There is a need for a universal tool which both professionals and amateurs can use to get the best positions of minor planets out of their CCD-frames. The task of the program is not to detect new asteroids, but to assist follow-up observations of known ones. To stand out against the other applications it should be

- suitable for most equipment (observation and processing environment),
- as non-interactive as possible,
- easy to handle,
- giving best possible results,

or short universal.

2. CONCEPTS OF UNIVERSALITY

Portable code. An important characteristic of a universal computer program is the possibility to run it on different platforms and different operating systems. The best way to fulfil this requirement is to write portable code which can be run on most computers without any modifications. The current version of the program uses C++ and follows strictly the ANSI standards. Since there is no need for a graphical user interface in a non-interactive application, the ANSI instruction set should be sufficient.

Language. It is very desirable to give statements in the users native language. Currently the program reads all statements from a simple text file that can be altered to any language.

Interfaces. Universality implies flexibility for data input and output. Open interfaces programmable by the user with the help of an intuitive language would be useful. The current program version uses open interfaces for reading from a star catalog and producing output files.

Automatic algorithms. To become non-interactive a universal program must include smart algorithms that routinely do the work the user would normally have to do. As an example, the matching of stars found on the picture and in the star catalog is done by a program routine using an algorithm described in Valdez et al. (1995).

3. CURRENT STATUS

In Dresden we started with the development of an astrometric tool that fits the requirements to a universal program. The program was designed to run in batch mode. Thus, no graphic user interface is intended.

The frame is read and if needed preprocessed (dark field, flat field etc.). There is a possibility to create or load a defect pixel mask which marks pixels with unusual behavior to not use them in the measurement process. Then the objects on the picture are extracted and their properties (elongation, approximate center etc.) are determined. Accurate positions and magnitudes of all (suitable) objects are calculated next by least squares fit of the individual object images and a modelled point spread function (PSF). There are some analytical and one empirical PSF available at present. Afterwards the frame's corresponding star catalog window is loaded. The positions of the catalog stars are reduced to their apparent places. In the next step the stars on the picture are matched with the catalog stars automatically. Afterwards the exact orientation of the picture with respect to the celestial sphere is reconstructed. For this purpose, several projections are available depending on the used telescope-camera combination and the number of catalog stars on the picture. At the end the coordinates and magnitudes of all objects which were not found in the catalog are determined and the results are put out to a data file.

4. SOME PLANNED IMPROVEMENTS

New models for spread functions. There should be elongated models of spread functions for the case when the MP appears as a short line because of its movement during the exposure.

Approximate minor planets position from number. Because it is intended to use the program for tracking known minor planets it is possible to determine the coordinates of the frame from a given more or less accurate set of orbital elements and the observation time. Then it is not necessary to supply this position as an input parameter any longer.

Color refraction. Langhans et al. (2002) showed that color refraction has to be taken into account when trying to find accurate positions. An appropriate routine should be included in the program

JAVA-GUI for setup. Although the program works in batch mode there are still some configurations to be done. To assist the user in creating the appropriate files it is desirable to have a graphic user interface in a portable manner, maybe in JAVA.

5. REFERENCES

Valdez, F.G., Campusano, L.E., Velasquez, J.D., Stetson, P.B.: 1995, PASP 107, 1119

Langhans, R., Malyuto, V., Potthoff, H.: 2002, Calculated differential color refraction confronted with observed stellar positions, Poster for Journées 2002

CALCULATED DIFFERENTIAL COLOR REFRACTION CONFRONTED WITH OBSERVED STELLAR POSITIONS

R. LANGHANS[1], V. MALYUTO[2], AND H. POTTHOFF[1]

[1] Lohrmann Observatory Dresden, Mommsenstrasse 13, 01069 Dresden, Germany
[2] Tartu Observatory, 61602 Tartumaa, Tõravere, Estonia
e-mail: langhans@astro.geo.tu-dresden.de

ABSTRACT. We compare the calculations of differential color refraction with the observed effect found in some observed stellar positions. Special observations have been performed in a selected field where there are some Tycho-2 stars with well determined spectral types (from A to M). The observations cover the wide range of zenith distances from 72° to 27°. Our analysis demonstrates that differential color effects in refraction are significant.

1. INTRODUCTION

To determine the exact positions of celestial objects relative to reference stars it is necessary to include all the displacements and motions involved in the reference system. Among them the atmospheric color refraction should be taken into account. The best source for a comparison of calculated and observed color refraction are special observations in an area where there are some stars with available color information (covering a wide range of spectral types and/or color indices) as well as exact extraterrestrial stellar positions. Such observations and their treatment in the context of color refraction are the content of the present work.

2. OBSERVATIONS

Table 1: Data of the stars under study

No.	Tycho-2	V_T	$B_T - V_T$	$B - V^*$	Sp. Type
1	TYC 2665-0058-1	9.768	0.357	0.332	A7-F0IV-V
2	TYC 2665-0096-1	11.130	0.606	0.555	F5V
3	TYC 2666-0449-1	11.124	0.338	0.313	A5V
4	TYC 3134-1985-1	10.006	0.270	0.246	A7V
5	TYC 2666-1479-1	10.256	1.854	1.545	M0III
6	TYC 2665-0098-1	9.681	2.084	1.742	M0
7	TYC 2665-0678-1	11.876	0.350	0.325	
8	TYC 3134-1746-1	12.383	1.431	1.214	

*Transformed from $B_T - V_T$ to $B - V$ of the Johnson system (Bessell 2000).

For our observations we have chosen an area centered at NGC 6791 (Fig. 1). In our area there are eight stars, whose positions and $B_T - V_T$ are available in Tycho-2 catalog. For five of

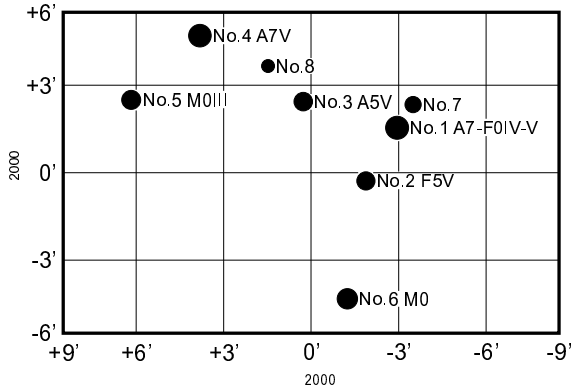

Figure 1: The star chart for the observed area ($18' \times 12'$). The center is $\alpha_{2000} = 19^h 21^m 00^s, \delta_{2000} = +37°27'00''$.

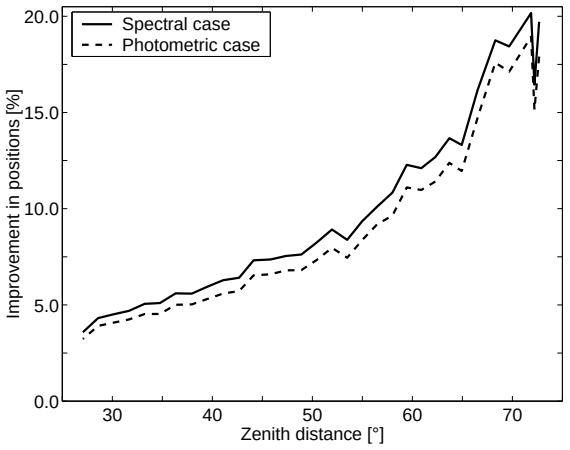

Figure 2: The positional improvement (as given in expressions 1) for spectral and photometric case, respectively, as function of the zenith distance for the area.

them there are spectral types derived from the color indices of the Vilnius photometric system (Cernis et al. 1997). For one further star (TYC 2665-0098-1) there is a spectral type (M0) in the Simbad database. All available information for the stars under study is summarized in Table 1.

We have performed our astrometric observations in Dresden during one night (April 24/25, 2001). The Meade LX200 telescope in combination with the SBIG ST-8 CCD detector leads to a frame which is $18'$ wide and $12'$ high. We started observations when the ascending area was at a zenith distance of about 72°. Then we were producing digital pictures every 10 minutes until the area reached a zenith distance of about 27°. In total we took 32 pictures. We did not use any filters. During observations we have registered the meteorological parameters: temperature, pressure and humidity.

3. DATA TREATMENT

To calculate refraction we used a computer program of Stone (1996) which was modified by Malyuto & Meinel (2000). Further modifications were carried out to be able to use the extended empirical library of energy distributions (Sviderskiene 1988) and to calculate refraction as a function of synthetic color indices ($B-V$, $V-R$ and $V-I$).

We have calculated the refraction values for every observation of the stars in Table 1. To compare different available possibilities, we distinguish two cases: (1) a photometric case where photometric color indices $B-V$ are used in the refraction calculations and (2) a spectral case where spectral types and luminosity classes are used in the refraction calculations.

Normally the refraction effects are subtracted from the observed stellar positions. However, the orientation of the CCD-matrix with respect to the celestial sphere is not known exactly from the beginning. To overcome this difficulty we modified the catalog positions by subtracting the refraction values from their calculated zenith distances. Then we determined the best transformation parameters of the observed and the modified catalog positions by least squares fit. From the residuals we calculated the standard deviation m_0.

As a result we have two values for m_0: the value $m_{0,sp}$ in the spectral case and the value $m_{0,phot}$ in the photometric case for every picture. To estimate the positional improvement in comparison with the case when there is no color information for stars, we have also calculated the value $m_{0,u}$ (when catalog coordinates are used without modifications). The improvement I in stellar positions is characterized by the following expressions (in percent for every picture):

$$I_{sp} = \left(1 - \frac{m_{0,sp}}{m_{0,u}}\right) \cdot 100, \qquad I_{phot} = \left(1 - \frac{m_{0,phot}}{m_{0,u}}\right) \cdot 100 \tag{1}$$

for the spectral and photometric case, respectively. This makes I rather independent of quality changes through the pictures series. The results are presented in Fig. 2.

4. CONCLUSIONS

Refraction calculations are necessary in order to extract accurate stellar positions from ground based observations at large zenith distances if an instrument without filters is used. The availability of broad-band indices is generally enough for accurate refraction calculations. The modified Stone refraction code will be inserted in the universal computer program for high precision position determination of minor planets on CCD frames (Langhans 2002).

5. REFERENCES

Bessell, M.S.: 2000, PASP 112, 961
Cernis, K., Bartasiute, S., Straizys, V., Janulius, R.: 1997, BaltA 6, 573
Langhans, R.: 2002, A Universal Computer Program for High Precision Position Determination of Minor Planets on CCD Frames, Poster for Journées 2002
Malyuto, V., Meinel, M.: 2000, A&AS 142, 157
Stone, R.C.: 1996, PASP 108, 1051
Sviderskiene, Z.: 1988, Bull. Viln. Astron. Obs. 35

APPLICATION OF THE "SCANNER+MIDAS" COMPLEX FOR PROCESSING ASTROMETRIC PHOTOGRAPHIC PLATES

M. POGORELTSEV, Yu. BABENKO, O. VERTYPOLOKH
Astronomical Observatory of the Kyiv National University
Observatornaya 3, 04053 Kyiv-53, Ukraine
e-mail: verto@observ.univ.kiev.ua

ABSTRACT. Researches of an opportunity of use in the astrometric purposes of the photographic plates digital images received with the scanner ScanMaker-4 manufactured by Microtec were carried out by the authors. Photographic plates with the images of star fields received with different telescopes were used for researches. The processing of digital images of photoplates was made with the ESO-MIDAS and with the programs developed by one of the authors. The researches have shown, that this technology provides results with acceptable quality level. That makes possible use of the given scanner for mass processing of the stored photographic material.

A rich observational photographic material have been saved by many observatories for many years. The processing of this material by means of modern technology will allow to take the new astrometric and photometric data. As the special measuring machines for work with photographic plates are available only on several observatories, the opportunity of use for these purposes of the film-scanner essentially would simplify and quicken this work. The scanner in such case will carry out primary operation - scanning or digitizing of photographic plates. The digital images, received after such operation, can be processed by the same means, as CCD-images.

For our researches the scanner ScanMaker-4 manufactured by Microtek was used. According to the technical description it allows scanning with optical resolution 600x1200 dpi and color depth of 36 bits. The photographic plates received within the PIRS program (Gubanov et al., 1989) of Astronomical Observatory of Kyiv National University in 1991 and the plates received on the AGK-2 program at Pulkovo Astronomical Observatory (Beljavsky, 1947) in 1929 were used for our work. PIRS photographic plates were received with the astrograph (F=426mm, size of a field - $108'$, scale - $50''$/mm) of Astronomical Observatory at Kyiv. AGK-2 plates were received with the zone astrograph (D=160 mm, F=2049 mm, working field $5^\circ \times 5^\circ$, scale - $100''$/mm) of Pulkovo Observatory.

The analysis of the received images has shown, that the accuracy of 256-color scanning is enough to reproduce a color gradient of photographic emulsion. So for scanning the color mode with 8 bits color depth was chosen. The scanning were carried out in a mode $900^\circ \times 900^\circ$ dpi. These modes were chosen specially for the given plates proceeding from resolution ability of the scanner and received scale of the electronic image. After scanning the image was kept in the tiff format (Tagged Image File Format). For the subsequent processing the image was converted in

the fits (Flexible Image Transport System) format.

The processing of the received digital images was made as follows. A search of the images of stars on a field and determination of coordinates of the centers of the star images and their photometric characteristics were performed through the ESO-MIDAS package. TYCHO-2 catalogue was chosen as a reference. The calculation of spherical coordinates α, δ was carried out with the program developed by one of the authors. Under calculations different models for astrometric reduction where used.

In our case the process of scanning consists in moving the scanning device along a plate. It was found, that the errors of definition of coordinates in a direction of CCD ruler, that is across the movement of the scanning device, are less than errors in a direction along movement of the scanning device, which reaches 2 arcsec. It makes the scanner actually one-coordinate measuring device. Thus, in order to receive both coordinates it is necessary to execute two scannings with turn of a plate by 90 degrees. In turn the scanning device consists of some CCD-rules and the specific joint error in coordinate is risen. For definition of an optimum scanning technique the multiple scannings with turn of a plate by 90, 180 and 270 degrees were executed. Finally we have chosen four-multiple scanning with subsequent turn of a plate by 90, 180 and 270 degrees. Then tool coordinates were averaged to exclude non-uniformity of movement of the scanner and to compensate discrepancy coupling of CCD-rulers. That is for reception of each coordinate only two scans were used from four ones, which orientations differ by 180 degrees. For reduction of an error splitting the plate image into zones also was executed which were scanned only by one CCD-ruler. The results for a plate received within the PIRS program are given in Table 1.

Table 1: Dependence of mean error in spherical coordinates on numbers and methods of scans

Numbers of scans (orientation)	all plate σ (stars in solution)	zone of one CCD-rule σ (stars in solution)
$1(0^\circ)$	247 (115)	205 (61)
$4(2\times 0^\circ, 2\times 180^\circ)$	205 (101)	159 (42)
$8(4\times 0^\circ, 4\times 180^\circ)$	160 (102)	120 (43)

From Table 1 it follows that mean errors decreases both with increasing of number of scans and under transition from all plate to one CCD-rule zone, reaching 120 mas. That is quite acceptable value for mass processing.

The carried out researches have shown, that use of the scanner for the astrometric purposes is quite possible. In conclusion we shall note, that it is possible to expect, that use of the scanner with the optical resolution up to 2400×2400 dpi will allow to reduce errors of definition of measured coordinates.

REFERENCES

Beljavsky S.I., 1947, Astrographic catalogue of 11322 stars between 70° North declination and North Pole., in *Transactions MAO in Pulkovo part II, volume LX (Koetzting)*, Leningrad.

Gubanov V.S., Kumkova I.I., Tel'nyuk-Adamchuk V.V. 1989, Confor: a new program for determining the Connection between radio and optical reference frames, *IAU Symp. N 141 "Inertial coordinate system on the sky". Pulkovo obs., 17-21 Oct., Leningrad, p.75.*

APPLICATION OF BLOCK-ADJUSTMENT ON EXTENDING FOV OF CCD [1]

Z. TANG (1)(2)(3), Y. YU (1)(2), J. LI (1)(2)
Ming ZHAO (1)(2), Shuhe WANG (1)(2), Wenjing JIN (1)(2)

(1) Shanghai Astronomical Observatory, Chinese Academy of Sciences
Shanghai 200030, China
(2) 2 National Astronomical Observatories, Chinese Academy of Sciences
Beijing 100021, China
(3) Purple Mountain Observatory, Chinese Academy of Sciences
Nanjing 210008, China

1. INSTRUCTION

To minimize the systematic errors caused by plate parameter variance, overlapping-plate technique was first applied to reduce plates in astrometry by Donner & Furuhjelm in 1929. This technique was usually called Block-adjustment (BA) since a block of plates were reduced together at the same time when it used. Eichhorn (1960) was the first to publish a rigorous formalism for BA. BA had been used to reduce the AC data (Eichhorn 1962-1983) and CPC plates (de Vegt, et al., 1967-1981, Zacharias, 1988) since 1960.

There are two causes that had obstructed the wide application of BA before 1990s. One is the systematic error that cannot be represented by polynomial models. The precision of the results of BA was depressed severely by such errors, which usually were caused by the defect of optics of telescopes and sometimes plate curve in Schmidt telescopes. Another is the computer capability. With positions of all stars covered by all plates and all plate parameters as unknowns, the system of normal equations was so big that it is difficult to solve without powerful computers. Except such two reasons, BA would have been used usually to construct the photographic catalogues covering all the sky.

When compared with photographic plates, CCD detectors have three advantages : higher quantum efficiency, higher linearity and greater convenience. But there is an obvious shortcoming for CCD, the field of view (FOV) of a CCD is often much smaller than that of photographic plate, especially for astrometric telescope with long focal length. It is difficult to use CCD in many research fields that need large FOV. On the other hand, small FOV of CCD implies that the influence of the defect of optics of telescope should be small, or even negligible. Along with the much smaller size, CCD doesn't suffer from the systematic error that obstructs the application of BA. At the same time, nowadays the capability of the computer is much more developed than before.

[1]Based on observations of Schmidt telescope in Xinglong Station of National Astronomical Observatories of China.

Since both problems mentioned in the second paragraph have been solved, it is natural to apply BA to reduce overlapped CCD frames together. At the same time, the FOV of the CCD will be extended to what all CCD frames covering with high precision, which will be much useful to all research fields that need large FOV. To validate the effect of BA, we used it to reduce some CCD observations, the preliminary results will be presented in next section.

2. SOME PRELIMINARY RESULTS OF THE APPLICATION OF BA

The observations were obtained from the 60/90cm Schmidt Telescope (F/3, CCD: 2048*2048, Scale: 0.015mm/pixel, FOV: 1*1). The overlapping style of CCD frames is corner-center. The exposure time for all observations was 120s. With Astrometry Calibration Region (ACR, Stone1999) as reference catalogue, all CCD frames were reduced with BA.

Results show that when compared with single CCD solution, BA can weaken the influence of positional errors of reference star, improve the results when reference stars were not distributed uniformly and obtain rather good results even when the reference stars are too insufficient to carry out single solution. The following figures show the differences between positions obtained from CCD reduction and those of ACR catalogue. In each figure, left : distribution of reference stars; center : differences of single solution; right : differences of BA solution, and the unit of (x, y) are pixel of CCD.

3. REFERENCES

Stone R., et al. 1999, AJ, 118, 2488
All references can be found in: Eichhorn H., 1988, IAU Symp.133, 177.

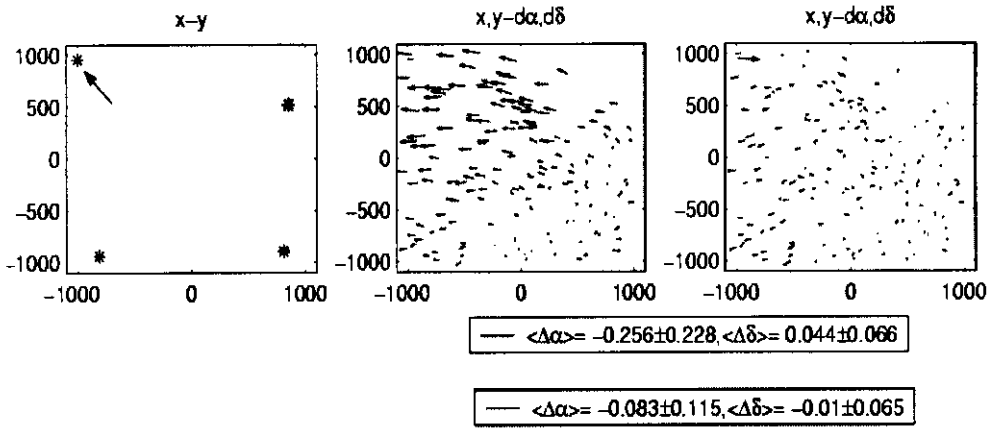

Figure 1: When R.A. of one reference star (arrow) was added 1" artificially

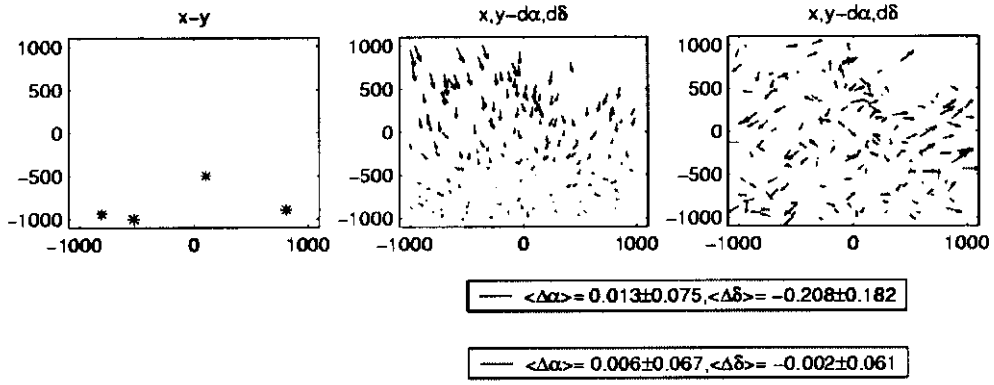

Figure 2: When reference stars were not distributed uniformly

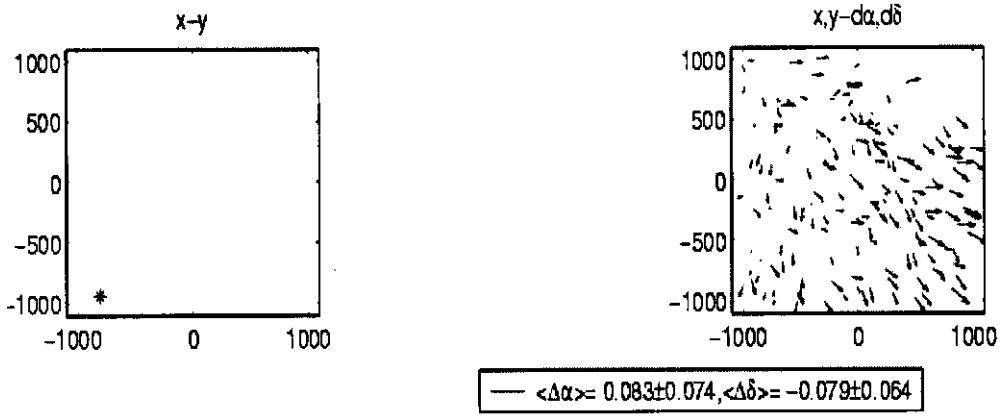

Figure 3: When reference stars are too insufficient to carry out single solution

DEVICES FOR REDUCTION OF CCD DISTORTION UNDER SCAN MODE OBSERVATIONS

O. VERTYPOLOKH[1], YU. BABENKO[1], P. LAZORENKO[2]

[1]Astronomical Observatory of Kyiv University
Observatorna St.,3, Kyiv, 04053, Ukraine
e-mail: verto@observ.univ.kiev.ua, babenko@observ.univ.kiev.ua

[2]Main Astronomical Observatory of National Academy of Sciences of Ukraine
Akademica Zabolotnogo St.,27, Kyiv, 03680, Ukraine
e-mail: laz@mao.kiev.ua

ABSTRACT. Practical experience on application of CCD detectors in a precise astrometry has shown, that one from the essential factors affecting a positional accuracy of an observation of stars in a scanning mode, especially for high declinations, is so-called CCD distorsion caused by the lack of co-incidence of projections of small circles of the celestial orbits on a plane of CCD with straight-line trajectories of moving charges. On the base of performed theoretical analysis of CCD distortion the authors have offered the devices essentially decreasing influence of CCD distortion on a positional accuracy of star observations in the scanning mode.

1. INTRODUCTION

The deterioration of positional accuracy of CCD scan mode observations at increase of declinations because of smearing of the star images owing to CCD - distortion is the well-known fact (Stone et al. 1996). The purpose of the given work consists in search of effective instrumental methods of reduction of influence CCD - distortion on positional accuracy of observations in scan mode.

2. CCD DISTORTION ANALYSIS AND DEVICES FOR REDUCTION OF CCD DISTORTION UNDER SCAN MODE OBSERVATIONS

Theoretical analysis of expressions for estimation of the smearing of the star image in both coordinates because of the CCD distortion taking place under scane mode observations with the MAC (Meridian Axial Circle) shows, that: a) the distortions of the star image in declination and right ascension have different character; b) with accuracy up to the second order terms concerning such small values as an hour angle $t_\circ$ of a star at the moment of a beginning of its electronic tracking, the difference of declinations $\Delta\delta$ of an observable star and projection of

the CCD centre on the celestial sphere and a time interval of scanning ΔT of a star, the size of the smearing in declination does not depend on size $\Delta\delta$ and has parabolic dependence on duration ΔT, that produces asymmetrical distribution of brightness in the image of a star in appropriate coordinate; c) with the above-stated accuracy the size of the smearing in a right ascension is proportional to the electronic scan duration ΔT and to the parameter $\Delta\delta$, but symmetric distribution of brightness in the star image in appropriate coordinate is remained; d) the errors of definition both declination and right ascension increase with the increasing of declinations and are especially great for the nearpole zone. From stated the obvious "tactical" instrumental improvement of the MAC suggests itself, which will supply essential reduction of the scan smearing. The essence of such improvement is that in front of the light-sensitive field of the CCD - matrix in parallel to it the rectangular diaphragm with variable width is established. Width and height of the diaphragm are accordingly guided lengthways and across with respect to the direction of charge transfer in a plane of the CCD-matrix. Width of the diaphragm is adjusted according to the formula: $\Delta l = lcos\delta_\circ$, where Δl is width of the diaphragm, l is width of the light-sensitive field of the CCD - matrix, $\delta_\circ$ - declination of a point in the sky in a plane of a meridian, to which sighting axis of the MAC is directed. In this case the smearing of the star image in declination reaches the maximal value at declination 45° and is equal to zero both for the equator and for the celestial pole, and in right ascension it reaches maximal, but not infinite value at the pole. It is necessary also to emphasize, that the offered design of a meridian telescope provides an opportunity to carry out scan mode observations independently on declination of observable stars down to the celestial pole.

On the base of performed theoretical analysis of the CCD distortion taking place under scan mode observations it follows as well that it is the uniform total smearing of the images of all objects along the circles. The centres of these circles coincide with the beginning of the CCD-matrix coordinate system. This total smearing is characterized by angular velocity, which in one's turn depends on the angular velocity of daily rotation of the Earth and on declination $\delta_\circ$. Basing on this conclusion, the authors offer to supply the meridian telescope with an additional optical element - the Dove prism, which should be mounted in an optical path of the tool in parallel beams and completely block its aperture. The distinctive features of the offered meridian telescope consist in the following. Two collimation objectives and Dove prism are entered into its optical tract. The Dove prism is established with an opportunity of rotation around of an optical axis of a telescope in the bearings, rigidly attached to a pipe, and has the appropriate drive, connected with the personal computer. The angular velocity of rotation of the Dove prism is adjusted according to the formula: $\omega = (1/4)Sin\delta_\circ \times k[rad/sec]$, where k $= 2\pi/(2 \times 24 \times 3600)$ is a constant factor. Its numerical value is small. Use of the Dove prism in a design of the MAC allows essentially to reduce the smearing of the star images in a plane of a CCD-matrix during scan mode observation, namely, to reduce the smearing in declination up to values about 3-rd order terms concerning instrumental parameters $t_\circ$, $\Delta\delta$ and ΔT, and to reduce twice the smearing in right ascension. Accordingly at the expense of instrumental reduction of CCD - distortion offered transit telescope allows essentially raising an accuracy of determination of star coordinates. It is necessary to note, that offered by the authors the improvements of a design of the MAC, namely auxiliary assembly with the Dove prism or assembly of the diaphragm with adjustable width, can be successful applied in a design of anyone meridian telescope, on which the scan mode observations are carried out. The authors have received the patents of Ukraine for the inventions concerning technical improvements, considered in this paper.

3. REFERENCES

R.S.Stone, D.G.Monet, A.K.B.Monet, R.L.Walker, H.D.Ables, A.R.Bird, F.H.Harris. 1996, AJ, 111, 1721.

Session IV

TIME, TIME TRANSFER AND EARTH ROTATION

TEMPS, TRANSFERT DE TEMPS ET ROTATION DE LA TERRE

LA ROTATION DE LA TERRE DE L'ANTIQUITÉ À L'AUBE DU XXème SIÈCLE

S. DÉBARBAT, M.-P. LERNER
SYRTE - UMR8630/CNRS, Observatoire de Paris
61 avenue de l'Observatoire 75014 Paris, FRANCE

ABSTRACT. The rotation of the Earth is reviewed from its round shape well known at the time of Antiquity up to the various aspects of its rotation at the end of the XIXth, via Copernicus, Galileo, Riccioli, Kant, Lalande, Foucault, Küstner, Chandler, Newcomb and others.

1. LA TERRE EST-ELLE RONDE?

Pour que la Terre puisse tourner, il fallait qu'elle fût ronde. C'était là une condition nécessaire : les adeptes de cette idée contraire à toute perception immédiate, et donc au sens commun, devaient au moins postuler pour la Terre une figure identique à celle des astres errants que tout un chacun pouvait voir tourner dans le ciel.

La notion même de la Terre sphérique ne s'est dégagée que lentement et n'a fini par s'imposer dans le monde grec qu'avec Platon et Aristote. Avant eux, comme nous l'apprend le Pseudo Plutarque (I^{er}-II^{e} s.) dans ses *Opinions des philosophes*, les idées relatives à la forme de la Terre étaient des plus variées. Pour Anaxagore (500-428), la Terre était comparable à une colonne de pierre; pour Anaximène (-VI^{e} s.), elle avait la forme d'une table; pour Leucippe, celle d'un tambour; pour Démocrite (460-370), celle d'un disque dans sa largeur, mais concave en son milieu. Seul Thalès (625-547) au dire du Pseudo Plutarque, aurait donné une figure sphérique à la Terre, mais cela est contredit par le témoignage d'Aristote, sans aucun doute plus fiable. D'après ce que rapporte ce dernier, Thalès faisait flotter la Terre sur l'eau, à l'instar d'une bûche ou de quelque chose de semblable [1].

Si l'on regarde maintenant du côté de la Bible, source d'un savoir révélé sur l'origine du monde qu'il est impossible de passer sous silence, la Terre est tout sauf sphérique - probablement, comme pour les Babyloniens, un disque plus ou moins plat couvert de vallées et de montagnes - et elle est tenue bien évidemment pour immobile.

Au total, excessivement rares avant Platon (428-348) sont les auteurs qui ont non seulement pensé que la Terre devait être sphérique, comme les Pythagoriciens (VI^{e}-V^{e} s.), mais surtout qui ont apporté des arguments propres à justifier cette thèse. Aristote (384-322) est le premier, dans son traité *Du ciel*, à avoir exposé des idées claires et des arguments, à la fois d'ordre physique et astronomique - notamment l'argument tiré des éclipses de Lune [2].

[1] Pseudo Plutarque, *op. cit.*, III 10; Aristote, *Du Ciel*, II, 13. - On trouvera une traduction française des principaux textes de Platon, Aristote, Ptolémée, Copernic, et Galilée évoqués ci-après dans l'anthologie publiée par J.-P. Verdet sous le titre *Astronomie et astrophysique* [Textes essentiels], Larousse, Paris 1993.

[2] Aristote, *loc. cit.*

En revanche, si Aristote a bien vu que la Terre était de figure (approximativement) ronde, et même de dimensions modestes au regard de l'univers enclos dans la sphère des étoiles fixes, il a pris, touchant l'immobilité de la Terre, une position qui engagera l'avenir pour longtemps.

2. ARISTOTE ET PTOLÉMÉE : LA TERRE RONDE EST IMMOBILE

Aristote évoque des "gens d'Italie connus sous le nom de Pythagoriciens" qui comptaient la Terre au nombre des astres en révolution autour du feu central, et qui la faisaient en outre tourner sur elle-même, expliquant par là le phénomène du jour et de la nuit. Aristote cite encore Platon qui, dans le *Timée*, maintenait la Terre au centre du monde, tout en la faisant tourner autour de son axe médian - opinion également partagée par Héraclide du Pont (388-315). Aux uns comme aux autres, Aristote oppose que la rotation propre de la Terre, peut-être concevable dans l'abstrait, est en fait impossible essentiellement pour une raison d'ordre physique tirée de la nature des éléments, et qui fait que c'est une nécessité manifeste pour la Terre d'être au centre du monde et d'y rester immobile. Conclusion confirmée par l'observation : les "lourds" lancés vers le haut retombent à leur point de départ, ce qui ne serait pas le cas si la Terre tournait sur elle-même [3].

Cet argument, tiré de l'expérience quotidienne, sera souvent invoqué pour réfuter une idée qui n'était pas absurde du point de vue astronomique, et même de nature à satisfaire un besoin rationnel de simplicité. Dans sa *Grande Syntaxe*, plus connue sous le nom d'*Almageste*, Ptolémée (100-170) sera lui aussi sensible à cette idée, mais il n'en rejettera pas moins la réalité de la rotation propre de la Terre au nom des conséquences qu'un tel mouvement entranerait pour nous [4].

3. LA PÉRIODE MÉDIÉVALE : DES ARGUMENTS PROBABLES EN FAVEUR DE LA ROTATION

Il faudra attendre pour l'essentiel le Moyen Age, et plus précisément le XIVe siècle, pour que l'idée d'une rotation propre de la Terre bénéficie à nouveau d'un examen attentif. Parmi les auteurs les plus notables, on mentionnera Jean Buridan (1295-1358), Thémon Juif (? - 1360?) et Nicole Oresme (1323-1382). Aucun d'eux n'a accepté la réalité d'un tel mouvement, mais ils ont exposé avec un certain détail les arguments en sa faveur.

Oresme ira le plus loin dans le sens de cette thèse en affirmant qu'on ne peut démontrer la fausseté de la rotation propre de la Terre ni par l'expérience, ni par la raison. Le principe d'économie des opérations de la nature accepté, selon Oresme, "par tous les philosophes", joue ici un rôle de premier plan. Admettre "le mouvement journal de la terre qui est tres petite ou resgart du ciel" permettrait de sauver les apparences au moyen d'une petite opération en s'épargnant toutes les "operacions si outrageusement grandes" qu'impose la doctrine traditionnelle.

Pourtant, Oresme ne sera pas convaincu par cet argument, ni par les autres, notamment celui qui sauverait la trajectoire de la flèche tirée vers le haut et retombant à la verticale du tireur en disant qu'elle est solidaire du mouvement de l'air entrané par la rotation de la Terre. En effet, il conclut son analyse en déclarant que le mouvement des cieux autour de la Terre immobile est conforme à la raison naturelle et à l'Écriture [5]. Car si pour les médiévaux Dieu avait créé une Terre ronde - les Pères de l'Eglise, nourris de philosophie grecque, avaient depuis longtemps accepté l'idée d'une Terre sphérique, croyant même en retrouver la figure dans la *Genèse* - il l'avait aussi voulue "inébranlable pour les siècles des siècles" [6].

[3] Platon, *Timée*, 40 B C, et Aristote, *Du Ciel*, II 14.
[4] *Almageste*, I 4-7.
[5] *Le Livre du ciel et du monde*, II 25.
[6] *Psaume*, 92, 1.

Pour se libérer efficacement de l'absurde vitesse du dernier ciel en rapportant son apparence à un mouvement réel de la Terre, il fallait faire sauter au moins l'un des verrous physiques qui assuraient l'invincibilité du géostatisme : l'idée que le corps "lourd" qui occupe le centre de l'univers est par nature immobile. Il fallait surtout se libérer du dogme qui interdisait à la Terre de participer toute entière, de façon naturelle, et non violente, à un transport circulaire.

4. COPERNIC : LA TERRE PEUT ET DOIT TOURNER SUR ELLE-MEME

Dans le *De revolutionibus*, Copernic commence son exposé relatif à la mobilité de la Terre par la rotation diurne, car le plus évident des mouvements semble être celui de la révolution quotidienne qui entrane le monde entier à l'exception de notre globe. Or cette évidence peut aussi bien être sauvée en faisant tourner la Terre sur elle-même d'ouest en est, et cela parat même plus rationnel. Le ciel n'est-il pas immense au regard de la Terre? Celle-ci n'est-elle pas comme un point par rapport à un corps, et comme le fini par rapport à l'infini? D'où l'étonnement qu'il y aurait à voir tourner cette immensité en vingt-quatre heures plutôt que la Terre.

Toutefois, Copernic n'ignore pas que les objections principales des adversaires de cette thèse sont d'ordre physique. Il cite d'abord l'argument tiré de la gravité qui fait que tous les corps lourds tendent à s'immobiliser le plus près possible du centre de la Terre, et qu'elle-même occupe, immobile, le milieu du monde. Puis il mentionne la doctrine aristotélicienne des deux classes de mouvements naturels des corps simples : mouvement rectiligne appartenant en propre aux quatre éléments du monde sublunaire : vers le haut pour l'air et le feu, vers le bas pour l'eau et la terre; mouvement circulaire autour du centre immobile réservé au corps céleste éthéré qui occupe toute la région supralunaire, en montrant que cette distinction ne tient plus si l'on fait tourner la Terre sur elle-même.

Copernic rejette également la critique adressée par Ptolémée à l'hypothèse de la rotation diurne de la Terre en niant les effets prétendument dévastateurs de la rotation diurne pour ce qui est à la surface du globe terrestre et pour la Terre elle-même. Qui admet en effet au départ que ce mouvement appartient en propre à la Terre posera *ipso facto* son caractère "naturel" et non "violent" : or "ce qui est produit par la nature est en bon ordre et se conserve dans l'excellence de sa composition. Par conséquent, c'est en vain que Ptolémée craint que la terre et toutes les choses terrestres ne se dispersent sous l'effet d'une rotation produite par l'action de la nature" [7].

Le caractère purement dialectique de la réponse de Copernic à l'auteur de l'*Almageste* est évident. Tout son raisonnement repose sur l'antinomie entre mouvement "naturel" de la Terre et mouvement "violent" du ciel. Mais les géocentristes pouvaient nier que la révolution du ciel fût violente et considérer à bon droit que Copernic n'avait pas vraiment répondu - c'est-à-dire donné des contre-raisons d'ordre physique - à leurs arguments quant aux effets qu'entraneraient la rotation de la Terre (elle ne pouvait être à leurs yeux qu'un mouvement violent) sur les corps situés à sa surface ou en suspension dans l'air.

5. ARGUMENTS AVANCÉS PAR GALILÉE EN FAVEUR DE LA ROTATION DE LA TERRE

Galilée avance deux séries d'arguments pour établir dans un premier temps la possibilité de la rotation de la Terre, puis, dans un second temps, sa réalité.

[7] *De revolutionibus*, I 7-8 (voir l'édition de cette œuvre comprenant le texte latin critique, une traduction française et des notes, par M.-P. Lerner, A. Segonds et J.-P. Verdet, paratre aux éditions Les Belles Lettres).

5.1 La rotation n'entraîne pas d'effet mécanique

C'est à Galilée (1564-1642) qu'il reviendra de proposer dans le *Dialogue sur les deux plus grands systèmes du monde*, publié à Florence en 1632, les premières réponses sérieuses aux objections des philosophes traditionnels.

On peut ramener à trois les objections traditionnelles contre la rotation diurne tirées respectivement 1) du mouvement naturel des graves : la pierre lâchée du haut d'une tour ne tomberait jamais à son pied. 2) du mouvement violent : le mouvement du boulet de canon tiré dans le même sens que la rotation de la Terre serait absorbé par la vitesse plus grande de celle-ci, ou encore la portée des tirs vers l'est ou vers l'ouest ne serait pas la même. 3) du mouvement des corps en suspension : les oiseaux ou les nuages seraient entranés sans pouvoir se déplacer librement.

Autrement dit, ce sont les effets mécaniques supposés du mouvement diurne qu'objectent les adversaires de la théorie. Galilée va s'efforcer d'y répondre en montrant que, dans l'hypothèse de la rotation, aucun effet inconnu par rapport à l'état de repos ne survient. Pour ce faire, il étend à la Terre toute entière le principe de relativité mécanique démontré dans le cas des objets transportés par un navire, lesquels ne subissent aucune perturbation du fait de son déplacement en mer : quel que soit le mouvement attribué à la Terre, il est nécessaire qu'il reste totalement imperceptible pour ses habitants qui participent de son mouvement. Autrement dit, pour réfuter ses adversaires, Galilée postule que les corps ne partent pas d'un état de repos absolu comme le veulent ceux-ci, mais d'un état initial de mouvement, celui du système dont ils font partie et qu'ils conservent en eux aussi longtemps qu'ils se meuvent. Mais il ne va pas se contenter de cette simple affirmation.

Grâce à ses travaux sur le plan incliné, Galilée sait que sur une surface horizontale qui n'éloigne ni n'approche une boule du centre commun des graves, le moment de descente de ladite boule est nul et qu'elle devient indifférente au mouvement ou au repos. Plus précisément, si elle est repos, elle y restera. Si en revanche, on lui communique une certaine vitesse, elle va la conserver. Sur un plan horizontal un mouvement une fois commencé se perpétuerait indéfiniment et uniformément. Or ce mouvement inertial autour du centre de la Terre n'est par définition incompatible avec aucun autre mouvement, avec lequel il se combinera sans difficulté.

Fort de ce principe, Galilée croit pouvoir montrer que la pierre qui tombe le long de la tour, les boulets de canons tirés dans des directions différentes ou l'oiseau et le nuage, du fait de l'*impeto* circulaire auquel ils ont part, ne subissent aucune altération liée à la rotation de la Terre dans la mesure où chaque portion de sa surface peut être assimilée à un système inertial [8].

L'argumentation de Galilée souffre d'un double défaut. D'abord elle n'est pas de nature à mettre en évidence la réalité de la rotation de la Terre. Si le déplacement uniforme d'un système demeure sans influence sur les mouvements qui s'y déroulent, il s'ensuit qu'aucune observation ou expérience menée à l'intérieur du système ne pourra mettre en évidence sa translation.

En second lieu, parce qu'il tient le mouvement circulaire uniforme pour un mouvement simple - en quoi il reste pleinement aristotélicien - et non (comme on le saura plus tard, grâce à Huygens) pour un mouvement composé dont seule une accélération dirigée vers le centre assure l'entretien, Galilée se trompe en assimilant la rotation de la Terre à un système inertial à l'intérieur duquel aucune déviation d'un mobile ne pourrait se produire. Il est faux en effet que la rotation terrestre n'affecte pas le mouvement des corps à sa surface [9].

5.2 Preuve tirée des marées

Si, dans la Deuxième Journée du *Dialogue*, Galilée n'a pas su mettre en évidence la rotation propre de la Terre pour les raisons qu'on a dites, il s'est employé à en établir la réalité dans la

[8] *Dialogue sur les deux grands systèmes du monde*, Deuxième Journée (trad. fr., éd. Fréreux-De Gandt, Point Seuil, Paris 2000, p. 217 sq).

[9] Voir M. Clavelin, *La philosophie naturelle de Galilée*, 2e éd., Paris 1996, p. 232-276.

Quatrième Journée, celle où il expose sa fameuse théorie des marées. On peut résumer en ces termes l'argument de Galilée, qui appuie sa démonstration sur le modèle déférent-excentrique bien connu des astronomes.

Si la Terre tourne sur elle-même d'ouest en est, et accomplit en même temps une révolution annuelle autour du Soleil, les parties de la Terre auront chaque jour alternativement une vitesse égale à la somme et à la différence des deux vitesses. En conséquence, l'eau contenue dans les mers, qui ne peut pas suivre instantanément ces variations de vitesse, se comporte comme si elle se trouvait à l'intérieur d'un vase, ou encore d'une barque tantôt accélérée, tantôt ralentie, avec pour effet que l'eau se rassemblera alternativement vers la proue et vers la poupe [10].

L'idée consistant à expliquer l'élévation et l'abaissement périodique de l'eau, c'est-à-dire l'alternance du flux et du reflux, par la composition de deux rotations uniformes, a en général été considérée comme une théorie des marées fausse. Et ce pour deux raisons principales. D'abord ce modèle ne rend compte que d'une marée haute et une marée basse toutes les 24 heures. Ensuite, parce que Galilée prétend expliquer un phénomène dû essentiellement à d'autres causes. Comme on le sait, il faudra attendre Newton pour avoir une première théorie des marées satisfaisante des deux points de vue mentionnés à l'instant. Mais cela veut-il dire que la théorie galiléenne des marées soit véritablement et au sens propre "fausse", comme la majorité des historiens de la science le soutiennent?

Dans une étude récente, Pierre Souffrin s'est employé à rendre justice à cette théorie. Il rappelle que Galilée ne s'est pas contenté d'un discours théorique : il a construit un dispositif expérimental permettant de mettre en évidence l'engendrement de ce mouvement périodique de l'eau s'élevant et s'abaissant alternativement contre les parois du récipient comme résultante du double mouvement décrit ci-dessus. Cette machine n'a malheureusement pas été conservée, mais Souffrin en a construit une récemment qui confirme les dires du savant italien. Ce modèle simple suffirait pour démontrer l'essentiel, à savoir que la combinaison de ces deux mouvements a pour conséquence nécessaire des flux et des reflux des eaux superficielles de la même nature que ceux que l'on observe dans le phénomènes des marées. En ce sens, Galilée aurait eu raison de voir dans les marées une preuve du double mouvement de la Terre [11].

6. DE RICCIOLI FOUCAULT : QUELQUES TENTATIVES EXPÉRIMENTALES

Quoiqu'il en soit sur ce point, après 1632, date de parution du *Dialogue*, la théorie galiléenne des marées ne rencontra qu'incompréhension et refus de l'écrasante majorité des auteurs, attitude que la condamnation de l'héliocentrisme comme "fortement suspect d'hérésie" n'aida pas à surmonter surtout en Italie. On peut même dire qu'elle encouragea alors un certain nombre d'entre eux à reprendre l'étude de la trajectoire des corps en chute libre pour démontrer expérimentalement l'immobilité de la Terre et le bien fondé de la décision qu'avait prise l'Eglise de Rome sur la base de l'Ecriture sainte. On se bornera à citer ici Giambattista Riccioli (1598-1671), Stefano Degli Angeli (1623-1697), Diego Zerilli (XVII^{e} s.), auteurs plus ou moins connus aujourd'hui qui se sont parfois opposés sur les résultats de leurs observations alors qu'ils partageaient la même conviction géocentriste. Mais il faut aussi mentionner les travaux de Giovanni Alfonso Borelli (1608-1679), Adrien Auzout (1622-1691), Robert Hooke (1635-1703) et Isaac Newton (1642-1727) qui, eux, ont tenté de mettre en évidence la déviation vers l'est (et le sud pour les deux derniers) de la trajectoire des graves comme conséquence de la rotation propre de la Terre. Mais les résultats obtenus en ce sens ne paraissaient pas entièrement satisfaisants encore aux yeux d'un Laplace en 1796 [12].

[10] *Dialogue*, Quatrième Journée, trad. cit., p. 599 sq.

[11] P. Souffrin, "La théorie galiléenne des marées n'est pas une théorie fausse", *Epistémologies*, 1-2 (2000), p. 113-139.

[12] Sur tous ces auteurs, voir A. Koyré, *Chute des corps et mouvement de la Terre de Kepler Newton*, trad. fr.,

Cinq ans avant la parution du livre de Laplace, l'abbé Giambattista Guglielmini (1763-1817) avait fait des expériences du haut de la Torre degli Asinelli, la grande tour penchée de Bologne haute d'environ 78 mètres, en vue de confirmer les expériences de Robert Hooke prévoyant une déviation du grave arrivé au sol à la fois vers l'est et le sud. Mais l'imprécision des mesures rendit les résultats peu décisifs. Les expériences tentées en 1802 et 1804 par Johann Friedrich Benzenberg (1777-1846), puis par Ferdinand Reich (1799-1882) en 1831, furent plus concluantes. Au point que l'on crédite parfois Reich, qui utilisa un puits de mine de 158,50 mètres de profondeur, du mérite d'avoir été le premier à prouver la rotation de la Terre dans le cadre de la mécanique classique.

Aucune de ces expériences, qui exigeaient un rigoureux dispositif de mesure particulièrement délicat à mettre en oeuvre, ne mettaient en évidence de façon directement sensible le phénomène de la rotation de la Terre sur elle-même. Pour cela, il faudra attendre Léon Foucault.

7. LA ROTATION DE LA TERRE SELON FOUCAULT, CHANDLER ET D'AUTRES

En janvier 1851, Léon Foucault (1819-1868) parvient, dans la cave de la maison où il habite avec sa mère, à Paris rue d'Assas, à voir changer de direction le pendule qu'il a mis en oscillation. Arago (1786-1853), alors directeur des observations, et directeur délégué du Bureau des longitudes, à l'Observatoire de Paris, demande à Foucault de monter l'expérience dans la grande salle méridienne (de nos jours Salle Cassini) située au deuxième étage du bâtiment Perrault. La démonstration a lieu dès le mois suivant. Louis Napoléon Bonaparte fait installer par Foucault un troisième pendule sous les voûtes du Panthéon. Le grand public se presse, en mars 1851, pour voir les oscillations du pendule rendre sensible la rotation de la Terre. L'installation de tels pendules se développe immédiatement dans le monde, des Etats-Unis au Japon, en passant par tous les pays d'Europe.

Vers la même époque la construction d'instruments nouveaux, leur mise en oeuvre, l'analyse des données collectées, confirment à l'évidence deux phénomènes qui affectent la rotation de la Terre. Le premier d'entre eux, l'accélération séculaire de la Lune constatée dès l'apparition des horloges à pendule de Huygens (1629-1695), par Hevelius (1611-1687), et confirmée par la suite, pourrait s'expliquer par un ralentissement de la rotation terrestre. Le second phénomène, mis en évidence à l'Observatoire de Paris par Picard (1620-1682) grâce à ses instruments de précision équipés de lunettes et de micromètres, est une variation de la hauteur du pôle au-dessus de l'horizon [13]. Cette hauteur du pôle, latitude du lieu, fluctue et ses déterminations, dans les différents pays, confirment le phénomène.

Au XIXè siècle Yvon Villarceau (1813-1883), à l'Observatoire de Paris, passe vraisemblablement près d'une découverte lorsqu'il obtient de Le Verrier (1811-1877) que des moyennes mensuelles de la latitude de Paris soient effectuées sur six ans. C'est à l'Américain Chandler (1846-1913) que revient l'honneur de la découverte du terme périodique, phénomène dont Euler (1707-1783) avait dès 1765 établi la théorie. Dans son traité "Theoria motus corporum solidorum seu rigidorum" [14], il donne une période de 305 jours pour le déplacement, observé à la surface de la Terre, de son axe de rotation. Par la suite, nombre d'astronomes chercheront à confirmer cette valeur.

L'Allemand Kstner (1856-1936) utilise pour ses observations une lunette zénithale du type

Paris 1973; voir aussi, pour la période postérieure, J. Gapaillard, *Et pourtant elle tourne! Le mouvement de la terre*, Paris 1993.

[13] S. Débarbat, "Latitude Observations at Paris Observatory Prior to the ILS", *dans Polar Motion Historical and Scientific Problems*, IAU Coll. 178 (27-30 sept. 1999), Dick, McCarthy et Luzum eds, Astron. Soc. of the Pacific, 2000, p. 83-87.

[14] L. Euler, *Mémoires de l'Académie des Sciences de Berlin*, 1765, p. **194-218**.

de celle que Talcott (1797-1883), aux Etats-Unis, a imaginé en 1834, bientôt suivi par Airy (1801-1892), l'*Astronomer Royal* de Greenwich. Küstner décèle, en 1888, des variations de latitude que Bessel (1784-1846) avait soupçonnées dès 1843. Peu après Chandler, employant son almucantar, lequel exploite la méthode de Gauss (1777-1855) des hauteurs égales, fait connatre (1891/1892) qu'il existe dans la latitude une combinaison de deux mouvements. L'un est de période annuelle, l'autre mouvement - dit "terme de Chandler" - est de 427 jours. L'ensemble provoque une oscillation de l'axe de rotation de la Terre d'une durée de six années [15].

8. LA ROTATION DE LA TERRE : UNE SUITE SANS FIN

En 1754, Kant (1724-1804) émet l'idée que les marées pourraient être responsables d'un allongement de la durée du jour. Lalande (1732-1807), un peu plus tard, s'interroge sur les possibilités d'un tel ralentissement qui pourrait atteindre deux à trois secondes d'heure en un an [16]. Il évoque aussi, parmi les causes possibles, les mouvements de l'atmosphère ou de la mer, phénomènes de nature géophysique.

A la fin du XIXe siècle, l'Association Internationale de Géodésie (AIG) - qui a pris le relais en 1864 de l'Europäische Gradmessung, elle-même héritière de la Mitteleuropäische Gradmessung [17], créée en 1861 - va faire progresser la question. L'AIG s'intéresse aux variations de l'axe autour duquel s'effectue la rotation de la Terre pour expliquer les perturbations de la latitude. En 1898, elle se réunit et décide la création de stations bien réparties autour du globe terrestre, situées à la même latitude de $39°8'$. Le terme mis en évidence étant de six ans, nombreux sont ceux qui pensent qu'après une telle durée d'observations, le mouvement de l'axe de rotation de la Terre au sol sera élucidé.

Les stations établies dès 1899, équipées du même instrument zénithal et observant les mêmes étoiles, sont au nombre de quatre : une à Carloforte, dans une le proche de la Sardaigne, une à Mizusawa au Japon, deux aux Etats-Unis, une sur la côte est, l'autre sur la côte ouest. Deux autres stations se joindront à elles, l'une en Russie et l'autre aux Etats-Unis. Les circonstances feront varier de trois à six le nombre total des stations en activité, mais les impératifs de l'AIG demeureront au cours du temps. Le Service, qui a célébré en 1999 le centenaire des premières observations à Cagliari et à Carloforte [18], avait pris le nom de Service International des Latitudes (SIL), et l'Allemand Albrecht (1843-1915) s'était vu confier, dès 1900, la tâche d'en traiter les données. Des changements sont intervenus depuis, car les six années prévues n'ont pas suffi, mais c'est là une autre histoire.

A côté des études du mouvement du pôle terrestre, celles des variations de la vitesse de rotation se poursuivaient. C'est par la Lune et l'accélération de son mouvement que les Hansen (1795-1874) en Allemagne, les Newcomb (1835-1909) aux Etats-Unis et d'autres, entre 1857 et 1875, ont convaincu leurs collègues du ralentissement séculaire de cette vitesse. En particulier, Newcomb a utilisé les observations d'occultations d'étoiles par la Lune menées à l'Observatoire de Paris depuis sa fondation en 1667 : nouvel exemple de l'utilisation de données anciennes pour des recherches modernes. Newcomb a compilé lesdites données à l'Observatoire de Paris avec Delaunay (1816-1872), spécialiste réputé de la théorie de la Lune, pendant la Guerre de 1870.

Bientôt la découverte de la télégraphie sans fil (TSF), dès avant 1900 et qui va se développer rapidement, apportera grâce aux signaux horaires le moyen d'affiner l'étude de ce mouvement. Les premiers de ces signaux, d'une portée de 5 000 km, partiront de la Tour Eiffel. L'Observatoire de Paris, où s'effectuait la détermination de l'heure, indiquait l'instant d'émission du signal. La

[15] E.P. Fedorov, "Nutation and the forced motion of the earth's pole", Pergamon Press, 1962, xix + 152 pages.
[16] J. Lalande, *Astronomie*, 3e édition, Desaint, Paris, 1792.
[17] S. Débarbat, "The AIG and the Origin of the International Scientific Unions" dans *Global Change and History of Geophysics*, Schröder and Colacino eds, Bremen-Roennebeck, 1996, p. 155-160.
[18] Cf. *Op. cit.* note 13.

crue de la Seine, qui avait retardé les travaux d'aménagement du dispositif dans le laboratoire de la Tour, n'empêchera pas le début de l'expérience en novembre 1910.

9. UNE CONCLUSION QUI S'IMPOSE

Avec cette année fin de siècle s'achève la partie proprement historique des études de la rotation de la Terre. Ce qui appartient au XXème siècle est de l'histoire contemporaine, tandis que pour le XXIème siècle, il vous revient à vous - participants des J 2002 - de l'écrire.

DECADAL MODULATION IN THE SEASONAL VARIATIONS OF EARTH ROTATION : POSSIBLE RELATIONSHIP WITH SOLAR ACTIVITY

D. GAMBIS[1], R. ABARCA DEL RIO[2], D. SALSTEIN[3]

1 - Observatoire de Paris, SYRTE, UMR8630
61 Av de l'Observatoire, Paris, France

2 - Departamento de Fisica de la Atmosfera y de los Oceanos (DEFAO)
Facultad de Ciencias Fisicas y Matematicas, Universidad de Concepcion
Casilla 160-C, Concepcion, Chile

3 - Atmospheric and Environmental Research, Inc
131 Hartwell Ave., Lexington. MA 02421, USA

ABSTRACT. Linear correlations have been found at the decadal frequency band, between the modulation of amplitudes and phases of the seasonal variations of length of day (annual and semi-annual), and solar activity represented by the Wolf number index as well as the total radiative flux at 10.7 cm. A possible mechanism explaining this relation is hypothesized to involve the lower regions of the atmosphere, which have been observed to contain significant interannual variations of seasonal signals. Though the present results are suggestive, involving patterns of temperature and wind fluctuations, further physical explanation of the mechanism involved is needed.

1. INTRODUCTION

The Sun drives the thermal balance of our planet and determines the seasonal variations of the weather. However, until recently solar irradiance was assumed to be invariant and because of the absence of consensus regarding physical processes relating solar activity to climate variations, this topic has caused much speculation and controversy.

A variety of studies have sought to establish relationships between solar and atmospheric variability (Labitzke, 1987; Labitzke and van Loon, 1990 and 1997; Barnston and Livezey, 1987; Pittock, A. B., 1978; Friis-Christensen, E., and K. Lassen, 1991, Salby and Shea, 1991; Sadourny, 1994; Reid, 1995). Many of the relationships detected have been questioned principally for both physical and statistical reasons. The physical basis for the relationship is unclear; solar irradiance variations observed during the last 3 decades are very small, with amplitudes of only 0.4% of the total solar energy.

Following a recent study (Abarca et al, 2003) we have re-investigated more extensively (Gambis et al, 1993) a possible relationship between the atmosphere and solar activity at the decadal time scale using LOD, AAM and Solar activity indexes: Wolf number and solar flux at 10.7 cm in the analyses.

2. DATA: EARTH ROTATION, ATMOSPHERIC ANGULAR MOMENTUM, AND SOLAR ACTIVITY DATA SETS

2.1 Earth rotation, Length of day (LOD)

The LOD series is derived from Universal Time UT1-TAI obtained from the combination of astrometric and space-geodetic methods. Prior to the advent of space geodetic techniques, in the 1970s, optical astrometry measurements, provided by as many as 50 instruments, principally astrolabes and transit instruments, were used to determine these earth rotation parameters. Since that time, modern methods including lunar laser ranging and very long baseline interferometry VLBI have provided the Earth Orientation Parameters (EOP) with increasing accuracy. These series are homogeneous with respect to the conservation of the reference system but not to accuracy, the precision of UT determinations having improved considerably over time, from 0.3 ms in the 1960s to 0.015 ms in 2003. The effects of the known externally forced zonal tides have been removed. Prior to 1962, variations of LOD were filtered into various components: decadal, seasonal and intraseasonal variations. Figure 1 shows the results of this filtering over 1962 until now (Shiskin et al, 1970)

The zooming of the seasonal variation series is represented on figure 2. A decadal modulation can be roughly noticed. This series will be analyzed and compared to other series AAM and solar activity.

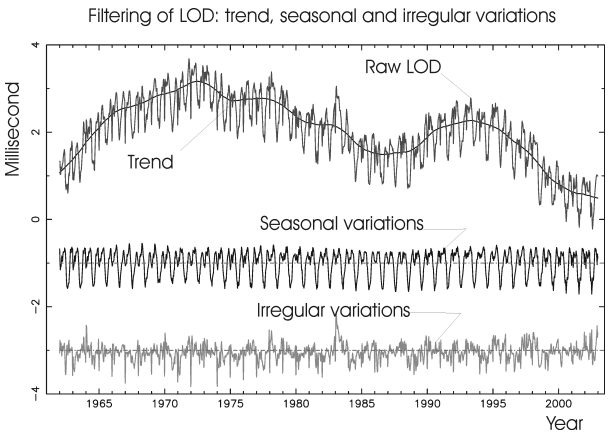

Figure 1: Filtering of LOD series into three components: trend, seasonnal and interannual

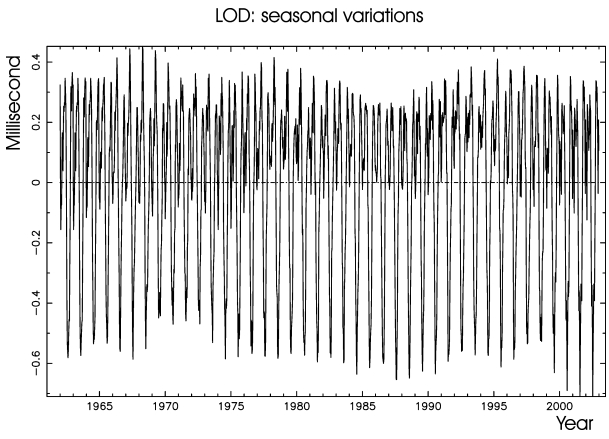

Figure 2: The seasonnal variations exhibit a significant decadal modulation

2.2 Atmospheric Angular Momentum

A fundamental measure of the dynamic state of the atmosphere is its angular momentum about the polar axis relative to the Earth. Variations in atmospheric winds and the distribution of surface pressure cause variations in Atmospheric Angular Momentum quantities. Because of the smallness of the external torques exerted by the sun and moon, and the limited role of the oceans, the angular momentum of the Earth-atmosphere system is largely conserved, and variations in AAM and LOD can be used as proxy indices for each other when decadal fluctuations attributed to the core mantle torque and known tidal terms are removed from the LOD series.

The AAM data can be expressed in millisecond (ms) of length of day (LOD) variability, assuming that changes in AAM for the entire atmosphere are accompanied by equivalent changes in the angular momentum of the Earth, through the following relation (Rosen and Salstein, 1983) :

$$\Delta LOD(ms) = 1.68.10^{-29} \Delta AAM(kg.m^2/s)$$

2.3 Solar variability

A number of different measures characterizing solar activity have been produced over the course of many years, and each is linked to some aspect of activity within the solar atmosphere, photosphere and corona. Nevertheless, these measures of solar activity are all well correlated with each other. The common indices that have been the most studied are those measuring the portion of the solar disc covered by sunspots, especially the composite "Wolf number", the solar radio flux at 10.7 cm, and total solar irradiance.

Although sunspots have been noted since at least 165 B.C. from China, the first scientific observations date from 1610. There are monthly data since 1650. The commonly used measure was introduced by Wolf, in 1852, as a specific index, based on a combination of a group number and a total spot number. The sunspot series reveals a cycle with average length of 11 years, but varying between 9 and 13 years. Indeed, the length of the cycle has been related to certain climate indices (Friis-Christiansen and Lassen, 1991) over a period longer than a century. The Wolf number index has already gone through 24 cycles since its start in 1755. The series has monthly data which vary significantly, partly because of the inclusion of active and inactive sunspots. Hence for sunspots, smoothed series, perhaps an annual mean, may be the scale of solar activity of interest here.

The spot number is well correlated to the solar flux, at 99% and a record of sunspots is available over a lengthy period.

3. ANALYSES

The seasonal LOD series presented on figure 2 was analysed. A least-square process allows the estimation of both annual and semi-annual components. amplitudes and phases are derived. Figure 3 and 4 show the amplitudes of the annual and semi-annual terms on the same plot that the solar activity. On most of the interval the agreement is striking (anti-correlation in the case of the semi-annual term). No significant phase shift between decadal AAM and solar activity. Similar agreements appear in the modulation of the phase (not represented). Figures 5 and 6 show that solar activity and the modulation of the amplitudes and phases of the annual and semi-annual terms of LOD exhibit a significant decadal period of 10-14 years.

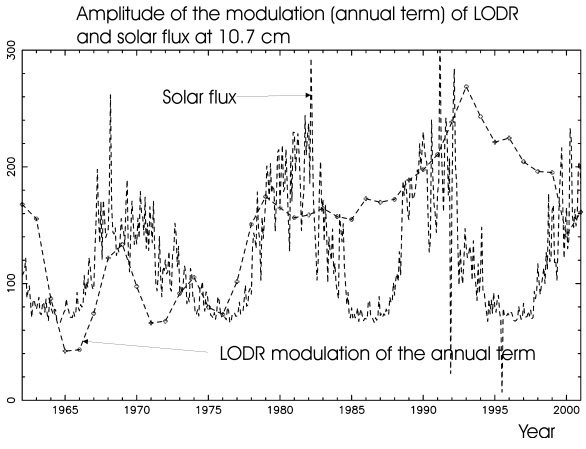

Figure 3: Amplitude of the modulation (annual term) of LOD and the annual flux at 10.7 cm

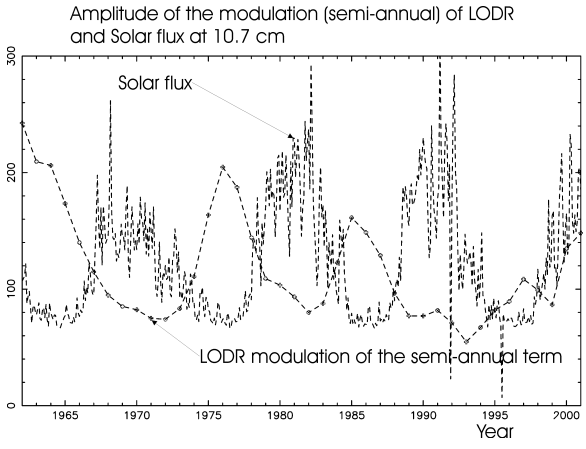

Figure 4: Amplitude of the modulation (semi-annual term) of LOD and the annual flux at 10.7 cm

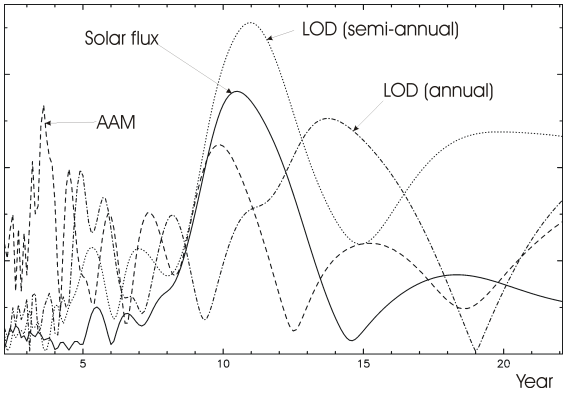

Figure 5: Periodogram of the solar flux, AAM and the amplitude of LOD modulation in the decadal frequency band

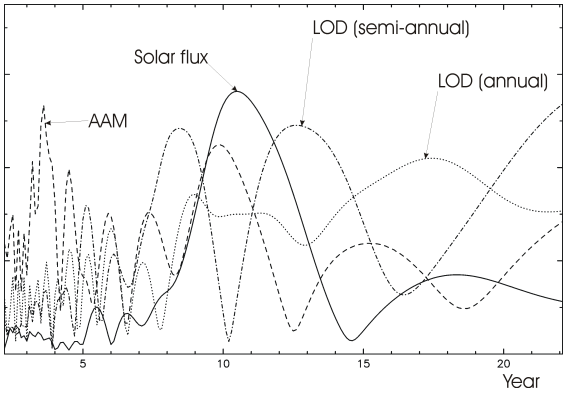

Figure 6: Periodogram of the solar flux, AAM and the phase of LOD modulation in the decadal frequency band

4. CONCLUSION

The present preliminary investigation reveals some significant relationships on seasonal time scales between solar activity and both atmospheric angular momentum and the length of day, which have been linked to each other. The strength and timing of the seasonal cycle in the terrestrial quantities appear to be modulated by the cycle of solar activity, when measured by either the 10.7 cm radio flux, the sunspot number. Though the mechanism is not clear, circumstantial evidence points to physical interactions in the lower troposphere as being responsible for the link in question, due to the known seasonal signal of that region relative to that of the entire atmosphere.

5. REFERENCES

Abarca del Rio, R., D. Gambis, and D. A. Salstein, 2003: *Solar Activity and Earth rotation variability*, Journal of Geodynamics, (D. Gambis, B. Kolaczek and D. Salstein, eds), in press.

Barnston A.G. and R.E. Livezey, 1987: *Classification, sesasonality and persistence of low-frequency atmospheric circulation, patterns*, Month. Wea. rev.115, 1083-1126.

Friis-Christensen and K. Lassen: *Length of the solar cycle: an indicator of solar activity closely associated with climate*. Science., 254, 698-700

Pittock, A. B., 1978: *A critical look at long-term sun-weather relationships*, Rev. Geophys. Space.

Friis-Christensen, E., and K. Lassen, 1991: *Length of the solar cycle: An indicator of solar activity closely associated with climate*, Science, 254, 698-700.

Gambis D., Bourget P, Lantos P. and D. Salstein, 1993: *Analysis of decadal signal in both the Earth rotation and atmospheric angular momentum.* Abstract Proc. Symp. IAG, Pkin, p332.

Labitzke, K., 1987: *Sunspots, the QBO, and the stratospheric temperature in the north polar region.*, Geophys. Res. Lett., 14, 535-537.

Labitzke, K. and H. van Loon, 1990: *Association between the 11-year solar cycle, the quasi-biennial oscillation and the atmosphere: A summary of recent work.*, Phil. Trans. Roy. Soc. London., A 330, 577-589.

Labitzke, K. and H. van Loon, 1997: *The signal of the 11-year sunspot cycle in the upper troposphere-lower stratosphere*. Space Science Reviews, 80, 393-410.

Nastrom, G.D and A.D. Belmont, 1980: *Evidence for a solar cycle signal in tropospheric winds*, J. Geophys. Res.,85, 443.

Reid, G.C.: *Solar total irradiance variations and the global sea surface temperature record.* J. Geophys. Res., 96, 2835-2844.

Rosen, R. D., and D. A. Salstein, 1983: *Variations in atmospheric angular momentum on global and regional scales and length of day.*, J. Geophys. Res., 88, 5451-5470..

Rosen. R. D., D. A. Salstein, and T. M. Wood, 1991: *Zonal contributions to global momentum variations on intraseasonnal through interannual time scales.* J. Geophys. Res., 96, 5145-5151.

Sadourny, R., 1994: *L'influence du Soleil sur le climat*, C.R. Acad. Sci. Paris, 319, 1325-1342.

Salby, M. L, and D. J. Shea, 1991: *Correlations between solar activity and the atmosphere: An unphysical explanation.* J. Geophys. Res., 96, 22579-22595.

Shiskin J., Young A.H., Musgrave J.C., 1965: *The X-11 variant of the Census Method II seasonal adjustment program*, U.S. Dept. of Commerce, Bureau of the Census, Technical Paper No 15.

EARTH'S ROTATION IN THE 7TH CENTURY DERIVED FROM ECLIPSE RECORDS IN JAPAN AND IN CHINA

M. SÔMA[1)], K. TANIKAWA[1)], and K.-A. KAWABATA[2)]

[1)] National Astronomical Observatory of Japan
Mitaka, Tokyo 181-8588, Japan
e-mail: somamt@cc.nao.ac.jp, tanikawa.ky@nao.ac.jp

[2)] Emeritus Professor of Nagoya University
Hanakoganei 4–39–15, Kodaira, Tokyo 187-0002, Japan
e-mail: kawabata-nagoya@jcom.home.ne.jp

ABSTRACT. It is generally accepted that the solar eclipse of AD 628 recorded as total in the Nihongi (Annals of Japan) was in fact a partial one. We compare the solar eclipses of AD 628 and AD 637 and the lunar occultation of Mars of AD 681 recorded in Japan and the solar eclipses of AD 616 and AD 702 recorded in China, and show that the eclipse of AD 628 could be indeed total, and we derive the Earth's rotation in the 7th century from these records.

1. INTRODUCTION

The solar eclipse of 628 April 10 was recorded as "The sun was totally eclipsed" in the Nihongi (The Nihongi is also known as the Nihon-Shoki; "Nihon" means Japan and "gi" or "Shoki" means Annals). This event is the first solar eclipse recorded in the Nihongi, and this is the only solar eclipse recorded as total in the Nihongi. Nine years later, on 637 April 1, there was another solar eclipse observed in Japan. It was also recorded in the Nihongi, but only recorded as "The sun was eclipsed". It is assumed that these records were based on the observations made at Asuka where the capital was located at that time (approximate longitude 135° 50′E, latitude 34° 30′N). Calculations made by Saito and Ozawa (1992) and Watanabe (1994) show that the magnitude of the eclipse of 637 was greater than that of the eclipse of 628, which contradicts with the reports in the Nihongi, and they concluded that the description of the AD 628 eclipse in the Nihongi was an exaggeration.

There was also a record of a lunar occultation of Mars of AD 681 in the Nihongi. Comparing these records with the Chinese eclipse records of AD 616 and AD 702, we show that it is possible that the AD 628 eclipse was indeed total at Asuka, and we derive the Earth's rotation (the value of TT − UT where TT is Terrestrial Time and UT is Universal Time) in the 7th century from these observations.

2. OBSERVATIONS AND CALCULATIONS

Stephenson (1997) obtained the values of $\Delta T = \mathrm{TT} - \mathrm{UT}$ from about 720 BC using mainly the ancient solar and lunar eclipses. According to the ΔT curve of his Fig. 14.4, the value of ΔT in the first half of the 7th century is about 4500 sec, but the figure also shows that there were few eclipse records used to derive the ΔT values in the 7th century, and the value does not fit with three points obtained from solar eclipses of around AD 700.

If we adopt the value $\Delta T = 4500$ sec in the first half of the 7th century, the magnitudes of the solar eclipses of AD 628 and AD 637 are 0.89 and 0.93, respectively. This is in accord with the calculations by Saito and Ozawa (1992) and by Watanabe (1994), but it contradicts with the eclipse records in the Nihongi as mentioned in Sect. 1.

Solar eclipses of AD 616 and AD 702 are recorded in China. The 616 May 21 solar eclipse is given as "chin" in Sui-shu (Annals of the Sui Dynasty). "Chin" usually means total, but it was also used for annular eclipses, and in fact the AD 616 eclipse was annular. The 702 September 26 eclipse is recorded as "almost complete" in Chiu-t'ang-shu (Old History of the T'ang Dynasty) and as "not complete and like a hook" in Hsin-t'ang-shu (New History of the T'ang Dynasty). It is assumed that the AD 616 eclipse was observed at Lo-yang (approximate longitude 112° 24′E, latitude 34° 48′N), and the 702 eclipse was observed at Ch'ang-an (approximate longitude 108° 55′E, latitude 34° 15′N).

From the condition that the AD 616 eclipse was annular at Lo-yang, the AD 628 eclipse was total at Asuka, and the AD 702 eclipse was not total at Ch'ang-an, the following ΔT values are derived:

Date	Place	Possible range of ΔT
616 May 21	Lo-yang, China	2278 sec $\leq \Delta T \leq$ 3002 sec
628 April 10	Asuka, Japan	2267 sec $\leq \Delta T \leq$ 2959 sec
702 Sept. 26	Ch'ang-an, China	$\Delta T \leq$ 1429 sec or 2728 sec $\leq \Delta T$

The common range of the ΔT value for the three eclipses is 2728 sec $\leq \Delta T \leq$ 2959 sec, but since it is hard to believe that the ΔT value was constant from 616 to 702, we conclude here that the ΔT value was about 3000 sec in the 7th century as opposed to about 4000 sec given by Stephenson (1997).

By adopting the value $\Delta T = 3000$ sec, the magnitudes of the AD 628 eclipse and the AD 637 eclipse at Asuka are 1.00 and 0.88, respectively, which agrees with the records in the Nihongi.

There is another record in the Nihongi which supports our value of ΔT. A lunar occultation of Mars of 681 November 3 was recorded as "Mars was occulted" in the Nihongi. Our calculations show that actually Mars was not occulted at Asuka but the apparent distance of Mars' center from the lunar limb at the closest approach depends on the adopted ΔT value as follows:

ΔT	Distance
3000 sec	$34''$
4000 sec	$71''$

The Moon's age was 17.3 days and the Moon's phase (fraction of the area of the apparent disk that is illuminated by the Sun) was 95%, but Mars' altitude was 70 deg above the horizon and Mars' magnitude was -1.3 so that Mars was bright enough to be seen near the Moon. Considering that the angular resolution of naked eyes should be usually better than about $60''$, $\Delta T = 4000$ sec cannot be accepted from the occultation report, but it is seen that $\Delta T = 3000$ sec is acceptable from the above calculations.

For the present calculations, $-13''T^2$ is adopted for the tidal term of the lunar mean longitude, where T is the time in centuries. This coefficient is the one obtained by Dickey et al. (1994)

from the analysis of the recent lunar laser ranging measurements, and it is consistent with that derived by Morrison and Ward (1975) from the comparison of the observations of transits of Mars and lunar occultations of stars which covered the period from 1677 to 1973. However it is questionable if this coefficient has been constant since the 7th century. The ΔT values obtained from the eclipse records depend on the coefficient of the tidal term. The dependence will be investigated elsewhere.

3. CONCLUSION

From the eclipse and occultation observations recorded in Japan and China, it is concluded that the ΔT value was about 3000 sec in the 7th century.

4. REFERENCES

Dickey J.O., Bender P.L., Faller J.E., Newhall X X, Ricklefs R.L., Ries J.G., Shelus P.J., Veillet C., Whipple A.L., Wiant J.R., Williams J.G., and Yoder C.F. 1994, *Science*, **265**, 482–490.

Morrison L.V. and Ward C.G. 1975, *Mon. Not. R. Astr. Soc.*, **173**, 183–206.

Saito K. and Ozawa K. 1992, *Ancient Astronomical Records in China*, Yûzankaku (in Japanese).

Stephenson F.R. 1997, *Historical Eclipses and Earth's Rotation*, Cambridge University Press.

Watanabe T. 1994, *Solar and Lunar Eclipses Recorded in China, Korea, and Japan*, Yûzankaku (in Japanese).

TIME TRANSFER AND FREQUENCY SHIFT UP TO THE ORDER $1/c^4$ IN THE FIELD OF AN AXISYMMETRIC ROTATING BODY

P. TEYSSANDIER
SYRTE/UMR 8630-CNRS
Observatoire de Paris, 61 avenue de l'Observatoire, F-75014 Paris, France
E-mail: pierre.teyssandier@obspm.fr

B. LINET
Laboratoire de Mathématiques et Physique Théorique, UMR 6083-CNRS
Université François Rabelais, F-37200 Tours, France
E-mail: linet@celfi.phys.univ-tours.fr

ABSTRACT. We present a general procedure to determine up to the order $1/c^4$ the relativistic influence of the mass and spin multipoles on the time transfers and the frequency shifts in the vicinity of an isolated, axisymmetric rotating body. This procedure is applied within the Nordtvedt-Will parametrized post-Newtonian formalism. We give explicit formulae for the contributions of the mass, of the quadrupole moment and of the angular momentum of the rotating body.

1. INTRODUCTION

The art of ultraprecise timekeeping is rapidly progressing. The laser-cooled atomic clock PHARAO scheduled to fly on the International Space Station (ISS) in 2006 or 2007 is expected to stick with an accuracy of 10^{-16} (ESA/ACES mission). The NIST/NASA/JPL PARCS experiment scheduled for launch in 2007 is projected to enter the 5×10^{-17} accuracy range. And new kinds of optical clocks extracting time from calcium atoms or mercury ions are expected to reach an accuracy of the order of 10^{-18} in the foreseeable future.

At a level of uncertainty about 10^{-18}, a fully relativistic calculation of the time and frequency transfers must be performed up to the order $1/c^4$ within the post-Newtonian formalism. We present here the results that we have recently obtained at this order of approximation for an isolated, axisymmetric rotating body having a stationary gravitational field (Linet and Teyssandier 2002, denoted by LT (2002) in what follows). The problem is treated within the Nordtvedt-Will parametrized post-Newtonian (PPN) formalism (Will 1993). It seems that in the previous works devoted to the time and frequency transfers between a satellite and the ground, the calculations were carried out only up to the order $1/c^3$, in the narrow context of general relativity (see Blanchet et al. (2001) and Refs. therein).

Our procedure gives means of determining the contributions of all the mass and spin multipoles of the rotating body. We obtain explicit expressions for the contributions of the mass, of the quadrupole moment and of the angular momentum. The numerical estimates are performed

for a photon emitted from a satellite A orbiting at the altitude $h = 400$ km and received by a terrestrial station B.

2. THE WORLD FUNCTION

We use the method of the world function (Synge 1964), which presents the great advantage to spare the trouble of solving the differential equations of light rays. So we recall the definition and the fundamental properties of this function. Spacetime is assumed to be covered by a global quasi-Cartesian coordinate system $(x^\mu) = (x^0, \boldsymbol{x})$, with $x^0 = ct$. The metric is denoted by $g_{\mu\nu}$. The signature of the metric is -2.

Consider two points $x_A = (ct_A, \boldsymbol{x}_A)$ and $x_B = (ct_B, \boldsymbol{x}_B)$. If these points are close enough to one another, they are connected by a unique geodesic path Γ_{AB}. The world function is the two-point function $\Omega(x_A, x_B)$ defined by

$$\Omega(x_A, x_B) = \frac{1}{2}\varepsilon_{AB}\left[s_{AB}\right]^2 , \tag{1}$$

where s_{AB} is the geodesic distance between x_A and x_B and $\varepsilon_{AB} = 1, 0, -1$ according to whether Γ_{AB} is a timelike, null or spacelike geodesic, respectively.

The world function has the following properties.

i) In a vacuum, a light ray is a null geodesic of the metric g. As a consequence, two points x_A and x_B are linked by a light ray if and only if the condition

$$\Omega(x_A, x_B) \equiv \Omega(ct_A, \boldsymbol{x}_A, ct_B, \boldsymbol{x}_B) = 0 \tag{2}$$

is fulfilled. Solving this equation for t_B yields the travel time $t_B - t_A$ of a photon emitted at x_A and received at x_B as a function of t_A, $\boldsymbol{x}_A$ and $\boldsymbol{x}_B$: $t_B - t_A = \mathcal{T}(t_A, \boldsymbol{x}_A, \boldsymbol{x}_B)$. This function is called the time transfer function.

ii) Let x_A and x_B be two points connected by a null geodesic Γ_{AB}. The covariant components of the vector $p^\alpha = dx^\alpha/d\lambda$ tangent to Γ_{AB}, respectively, at x_A and x_B are given by

$$(p_\alpha)_A \equiv \left(g_{\alpha\beta}\frac{dx^\beta}{d\lambda}\right)_A = -\frac{\partial\Omega}{\partial x_A^\alpha}, \qquad (p_\alpha)_B \equiv \left(g_{\alpha\beta}\frac{dx^\beta}{d\lambda}\right)_B = \frac{\partial\Omega}{\partial x_B^\alpha}, \tag{3}$$

where λ is the unique affine parameter along Γ_{AB} such that $\lambda_A = 0$ and $\lambda_B = 1$.

Thus, if $\Omega(x_A, x_B)$ is known, it is possible to determine the frequency shift between x_A and x_B. Indeed, let ν_A be the proper frequency of a photon as measured by an observer A at x_A moving with the unit 4-velocity $u_A^\alpha = (dx^\alpha/ds)_A$ and ν_B be the proper frequency of the same photon as measured by an observer B at x_B moving with the unit 4-velocity $u_B^\alpha = (dx^\alpha/ds)_B$. The frequency shift $\nu_A/\nu_B - 1$ is given by the well-known formula

$$\frac{\nu_A}{\nu_B} - 1 = \frac{u_A^\alpha (p_\alpha)_A}{u_B^\alpha (p_\alpha)_A} - 1 . \tag{4}$$

In what follows, we suppose that the light rays are propagating in a stationary gravitational field generated by an isolated, axisymmetric rotating body. The coordinates are chosen so that the metric does not depend on x^0. Then the world function is of the form $\Omega(x_B^0 - x_A^0, \boldsymbol{x}_A, \boldsymbol{x}_B)$ and the travel time of a photon propagating from x_A to x_B may be written as

$$t_B - t_A = \mathcal{T}(\boldsymbol{x}_A, \boldsymbol{x}_B) . \tag{5}$$

If the time transfer function $\mathcal{T}(\boldsymbol{x}_A, \boldsymbol{x}_B)$ is known, it is easy to determine the frequency shift between A and B since it can be shown that Eq. (4) reduces to

$$\frac{\nu_A}{\nu_B} - 1 = \frac{u_A^0}{u_B^0} \times \frac{1 + \boldsymbol{v}_A \cdot \nabla_{\boldsymbol{x}_A}\mathcal{T}}{1 - \boldsymbol{v}_B \cdot \nabla_{\boldsymbol{x}_B}\mathcal{T}} - 1 , \tag{6}$$

where $\boldsymbol{v}_A = (d\boldsymbol{x}/dt)_A$ and $\boldsymbol{v}_B = (d\boldsymbol{x}/dt)_B$ are the coordinate velocities of the clocks comoving with A and B, respectively.

3. TIME TRANSFER AND FREQUENCY SHIFT

The center of mass O of the rotating body is taken as the origin of the coordinates $(\boldsymbol{x})$, Ox^3 being both the axis of symmetry and the axis of rotation. The angular momentum of the body about Ox^3 is denoted by $\boldsymbol{S}$. The unit vector along the x^3-axis is denoted by $\boldsymbol{k}$. We write $\boldsymbol{S} = S\boldsymbol{k}$. We put $r = |\boldsymbol{x}|$, $r_A = |\boldsymbol{x}_A|$, $r_B = |\boldsymbol{x}_B|$. We denote by r_e the equatorial radius. We call θ the angle between $\boldsymbol{x}$ and $\boldsymbol{k}$. We denote by $\boldsymbol{v}_r$ the velocity of the center of mass O relative to the universe rest frame.

With a convenient choice of coordinates, the PPN metric may be written in the form

$$g_{00} = 1 - \frac{2}{c^2}W + \frac{2\beta}{c^4}W^2 + \frac{1}{c^4}f(\xi, \alpha_2, \alpha_3, \zeta_1, ..., \zeta_4) + O(6)\,, \tag{7}$$

$$\{g_{0i}\} = \frac{2}{c^3}\left[(\gamma + 1 + \frac{1}{4}\alpha_1)\boldsymbol{W} + \frac{1}{4}\alpha_1 \boldsymbol{v}_r\, W\right] + O(5)\,, \tag{8}$$

$$g_{ij} = -\left(1 + \frac{2\gamma}{c^2}\, W\right)\delta_{ij} + O(4)\,, \tag{9}$$

where $f(\xi, \alpha_2, \alpha_3, \zeta_1, ..., \zeta_4)$ denotes contributions involving post-Newtonian parameters that we do not take into account here and W and $\boldsymbol{W}$ are potentials which may be expanded in multipole series of the form

$$W(\boldsymbol{x}) = \frac{GM}{r}\left[1 - \sum_{n=2}^{\infty} J_n \left(\frac{r_e}{r}\right)^n P_n(\cos\theta)\right]\,, \tag{10}$$

$$\boldsymbol{W}(\boldsymbol{x}) = \frac{G\boldsymbol{S}\times\boldsymbol{x}}{2r^3}\left[1 - \sum_{n=1}^{\infty} K_n \left(\frac{r_e}{r}\right)^n P'_{n+1}(\cos\theta)\right] \tag{11}$$

in the region $r > r_e$.

In these equations, the P_n are the Legendre polynomials; M, J_2, ..., J_n, ..., $\boldsymbol{S}$, ..., K_n, ... correspond to the generalized Blanchet-Damour mass and spin multipole moments (Blanchet 1989, Damour et al 1991 , Klioner and Soffel 2000). Note that the coefficients K_n in Eq. (11) coincide up to $1/c^2$ terms with the spin multipole moments calculated by one of us (Teyssandier 1977 and 1978).

Putting $\boldsymbol{R}_{AB} = \boldsymbol{x}_B - \boldsymbol{x}_A$ and $R_{AB} = |\boldsymbol{x}_B - \boldsymbol{x}_A|$, we have shown that the world function $\Omega(x_A, x_B)$ may be written in the form

$$\begin{aligned}\Omega(x_A, x_B) = {} & \frac{1}{2}\left[(x_B^0 - x_A^0)^2 - R_{AB}^2\right] - \frac{1}{c^2}\left[(x_B^0 - x_A^0)^2 + \gamma R_{AB}^2\right]\mathcal{W}(\boldsymbol{x}_A, \boldsymbol{x}_B) \\ & + \frac{2}{c^3}(\gamma + 1 + \frac{1}{4}\alpha_1)(x_B^0 - x_A^0)\boldsymbol{R}_{AB}\cdot\boldsymbol{\mathcal{W}}(\boldsymbol{x}_A, \boldsymbol{x}_B) \\ & + \frac{1}{2c^3}\alpha_1(x_B^0 - x_A^0)(\boldsymbol{R}_{AB}\cdot\boldsymbol{v}_r)\mathcal{W}(\boldsymbol{x}_A, \boldsymbol{x}_B) + O(4)\,,\end{aligned} \tag{12}$$

where $\mathcal{W}(\boldsymbol{x}_A, \boldsymbol{x}_B)$ and $\boldsymbol{\mathcal{W}}(\boldsymbol{x}_A, \boldsymbol{x}_B)$ are given by the following multipole expansions when $r > r_e$:

$$\mathcal{W}(\boldsymbol{x}_A, \boldsymbol{x}_B) = GM\left[1 - \sum_{n=2}^{\infty}\frac{1}{n!}J_n r_e^n \frac{\partial^n}{\partial z^n}\right] F(\boldsymbol{x}, \boldsymbol{x}_A, \boldsymbol{x}_B)\Big|_{\boldsymbol{x}=0}\,, \tag{13}$$

$$\boldsymbol{\mathcal{W}}(\boldsymbol{x}_A, \boldsymbol{x}_B) = -\frac{1}{2}G\boldsymbol{S}\times\nabla\left[1 - \sum_{n=1}^{\infty}\frac{1}{n!}K_n r_e^n \frac{\partial^n}{\partial z^n}\right] F(\boldsymbol{x}, \boldsymbol{x}_A, \boldsymbol{x}_B)\Big|_{\boldsymbol{x}=0}\,, \tag{14}$$

the kernel function $F(\boldsymbol{x},\boldsymbol{x}_A,\boldsymbol{x}_B)$ being defined as

$$F(\boldsymbol{x},\boldsymbol{x}_A,\boldsymbol{x}_B)=\frac{1}{R_{AB}}\ln\left(\frac{\mid \boldsymbol{x}-\boldsymbol{x}_A\mid+\mid \boldsymbol{x}-\boldsymbol{x}_B\mid+R_{AB}}{\mid \boldsymbol{x}-\boldsymbol{x}_A\mid+\mid \boldsymbol{x}-\boldsymbol{x}_B\mid-R_{AB}}\right). \tag{15}$$

These formulae show that the multipole expansion of $\Omega(x_A,x_B)$ can be thoroughly calculated up to the order $1/c^3$ by straightforward differentiations of the kernel function given by (15). Note that integral expressions of $\mathcal{W}$ and $\boldsymbol{\mathcal{W}}$ valid everywhere are also given in LT (2002).

We have shown that the time transfer $\mathcal{T}(\boldsymbol{x}_A,\boldsymbol{x}_B)$ and its multipole expansion can be explicitly calculated up to the order $1/c^4$ when $\Omega(x_A,x_B)$ is known up to the order $1/c^3$. In the present communication, we retain only the contributions due to M, J_2 and $\boldsymbol{S}$. Thus, putting

$$\boldsymbol{n}_A=\frac{\boldsymbol{x}_A}{r_A},\quad \boldsymbol{n}_B=\frac{\boldsymbol{x}_B}{r_B},\quad \boldsymbol{N}_{AB}=\frac{\boldsymbol{x}_B-\boldsymbol{x}_A}{R_{AB}}, \tag{16}$$

and using the identity $(r_A+r_B)^2-R_{AB}^2=2r_Ar_B(1+\boldsymbol{n}_A\cdot\boldsymbol{n}_B)$, we get

$$\mathcal{T}(\boldsymbol{x}_A,\boldsymbol{x}_B)=\frac{1}{c}R_{AB}+\mathcal{T}_M(\boldsymbol{x}_A,\boldsymbol{x}_B)+\mathcal{T}_{J_2}(\boldsymbol{x}_A,\boldsymbol{x}_B)+\mathcal{T}_{\boldsymbol{S}}(\boldsymbol{x}_A,\boldsymbol{x}_B)+\mathcal{T}_{\boldsymbol{v}_r}(\boldsymbol{x}_A,\boldsymbol{x}_B)+\cdots,$$

where

$$\mathcal{T}_M(\boldsymbol{x}_A,\boldsymbol{x}_B)=(\gamma+1)\frac{GM}{c^3}\ln\left(\frac{r_A+r_B+R_{AB}}{r_A+r_B-R_{AB}}\right), \tag{17}$$

$$\mathcal{T}_{J_2}(\boldsymbol{x}_A,\boldsymbol{x}_B)=-\frac{\gamma+1}{2}\frac{GM}{c^3}\frac{J_2r_e^2}{r_Ar_B}\frac{R_{AB}}{1+\boldsymbol{n}_A\cdot\boldsymbol{n}_B}\left[\left(\frac{1}{r_A}+\frac{1}{r_B}\right)\frac{(\boldsymbol{k}\cdot\boldsymbol{n}_A+\boldsymbol{k}\cdot\boldsymbol{n}_B)^2}{1+\boldsymbol{n}_A\cdot\boldsymbol{n}_B}-\frac{(\boldsymbol{k}\times\boldsymbol{n}_A)^2}{r_A}-\frac{(\boldsymbol{k}\times\boldsymbol{n}_B)^2}{r_B}\right], \tag{18}$$

$$\mathcal{T}_{\boldsymbol{S}}(\boldsymbol{x}_A,\boldsymbol{x}_B)=-(\gamma+1+\frac{1}{4}\alpha_1)\frac{GS}{c^4}\left(\frac{1}{r_A}+\frac{1}{r_B}\right)\frac{\boldsymbol{k}\cdot(\boldsymbol{n}_A\times\boldsymbol{n}_B)}{1+\boldsymbol{n}_A\cdot\boldsymbol{n}_B}, \tag{19}$$

$$\mathcal{T}_{\boldsymbol{v}_r}(\boldsymbol{x}_A,\boldsymbol{x}_B)=-\alpha_1\frac{GM}{2c^4}(\boldsymbol{N}_{AB}\cdot\boldsymbol{v}_r)\ln\left(\frac{r_A+r_B+R_{AB}}{r_A+r_B-R_{AB}}\right). \tag{20}$$

The term of order $1/c^3$ given by (17) is the well-known Shapiro time delay. Equations (18) and (19) extend results previously found for $\gamma=1$ and $\alpha_1=0$ (Klioner 1991, Klioner and Kopeikin 1992 ; see also, e.g., Ciufolini et al 2003 and Refs. therein).

Using Eq. (6) and Eqs. (17)-(20), it is possible to perform the calculation of the ratio ν_A/ν_B up to the order $1/c^4$ if the terms of the same order in g_{00} are taken into account. For the sake of simplicity, we henceforth confine ourselves to the fully conservative metric theories of gravity without preferred location effects, in which all the PPN parameters vanish except β and γ. Since the gravitational field is assumed to be stationary, the chosen coordinate system is then a standard post-Newtonian gauge and the metric takes its usual post-Newtonian form (Klioner and Soffel 2000). Then, retaining only the contributions due to M, J_2 and $\boldsymbol{S}$ in the terms of orders $1/c^3$ and $1/c^4$, we have found that the frequency shift ν_A/ν_B-1 may be written as

$$\frac{\nu_A}{\nu_B}-1=\left(\frac{\delta\nu}{\nu}\right)_c+\left(\frac{\delta\nu}{\nu}\right)_g, \tag{21}$$

where $(\delta\nu/\nu)_c$ is the special relativistic Doppler effect given by

$$\begin{aligned}\left(\frac{\delta\nu}{\nu}\right)_c &= -\frac{1}{c}\left[\boldsymbol{N}_{AB}\cdot(\boldsymbol{v}_A-\boldsymbol{v}_B)\right]+\frac{1}{c^2}\left[\frac{1}{2}v_A^2-\frac{1}{2}v_B^2-[\boldsymbol{N}_{AB}\cdot(\boldsymbol{v}_A-\boldsymbol{v}_B)](\boldsymbol{N}_{AB}\cdot\boldsymbol{v}_B)\right]\\ &\quad-\frac{1}{c^3}[\boldsymbol{N}_{AB}\cdot(\boldsymbol{v}_A-\boldsymbol{v}_B)]\left[\frac{1}{2}v_A^2-\frac{1}{2}v_B^2+(\boldsymbol{N}_{AB}\cdot\boldsymbol{v}_B)^2\right] \qquad (22)\\ &\quad+\frac{1}{c^4}\left\{\frac{3}{8}v_A^4-\frac{1}{4}v_A^2v_B^2-\frac{1}{8}v_B^4\right.\\ &\quad\left.-[\boldsymbol{N}_{AB}\cdot(\boldsymbol{v}_A-\boldsymbol{v}_B)](\boldsymbol{N}_{AB}\cdot\boldsymbol{v}_B)\left[\frac{1}{2}v_A^2-\frac{1}{2}v_B^2+(\boldsymbol{N}_{AB}\cdot\boldsymbol{v}_B)^2\right]\right\}+O(5)\end{aligned}$$

and $(\delta\nu/\nu)_g$ is the gravitational part given by

$$\left(\frac{\delta\nu}{\nu}\right)_g=\frac{1}{c^2}(W_A-W_B)+\frac{1}{c^3}\left(\frac{\delta\nu}{\nu}\right)_M^{(3)}+\frac{1}{c^3}\left(\frac{\delta\nu}{\nu}\right)_{J_2}^{(3)}+\frac{1}{c^4}\left(\frac{\delta\nu}{\nu}\right)_M^{(4)}+\frac{1}{c^4}\left(\frac{\delta\nu}{\nu}\right)_{\boldsymbol{S}}^{(4)}+\cdots,$$

the different terms being separately made explicit and briefly estimated in what follows.

The term $(\delta\nu/\nu)_M^{(3)}$ due to the mass reads

$$\begin{aligned}\left(\frac{\delta\nu}{\nu}\right)_M^{(3)} &= -GM\left(\frac{1}{r_A}+\frac{1}{r_B}\right)\left\{\left(\frac{\gamma+1}{1+\boldsymbol{n}_A\cdot\boldsymbol{n}_B}-\frac{r_A-r_B}{r_A+r_B}\right)[\boldsymbol{N}_{AB}\cdot(\boldsymbol{v}_A-\boldsymbol{v}_B)]\right.\\ &\quad\left.+(\gamma+1)\frac{R_{AB}}{r_A+r_B}\frac{\boldsymbol{n}_A\cdot\boldsymbol{v}_A+\boldsymbol{n}_B\cdot\boldsymbol{v}_B}{1+\boldsymbol{n}_A\cdot\boldsymbol{n}_B}\right\}. \qquad (23)\end{aligned}$$

With K_{AB} defined as

$$K_{AB}=\frac{(r_A-r_B)^2}{r_Ar_B} \qquad (24)$$

the term $(\delta\nu/\nu)^{(3)}_{J_2}$ may be written as

$$\begin{aligned}
\left(\frac{\delta\nu}{\nu}\right)^{(3)}_{J_2} &= \frac{GMJ_2}{2r_e}[\boldsymbol{N}_{AB}\cdot(\boldsymbol{v}_A-\boldsymbol{v}_B)]\left[\left(\frac{r_e}{r_A}\right)^3\left[3(\boldsymbol{k}\cdot\boldsymbol{n}_A)^2-1\right]-\left(\frac{r_e}{r_B}\right)^3\left[3(\boldsymbol{k}\cdot\boldsymbol{n}_B)^2-1\right]\right]\\
&+\frac{\gamma+1}{2}\,\frac{GM\,J_2r_e^2(r_A+r_B)}{r_A^2r_B^2}\,\frac{1}{(1+\boldsymbol{n}_A\cdot\boldsymbol{n}_B)^2}\\
&\times\Bigg\{[\boldsymbol{N}_{AB}\cdot(\boldsymbol{v}_A-\boldsymbol{v}_B)]\left[(\boldsymbol{k}\cdot\boldsymbol{n}_A+\boldsymbol{k}\cdot\boldsymbol{n}_B)^2\,\frac{5-3\boldsymbol{n}_A\cdot\boldsymbol{n}_B+2K_{AB}}{1+\boldsymbol{n}_A\cdot\boldsymbol{n}_B}\right.\\
&\left.-\left(1-\frac{r_A(\boldsymbol{k}\cdot\boldsymbol{n}_B)^2+r_B(\boldsymbol{k}\cdot\boldsymbol{n}_A)^2}{r_A+r_B}\right)(3-\boldsymbol{n}_A\cdot\boldsymbol{n}_B+K_{AB})\right]\\
&+\frac{R_{AB}}{r_A+r_B}(\boldsymbol{n}_A\cdot\boldsymbol{v}_A+\boldsymbol{n}_B\cdot\boldsymbol{v}_B)(\boldsymbol{k}\cdot\boldsymbol{n}_A+\boldsymbol{k}\cdot\boldsymbol{n}_B)^2\,\frac{7-\boldsymbol{n}_A\cdot\boldsymbol{n}_B+2K_{AB}}{1+\boldsymbol{n}_A\cdot\boldsymbol{n}_B}\\
&-\frac{R_{AB}}{r_A}(\boldsymbol{n}_A\cdot\boldsymbol{v}_A)\left[1-3(\boldsymbol{k}\cdot\boldsymbol{n}_A)^2\right]\frac{r_A+r_B(2+\boldsymbol{n}_A\cdot\boldsymbol{n}_B)}{r_A+r_B}\\
&-\frac{R_{AB}}{r_B}(\boldsymbol{n}_B\cdot\boldsymbol{v}_B)\left[1-3(\boldsymbol{k}\cdot\boldsymbol{n}_B)^2\right]\frac{r_A(2+\boldsymbol{n}_A\cdot\boldsymbol{n}_B)+r_B}{r_A+r_B}\\
&+R_{AB}\left[2\left(\frac{\boldsymbol{n}_A\cdot\boldsymbol{v}_A}{r_A}+\frac{\boldsymbol{n}_B\cdot\boldsymbol{v}_B}{r_B}\right)(\boldsymbol{k}\cdot\boldsymbol{n}_A)(\boldsymbol{k}\cdot\boldsymbol{n}_B)\right.\\
&\left.-(\boldsymbol{n}_A\cdot\boldsymbol{v}_A)\frac{1-(\boldsymbol{k}\cdot\boldsymbol{n}_B)^2}{r_B}-(\boldsymbol{n}_B\cdot\boldsymbol{v}_B)\frac{1-(\boldsymbol{k}\cdot\boldsymbol{n}_A)^2}{r_A}\right]\\
&-2\,\frac{R_{AB}}{r_A}(\boldsymbol{k}\cdot\boldsymbol{v}_A)\left[\boldsymbol{k}\cdot\boldsymbol{n}_A\frac{r_A+r_B(2+\boldsymbol{n}_A\cdot\boldsymbol{n}_B)}{r_A+r_B}+\boldsymbol{k}\cdot\boldsymbol{n}_B\right]\\
&-2\,\frac{R_{AB}}{r_B}(\boldsymbol{k}\cdot\boldsymbol{v}_B)\left[\boldsymbol{k}\cdot\boldsymbol{n}_A+\boldsymbol{k}\cdot\boldsymbol{n}_B\frac{r_A(2+\boldsymbol{n}_A\cdot\boldsymbol{n}_B)+r_B}{r_A+r_B}\right]\Bigg\}.
\end{aligned}\tag{25}$$

A crude estimate for the ISS shows that if $\gamma=1$, then

$$\left|\frac{1}{c^3}\left(\frac{\delta\nu}{\nu}\right)^{(3)}_{J_2}\right|\leq\ 1.3\times10^{-16}\,.\tag{26}$$

So, it will perhaps be necessary to take into account this effect of J_2 in ACES or PARCS experiments. However, a lower bound will be found if the inclination of the orbit of the ISS and the latitude of the terrestrial station are taken into account.

At the order $1/c^4$, the contribution of the mass is given by

$$\begin{aligned}
\left(\frac{\delta\nu}{\nu}\right)^{(4)}_{M} &= (\gamma+1)\left(\frac{GM}{r_A}v_A^2-\frac{GM}{r_B}v_B^2\right)-\frac{1}{2}\frac{GM(r_A-r_B)}{r_Ar_B}(v_A^2-v_B^2)\\
&-GM\left(\frac{1}{r_A}+\frac{1}{r_B}\right)\left[\left(\frac{2(\gamma+1)}{1+\boldsymbol{n}_A\cdot\boldsymbol{n}_B}-\frac{r_A-r_B}{r_A+r_B}\right)[\boldsymbol{N}_{AB}\cdot(\boldsymbol{v}_A-\boldsymbol{v}_B)](\boldsymbol{N}_{AB}\cdot\boldsymbol{v}_B)\right.\\
&\left.+\frac{\gamma+1}{1+\boldsymbol{n}_A\cdot\boldsymbol{n}_B}\frac{R_{AB}}{r_A+r_B}\left\{(\boldsymbol{n}_A\cdot\boldsymbol{v}_A)(\boldsymbol{N}_{AB}\cdot\boldsymbol{v}_B)-[\boldsymbol{N}_{AB}\cdot(\boldsymbol{v}_A-2\boldsymbol{v}_B)](\boldsymbol{n}_B\cdot\boldsymbol{v}_B)\right\}\right]\\
&+\frac{1}{2}\left(\frac{GM}{r_Ar_B}\right)^2\left[(r_A-r_B)^2+2(\beta-1)(r_A^2-r_B^2)\right]\,.
\end{aligned}\tag{27}$$

The dominant term $(\gamma+1)GM/r_Av_A^2$ in (27) induces a correction to the frequency shift which amounts to 10^{-18}. So, it will certainly be necessary to take this term into account in experiments performed in the foreseeable future.

Finally, the term $c^{-4}(\delta\nu/\nu)^{(4)}_{\boldsymbol{S}}$ due to the angular momentum is

$$\begin{aligned}\left(\frac{\delta\nu}{\nu}\right)^{(4)}_{\boldsymbol{S}} &= (\gamma+1)\,\frac{GS}{r_A r_B}\,\boldsymbol{v}_A\cdot\left\{\left(1+\frac{r_B}{r_A}\right)\frac{\boldsymbol{k}\times\boldsymbol{n}_B}{1+\boldsymbol{n}_A\cdot\boldsymbol{n}_B}-\frac{r_B}{r_A}\,(\boldsymbol{k}\times\boldsymbol{n}_A)\right.\\ &\quad\left.+\,\frac{\boldsymbol{k}\cdot(\boldsymbol{n}_A\times\boldsymbol{n}_B)}{(1+\boldsymbol{n}_A\cdot\boldsymbol{n}_B)^2}\left[\left(1+\frac{r_B}{r_A}(2+\boldsymbol{n}_A\cdot\boldsymbol{n}_B)\right)\boldsymbol{n}_A+\left(1+\frac{r_B}{r_A}\right)\boldsymbol{n}_B\right]\right\}\\ &\quad-(\gamma+1)\,\frac{GS}{r_A r_B}\,\boldsymbol{v}_B\cdot\left\{\left(1+\frac{r_A}{r_B}\right)\frac{\boldsymbol{k}\times\boldsymbol{n}_A}{1+\boldsymbol{n}_A\cdot\boldsymbol{n}_B}-\frac{r_A}{r_B}\,(\boldsymbol{k}\times\boldsymbol{n}_B)\right.\\ &\quad\left.-\,\frac{\boldsymbol{k}\cdot(\boldsymbol{n}_A\times\boldsymbol{n}_B)}{(1+\boldsymbol{n}_A\cdot\boldsymbol{n}_B)^2}\left[\left(1+\frac{r_A}{r_B}(2+\boldsymbol{n}_A\cdot\boldsymbol{n}_B)\right)\boldsymbol{n}_B+\left(1+\frac{r_A}{r_B}\right)\boldsymbol{n}_A\right]\right\}.\end{aligned}\tag{28}$$

Taking for the Earth $S = 5.86\times10^{33}$ kg m^2 s^{-1}, we obtain the inequality

$$\left|\frac{1}{c^4}\left(\frac{\delta\nu}{\nu}\right)^{(4)}_{\boldsymbol{S}}\right| \le (\gamma+1)\times10^{-19}\,.\tag{29}$$

Thus, our formula confirms that the effect of the angular momentum of the Earth on the frequency shift will not affect the ACES or PARCS experiments.

4. REFERENCES

Blanchet, L., Salomon, C., Teyssandier, P. and Wolf, P., 2001, *Astron. Astrophys.* **370**, 320.

Blanchet, L. and Damour, T., 1989, Ann. Inst. H. Poincaré Phys. Théor. **50**, 377.

Ciufolini, I., Kopeikin, S. M., Mashhoon, B., and Ricci, F., Phys. Lett. A, 2003, **308**, 101.

Damour, T., Soffel, M. and Xu, C., 1991, *Phys. Rev. D* **43**, 3273.

Klioner, S. A., 1991, *Sov. Astron.* **35**, 523.

Klioner, S. A. and Kopeikin, S. M., 1992, *Astron. J.* **104**, 897.

Klioner, S. A. and Soffel, M., 2000 *Phys. Rev. D* **62**, 024019.

Linet, B. and Teyssandier, P., 2002, *Phys. Rev. D* **66**, 024045.

Synge, J. L., 1964, *Relativity: the General Theory* (North-Holland).

Teyssandier, P., 1977, *Phys. Rev. D* **16**, 946; 1978, *Phys. Rev. D* **18**, 1037.

Will, C. 1993, *Theory and Experiment in Gravitational Physics*, revised edition (Cambridge University Press).

ATOMIC FREQUENCY STANDARDS AND TIME MEASUREMENT

C. MANDACHE[(1)], Y. SORTAIS[(2)], S. BIZE[(2)], F. PEREIRA DOS SANTOS[(2)],
M. ABGRALL[(2)], S. ZHANG[(2)], D. CALONICO[(2)], H. MARION[(2)],
Y. MACSIMOVIC[(2)], P. LEMONDE[(2)], G. SANTARELLI[(2)],
P. LAURENT[(2)], C. SALOMON[(3)] and A. CLAIRON[(2)]

(1) Institutul National de Fizica Laserilor, Plasmei si Radiatiei
P.O.Box-MG36, Bucuresti, Magurele, Romania
(2) BNM-SYRTE, Observatoire de Paris
61 Av. de l'Observatoire, 75014 Paris, France
(3) Laboratoire Kastler Brossel, Ecole Normale Superieure
24 rue Lhomond, F-75231 Paris Cedex 05, France

"What is the time?"
"If no one asks me, I know. If I wish to explain it to one that asketh I know not."
St. Augustine of Hippo

1. INTRODUCTION

In the history of mankind, in his explorations and quest for knowledge, time has always played a crucial role. Without a precise measurement of time, many human activities, in particular space exploration, would hardly be feasible at the level of precision we know.

Time is a concept most difficult to comprehend. It has generated a multitude of essays of either philosophical or physical nature. However, for essentially all practical requirements, the notion of time has been reduced to one of measurement, without reference to its philosophical aspect.

To count the time that passes, or almanac (in Arabic, "almanac" means "to count"), is very simple for a child. He sees the Sun rising every morning and lying down every evening. The child is right on a short term scale. To evaluate time over millions of years is more complex and beyond our terrestrial concept of the length of a day. However, can we measure time well?

A first obvious thing to note is that the Moon turns around the Earth in a little less than 30 sunrises. One second obvious thing, discovered at least 3000 years ago, but accepted universally only 400 years ago is that the earth turns around the Sun. Celestial bodies - the Sun, the Moon, the planets, and the stars - have provided us with a reference frame for measuring the passage of time throughout our existence as human beings. Ancient civilizations relied upon the apparent motion of these celestial bodies to determine seasons, months, and years.

2. PEOPLE, CIVILIZATIONS AND TIME

Ice-age hunters in Europe over 20,000 years ago scratched lines and made holes in sticks and bones, possibly counting the days between phases of the moon. The earliest Egyptian calendar was based on the moon's cycles. Before 2000 BC, the Babylonians used a year of 12 alternating

29 day and 30 day lunar months, giving a year of 354 days. In contrast, the Mayas of Central America relied not only on the Sun and the Moon, but also on the planet Venus, to establish 365 day calendars.

As far as we know, great civilizations in the Middle East and North Africa began making clocks to improve their calendars about 5000 to 6000 years ago. Obelisks (slender, tapered, four-sided monuments) were built as early as 3500 BC. Their moving shadows formed a kind of sundial, enabling people to partition the day into morning and afternoon. Another Egyptian shadow clock or sundial, possibly the first transportable timepiece, came into use around 1500 BC. *The merkhet*, the oldest known astronomical tool, was an Egyptian invention developed around 600 BC. A pair of merkhets was used to establish a north-south line (or meridian) by aligning them with the Pole Star.

The history of time keeping is the story of the search for ever more consistent actions or processes to regulate the rate of a clock. Water clocks were among the earliest timekeepers that didn't depend on the observation of celestial bodies. The "water thief" later named by the Greeks *clepsydra*, one of the oldest clock, was found in the tomb of the Egyptian pharaoh Amenhotep I, and began to be used about 325 BC. More elaborate and impressive mechanized water clocks were developed between 100 BC and 500 AD by Greek and Roman clock-makers and astronomers. In the first half of the first century BC, a Macedonian astronomer, Andronikos, supervised the construction of his *Horologion*, known today as the Tower of the Winds, in Athens market place. In the first half of the 14th century, large mechanical clocks began to appear in the towers of several large Italian cities. In 1656, Christian Huygens, a Dutch scientist, made the first pendulum clock, regulated by a mechanism with a "natural" period of oscillation. Around 1675, Huygens developed the balance wheel and spring assembly, still found in some of today's wristwatches. Those improvements allowed portable 17th century watches to keep time with an accuracy of 10 minutes per day. In 1721, George Graham improved the pendulum clock's accuracy to 1 second per day by compensating for changes in the pendulum's length due to temperature variations. John Harrison, a carpenter and self-taught clock-maker, refined Graham's temperature compensation techniques and developed new methods for reducing friction. The performance of those clocks was overtaken by that of quartz crystal oscillators and clocks developed in the 1920s. Nowadays, the timekeeping performance of quartz clocks has been substantially surpassed by atomic clocks. Fig.1 shows in a dramatic way the evolution of time keeping.

Figure 1: Dramatic representation of time keeping evolution

The evolution of the quality of clocks during the century is illustrated in the Fig.2. There

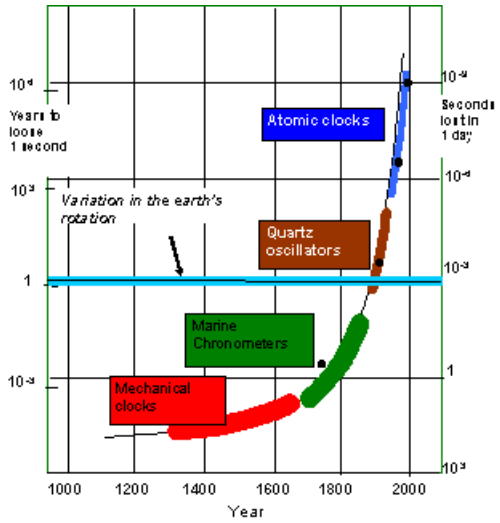

Figure 2: Evolution of the quality of clocks with time

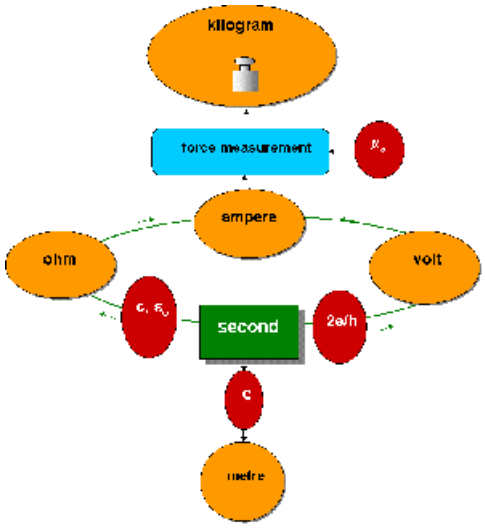

Figure 3: The unit of time - the second- as a central unit in the SI

has been a continuous improvement in quality and there is no end in sight.

3. THE UNIT OF TIME: THE SECOND

Time is the basic quantity in the International System of units (SI), whose representative unit, the second, was the first to be defined in terms of an atomic property: the hyperfine frequency of the cesium atom in its ground state. It is also the quantity that can be measured with the greatest accuracy due to the extraordinary development that has taken place in the field of atomic and laser physics. In present times, an accuracy of one part in 10^{15} in the implementation of the second is obtained routinely in the laboratory. Furthermore, the second plays a central role in the international system of units. Fig. 3 illustrates this concept by showing how all four independent basic quantities, length, current, mass and time are interconnected by means of fundamental constants. First the meter is directly connected to the second by means of the speed of light, c. The volt is connected directly to the second by means of h/2e (Josephson effect), where h is Plankc's constant and e is the charge of the electron. The ohm is related to the second by means of ϵ_0 and c (via the calculable capacitor) where ϵ_0 is the vacuum dielectric constant. Finally, the ampere is obtained by means of ohm's law. In principle, it is then possible to measure or monitor the kilogram by means of an ampere balance, a measurement that relies on the constant μ_0, the permeability of free space. All base units are then connected to fundamental constants. In this scheme, the kg could be lost and it would be possible to reconstitute it to an accuracy somewhat better than 10^{-7}.

4. Cs AND Rb FOUNTAINS AT SYRTE

At SYRTE, in Paris, one ^{87}Rb and two Cs fountains have been already constructed. A dual Cs and Rb fountain has been implemented in a (1,1,1) configuration (fig.4). Two optical benches, one for Rb and one for Cs, provide all the radiation fields required. They are completely separated and independent of each other and of the fountain mechanical structure. The benches are coupled to the vacuum chamber by means of polarizing optical fibres and through prealigned collimators. In the same trapping region Rb and Cs molasses are loaded by two atomic beams, pre-cooled by means of a chirping laser technique. The atomic beam flux at the exit of the oven

is about 10^{12} atoms/s for an oven temperature of 383 K. We collect up to 10^9 Cs atoms and detect up to 10^7 atoms for a 0.3 s loading time. A typical Ramsey fringes pattern is shown in Fig. 5, for a launching height is typically 0.865 m above the trapping region. This corresponding for a 0.53 s period between the two microwave interaction times, producing a 0.94 Hz FWHM for the central Ramsey fringe.

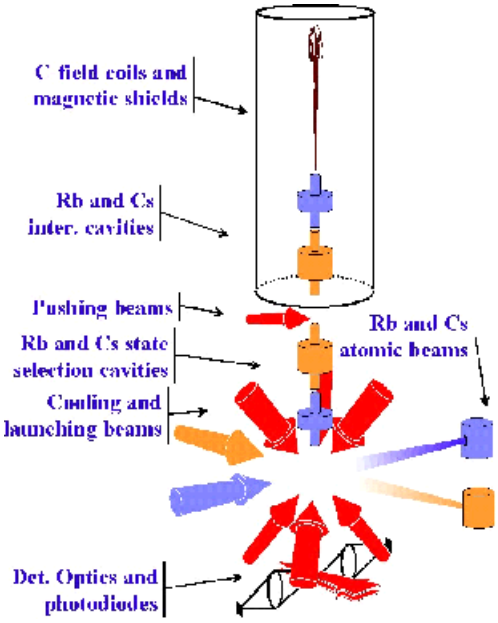

Figure 4: Dual atomic fountain FO2

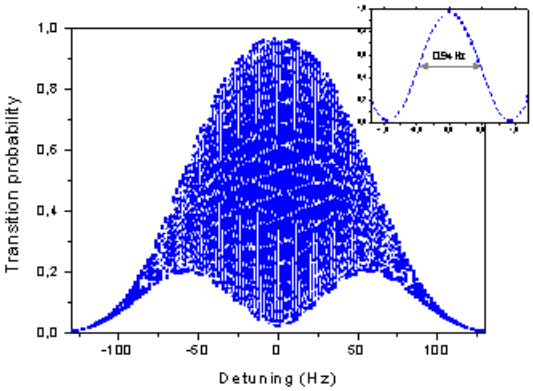

Figure 5: Ramsey fringes observed in fountain FO2

An atomic frequency standard is characterized by its stability and its accuracy. With an ultra-stable cryogenic sapphire oscillator as flywheel oscillator, a cesium fountain operates at the quantum projection noise limit. With 10^6 detected atoms, the relative frequency stability is $4.10^{-14}\tau^{-1/2}$. At t = 2.10^4 s the measured stability reaches 6 10-16. The accuracy of our fountain FO2 is presently slightly better than 10^{-15}. The error budget of the atomic fountain is given in Table 1

Effect	Rb	Cs
2nd order Zeeman	$(320{,}7 \pm 0{,}47).10^{-15}$	$(177{,}3 \pm 0{,}52).10^{-15}$
Blackbody Radiation	$(-12{,}7 \pm 0{,}21).10^{-15}$	$(-17{,}3 \pm 0{,}23).10^{-15}$
Cold collision and cavity pulling	$(0 \pm 0{,}1).10^{-15}$	$(-9{,}5 \pm 0{,}46).10^{-15}$
First order Doppler	$(0 \pm 0{,}2).10^{-15}$	$(0 \pm 0{,}2).10^{-15}$
Other	$(0 \pm 0{,}4).10^{-15}$	$(0 \pm 0{,}4).10^{-15}$
Quadratic Somme	$\mathbf{0,7.10^{-15}}$	$\mathbf{0,8.10^{-15}}$
Gravitational correction	$(6,5 \pm 0,1).10^{-15}$	$(6,5 \pm 0,1).10^{-15}$

Table 1: Error budget of the FO2 fountain

5. NEW METHOD FOR THE MEASUREMENT OF THE COLLISION SHIFT

To obtain a good frequency stability it is necessary to implement a fountain clock operating with as great a number of atoms as possible. In that case the collision displacement becomes very significant (a few 10^{-14} for Cs). Methods traditionally used to measure this displacement

result in a precision of the order of 15-20 %, which is insufficient. A new method using the adiabatic passage was developed and makes possible the preparation of an atomic clouds having a stable density ratio. The difference of atomic frequency between high and low density should allow the determination of the collision displacement to one part in 10^{-16}.

6. TESTING THE EQUIVALENCE PRINCIPLE USING COLD ATOM FOUNTAINS

Due to their high accuracy, atomic fountains can be used to perform very stringent tests of the fundamental physical laws. We have made an experiment to perform a new test of the variation of with time at the laboratory scale. The principle of the method is to compare at various times the hyperfine frequency (hyperfine separation energy) of ^{87}Rb and ^{133}Cs. We have compared a Rb fountain and two Cs fountains during a period of 5 years, and we have shown that $\frac{\dot{\alpha}}{\alpha}$ is less than $(-0.4 \pm 16)10^{-16}$ per year.

7. ATOMIC CLOCKS ON EARTH AND IN SPACE

Because micro-gravity allows long interaction times between the atoms and the microwave field and because the velocity is constant and smaller than in the earth fountains, we expect an excellent accuracy for a cold atom space clock. The space mission, ACES (Atomic Clocks Ensemble in Space), carries ultra-stable clocks. ACES have been selected by the European Space Agency to fly on the International Space Station in 2006. It consists of two clocks, a cold atom clock (PHARAO-SYRTE) and a hydrogen maser (Observatory of Neuchtel) together with microwave and optical links for time and frequency transfer to ground users . The scientific objectives of ACES include a measurement of the gravitational red-shift with a 25-fold improvement over the relativity experiment carried by Vessot and Levine in 1976, a better test of the isotropy of the speed of light and a search for a possible variation of the fine structure constant a with time. Finally, with appropriate time transfer equipment, ACES will allow synchronization of time scale of distant ground laboratories with 30 ps accuracy and frequency comparisons at the 10^{-16} accuracy level.

8. CONCLUSION

Microwave frequency standards using atomic fountains have now reached a high level of maturity. Their frequency stability of $3.10^{-14}\tau^{-1/2}$ makes possible the maintenance of time scales to an unsurpassed precision. They presently allow the determination of the unit second to an accuracy of few 10^{-16}. They also make possible the study of physical phenomena such as relativity and time variation of fundamental constants with unprecedented accuracy.

9. REFERENCES

J.Vanier and C.Audoin: *The Quantum Physics of Atomic Frequency Standards*, Adam Hilger, editor, Bristol, 1989.

The Mystery of Time, The National Geographic Society, 2002

F. Pereira Dos Santos et al, Phys. Rev. Lett. 89, 233004 (2002)

H. Marion et al, Phys. Rev. Lett. 90, 150801 (20033)

Vessot et al: *"Test of relativistic gravitation with a space-borne hydrogen maser"*, Phys. Rev. Lett., vol. 45, p 2081,dec. 1980

LONG-TERM STABILITY OF RHODE & SCHWARZ QUARTZ CLOCKS

P. PARASCHIV, P. POPESCU
Astronomical Institute of the Romanian Academy
Str. Cuţitul de Argint 5, RO-752121 Bucharest, Romania
e-mail: paras@aira.astro.ro, petre@aira.astro.ro

ABSTRACT. Modern time measurements in Romania started in 1967 with the installation of Rhode & Schwarz Quartz Clocks. The paper shows both the evolution of these measurements and the stability of the system, which became a few times better than in the beginning, 35 years ago. The evolution of the original R1, R2, R3, R4 oscillators was analyzed. After 1994, the receivers were connected to a digital chronometer, in order to perform the acquisition of the measuring data. New comparisons of R1, R2, R3 with M1, M2, M3 quartz clocks and GNST GPS receiver were made.

1. THE 1967 - 1990 PERIOD

In 1967, at Bucharest Astronomical Observatory a system of quartz clocks, model Rohde & Schwarz was installed. The system was made up of 4 frequency standards, XST type, with crystal oscillator and a complete set of accessories, including a comparing oscilloscope and signal receivers. The estimated standard stability (aging after 100 days of operation) was maximum 2×10^{-9}. The four frequency standards denominated RS1, RS2, RS3, RS4 were in operation in the interval 1967 - 1990.

Their main work was to synchronize and guide sidereal clocks and secondary clocks in the institute, as required by the status of Time Service Department. At the same time, the functional parameters were measured by means of time signals comparisons for RS1, RS2, RS3, RS4 using the oscilloscopic method and intercomparisons between clocks and time signals.

The Zeiss Transit Instrument was used for the study of irregularities of Earth Rotation, connected with the rezults of BIH and IPMS. An interesting, new method of time system inter-comparison, by means of television signals, was proposed by Vladimir Ptacek (Prague Astronomical Observatory) and Victor Stavinschi (Bucharest Astronomical Observatory). The accuracy was of the order of milliseconds.

The quartz clocks were also compared using the so called "flying clock" method, initiated by Hewlet Packard Company. The Earth Rotation research group also joined MERIT campaign, performing observation and time comparisons. Visual observations were stopped in 1988 due to the MERIT conclusion.

Between 1982-1985 a set of hydrogen masers, built by the Romanian Institute of Materials Technology was installed in the Astronomical Institute. Victor Stavinschi, the chief of Time Service, started to test the accuracy and the stability of the new frequencies standards. The results were not satisfactory in comparison with the old Rohde&Schwarz clocks. The measurements were performed in order to determine the parameters of frequency standards, determined fre-

quency standards errors, relative error in frequency, daily variation of relative error in frequency, sidereal time error, frequency dependence by ambient temperature and frequency dependence by power supply. The measurements performed in order to determine the parameters of frequency standards related to comparisons of time signals for RS1, RS2, RS3, RS4 by means of the oscilloscopic method and also the relative error in frequency and daily variation of relative error in frequency. To determine the sidereal time errors the coincidence method has been used with a CAO comparing oscilloscope. These measurements has been performed continuously.

2. DEVELOPMENTS FROM 1990 TILL NOW

After 1990, the RS3, RS4 were eliminated due to their frequency - different with 1.1×10^{-6} (RS3) and 1.8×10^{-6} (RS4) from the nominal one. In 1994, RS3 started operate with a new crystal oscillator, mounted by Tiberiu Bocaniciu, the chief of Time Service. Due to their instability, maser clocks were discharged from the system, only their Thompson quartz clocks remaining in operation, named M1, M2, M3, with a standard stability of maximum1.0×10^{-10}.

In 1998, a GPS time receiver type GNSS 300T was mounted in order to receive both GPS and GLONASS signals, with an error of $\pm 0.1 \mu s$ from UTC. It is possible to determine the error of the compared standard $\pm 0.1 \mu s$, instead of $\pm 1.0 ms$ by the time signal comparison. A computer assists all the measurements, performed with an accuracy of $0.1 ns$.

By means of the method of BIPM, the Group standard (RS1, RS2, RS3, M1, M2, M3) made of these 6 frequency standards was established. The polynomial coefficients of the evolution of the clocks were computed and a prognosis of the evolution of their mean error was made. The differences between the prognosis and the results didn't exceed $\pm 0.1 ms$.

3. COMPARISON RESULTS

Statistical studies were continuously performed in order to have a complete image of the process. We have tried underline the Rode & Schwarz clocks, their stability and fiability.

The results are contained in the following figures.

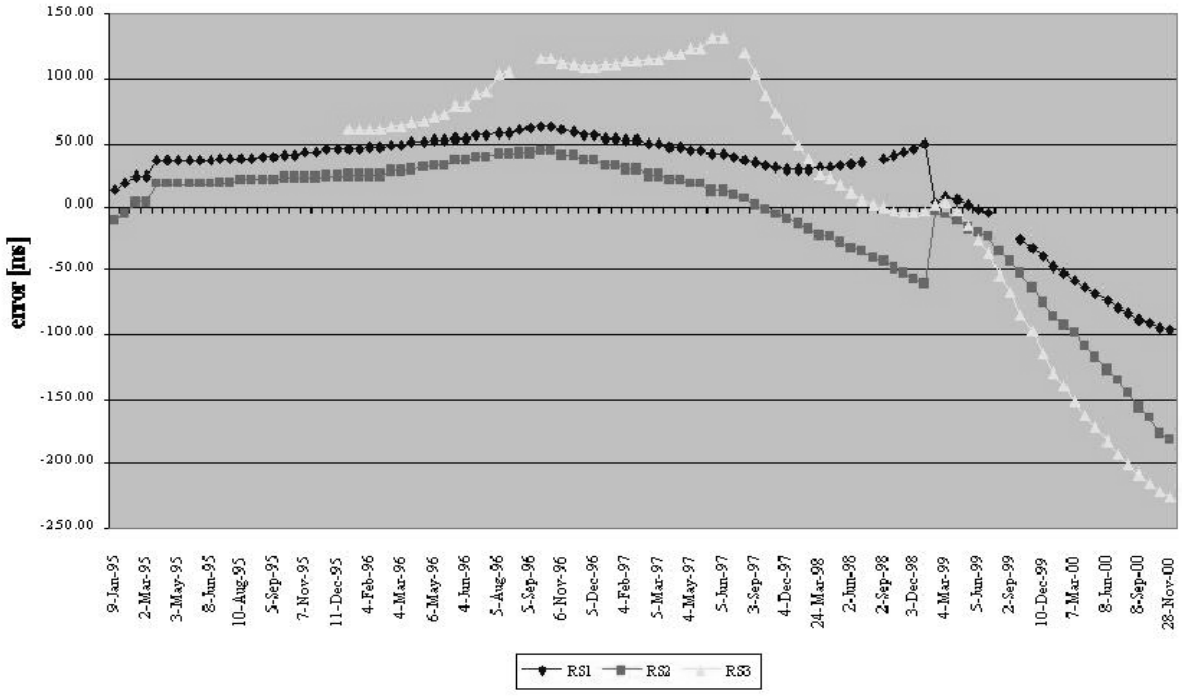

Figure 1. Time differences RSi - UTC.

From the graph one can see the better correlation of the RS1 and RS2 frequency standards with UTC. After the adjustment from 1999, we have noticed that the slope increased due to the frequency variation.

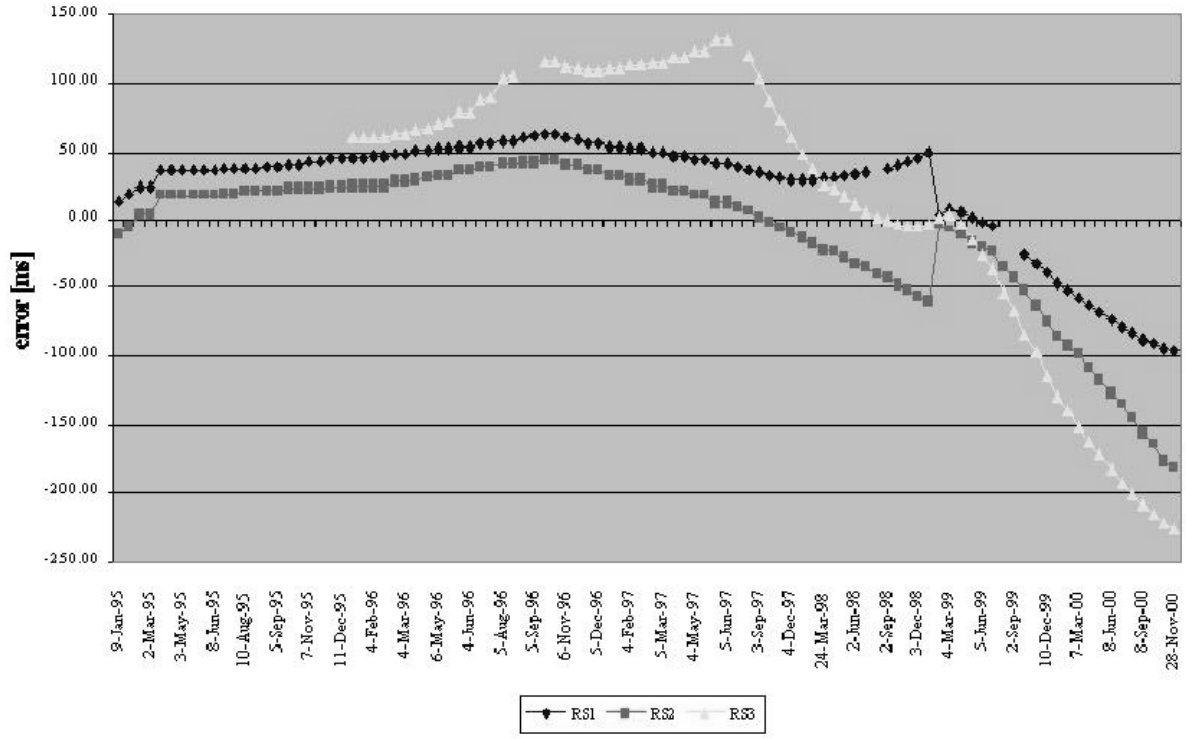

Figure 2. Frequency long term stability.

For the standards R1 and R2, their frequency variations were positive and the linear time dependent; R3 having a new crystal, his stability is not of the same order. The monthly variation of relative frequency for RS1 and RS2 standards were 1.4×10^{-10} and 0.4×10^{-10}, respectively. Annual variation is less than 17×10^{-10} and 6×10^{-10}, respectively. The values of the frequency stability, computed with Allan's formula are, for RS1, RS2 and RS3, $0.11, 0.09, 0.22 (\times 10^{-10})$, respectively.

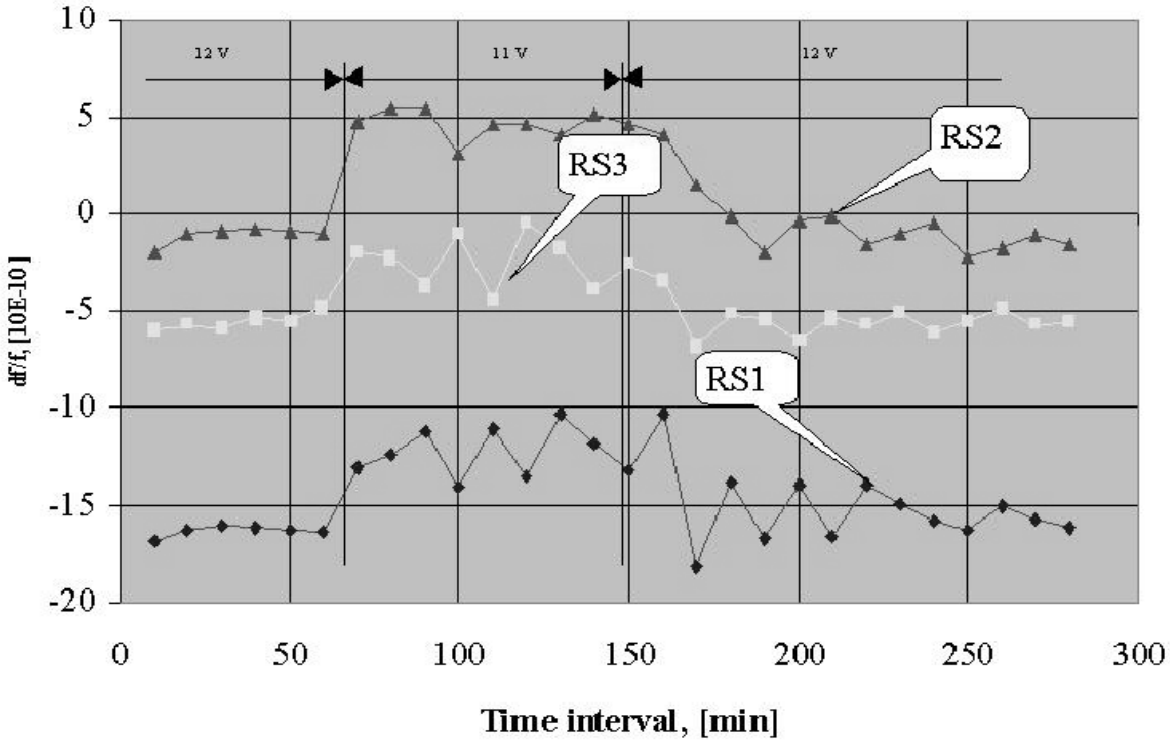

Figure 3. Effect of operating voltage.

A variation of 10% of the power voltage determined a 5×10^{-10} variation of the relative frequency of the standards.

In a similar way a temperature variation of 10^0C implies a variation of the relative frequency less than 1.0×10^{-10}.

4. CONCLUDING REMARKS

The evolution of Rohde&Schwarz frequency standards which was analyzed shows that the stability of the system has become a few times better than in the beginning, 35 years ago. In spite of the fact that the system is old, it represents a good time reference for astronomical observations connected with the GNSS 300T GPS receiver.

5. REFERENCES

Stavinschi, M. : 1984, *St. Cerc Fiz.*, **36**, 448. Bocaniciu, T., Paraschiv, P., Stavinschi, M., Popescu, P., Popescu, R.: 2001, *Proceedings of International Conference of Metrology*, Bucharest, 18-20 Sept. 2001, vol. 3, 641.

POSTFACE

JOURNÉES 2003 SYSTÈMES DE RÉFÉRENCE SPATIO-TEMPORELS

"Astrometry, geodynamics and solar system dynamics: from milliarcseconds to microarcseconds"

Scientific Organizing Committee :
N. Capitaine, France (Chair); A. Brzeziński, Poland; P. Defraigne, Belgium; A.Finkelstein, Russia; M. Soffel, Germany; J. Vondrák, Czech R.; Ya. Yatskiv, Ukraine

Local Organizing Committee :
A.Finkelstein (Chair), V.Brumberg, V.Gubanov (vice-Chair), I. Kumkova, G.Krasinsky, Z.Malkin, N.Panafidina (secretary), N.Shuygina, E.Yagudina

Conference location : Institute of Applied Astronomy of Russian Academy of Sciences, St.Petersburg

Scientific objectives :
The Journées 2003 "Systèmes de référence spatio-temporels", with the sub-title "Astrometry, geodynamics and solar system dynamics: from milliarcseconds to microarcseconds", will be held from 22 to 25 September 2003 in St Petersburg, at Institute of Applied Astronomy of Russian Academy of Sciences (IAA), organized jointly by the IAA and Paris Observatory. These Journées will be the fifteenth conference in this series whose purpose is to discuss the problems, from the concepts and realizations of space and time reference systems to the scientific interpretations of precise observations referred to these systems.

The conference is intended to provide a forum for researchers in the fields of Earth rotation, reference frames, astrometry and time. One of the purposes of this meeting is to discuss the latest scientific developments in these topics after the 25th General Assembly of the International Astronomical Union in July 2003 in Sydney. These Journées will thus include, as usual, sessions related to celestial and terrestrial reference sytems and frames, rotation of the Earth and planets, geophysical effects, dynamics of the Solar System, Relativity and time and an additional session providing information relative to the 25th IAU GA.

Scientific programme :
The programme of the Journées 2003 includes the six following sessions :

Session 1 : Celestial and terrestrial reference frames: techniques, definition and links

Session 2 : Rotation of the Earth and other planets: observations and models
(as a special session in the tradition of the Orlov's conferences)

Session 3 : Plate tectonics and crustal deformations and geophysical fluids

Session 4 : Solar System Dynamics

Session 5 : Relativity and Time

Session 6 : Information and discussion relative to the 25th IAU General Assembly

Contact : Institute of Applied Astronomy of Russian Academy of Sciences,
10 Kutuzov Quay, 191187, St.Petersburg, Russian Federation,
Phone : +7-(812)275-11-18; Fax : +7-(812)275-11-19; e-mail : gubanov@quasar.ipa.nw.ru,

or see : http://quasar.ipa.nw.ru/conference/2003/